The theory and properties of randomly disordered crystals and related physical systems

R. J. Elliott

Department of Theoretical Physics, Oxford University, Oxford, OX1-3PQ, England

J. A. Krumhansl

Laboratory of Atomic and Solid State Physics, Cornell University, Ithaca, New York 14850

P. L. Leath

Department of Physics, Rutgers University, New Brunswick, New Jersey 08903

We review the methods which have been developed over the past several years to determine the behavior of solids whose properties vary randomly at the microscopic level, with principal attention to systems having composition variation on a well-defined structure (random "alloys"). We begin with a survey of the various elementary excitations and put the dymanics of electrons, phonons, magnons, and excitons into one common descriptive Hamiltonian; we then review the use of double-time thermodynamic Green's functions to determine the experimental properties of systems. Next we discuss these aspects of the problem which derive from the statistical specification of the microscopic parameters; we examine what information can and cannot be obtained from averaged Green's functions. The central portion of the review concerns methods for calculating the averaged Green's function to successively better approximation, including various self-consistent methods, and higher-order cluster effects. The last part of the review presents a comparison of theory with the experimental results of a variety of properties—optical, electronic, magnetic, and neutron scattering. An epilogue calls attention to the similarity between these problems and those of other fields where random material heterogeneity has played an essential role.

CONTENTS

I. PREAMBLE

The subject of randomness in physics is probably familiar to most physicists only in the form of statistical mechanics, or in applications of the Boltzmann and "master" equations. Yet much of the world we live in, particularly the materials we deal with, does not have the simplicity and regularity found in physical systems which have received most of our attention. If one consults recent reviews of related fields [Beran, 1968, 1971; Frisch, 1968] one begins to realize the tremendous range of real situations in which randomness is a central aspect of the problem.

For example, in geophysics the material properties of randomly polycrystalline rock, its pore and fissure structure, and elastic waves and transport in such media are all essential to the interpretation of geological situations. The motion of the sea, both underwater and surface, including sound propagation with turbulence or random density fluctuations, present similar analytical problems. And it goes on—atmosphere and ionosphere, astrophysical problems (going back to attempts to understand twinkling of stars), radiowave propagation, communication theory, neutron diffusion, partial coherence in modern optics. All of these have in common the problem of describing the dynamics of some field or particle motions in the presence of random irregularities in the parameters of the system. We will return to these similarities in the last section of this paper.

The study of matter which is random in either composition or structure had for years received considerably less attention by physicists than better definable crystalline materials for good reason. The definite structure of the latter allowed both considerable theoretical progress and dependable comparison of experiments between various workers, both of which are essential to good scientific progress. Nonetheless, results were obtained in some heterogeneous situations. Einstein (1906) concerned himself with the dielectric and optical properties of a suspension of small particles in a liquid. Rayleigh (1892) addressed the question of the average permitivity of a heterogeneous medium.

While those studies were primarily concerned with static response, progress was made on wave propagation [see J. B. Keller and F. C. Karal, Jr. (1964, 1966)]. Of particular importance to the developments which are the principal subject of the present review, Foldy (1945) showed how the effective index of a medium could be related to the averaged forward scattering amplitudes in a heterogeneous medium; this was primarily a strong scattering "low concentration" theory, and it was not self-consistent. Lax (1951, 1952) extended the theory by introducing an effective medium in which scattering fluctuations were imbedded, and whose parameters were determined by averaging similar to Foldy, but now this gave an implicit equation to determine self-consistently the effective index. In essence this is the philosophy, transposed to the context of alloys and random crystals, which has become known as "self-consistent" or "coherent potential approximation."

During the last decade the subject has evolved rapidly, and both theoretical and experimental interest in materials with randomness in their properties has increased substantially. The reasons are several. With regard to alloys, progress in metallurgical science, as well as in the physics of dilute magnetic and nonmagnetic alloys, led to the need for more realistic descriptions than rigid band or virtual crystal models. With regard to semiconductors, both compound (crystalline) semiconductors and amorphous semiconductors began to receive considerable attention as possibly presenting parametric flexibility, or even fundamentally new phenomena, for electronic applications.

At the same time, on the theoretical side, three principal developments drew the attention of theoretical physicists. First, the developments of sophisticated perturbation technique in many-body theory—particularly in the use of Green's functions—which has made it possible to avoid the cumbersome differential equation description of Schrödinger waves in a random medium, as well as to calculate needed experimental quantities directly. Second, the development of computers capable of determining information about reasonably large models of random systems. Third, new efforts toward understanding the topology and structure of random networks, both by physical model construction and by computer simulation. Many more physicists have now become involved in the study of random systems, and both experimental and theoretical progress has been made.

For the traditional methodology of solid state physics, and in the interpretation of experiments, the loss of lattice periodicity is a disaster. The methods of group theory, which one relies on because of translational symmetry, are no longer applicable, so the states are not simply characterized by a wave vector **k**; of course, it follows that "**k**-selection rules" also are lost. A point of some concern is the continued use of traditional band theory results in the interpretation of experiments on random systems, in spite of their self-evident inapplicability.

As we see it at the present time, there are three main sub-areas with definite concepts being developed and tested: direct computer modeling and experiments; theoretical and experimental work on random alloys and related systems; and theory and experiment for amorphous semiconductors. That order of listing is also, in our view, indicative of the degree of maturity of definite results and critical comparison with experiment—which bring us to the setting and purpose of the present review article.

Dean (1971) has presented an extensive review of the numerical studies of disordered systems. Mott and Davis (1971) and N. Mott, M. H. Cohen, P. W. Anderson, H. Fritzsche, and D. J. Thouless (J. Tauc, 1972), to mention a few, have stimulated considerable discussion (in various conference proceedings particularly) of amorphous semiconductors. However, there exists no comparable review of theory and experiment for random alloys and related systems; we believe that this subject has reached considerable definiteness in its development, so it is the aim of this paper to review it. There is one other recent review by Bell (1972) which lies somewhat between ours and Dean's, but we devote considerably more attention to formal methods and their relation to experiment. The plan of our review is as follows:

Section II has as its purpose the introduction of model Hamiltonians which show that to good approximation electron, phonon, magnon, and exciton problems reduce to the same formulation. In preparing this review we have noticed considerable duplication in the timing and content of ideas put forth by specialists in these particular topics, and hope by our presentation to supply the reader with a basis for comparing the literature of random systems no matter what the context. Having done this, we review the thermodynamic Green's function method for treating the dynamics of such systems, and relate it to desired experimental quantities. Illustrations of the method are given for simple defect problems.

Finally, in Sec. II, we address the general features which may be expected from randomness on the dynamics of systems. The numerical studies reviewed by Dean (1971) and Bell (1972), showed that the spectrum of random systems usually has two characteristically different regions—one continuous with primarily extended states, the other being "spiky" with localized states, frequently identifiable with clusters of defects. A main point of our discussion is the way in which configuration (or "ensemble"), averaging relates to the nature of the states, and particularly to those theoretical quantities which are typically measured experimentally.

Proceeding to Sec. III, which surveys approximation methods in various formal calculations to date, we show how both the equations of motion of the Green's functions and statistical considerations must be combined in a single expression, in order to incorporate both dynamics and structure in the physics of such systems. This is, of course, the essence of the formidable difficulty which theories of the dynamics of random systems must face.

Instead, one must explicitly introduce statistical consideration. In the general case the quantities desired are nonlinear functionals of the random parameters of the system (Frisch, 1968; Beran, 1968, 1971). No general methods exist for determining the stochastic properties of such systems; however, it is possible to compute low-order averages and correlation functions—which primarily are what is needed by the physicist.

A variety of methods have been developed for different applications. Some are algebraic "decoupling" approximations, while others make use of diagrammatic organization of perturbations and the statistics of series expansion; localized and band (Bloch) states have been used. In Sec. III we have brought together, in a comparative discussion, both formal methods and model computations based upon them, using examples from electron, phonon, exciton, and magnon applications. Low concentrations of simple defects may be discussed quite satisfactorily. However, extended defects, clusters, short-range order, and amorphous structure are much more difficult to treat, although progress is being made rapidly; we summarize what we know at this writing.

Finally, in Sec. IV we compare model methods and computations with experiment, including systems of electrons, phonons, magnons, and excitons. We show that by now it is indeed possible to take parameters determinable by measurement or inferred from perfect crystal data, put them into various theoretical models, and predict both semiquantitatively and phenomenologically the behavior found experimentally in various random systems.

We are limited still in our understanding of a few problem areas, particularly transport effects in semiconducting amorphous materials, which as noted earlier we consider to be outside of the scope of the present review. On the other hand, in the matter of random alloys and many related topics the ability to relate parameters, structure, and properties has been developed to a degree well worth reporting to physicists.

We conclude this introductory section with an apology to the authors of much recent work which we have not been able to cite here, but as a practical matter we had to limit our review to material published up until early 1973. Beyond that date we have only been able to include a few references.

II. INTRODUCTION

A. Model Hamiltonians

All types of excitation in disordered crystals may be discussed by the same theoretical methods. In this section we discuss Hamiltonians (and the equations of motion) for the specific types of excitation which are most commonly studied in solid state physics: electrons, phonons, excitons, and magnons. By a suitable change of notation it is shown that all these problems may be made formally identical, and a universal notation is developed which can be used throughout the paper and specialized to specific situations as required. In the literature, workers interested in one application have often ignored the parallel work in related fields, although the formal similarities have been stressed by a number of authors [e.g., Anderson (1967), Matsuda (1966), Onodera and Toyozawa (1968), Maradudin (1966), Aiyer *et al.* (1969)].

Since most of the paper will be considering alloys with substitutional disorder, we shall confine our attention to the Hamiltonians appropriate to this case. In Sec. IV a brief discussion of structural (glass-like) disorder is given.

1. Fermions–electrons

In a perfect crystal, the translational symmetry ensures that any excitation is specified by a wave vector **k** which lies inside the first Brillouin zone, and a band, or branch j. If $a_j^+(\mathbf{k})$ and $a_j(\mathbf{k})$ are the usual creation and destruction operators, the Hamiltonian may be written

$$\mathcal{H}_0 = \sum_{j\mathbf{k}} E_j(\mathbf{k})\, a_j^+(\mathbf{k})\, a_j(\mathbf{k}), \tag{2.1}$$

with a suitable choice of origin. The energy of the $(j, \mathbf{k})$ excitation is $E_j(\mathbf{k})$. The a's satisfy the usual anticommutation relations for fermions (e.g., electrons),

$$[a_j(\mathbf{k}), a_{j'}^+(\mathbf{k}')]_+ = \delta_{jj'}\delta(\mathbf{k}-\mathbf{k}'). \tag{2.2}$$

The Hamiltonian can be transformed into the site representation by defining operators which create excitations centered on particular unit cells in the crystal. In the electron case this is the well-known transformation to Wannier functions. If we can, for physical reasons, confine our attention to b branches, we shall need b separate local functions at each site. In the electron case it is always an approximation to restrict b since the number of bands is, in principle, infinite. Nevertheless it usually is a good approximation to consider a few, or even only one band. If α specifies the b functions, and l specifies the unit cell at lattice position $\mathbf{R}(l)$, $\mathcal{H}_0$ can be written

$$\mathcal{H}_0 = \sum_{\alpha l} E_\alpha(l)\, a_\alpha^+(l)\, a_\alpha(l) + \sum_{\alpha\alpha', ll,} W_{\alpha\alpha'}(l, l')\, a_\alpha^+(l)\, a_{\alpha'}(l'), \tag{2.3}$$

where $W(l, l')$ depends only on $[\mathbf{R}(l) - \mathbf{R}(l')]$ and not explicitly on the positions separately, while $E_\alpha(l)$ is independent of l. The Heisenberg equations of motion give

$$i\hbar\frac{\partial}{\partial t}a_\alpha(l,t) = [a_\alpha(l,t),\mathcal{H}] = E_\alpha(l)a_\alpha(l,t) + \sum_{\alpha' l'} W_{\alpha\alpha'}(l,l')a_{\alpha'}(l',t). \tag{2.4}$$

If this is Fourier analyzed, the eigenvalues $E_j(\mathbf{k})$ are the solutions of the secular equation

$$|(E-E_\alpha)\delta_{\alpha\alpha'} - W_{\alpha\alpha'}(\mathbf{k})| = 0, \tag{2.5}$$

where $W_{\alpha\alpha'}(\mathbf{k}) = \sum_{l'} W_{\alpha\alpha'}{}^0(l,l')\exp\{i\mathbf{k}\cdot[\mathbf{R}(l)-\mathbf{R}(l')]\}$ and $E = \hbar\omega$.

In the presence of imperfections the excitations are no longer specified by $\mathbf{k}$, and terms like

$$\sum_{jj',\mathbf{kk}'} V_{jj'}(\mathbf{k},\mathbf{k}')a_j{}^+(\mathbf{k})a_{j'}(\mathbf{k}') \tag{2.6}$$

must be added to Eq. (2.1). In this paper we are concerned with defects which cause a local change in the crystal. This is most conveniently dealt with in the site representation of Eq. (2.3). $E_\alpha(l)$ and $W_{\alpha\alpha'}(l,l')$ are changed in the vicinity of a defect from their perfect values. We denote this by

$$V_{\alpha\alpha'}(l,l') = (E_\alpha(l) - E_\alpha{}^0)\delta_{\alpha\alpha'}\delta(l,l') + [W_{\alpha\alpha'}(l,l') - W_{\alpha\alpha'}{}^0(l,l')]. \tag{2.7}$$

In some systems it is a good approximation to consider only a single band, and this case will be studied in most detail since the algebra is simple and the methods may be followed more directly. We may also take the origin arbitrarily and it is therefore often chosen to assist in the calculations, for example to improve the convergence of the perturbation theory. In this single band case the suffices are dropped and

$$V(l,l') = (E(l) - E^0)\delta(l,l') + \Delta W(l,l'). \tag{2.8}$$

Often the first term in Eq. (2.8) is the most important, and this greatly simplifies the theory. If we neglect $\Delta W(l,l')$ the defects described by Eq. (2.8) do not overlap; V is simply determined by whether site l has a defect or host atom on it. Physically this means that the impurity atom has a different core potential but essentially the same valence electron distribution. This is satisfactory in some real situations, but not by any means in all.

2. *Bosons*

In discussing the vibrational excitation of solid helium, and for excitons, we deal with bosons. The fundamental Hamiltonian for the perfect crystal can still be written in the form (2.1) although the total energy will contain a contribution from the zero-point energy. The $a_j{}^+(\mathbf{k})$ now satisfy commutation relations

$$[a_j(\mathbf{k}), a_{j'}{}^+(\mathbf{k}')] = \delta_{jj'}\delta(\mathbf{k}-\mathbf{k}'). \tag{2.9}$$

When this is transformed into the site representation $\mathcal{H}$ takes the simple form (2.3) only if the $a_\alpha{}^+(l)$ etc. have been defined to create local excitations from the true ground state of the system. If the a are not so chosen, terms in $a_\alpha(l)a_\beta(l')$ and $a_\alpha{}^+(l)a_\beta{}^+(l')$ will occur in $\mathcal{H}_0$. In these circumstances a Bogoliubov transformation is required, and the secular equation like Eq. (2.5) giving the characteristic excitation energies is always an equation in E^2.

The effect of an impurity is again to introduce terms like Eq. (2.6). Now that particle number need not be conserved as in the fermion case, terms in $a_j{}^+(\mathbf{k})a_{j'}{}^+(\mathbf{k}')$ and $a_j(\mathbf{k})a_j(\mathbf{k}')$ can also occur. This means that the ground state of the system and the zero-point energy is changed by the addition of the defects. The Hamiltonian must be diagonalized by a Bogoliubov transformation in this case and the secular equation (2.5) is quadratic in E.

3. *Excitons*

There is one physical situation—that of excitons—where the above complications are immaterial. The ground state of the system corresponds to full bands, with the electrons in closed valence shells. The singlet excited states correspond to a transfer of an electron to the conduction band leaving behind a hole with the same spin. In the lowest excited states these electron–hole pairs are bound together. In the simplest model—the 'Frenkel' exciton—this binding is close, and the electron and hole are effectively bound at the same site. This excited atom behaves as a boson. The $a_\alpha{}^+(l)$ is therefore defined as the operator which creates an excitation of type α at atom l. The exciton moves across the crystal because of overlap with adjacent atoms. The excitation energies are normally large, so relatively few excitons are usually excited except in special circumstances. In this case the Hamiltonian takes exactly the form (2.3) except the a's are now boson operators. The E_α are here the excitation energies and $W_{\alpha\alpha'}(l,l')$ the hopping integrals. The effects of impurities can be described by Eq. (2.7).

The most important application to disordered systems was given by Onodera and Toyozawa (1968) in a description of optical absorption by excitons in mixed alkali halides.

4. *Phonons*

For lattice vibrations in disordered systems it is convenient to work with momentum and displacement operators p and u rather than the a's. The Hamiltonian is given most naturally in a site representation

$$\mathcal{H} = \sum_{l,\alpha}\frac{p_\alpha(l)^2}{2M_\alpha(l)} + \tfrac{1}{2}\sum_{\alpha,\alpha',l,l'}\Phi_{\alpha\alpha'}(l,l')u_\alpha(l)u_{\alpha'}(l'). \tag{2.10}$$

As before, l specifies the unit cell at $\mathbf{R}(l)$ and here α specifies one of the 3ν Cartesian coordinates of the ν atoms in the cell. In the perfect lattice $M_\alpha(l)$ is independent of l and depends only on atom type, while Φ is a function only of $[\mathbf{R}(l)-\mathbf{R}(l')]$.

The Heisenberg equations of motion are

$$i\hbar \frac{\partial}{\partial t} u_\alpha(l,t) = [u_\alpha(l,t), \mathcal{H}] = M_\alpha(l)^{-1} p_\alpha(l,t) \qquad (2.11a)$$

$$\begin{aligned} i\hbar \frac{\partial}{\partial t} p_\alpha(l,t) &= [p_\alpha(l,t), \mathcal{H}] \\ &= -\sum_{l',\alpha'} \Phi_{\alpha\alpha'}(l,l') u_{\alpha'}(l',t), \end{aligned} \qquad (2.11b)$$

so that

$$M_\alpha(l) \frac{\partial^2}{\partial t^2} u_\alpha(l,t) = -\sum_{l'\alpha'} \Phi_{\alpha\alpha'}(l,l') u_{\alpha'}(l',t). \qquad (2.12)$$

When Fourier transformed, this expression becomes

$$\sum_{\alpha' l'} [M_\alpha(l)\delta_{\alpha\alpha'}\delta(l,l')\omega^2 - \Phi_{\alpha\alpha'}(l,l')] u_{\alpha'}(l') = 0. \qquad (2.13)$$

These equations are, of course, the same as would have been obtained classically, since the system is harmonic (Messiah, 1962).

In the perfect crystal the characteristic frequencies and normal modes may be readily obtained because of the translational symmetry. Transforming to **k** representation, the matrix reduces to $3\nu \times 3\nu$ blocks. The normal modes are found in the form

$$\phi_j(\mathbf{k}) = \sum_{\alpha,l} \sigma_j^\alpha(\mathbf{k}) \exp[i\mathbf{q}\cdot\mathbf{R}(l)] u_\alpha(l) (M_\alpha/N)^{1/2}. \qquad (2.14)$$

With impurities we write

$$M_\alpha(l) = M_\alpha^0 - \Delta M_\alpha(l) = M_\alpha^0(1 - \epsilon_\alpha(l)), \qquad (2.16a)$$

$$\Phi_{\alpha\alpha'}(l,l') = \Phi_{\alpha\alpha'}^0(l-l') + \Delta\Phi_{\alpha\alpha'}(l,l'). \qquad (2.16b)$$

Equation (2.13) now reads

$$\begin{aligned} \sum_{\alpha' l'} [M_\alpha^0 \omega^2 \delta_{\alpha\alpha'}\delta(l,l') &- \Phi_{\alpha\alpha'}^0(l,l') \\ &- V_{\alpha\alpha'}(l,l')] u_{\alpha'}(l') = 0, \end{aligned} \qquad (2.17)$$

where

$$V_{\alpha\alpha'}(l,l') = M_\alpha^0 \omega^2 \epsilon_\alpha(l) \delta_{\alpha\alpha'}\delta(l,l') + \Delta\Phi_{\alpha\alpha'}(l,l'). \qquad (2.18)$$

V plays the same role in these equations as does that defined by Eq. (2.7) in Eq. (2.5). We shall utilize this fact to establish a common notation below.

For simple mass defects, when changes in force constants are neglected, **V** is diagonal in the site representation. In a crystal with one atom per cell, the α index may be dropped from **M** and Eq. (2.18). Many of the more detailed calculations reported here have been done for this simplified case. Fortunately in many crystals mass changes are larger than corresponding force constant changes.

5. *Magnons*

The excitations in ordered magnetic materials are spin waves or magnons [for a review see Keffer (1966)]. Most systems of interest can be described in terms of an interaction between the spins of the form

$$\begin{aligned} \mathcal{H} = \sum_{l,l'} I(l,l') S_z(l) S_z(l') &+ J(l,l') \\ &\times [S_x(l)S_x(l') + S_y(l)S_y(l')], \end{aligned} \qquad (2.19)$$

where we have labelled magnetic atoms, rather than cells by l. If $J = 0$ we have the Ising model, if $I = J$ we have the Heisenberg model. For $l = l'$ both I and J will vanish. Some systems require further terms in the Hamiltonian for a realistic description. Assuming that spins order along the z direction, the excitations are described through the equations of motion of the operators $S_\pm = S_x \pm iS_y$ which increase or decrease the spin component along the z directions; we find

$$\begin{aligned} i\hbar \frac{\partial S_-(l)}{\partial t} = 2\sum_{l'} [I(l,l') S_-(l) S_z(l') \\ - J(l,l') S_-(l') S_z(l)]. \end{aligned} \qquad (2.20)$$

The equations may be linearized by replacing $S_z(l)$ by its appropriate equilibrium value $\langle S_z(l) \rangle$.

For a simple homogeneous ferromagnet we denote

$$\langle S_z(l) \rangle = S. \qquad (2.21)$$

The Fourier transform

$$N^{-1/2} \sum_l \exp[i\mathbf{k}\cdot\mathbf{R}(l)] S_-(l) = S_-(\mathbf{k}) \qquad (2.22)$$

satisfies the equation

$$\begin{aligned} \omega S_-(\mathbf{k}) = (2S \sum_{l'} I(l,l') &- J(l,l') \\ &\times \exp\{i\mathbf{k}\cdot[\mathbf{R}(l) - \mathbf{R}(l')]\}) S_-(\mathbf{k}), \end{aligned} \qquad (2.23)$$

and the quantity multiplying $S_-(\mathbf{k})$ is $\omega(\mathbf{k})$, the excitation frequency of the spin wave. In terms of the Fourier transform of I and J in this periodic crystal case

$$\omega(k) = 2S[I(0) - J(k)]. \qquad (2.24)$$

It is possible to define a set of creation and destruction operators with approximate boson properties to describe this system. We write

$$S_-(l) = (2S(l))^{1/2} a^+(l), \qquad S_+(l) = [2S(l)]^{1/2} a(l), \qquad (2.25)$$

and

$$S_z(l) = S(l) - a^+(l) a(l).$$

The Hamiltonian may then be written

$$\begin{aligned} \mathcal{H} = -\sum_{l,l'} \{2S(l') I(l,l') a^+(l) a(l) &+ 2[S(l)S(l')]^{1/2} \\ \times J(l,l') a^+(l) a(l') \} \end{aligned} \qquad (2.26)$$

in the same general form as Eq. (2.3).

If a defect is introduced, $S(l)$, $I(l, l')$, and $J(l, l')$ will all change. The change V as defined in Eq. (2.7) is here

$$V(l, l') = 2[S(l)S(l')]^{1/2}J(l, l') - 2SJ_0(l, l') \qquad \text{for } l \neq l' \tag{2.27a}$$

and

$$V(l, l) = \sum_{l'} [S(l')I(l, l') - SI_0(l, l')]. \tag{2.27b}$$

In this case no simple physical defect corresponds to a purely diagonal change. Furthermore, if the sign of I and J change, the ground state will change, since the defect spin will prefer to orient itself antiparallel to the host spins. This situation requires a redefinition of the a operators. If the ground state remains ferromagnetic, however, the system may be treated in a similar way to the electron and phonon systems already described.

For an antiferromagnet the situation is slightly more complicated. In the simplest case there are two types of magnetic spin where

$$\langle S_z(l) \rangle = \pm S. \tag{2.28}$$

Substituting in Eq. (2.20) gives two equations for different l depending on the sublattice. As a result the characteristic frequencies are given by

$$\omega^2(\mathbf{k}) = (2S)^2[I(\mathbf{0})^2 - J(\mathbf{k})^2]. \tag{2.29}$$

In the presence of impurities with the same antiferromagnetic order the excitations are still given by equations like (2.20) with appropriate changes in $\langle S_z(l) \rangle$, I, and J.

B. Green's functions

In the last section it was shown that the problem of determining the excitation spectra in disordered crystals was essentially the same for several types of excitation. Within the approximations adopted the excitations are noninteracting, and it is only necessary to determine the spatial form and energy of each excitation. In the vibrational case this is the same as saying that we have used the harmonic approximation and that we now must determine the normal modes. This could be done in principle by finding the eigenvalues and eigenvectors of the set of linear equations (2.4) or (2.13). In a general imperfect crystal, without translational symmetry, this is an impossible task. Much important information has been obtained by a direct numerical attack on the secular determinant for a finite sample of crystal, but computerized models have been reviewed elsewhere (Dean, 1971), so that we shall only refer to those approaches for comparison with the analytic methods used here. In addition, special techniques have been developed for the one-dimensional crystal, notably the 'transfer matrix' method of Hori (1968); however, this method fails in three dimensions.

Although numerical studies have been very useful, the essential requirement of a theory is that it explain the experimental facts, and we therefore need to predict various crystal properties. It is seldom possible, in an imperfect crystal, to examine experimentally a particular normal mode. It is possible, for example by optical absorption, to examine all the crystal modes at a particular frequency. It is also possible, by inelastic neutron scattering, to examine the **k**-component content of these modes. In the perfect crystal this leads to the properties of specific modes because **k** is a good quantum number in a periodic system. But in the imperfect crystal all modes are sampled by this technique.

There are two types of common observational methods: responses to macroscopic external fields, such as mechanical forces or electromagnetic fields, and inelastic scattering cross sections with such scatterers as neutrons, electrons, and photons. These properties are in fact closely related, and all depend on correlation functions between appropriate operators. A well-defined formalism which leads directly to these quantities without the necessity of a complete normal mode solution is that of thermodynamic Green's functions, which we now review.

1. Double-time Green's functions

Complete details of Green's functions can be found in the review by Zubarev (1960). Their application to lattice vibrations in defect lattices has been discussed, for example, by Elliott and Taylor (1967). The application to defect magnetic (spin-wave) systems has been discussed by, for example, Wolfram and Callaway (1963) and Izyumov (1966).

These functions contain, at least as regards the experimental variables which enter their definition: (i) information on the dynamics of these variables, (ii) the density of the excitation states of the system, and (iii) the information needed to compute correlation functions, and therefore scattering and response properties of the system.

Several kinds of Green's functions are used in general applications: causal, retarded, and advanced:

$$\begin{aligned} G_c &= (2\pi/i\hbar)\langle T_\eta A(t)B(t')\rangle \equiv \langle\langle A(t); B(t')\rangle\rangle_c, \\ G_R &= (2\pi/i\hbar)\theta(t-t')\langle[A(t), B(t')]_\eta\rangle \\ &\equiv \langle\langle A(t); B(t')\rangle\rangle_R, \\ G_A &= (-2\pi/i\hbar)\theta(t'-t)\langle[A(t), B(t')]_\eta\rangle \\ &= \langle\langle A(t); B(t')\rangle\rangle_A, \end{aligned} \tag{2.30}$$

where $\eta = +1(-1)$ for bosons (fermions) is conventional and where T is the time ordering operator referring to ordinary commutation or anticommutation, θ is the unit step function, and averages are both quantum mechanical and thermal, over an equilibrium distribution. For the most part the retarded function is used in applications.

The Green's functions are closely related to the correlation functions

$$\mathfrak{F}_{AB}(t, t') = \langle A(t)B(t')\rangle. \tag{2.31}$$

Hence, for example,

$$G_R = (2\pi/i\hbar)\theta(t-t')[\mathfrak{F}_{AB}(t, t') - \eta\mathfrak{F}_{BA}(t', t)], \tag{2.32}$$

from which it may be expected that the Fourier transforms of G and $\mathfrak{F}$ are related. In fact, most calculations are done on

$$G_R(E) = (2\pi)^{-1}\int_{-\infty}^{\infty} G_R(t-t') \times \exp[iE(t-t')/\hbar]\, d(t-t'). \tag{2.33}$$

Since only $(t-t')$ appears in these expressions, we can set $t'=0$ without loss of generality. For real E we replace E by $E+i\epsilon$ for convergence.

It is not appropriate in this review to repeat all of the formal detail which is covered by Zubarev and others. Rather, we state the main results which can be found if the Green's functions are expressed in appropriate manner, and then we indicate how the Green's functions are usually calculated.

Double-time Green's functions may be expressed in a "spectral representation." Given a complete set of states, determined by the Hamiltonian, we may formally write

$$G_R(E) = \hbar\int_{-\infty}^{\infty} [\exp(\hbar\omega/k_BT)-\eta]J(\omega)\,\frac{d\omega}{E-\hbar\omega+i\epsilon}, \tag{2.34a}$$

where the spectral density is

$$J(\omega) = Q^{-1}\sum_{\nu,\mu}\exp(-E_\mu/k_BT)\langle\nu\mid A\mid\mu\rangle\langle\mu\mid B\mid\nu\rangle \times \delta(E_\mu-E_\nu-\hbar\omega). \tag{2.34b}$$

Here A and B are Schrödinger operators, Q is the (grand) partition function, μ and ν label the exact eigenstates of the system. If the imaginary part of E is positive, we define $G(E)=G_R(E)$; if negative, we define $G(E)=G_A(E)$. There is then the relation

$$\begin{aligned} J(\omega) &= (2\pi)^{-1}i[\exp(\hbar\omega/k_BT)-\eta]^{-1} \times \lim_{\epsilon\to 0}[G(\hbar\omega+i\epsilon)-G(\hbar\omega-i\epsilon)] \\ &= -(\pi)^{-1}[\exp(\hbar\omega/k_BT)-\eta]^{-1}\,\mathrm{Im}[G_R(\hbar\omega)]. \end{aligned} \tag{2.35}$$

In these equations the energy zero is to be taken as the chemical potential; for magnons and phonons this is zero, but for fermions it is the Fermi energy. From the analytic form (2.34) it is clear that $G_{R(A)}(E)$ is analytic in the upper (lower) half complex E plane, and thus that the real and imaginary parts of $G_{R(A)}$ are related by the Kramers–Kronig relations,

$$\mathrm{Re}G_R = \frac{1}{\pi}\int_{-\infty}^{\infty}\frac{\mathrm{Im}G_R(E')}{E-E'}\,dE' \tag{2.36a}$$

and

$$\mathrm{Im}G_R(E) = \frac{-1}{\pi}\int_{-\infty}^{\infty}\frac{\mathrm{Re}G_R(E')}{E-E'}\,dE'. \tag{2.36b}$$

With these formal relations, several experimental quantities may be found.

A correlation function is defined:

$$\mathfrak{F}_{AB} = \langle A(t)B(0)\rangle = \hbar\int_{-\infty}^{\infty} d\omega\,\exp(\hbar\omega/k_BT)J(\omega)\exp(-i\omega t), \tag{2.37a}$$

and thus, from Eq. (2.35)

$$\mathfrak{F}_{AB}(\omega) = -(\hbar/\pi)\exp(\hbar\omega/k_BT) \times [\exp(\hbar\omega/k_BT)-\eta]^{-1}\,\mathrm{Im}[G_R(\hbar\omega)]. \tag{2.37b}$$

There are also relations between this and other correlation functions. In particular

$$\mathfrak{F}_{BA} = \langle B(t)A(0)\rangle = \hbar\int_{-\infty}^{\infty} d\omega\,\exp(i\omega t)J(\omega). \tag{2.37c}$$

In general also

$$\langle\langle A;B,E\rangle\rangle_R = \langle\langle B;A,-E\rangle\rangle_A. \tag{2.38}$$

The response of observable $A(t)$ to applied force $B\exp(-i\omega t+\gamma t)$ ($\lim\gamma = 0+$) is also simply related to the Green's function through the formula

$$\langle A(t)\rangle = \langle A\rangle_0 = \chi_{AB}(\omega)\exp(-i\omega t+\gamma t),$$

where the generalized susceptibility $\chi_{AB}(\omega)$ is

$$\begin{aligned}\chi_{AB}(\omega) &= -G_R(A,B;E=\hbar\omega) \\ &= -G(A,B;E=\hbar\omega+i\epsilon).\end{aligned} \tag{2.39}$$

The major experimental quantities can be determined if the Green's functions can be found from the equations of motion which we therefore proceed to discuss.

2. *Equations of motion of the Green's functions*

The quantities entering the definition of the Green's functions are Heisenberg operators. Thus differentiation of the defining equation with respect to t yields

$$\begin{aligned} i\hbar(\partial/\partial t)\langle\langle A(t);B(0)\rangle\rangle &= 2\pi\delta(t)\langle[A(t),B(0)]_\eta\rangle \\ &\quad + \langle\langle[A(t),\mathcal{H}(t)];B(0)\rangle\rangle. \end{aligned} \tag{2.40}$$

The double-time Green's function on the right-hand side is in general different, and usually of higher order than the initial one. This leads to a chain of coupled equations; in general these cannot be solved exactly, but are decoupled in some way in practical approximations.

However, for the harmonic lattice Hamiltonian and for the model Hamiltonians of Sec. IB for electron, exciton, and spin-wave excitations, the chain of equations terminates exactly. The simplest example is obtained from the Green's function

$$\langle\langle a_\alpha(l,t);a_{\alpha'}^{+}(l',0)\rangle\rangle = G_{\alpha\alpha'}(l,l',t). \tag{2.41}$$

The causal, retarded, and advanced Green's function are chosen by inserting the appropriate complex energy in their Fourier transform. Using Eq. (2.4) for the derivative of a in Eq. (2.40) gives

$$\begin{aligned} i\hbar \frac{\partial}{\partial t} G_{\alpha\alpha'}(l, l', t) &= 2\pi\delta(t)\langle[a_\alpha(l), a_{\alpha'}{}^{+}(l')]_\eta\rangle + E_\alpha(l) G_{\alpha\alpha'}(l, l', t) \\ &\quad + \sum_{\alpha'' l''} W_{\alpha\alpha''}(l, l'') G_{\alpha''\alpha'}(l'', l', t). \end{aligned} \tag{2.42}$$

Since the appropriate commutation in the first term is unity, transforming to frequency space gives $\delta_{\alpha\alpha'}\delta(l, l')$ for this term. The equation is now a matrix equation which can be written for $G_{\alpha\alpha'}(l, l', E)$ defined by Eq. (2.33)

$$\mathsf{G}(E) = (E\mathsf{1} - \mathcal{H})^{-1}, \tag{2.43}$$

where $\mathcal{H}$ is the matrix of the numbers in Eq. (2.3).

If the eigenstates s are known (and are created by $a_s{}^{+}$) G can be diagonalized by the transformation to this representation

$$\langle\langle a_s; a_{s'}{}^{+}, E\rangle\rangle = \delta_{ss'}/(E - E_s). \tag{2.44}$$

In the perfect crystal, defined by Eq. (2.1), the states s are known and specified by $j\mathbf{k}$. In the imperfect crystal they are not known.

For the case of lattice vibrations, using the Hamiltonian (2.10) and equations of motion (2.11) and (2.40) gives

$$\begin{aligned} i\hbar(\partial/\partial t)\langle\langle u_\alpha(l, t); u_{\alpha'}(l, 0)\rangle\rangle &= 2\pi\delta(t)\langle[u_\alpha(l), u_{\alpha'}(l')]\rangle \\ &\quad + \langle\langle[u_\alpha(l, t), \mathcal{H}]; u_{\alpha'}(l', 0)\rangle\rangle \\ &= O + i\hbar\langle\langle p_\alpha(l, t)/M_\alpha(l); u_{\alpha'}(l', 0)\rangle\rangle. \end{aligned} \tag{2.45}$$

This contains a different Green's function, so, proceeding to the next equation,

$$\begin{aligned} i\hbar(\partial/\partial t)\langle\langle p_\alpha(l, t)/M_\alpha(l); u_{\alpha'}(l', 0)\rangle\rangle &= 2\pi\delta(t)\langle[p_\alpha(l)/M_\alpha(l); u_{\alpha'}(l')]\rangle \\ &\quad + \langle\langle[p_\alpha(l, t)/M_\alpha(l), \mathcal{H}]; u_{\alpha'}(l', 0)\rangle\rangle \\ &= \frac{-2\pi i\hbar}{M_\alpha(l)}\delta(t)\delta_{\alpha\alpha'}\delta_{ll'} \\ &\quad - \frac{i\hbar}{M_\alpha(l)}\sum_{\alpha'' l''}\Phi_{\alpha\alpha'}(l, l'') \\ &\quad \times \langle\langle u_{\alpha''}(l'', t); u_{\alpha'}(l', 0)\rangle\rangle. \end{aligned} \tag{2.46}$$

Defining

$$G_{\alpha\alpha'}(l, l'; t) = \langle\langle u_\alpha(l, t), u_{\alpha'}(l', 0)\rangle\rangle, \tag{2.47}$$

we find

$$\begin{aligned} M_\alpha(l)(\partial^2/\partial t^2) G_{\alpha\alpha'}(l, l', t) &= -2\pi\delta(t)\delta_{ll'}\delta_{\alpha\alpha'} - \sum_{\alpha'' l''}\Phi_{\alpha\alpha''}(l, l'') \\ &\quad \times G_{\alpha''\alpha'}(l'', l'; t). \end{aligned} \tag{2.48}$$

The Fourier transform to frequency, Eq. (2.33), gives

$$\begin{aligned} M_\alpha(l)\omega^2 G_{\alpha\alpha'}(l, l'; \omega) &= \delta_{\alpha\alpha'}\delta(l, l') + \sum_{\alpha'' l''}\Phi_{\alpha\alpha''}(l, l'') \\ &\quad \times G_{\alpha''\alpha'}(l'', l'; \omega). \end{aligned} \tag{2.49}$$

Condensed to matrix form this is written

$$[\mathsf{M}\omega^2 - \mathbf{\Phi}]\mathsf{G}(\omega) = \mathsf{1}, \tag{2.50}$$

where $\mathsf{1}$ is the unit matrix.

The transformation to normal modes will also diagonalize this matrix. In the case of the perfect crystal the result is

$$\begin{aligned} G_{jj'}(\mathbf{k}, \mathbf{k}'; \omega) &= \langle\langle \phi_j(\mathbf{k}); \phi_{j'}(\mathbf{k}'), \omega\rangle\rangle \\ &= \delta_{jj'}\delta(\mathbf{k} - \mathbf{k}')[\omega^2 - \omega_j{}^2(\mathbf{k})]^{-1}. \end{aligned} \tag{2.51}$$

In the spin-wave case the Green's function of interest is $\langle\langle S_-(l, t), S_+(l', 0)\rangle\rangle$. Using the Hamiltonian (2.19) and the equation of motion (2.20), Eq. (2.40) becomes more complicated:

$$\begin{aligned} i\hbar\langle\langle S_-(l, t); S_+(l', 0)\rangle\rangle &= 4\pi\delta(t)\delta(l, l')\langle S_z(l)\rangle \\ &\quad + 2\sum_{l''} I(l, l'')\langle\langle S_-(l, t) S_z(l'', t); S_+(l', 0)\rangle\rangle \\ &\quad + 2\sum_{l''} J(l, l'')\langle\langle S_-(l'', t) S_z(l, t); S_+(l', 0)\rangle\rangle. \end{aligned} \tag{2.52}$$

This can again be linearized by decoupling out the $S_z(l, t)$ and replacing it by its equilibrium value. In the imperfect crystal we see that the inhomogeneous term will not give a unit matrix unless all the $\langle S_z(l)\rangle$ are equal. This leads to difficulty in the subsequent analysis. It is therefore usual to transform to variables like the a defined by Eq. (2.25). We write

$$\begin{aligned} G(l, l', t) &\equiv \langle\langle S_-(l, t); S_+(l', 0)\rangle\rangle / 2[S(l) S(l')]^{1/2} \\ &= \langle\langle \hat{a}^{+}(l, t); \hat{a}(l', t)\rangle\rangle. \end{aligned} \tag{2.53}$$

In the ferromagnet, therefore, on transforming to frequency space Eq. (2.52) becomes

$$\begin{aligned} EG(l, l', E) &= \delta(l, l') + \sum_{l''} 2S(l'') I(l, l'') G(l, l', E) \\ &\quad + \sum_{l''} 2[S(l'') S(l)]^{1/2} J(l, l'') G(l'', l', E). \end{aligned} \tag{2.54}$$

This is formally the same as Eq. (2.42) and has a solution like Eq. (2.43) with appropriate definitions.

C. Experimental quantities

1. Density of states

A basic property of an excitation spectrum is its density of states per unit energy range $\rho(E)$. This can be determined from the Green's function (Zubarev, 1960); from Eq. (2.44) we see that the poles of $\langle\langle a; a^+, E\rangle\rangle$ occur at the characteristic energies. Defining the sum over all states s as the trace of G

$$\begin{aligned}-\pi^{-1}\operatorname*{Im}_{\epsilon\to 0}&[\operatorname{Tr}\langle\langle a_s; a_s^+, E\rangle\rangle]\\ &= -\pi^{-1}\operatorname{Im}[\sum_s (E - E_s + i\epsilon)^{-1}]\\ &= \sum_s \delta(E - E_s) = \rho(E).\end{aligned}\tag{2.55}$$

In the imperfect crystal the E_s are not known, but since Eq. (2.55) is a trace it may be evaluated in any representation. In particular, using the site representation for the trace $l = l'$

$$\rho(E) = -\pi^{-1}\operatorname*{Im}_{\epsilon\to 0}\sum_{\alpha,l}\langle\langle a_\alpha(l); a_\alpha^+(l), E\rangle\rangle.\tag{2.56}$$

For the phonon case the displacement Green's function G defined by Eq. (2.47) will not give the density of states directly whenever the mass varies from site to site. In the perfect lattice case the transformation (2.14) must be applied before a simple form like Eq. (2.51) is obtained. It is the "mass-weighted" displacement Green's function which gives the density of states in the general case, namely

$$\begin{aligned}\pi^{-1}\operatorname*{Im}_{\epsilon\to 0}&\{\operatorname{Tr}[M_\alpha(l)^{1/2}\langle\langle u_\alpha(l); u_{\alpha'}(l'), \omega + ie\rangle\rangle M_{\alpha'}(l')^{1/2}\omega]\}\\ &= \sum_s [\delta(\omega - \omega_s) + \delta(\omega + \omega_s)] = \rho(\omega) + \rho(-\omega).\end{aligned}\tag{2.57}$$

By writing Eq. (2.46) in matrix form we can also find that

$$i\omega\langle\langle p; u\rangle\rangle = 1 + \mathbf{\Phi}\mathsf{G}(\omega) = \mathsf{M}\omega^2(\mathsf{M}\omega^2 - \mathbf{\Phi})^{-1}.\tag{2.58}$$

Therefore, using Eq. (2.50), the trace of the Green's function $i\langle\langle p, u\rangle\rangle$ is the same as the mass-weighted G used in Eq. (2.57), and will give the density of states $\rho(\omega) = \rho(-\omega)$ in the harmonic oscillator case.

Similarly, the spin-wave density of states may be constructed from the trace of $G(l, l', E)$ defined from Eq. (2.53).

2. Thermal properties

The ordinary thermal properties of these systems involve correlation functions. The internal energy $\langle\mathcal{H}\rangle$ of the system described by Eq. (2.3) requires a knowledge of $\langle a_\alpha^+(l)a_{\alpha'}(l')\rangle$ which may be determined from $\langle\langle a_\alpha^+(l); a_{\alpha'}(l'), E\rangle\rangle$ using the prescription given in Eqs. (2.36) and (2.37). This Green's function is related to the G defined in Eq. (2.41) by Eq. (2.38). The average energy is therefore (with respect to the chemical potential μ)

$$\langle\mathcal{H}\rangle = \pi^{-1}\int dE\,\frac{(E-\mu)\operatorname{Im}[\operatorname{Tr}G(E)]}{\exp[(E-\mu)/k_BT] + 1},\tag{2.59a}$$

while specific heat is obtained by differentiating. Using the properties of the Fermi distribution, it is given approximately at low T by

$$C_v(T) = \tfrac{1}{3}\pi^2\rho(\mu)k_B{}^2T = \gamma T\tag{2.59b}$$

which is proportional to the density of states at the Fermi level. The paramagnetic Pauli spin susceptibility is also an important quantity in metals:

$$\chi = \mu_B{}^2\rho(\mu).\tag{2.59c}$$

In the vibrational case $\langle\mathcal{H}\rangle$ involves averages which can be obtained from $\langle\langle u, u\rangle\rangle$ and $\langle\langle p, p\rangle\rangle$. The latter is governed by an equation similar to Eq. (2.46),

$$\omega\langle\langle p; p\rangle\rangle = -i\mathbf{\Phi}\cdot\langle\langle u; p\rangle\rangle.\tag{2.60a}$$

Using Eqs. (2.58) and (2.38) this formula gives a formal matrix result

$$\mathsf{M}^{-1}\langle\langle p, p\rangle\rangle = \mathbf{\Phi}\cdot(\mathsf{M}\omega^2 - \mathbf{\Phi})^{-1}.\tag{2.60b}$$

Thus the mean kinetic energy which can be obtained from $\frac{1}{2}\langle\langle p, p\rangle\rangle\mathsf{M}^{-1}$ is the same as the mean potential energy from $\frac{1}{2}\mathbf{\Phi}\langle\langle u, u\rangle\rangle$ as expected from equipartition. Using Eqs. (2.36) and (2.37) and differentiating with respect to T gives the specific heat

$$\begin{aligned}C_v = \int_0^\infty &\frac{d\omega h\omega^3}{k_BT^2}\,\frac{\exp(\hbar\omega/k_BT)}{[\exp(\hbar\omega/k_BT) - 1]^2}\\ &\times\operatorname{Im}\{\operatorname{Tr}(\mathsf{M}\cdot\mathsf{G})\}.\end{aligned}\tag{2.60c}$$

The $\langle\langle u, u\rangle\rangle$ Green's function may also be used to calculate the mean-square atomic displacement as required in the Debye–Waller factor, and so on.

In the spin-wave problem, the simple decoupling procedure employed in Eq. (2.21) is only valid at $T = 0$ so the calculation of thermal averages from the Green's function are not straightforward. We shall confine our attention here to $T = 0$ K.

3. Neutron scattering

Inelastic neutron scattering experiments give the most detailed information about the spectra of phonons and magnons. Sjölander (1964) has given a detailed discussion of the interaction between phonons, and all sorts of radiation, while Lovesey and Marshall (1966, 1971) have reviewed the interaction between neutrons and condensed matter. We therefore give only the essential formulas here. The interaction between a nucleus at $\mathbf{x}_\alpha(l)$ and a neutron can be described by a Fermi pseudopotential,

$$\mathcal{H}_{\text{int}} = \sum_{\alpha l} \frac{2\pi\hbar^2}{m} b_\alpha(l)\delta[\mathbf{r} - \mathbf{x}_\alpha(l)], \tag{2.61}$$

where $b_\alpha(l)$ is the scattering length. It depends on the nuclear species and in general also on the nuclear spin.

If a neutron is scattered from state $\mathbf{k}$ to state $\mathbf{k}'$ with energy change

$$E = (\hbar^2/2M_n)(k^2 - k'^2), \tag{2.62}$$

and wave-vector change

$$\mathbf{q} = \mathbf{k} - \mathbf{k}' + \mathbf{Q}, \tag{2.63}$$

where $\mathbf{Q}$ is a reciprocal lattice vector, the differential cross section per unit energy range consists of two parts (Van Hove, 1954). The coherent cross section from the average of b over nuclear spin states b^c is

$$\begin{aligned}\frac{d^2\sigma^c}{d\Omega dE} = \frac{1}{2\pi\hbar}\frac{k'}{k}\sum_{\alpha l,\alpha' l'}\int dt \exp(iEt/\hbar) \\ \times \langle b_\alpha{}^c(l) \exp[i\mathbf{q}\cdot\mathbf{x}_\alpha(l,t)] \\ \times b_{\alpha'}{}^c(l') \exp[-i\mathbf{q}\cdot\mathbf{x}_{\alpha'}(l',0)]\rangle.\end{aligned} \tag{2.64}$$

It is therefore directly related to the frequency transform of a thermally averaged, time-dependent correlation function. In most solids the actual nuclear position is always close to the equilibrium position, and we can therefore write $\mathbf{x}$ in terms of the displacement $\mathbf{u}$ as

$$\mathbf{x}_\alpha(l) = \mathbf{R}_\alpha(l) + \mathbf{u}_\alpha(l). \tag{2.65}$$

Expanding the expression in Eq. (2.64) gives in the first nonvanishing order the $\langle u, u\rangle$ correlation. A more complete treatment shows that the effective scattering lengths should be modified by the Debye–Waller factor so that

$$\begin{aligned}\frac{d^2\sigma}{d\Omega dE} = \frac{1}{2\pi\hbar}\frac{k'}{k}\int dt \exp(iEt/\hbar) \\ \times \sum_{\alpha,\alpha',l,l'} B_\alpha(l)B_{\alpha'}(l') \\ \times \langle[\mathbf{q}\cdot\mathbf{u}_\alpha(l,t)][\mathbf{q}\cdot\mathbf{u}_{\alpha'}(l',0)]\rangle \\ \times \exp\{i\mathbf{q}\cdot[\mathbf{R}(l) - \mathbf{R}(l')]\},\end{aligned} \tag{2.66}$$

where for harmonic systems

$$B_\alpha(l) = b_\alpha{}^c(l) \exp\{-\tfrac{1}{2}\langle[\mathbf{q}\cdot\mathbf{u}_\alpha(l)]^2\rangle\}. \tag{2.67}$$

The incoherent cross section involves correlations only in the motion of individual atoms,

$$\begin{aligned}\frac{d^2\sigma^i}{d\Omega dE} = \frac{1}{2\pi\hbar}\frac{k'}{k}\int dt \exp(iEt/\hbar) \sum_{\alpha l}\beta_\alpha{}^2(l) \\ \times \langle[\mathbf{q}\cdot\mathbf{u}_\alpha(l,t)][\mathbf{q}\cdot\mathbf{u}_\alpha(l,0)]\rangle,\end{aligned} \tag{2.68}$$

where β contains the incoherent scattering length and the Debye–Waller factor as in Eq. (2.67).

The correlation functions in Eqs. (2.66) and (2.68) can be obtained from weighted sums of $G_{\alpha\alpha'}(l, l', E)$ defined by Eqs. (2.47) and (2.49). Using Eqs. (2.37b) and (2.66) one finds

$$\begin{aligned}\frac{d^2\sigma}{d\Omega dE} = \frac{1}{\pi}\frac{k'}{k}\sum_{\alpha\alpha',ll'} B_\alpha(l)B_{\alpha'}(l')n(E) \\ \times \operatorname{Im}\langle\langle\mathbf{q}\cdot\mathbf{u}_\alpha(l); \mathbf{q}\cdot\mathbf{u}_{\alpha'}(l'), E\rangle\rangle_R \\ \times \exp\{i\mathbf{q}\cdot[\mathbf{R}(l) - \mathbf{R}(l')]\},\end{aligned} \tag{2.69}$$

where

$$n(E) = [\exp(E/k_BT) - 1]^{-1} \tag{2.70}$$

is the usual Bose–Einstein factor. Thus if E is positive the cross section corresponds to phonon destruction and is proportional to the number of phonons present in equilibrium. G in Eq. (2.49) is an even function of E, so the contribution to $\operatorname{Im}G(-E)$ is opposite in sign. That is, there is a similar contribution at $(-E)$ corresponding to phonon creation proportional to

$$-n(-E) = [1 - \exp(-E/k_BT)]^{-1} = n(E) + 1. \tag{2.71}$$

In the perfect crystal the $B_\alpha(l)$ are the same in each cell and the $\mathbf{q}$ transform gives a cross section proportional to the Green's function (2.51). The imaginary part is then a delta function, $\delta[\omega^2 - \omega_j{}^2(\mathbf{q})]$, so that $\omega_j(\mathbf{q})$ can be determined directly. In the imperfect crystal, of course, $\mathbf{q}$ is not a good quantum number, and in principle the cross section will be continuous in frequency.

Neutron scattering can also be observed from spin waves. Here the cross section is

$$\begin{aligned}\frac{d^2\sigma}{d\Omega dE} = \frac{g^2}{2\pi\hbar}\frac{k'}{k}\sum_{l,l'}\exp\{i\mathbf{q}\cdot[\mathbf{R}(l) - \mathbf{R}(l')]\} \\ \times \int dt \exp(iEt/\hbar) \\ \times \langle S_+(l,t)S_-(l',0) + S_-(l,t)S_+(l',0)\rangle \\ \times f(l)f(l'),\end{aligned} \tag{2.72}$$

where $f(l)$ is the form factor of the magnetic moment distribution on atom l and $g = (1.9e^2/mc^2)$ is a scattering length which is a measure of the electron–neutron interaction. The correlation function involved is again directly related to a weighted sum of G's defined by Eq. (2.53).

4. *Optical properties—vibrational*

The predominant interaction between lattice vibrations and an electromagnetic field is of the electric dipole type:

$$\mathcal{H}_{\text{int}} = \sum_l e_\alpha(l)\mathbf{u}_\alpha(l)\cdot\boldsymbol{\varepsilon}\exp(i\omega t), \tag{2.73}$$

where $e_\alpha(l)$ is the effective charge of the (α, l) atom and is assumed to include the effects of atomic polarizability. In this model the polarization of the medium is

$$P = \langle \sum_{l} e_\alpha(l) u_\alpha(l) \rangle. \tag{2.74}$$

From Eq. (2.39) the polarizability is

$$\chi(\omega) = -\sum_{\alpha\alpha';\,ll'} e_\alpha(l) e_{\alpha'}(l') \langle\langle u_\alpha(l); u_{\alpha'}(l'), \omega\rangle\rangle_R. \tag{2.75}$$

The absorption coefficient for infrared radiation is

$$\mathcal{K} = 4\pi\omega\, \mathrm{Im}\chi(\omega)/c', \tag{2.76}$$

where c' is the velocity of light in the medium. As in the neutron scattering case it is simply related to a weighted sum over $\langle\langle u, u\rangle\rangle$; however, the wave vector of light is so small that only the $\mathbf{q} \simeq 0$ response is determined. In the perfect crystal where e_α is the same in each cell, Eq. (2.76) contains $\delta[\omega - \omega_j(0)]$ using Eq. (2.51).

Raman scattering by phonons is formally very similar to the neutron scattering problem except that the photons have $\mathbf{q} \simeq 0$. Defining an effective Raman polarizability for an (α, l) atom as $C_\alpha(l) u_\alpha(l)$, the Raman cross section is proportional to

$$\begin{aligned}\frac{d^2\sigma}{d\Omega dE} \propto \sum_{\alpha,l;\alpha,l'} & C_\alpha(l) C_{\alpha'}(l') n(E) \\ & \times \mathrm{Im}\langle\langle u_\alpha(l) \cdot u_{\alpha'}(l'), E\rangle\rangle_R.\end{aligned} \tag{2.77}$$

In general C depends on the direction of the photons and the polarization (Barker and Loudon, 1972).

5. *Transport properties*

The transport properties of the systems under consideration can also be written in the Green's function formalism. The Kubo (1957) formula for the electrical conductivity is

$$\begin{aligned}\sigma_{\mu\nu}(\omega) = \lim_{\eta\to 0^+} \frac{1}{V} \int_0^\infty & dt \exp(-i\omega t) \exp(-\eta t) \\ & \times \int_0^\beta d\lambda\, \langle J_\mu(0) J_\nu(t + i\hbar\lambda)\rangle,\end{aligned} \tag{2.78a}$$

where $\mathbf{J}$ is the charge current density operator and $\beta = (k_BT)^{-1}$. For the Hamiltonian (2.3), $\mathbf{J}$ takes the form

$$\begin{aligned}J_\mu &= ie/\hbar \sum_{l,l'} [\mathbf{R}(l) - \mathbf{R}(l')]_\mu W(l, l') a^+(l') a(l) \\ &= \sum_{l,l'} B(l, l')_\mu a^+(l') a(l).\end{aligned} \tag{2.78b}$$

For the thermal conductivity, the Kubo formula takes a similar form [see, for example, Mori *et al.* (1962)],

$$\begin{aligned}\kappa_{\mu\nu}(\omega) = \lim_{\eta\to 0^+} \frac{1}{VT} \int_0^\infty & dt \exp(-i\omega t) \exp(-\eta t) \\ & \times \int_0^\beta d\lambda\, \langle J_\mu^E(0) J_\nu^E(t + i\hbar\lambda)\rangle,\end{aligned} \tag{2.79a}$$

where in the phonon problem [see, for example, Flicker and Leath (1973)] the energy current density operator, using Eq. (2.10), is

$$\begin{aligned}J_\mu^E &= \tfrac{1}{2} \sum_{\nu,\gamma,l,l'} [\mathbf{R}(l) - \mathbf{R}(l')]_\mu \Phi_{\nu\gamma}(l, l') \\ &\quad \times u_\gamma(l') p_\nu(l)/M_\nu(l) \\ &= \sum_{\nu,\gamma,l,l'} A_\mu^{\nu\gamma}(l, l') u_\gamma(l') p_\nu(l)/M_\nu(l).\end{aligned} \tag{2.79b}$$

These correlation functions are related to two-particle Green's functions (2.37b) involving four a operators [or u and p operators). For the harmonic Hamiltonians we are using, such two-particle Green's functions can always be decoupled exactly into sums of products of two one-particle functions. This becomes clear if we assume that the transformation which diagonalizes G in Eq. (2.44) is known; then since these normal modes cannot interact with each other,

$$\begin{aligned}&\langle\langle a_s^+(t) a_{s'}(t); a_{s'}^+(0) a_s(0)\rangle\rangle \\ &\quad = \langle a_s^+(t) a_s(0)\rangle \langle\langle a_{s'}(t); a_{s'}^+(0)\rangle\rangle \\ &\qquad + \langle a_{s'}^+(0) a_{s'}(t)\rangle \langle\langle a_s^+(t); a_s(0)\rangle\rangle.\end{aligned} \tag{2.80}$$

Using this result and manipulating the formula (2.78) in the spectral representation to eliminate the integral over λ gives, for the dc electrical conductivity,

$$\begin{aligned}\sigma_{\mu\nu}(0) = \frac{2e^2}{\pi\hbar^2 V k_B T} \sum_{ll',nn'} & [\mathbf{R}(l) - \mathbf{R}(l')]_\nu W(l, l') \\ & \times [\mathbf{R}(n) - \mathbf{R}(n')]_\mu W(n, n') \\ & \times \int_{-\infty}^\infty \frac{d\epsilon \exp[(\epsilon - \mu)/k_BT]}{[\exp((\epsilon - \mu)/k_BT) + 1]^2} \\ & \times \mathrm{Im}G(l, n, \epsilon)\, \mathrm{Im}G(l', n', \epsilon).\end{aligned} \tag{2.81}$$

The ac electrical conductivity $\sigma(\omega)$ can be put in another form [see Velický and Levin (1970)] which is convenient for studying its high-frequency behavior,

$$\begin{aligned}\sigma_{\mu\nu}(\omega) = \frac{i}{\hbar\pi\omega V} \int_{-\infty}^\infty & \frac{d\epsilon}{\exp[(\epsilon - \mu)/k_BT] + 1} \\ & \times \mathrm{Tr}\{\mathrm{Im}\mathbf{G}(\epsilon - i\eta) e^2 (M^{-1})_{\mu\nu} \\ & + \mathbf{B}_\nu\, \mathrm{Im}\mathbf{G}(\epsilon - i\eta) \mathbf{B}_\mu \\ & \times [\mathbf{G}(\epsilon + \hbar\omega + i\eta) + \mathbf{G}(\epsilon - \hbar\omega - i\eta)]\},\end{aligned} \tag{2.82}$$

where (M^{-1}) is the effective mass tensor, which in k representation takes the form $\hbar^{-2}\partial^2\epsilon(k)/\partial k_\mu \partial k_\nu$. The high-frequency Drude behavior of this formula for metals has been discussed by Velický and Levin (1970).

In the case of phonons, the dc lattice thermal conductivity becomes [see, for example, Flicker and Leath (1973)]

$$\begin{aligned}K_{\mu\nu}(0) = \frac{-2\hbar^2}{\pi V k_B T} \int_{-\infty}^\infty & d\omega \frac{\omega^2 \exp(\hbar\omega/k_BT)}{[\exp(\hbar\omega/k_BT) - 1]^2} \\ & \times \mathrm{Tr}[\mathbf{A}_\mu\, \mathrm{Im}\mathbf{G}(\omega) \mathbf{A}_\nu \mathbf{G}(\omega)].\end{aligned} \tag{2.83}$$

6. *Optical Properties—electronic*

In addition to the dc conductivity, various experiments involving the interaction of light with metal and semiconductor alloys are also directly related to two-particle Green's functions. The interaction Hamiltonian between the electrons and the light has the form

$$\sum_{\alpha\beta;ll'} D_{\alpha\beta}(l,l')a_\alpha(l)a_\beta^+(l')\exp(i\omega t), \tag{2.84}$$

where $D_{\alpha\beta}(l,l')$ is the matrix element of $\mathbf{j}\cdot\mathbf{A}$ between Wannier functions of bands α and β, sites l and l'; $\mathbf{j}$ and $\mathbf{A}$ are the electron current and vector potential, respectively.

Transitions within a band are related to the conductivity described by Eq. (2.78); optical absorption involves interband transitions $\alpha\neq\beta$. The sum over all sites in Eq. (2.84) arises because the light waves have $\mathbf{k}\simeq 0$ and interact nearly in phase with all sites. In a perfect lattice where $\mathbf{D}$ will depend only on $\mathbf{R}(l)-\mathbf{R}(l')$ and not explicitly on l, Eq. (2.84) may be written

$$\sum_{\mathbf{k}}\sum_{\alpha\beta} D_{\alpha\beta}(\mathbf{k})a_\alpha(\mathbf{k})a_\beta^+(\mathbf{k})\exp(i\omega t), \tag{2.85}$$

and transitions conserve $\mathbf{k}$ values. In the imperfect case $\mathbf{D}(l,l')$ will depend on whether the sites are defects or not, and a weighted sum will develop as in the other properties discussed above. The polarizability, from which the other properties may be calculated, is given by an expression like (2.75). For a particular pair of bands

$$\begin{aligned}\chi_{\alpha\beta}(\omega) &= -2\pi\omega^2\sum_{ll';nn'} D_{\alpha\beta}(l,l')D_{\alpha\beta}(n,n')\\ &\quad\times\langle\langle a_\alpha(l)a_\beta^+(l');a_\alpha^+(n)a_\beta(n'),E\rangle\rangle_R.\end{aligned} \tag{2.86}$$

Using the relation (2.81), transformed to ω, gives

$$\begin{aligned}\chi_{\alpha\beta}(\omega) &= \omega^2\sum_{ll';nn'} D_{\alpha\beta}(l,l')D_{\alpha\beta}(n,n')\\ &\quad\times\int_0^\infty\frac{dE'}{\exp(E'/k_BT)+1}[\mathrm{Im}G_{\alpha\alpha}(l,n;E')\\ &\quad\times G_{\beta\beta}(l',n';E-E')-G_{\alpha\alpha}(l,n,E-E')\\ &\quad\times\mathrm{Im}G_{\beta\beta}(l',n',E')].\end{aligned} \tag{2.87}$$

The Fermi distribution function appears in order to ensure the occupation of one of the states involved in the transition. For a perfect crystal this reduces to

$$\chi_{\alpha\beta}(\omega) = \omega^2\sum_{\mathbf{k}}\frac{f(E_\alpha(k)(D_{\alpha\beta}(k))^2}{E+E_\alpha(\mathbf{k})-E_\beta(\mathbf{k})+iE}. \tag{2.88}$$

Several simplifications are commonly made in applying Eq. (2.88). One is to assume that the intraband matrix element D of Eq. (2.84) vanishes between sites [i.e., that $\mathbf{D}(l,l')=0$ unless $l=l'$]; this makes $D_{\alpha\beta}(\mathbf{k})=D_{\alpha\beta}$ independent of $\mathbf{k}$. The perfect lattice result is now proportional to the joint density of states of the two bands,

$$\chi_{\alpha\beta}''(\omega) = \omega^2\sum_{\mathbf{k}} f(E_\alpha(k))\delta[E+E_\alpha(\mathbf{k})-E_\beta(\mathbf{k})]D_{\alpha\beta}^2. \tag{2.89}$$

We may devise an approximate theory when impurities are present for the case when the α band is full and the β band empty. The unperturbed crystal has a joint band with energy

$$\begin{aligned}E(\mathbf{k}) &= E_\beta(\mathbf{k})-E_\alpha(\mathbf{k})\\ &= E(l)-\sum_{l'} W(l,l')\\ &\quad\times\exp\{i\mathbf{k}\cdot[\mathbf{R}(l)-\mathbf{R}(l')]\}\end{aligned} \tag{2.90}$$

and an appropriate $E(l)$ and $W(l,l')$ may be defined as in Eq. (2.3). If the perturbation V is different in each band we define

$$V(l) = V_{\alpha\alpha}(l)-V_{\beta\beta}(l). \tag{2.91}$$

Then if G is the Green's function for this new effective band,

$$\chi_{\alpha\beta}(\omega) = \omega^2 D_{\alpha\beta}(l)^2\sum_l G(l,l;E). \tag{2.92}$$

If one band is partly full it is difficult to use this approximation, since it is not possible to translate the Fermi function in one band in a simple manner. Finally we note the neglect of any correlation effects between the two G's which appear in Eq. (2.87) and all many-body and exciton effects in the above.

For the case of x-ray spectra where one of the bands α is a tightly bound band of inner shell electrons it is a good approximation to neglect the variation $E_\alpha(\mathbf{k})$. Then G in Eq. (2.92) is just that of the conduction band.

In photoelectric experiments (Spicer, 1972) the emission current depends not only on the absorption process but also on the probability of emission. It is commonly assumed, without much justification, that the $\mathbf{k}$ conservation breaks down. In that case the electrons are assumed to be excited and emitted at the same point in space so that $l=n$ in Eq. (2.87) and the emission probability is then

$$\begin{aligned}S_{\alpha\beta}(\omega) &\propto D^2\int_0^\infty dE'\,f(E')\,\mathrm{Im}G_{\alpha\alpha}(l,l;E')\\ &\quad\times\mathrm{Im}G_{\beta\beta}(l,l'E-E'),\end{aligned} \tag{2.93}$$

i.e., is proportional to the joint density of states $\int dE'\,\rho_\alpha(E')\rho_\beta(E-E')$.

D. Systems with few defects

1. *Standard manipulations*

The Green's functions which were defined in Sec. IIB were written in a shorthand matrix form as in Eqs. (2.43) and (2.50). If we know the properties of the perfect lattice as given by Eqs. (2.44) and (2.51) we may write the result for a general lattice in terms of the known result in the perfect case, denoted by P. Then G differs from P by the inclusion of an extra matrix V as defined in Eqs. (2.8) and (2.18). These quantities are related by the formal solution

$$\mathsf{G} = (1-\mathsf{PV})^{-1}\mathsf{P}. \tag{2.94}$$

This equation can be rearranged in various ways. For example,

$$\mathsf{G} = \mathsf{P} + \mathsf{PTP} \tag{2.95}$$

defines the T-matrix

$$\mathsf{T} = \mathsf{V}(1 - \mathsf{PV})^{-1}. \tag{2.96}$$

Alternatively, there is a Dyson equation,

$$\mathsf{G} = \mathsf{P} + \mathsf{PVG}. \tag{2.97}$$

Any of these expressions may be readily expanded so that

$$\mathsf{G} = \mathsf{P} + \mathsf{PVP} + \mathsf{PVPVP} + \cdots \tag{2.98}$$

giving a form of perturbation expansion about the perfect lattice. P represents the excitation propagating in the perfect crystal, V the scattering by the defects. Thus successive terms give the effect of multiple scattering. The various methods of approximate calculation of G correspond to summations over certain sets of terms in this perturbation expansion. Of course Eq. (2.98) is only meaningful if the series converges, which is usually not easily demonstrated.

2. *Single defects*

The problem of a lattice containing a single defect has been solved exactly in many instances where V is a matrix of limited size or range; experiments on crystals containing only a low concentration of such defects can be interpreted in terms of those results. An exhaustive review has been given by Maradudin (1966). We outline the solution for a single defect, since we may discuss the systems with a high defect concentration in terms of the single-defect results.

The simplest starting point is Eq. (2.95). The T-matrix (2.96) has the same small number of nonzero elements as V (these are a fraction of order N^{-2} of the whole, where N is the number of atoms). The excitation energies are given by the poles of G. These will generally be shifted from the poles of P by an amount of $O(N^{-1})$ [see, for example, Lifshitz (1956, 1964)], except that a few entirely new poles are possible from T. Such new states must be isolated in energy away from the bands of the perfect crystal, and represent localized states. Even though the band modes are modified by the presence of V to $O(1/N)$, this modification will be largely confined to the region of the crystal where V is nonzero, i.e., there will be large relative changes in the states in a region of the size $(1/N)$th of the crystal. These changes may be particularly large in certain narrow frequency ranges—an effect analagous to a resonance in scattering theory—when the frequency matches some characteristic frequency of the defect.

a. Single-site perturbations

These ideas can be clarified by considering a simple case. Suppose V contains only one diagonal element Δ at $l = 0$, in a single-band model. Then, from Eq. (2.96)

$$T(l, l') = \Delta/[1 - \Delta P(0)]\delta(l, 0)\delta(l, l') \tag{2.99}$$

which has poles whenever

$$1 - \Delta P(0) = 0 \tag{2.100}$$

is satisfied, where

$$\begin{aligned} P(0) &= P(l = 0, l' = 0; E) \\ &= N^{-1}\sum_{\mathbf{k}}[E - E(\mathbf{k})]^{-1}. \end{aligned} \tag{2.101}$$

FIG. 1. The diagrams occurring in the expansion (2.98) of $\mathbf{G}$ for the case of a crystal with a single defect.

This exact solution expressed in a diagrammatic notation corresponds to summing in G, the diagrams shown in Fig. (1) where the single horizontal line represents the perfect lattice propagator P and the dashed lines represent the scattering Δ by the impurity.

There is a local mode solution if Δ is very much larger than the bandwidth. For E well outside the band this reduces to

$$P(0) \simeq 1/[E - E_0], \tag{2.102}$$

and thus the condition (2.100) is satisfied when

$$E \simeq E_0 + \Delta. \tag{2.103}$$

In this case, the local mode is at the impurity-site energy. As Δ becomes comparable with the bandwidth we need the full solution of Eq. (2.99), and for small enough Δ no local mode will appear. The "excitation density" of the local mode at $l = 0$ may be assessed by using Eqs. (2.95) and (2.99) to give

$$\operatorname{Im}G(0, 0, E) = \pi\delta(E - E_L)[P(E_L)/(d/dE)\Delta P(E_L)] \tag{2.104}$$

(this is not a trace summed over l).

For E inside the band $P(0)$ has both a real and an imaginary part. If the density of states is $\rho_0(E)$, we can write the real and imaginary parts according to

$$P(0) = \mathcal{P}\int \frac{\rho_0(E')\,d(E')}{E - E'} + i\pi\rho_0(E) = P_R(0) + iP_I(0), \tag{2.105}$$

where $\mathcal{P}$ indicates the principal part of the integral. The value of $G(l = 0,\ l' = 0,\ E)$ is from Eqs. (2.95) and (2.99) just the scalar quantity

$$P(0)/[1 - \Delta P(0)]. \tag{2.106}$$

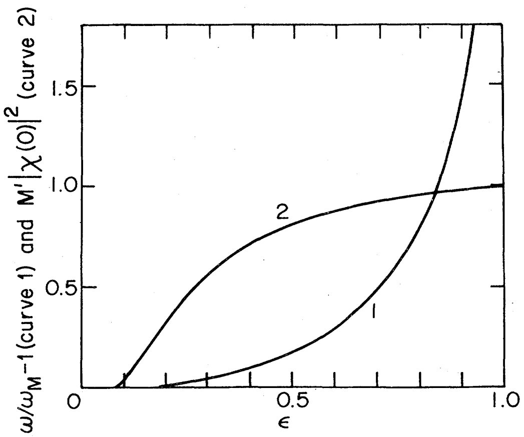

FIG. 2. The local mode frequency ($\omega_L/\omega_M - 1$) and fraction of the mode on the defect site $M'[\chi(0)]^2$, versus $\epsilon > 0$ for light masses in the three-dimensional Debye model [after Dawber and Elliott (1963)].

In particular

$$\mathrm{Im}G(0, 0, E) = \pi\rho_0(E)/\{[1 - \Delta\,\mathrm{Re}P(0)]^2 + [\Delta\pi\rho_0(E)]^2\}. \tag{2.107}$$

The response at the defect site is like that of the host lattice [the density of states $\rho_0(E)$] multiplied by the factor in the denominator. This may have a resonant form centered at the solution of

$$[1 - \Delta\,\mathrm{Re}\{P(0)\}] = 0, \tag{2.108}$$

with a width determined by $\mathrm{Im}P(0)$.

For a mass defect Eq. (2.16a) gives

$$\Delta = M\epsilon\omega^2. \tag{2.109}$$

In a cubic crystal with one atom per unit cell, symmetry gives the same result for each coordinate direction α. In this case

$$P(0) = \frac{1}{M}\left[\mathcal{P}\int_0^\infty \frac{d\omega'\,\rho_0(\omega')}{\omega^2 - \omega'^2} + \frac{i\pi}{2\omega}\rho_0(\omega)\right]. \tag{2.110}$$

A local mode will occur if the defect atom is sufficiently light, i.e., $\epsilon > 0$. Since $M(l)$ is always positive, we always have $\epsilon < 1$. For a heavy defect $\epsilon < 0$ there may be a resonance. These effects are demonstrated in Figs. 2 and 3, from the work of Dawber and Elliott (1963). Figure 2 shows the local mode frequency for a light mass in the Debye model together with the factor in Eq. (2.104) for $G(0)$ which determines the fraction of the local mode on the defect site. Figure 3 gives the factor in Eq. (2.107) for the same model, clearly showing resonance for $\epsilon < 0$ which shifts to lower frequencies and sharpens as the defect mass increases.

b. Two-site perturbations

If the perturbation involves two sites the algebra is slightly more complicated. The nonzero part of $\mathbf{V}$ is now a 2×2 matrix, as is $\mathbf{T}$. Specifying the sites by 1 and 2 we define

$$\mathsf{V} = \begin{pmatrix} \Delta(1) & \Lambda \\ \Lambda & \Delta(2) \end{pmatrix}. \tag{2.111}$$

The poles of $\mathbf{T}$, as given by Eq. (2.96), occur at the zeros of the determinant of $|\,1 - \mathsf{PV}\,|$, i.e., when

$$1 - [\Delta(1) + \Delta(2)]P(0) - 2\Lambda P(1, 2) + [\Delta(1)\Delta(2) - \Lambda^2][P(0)^2 - P(1, 2)^2] = 0. \tag{2.112}$$

This model allows the treatment of a number of cases. In particular it is a basic model problem in the treatment of crystals which have bond changes. For example, in the treatment of Blackman *et al.* (1971), electron energy bands are considered when the transfer integrals W of Eq. (2.3) are changed at random. This corresponds to putting

$$\Delta(1) = \Delta(2) = 0 \tag{2.113}$$

in Eq. (2.111). If a force constant is changed in the vibrational problem or an exchange coupling in the magnetic problem, then

$$\Delta(1) = \Delta(2) = -\Lambda \tag{2.114}$$

so that Eq. (2.112) becomes

$$1 - 2\Lambda[P(1, 2) - P(0)] = 0. \tag{2.115}$$

Changes in force constants (and exchange constants) are usually strongly correlated between the sites. For example, the introduction of a defect atom may change the interaction with all the neighbors, and these effects will interfere as discussed below.

Nevertheless this single bond change is sometimes used as a simple model.

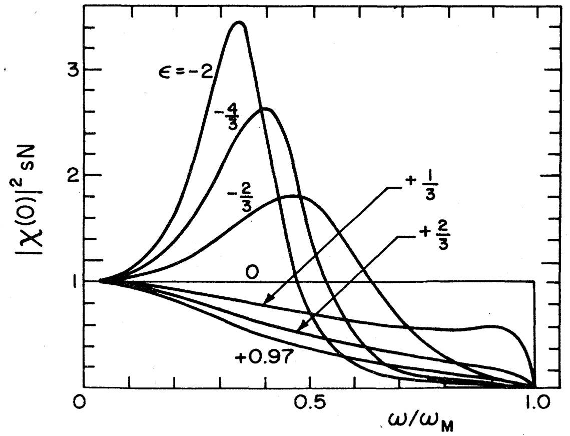

FIG. 3. The fraction of the mode of frequency ω on the heavy atom ($\epsilon < 0$) defect site versus ω/ω_M for the Debye model [after Dawber and Elliott (1963)].

c. Extended defects

We consider only one example of this, where a defect atom is coupled only to its nearest neighbors. A case discussed in some detail in the literature is that of a simple cubic Heisenberg ferromagnet (Wolfram and Callaway, 1963; Izyumov, 1966; subsequent work has been done by Walker, Chambers, Hone, and Callen (1972). Using Eq. (2.27) **V** becomes a 7 × 7 matrix arising from the defect and its six neighbors,

$$2JS\begin{pmatrix} \epsilon & -\gamma & -\gamma & -\gamma & -\gamma & -\gamma & -\gamma \\ -\gamma & \rho & 0 & 0 & 0 & 0 & 0 \\ -\gamma & 0 & \rho & 0 & 0 & 0 & 0 \\ -\gamma & 0 & 0 & \rho & 0 & 0 & 0 \\ -\gamma & 0 & 0 & 0 & \rho & 0 & 0 \\ -\gamma & 0 & 0 & 0 & 0 & \rho & 0 \\ -\gamma & 0 & 0 & 0 & 0 & 0 & \rho \end{pmatrix}, \qquad (2.116)$$

where

$$\epsilon = 6[(\mathbf{J}'/\mathbf{J}) - 1], \qquad \rho = (\mathbf{J}'S'/JS) - 1,$$

and

$$\gamma = [J'(S')^{1/2}/J(S)^{1/2}] - 1.$$

Because of the cubic symmetry **V** can be simplified by a transformation to symmetrized coordinates as discussed in Appendix C. For this simple cubic case the 7 × 7 reduces to one 2 × 2 matrix of Γ_1 (s-like) symmetry, three equal diagonal elements of Γ_5 (p-like) symmetry, and two of Γ_3 (d-like) symmetry. The matrix of $P(l, l')$ connecting sites of the cluster, and the T matrix also symmetrize in the same way. For the last two cases

$$t_i = 2JS\rho/(1 - 2JS\rho P_i), \qquad \text{for } i = p, d, \qquad (2.117)$$

where

$$P_p = P(0) - P(2\boldsymbol{\delta})$$

and

$$P_d = P(0) + P(2\boldsymbol{\delta}) - 2P(\boldsymbol{\delta} + \boldsymbol{\delta}').$$

Here $\boldsymbol{\delta}$, $\boldsymbol{\delta}'$ are the vectors to the nearest-neighbor sites $\boldsymbol{\delta} = a(1, 0, 0)$; $\boldsymbol{\delta}' = a(0, 1, 0)$, etc. For the s-like part

$$\mathbf{V}_s = 2JS\begin{pmatrix} \epsilon & -\gamma(6)^{1/2} \\ -\gamma(6)^{1/2} & \rho \end{pmatrix} \qquad (2.118)$$

$$\mathbf{P}_s = \begin{pmatrix} P(0) & 6^{1/2}P(\boldsymbol{\delta}) \\ 6^{1/2}P(\boldsymbol{\delta}) & P_s \end{pmatrix}, \qquad (2.119)$$

where $P_s = P(0) + P(2\boldsymbol{\delta}) + 4P(\delta + \delta')$. Thus the interference between the six changed bonds, symmetrically placed, gives a quite different t-matrix than that derived in Eq. (2.115) for single bond changes.

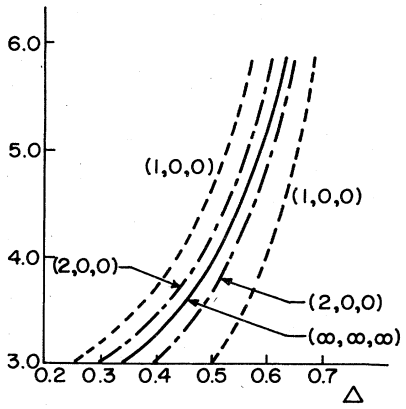

FIG. 4. The local mode frequencies for a pair (i, j) of light defects in a model simple-cubic crystal at separations $\mathbf{r}_{ij} = (1, 0, 0)$, $(2, 0, 0)$, and (∞, ∞, ∞) versus ϵ (Takeno, 1962).

The vibrational case for an extended defect is always more complicated because of the three degrees of freedom on each site. For example in this simple cubic case a 21 × 21 matrix results, although this too can be greatly simplified using the point symmetry. This situation has been considered in detail by a number of workers (e.g., Lakatos and Krumhansl, 1969; Yussouf and Mahanty, 1965, 1966, 1967), but since it has not been generalized to the case of many defects we shall not reproduce the results here.

The single impurity result is also of importance in the electronic case, as is discussed in Sec. IIIC2, where it is used to insure the correct dilute limit.

3. Defect pairs

Two defects with site-diagonal perturbations will interfere to produce changes in the single-defect modes. Two such defects can be described by Eq. (2.111) with $\Delta = 0$. The poles of Eq. (2.112) are shifted from the single-defect positions given by $1 - \Delta(1)P(0) = 0$. If the defects are identical they have two degenerate modes which are split as Eq. (2.112) becomes

$$1 - \Delta P(0) \pm \Delta P(1, 2) = 0, \qquad (2.120)$$

and the splitting depends on the size of $P(1, 2)$. Again for well localized modes the splitting will be small. A calculation of the pair modes frequencies for high-frequency phonons in a simple cubic crystal was made, for example, by Takeno (1962). The frequencies of the impurity modes are shown in Fig. 4 versus Δ for single defects and for pairs of defects that are separated by the vectors $a(1, 0, 0)$ and $a(2, 0, 0)$ in the crystal.

It is convenient to define here the two-defect **T**-matrix $\mathbf{T}^{(2)}$ in terms of the single-defect t-matrix.

$$t = \Delta/[1 - \Delta P(0)]. \qquad (2.121)$$

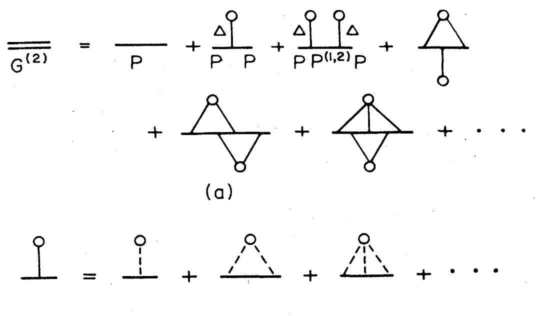

FIG. 5. (a) The diagrams occurring in the expansion (2.98) of **G** for the case of a crystal with two defects; (b) the scattering terms in the single-site t matrix (vertical solid line).

Manipulation of the 2×2 matrix in terms of Pauli spin matrices $\boldsymbol{\sigma}$ for convenience of representation gives:

$$\mathbf{T}^{(2)} = \Delta \mathbf{1}/[\mathbf{1} - \Delta \mathbf{P}^{(2)}]^{-1} = t\mathbf{1}/[\mathbf{1} - tP(i,j)\boldsymbol{\sigma}^x]^{-1}$$

$$= \frac{t}{[(1 - t^2P(i\cdot j)^2]}[\mathbf{1} + tP(i,j)\boldsymbol{\sigma}^x]. \qquad (2.122)$$

This calculation corresponds, in the diagrammatic notation defined above, to summing the diagrams corresponding to all scattering by the pair of defects as shown in Fig. 5(a), where the solid vertical line is the t-matrix for scattering by a single site as shown in Fig. 5(b).

E. General features of properties of disordered systems

For a crystal with many impurities the full solution of the problem clearly becomes intractable and approximations must be made. A formal solution involves a study of the T-matrix (2.96) for n defects. For a concentration c of defects in the crystal of N atoms this is a square matrix of dimension cN, involving many $P(l,l')$. Before proceeding to review the approximate methods currently in use we shall discuss a few general features of the system.

In the study of the single-defect problem it was shown that a single defect caused small modifications of most perfect crystal states, but introduced the possibility of isolated localized states. A pair of defects modifies the band states more, and, if the defects were of the type which give local states, two such states now appear on either side of that energy. The further addition of defects will continue this process of splitting impurity levels. Modification of the band will increase, and generally be particularly marked near resonances of the defects, which then produce the largest effects. The local modes for distant pairs and clusters will accumulate densely around the single-defect energy and give rise to an "impurity band." These features are seen prominently in computer studies.

While the total density of states is indicative of some properties, we recall that we often need suitably weighted densities of states. Transport properties on the other hand are given by two-particle Green's functions; here an essential question is whether the states involved can carry a current. These properties are related to the important question of state localization, as raised, for example, by Anderson (1958, 1970). This property is not reflected in the configuration-averaged density of states as Thouless (1970) has explicitly demonstrated. Recognizing that it is not the whole story, for the moment we consider what is known about the total density of states by way of exact results.

1. *Exact results*

The history of the theory of disordered systems has been singular in its dearth of exact solutions and precise general principles. Only highly idealized models have been solved exactly; nonetheless exact results on simple systems are invaluable, both in guiding physically motivated approximations and in disclosing unusual and unexpected features unique to disordered systems. An extensive review of numerical calculations has been given by Dean (1972), whose work, as mentioned in the introduction, complements ours.

The first exact analytical solution of the excitations of a disordered system was given by Dyson (1953), who considered a one-dimensional chain and found an integral equation for the density of states, for the case of a continuous distribution of masses and force constants. Unfortunately, the form of his result is such that it has not been of much practical use. Schmidt (1957) developed a method based on transfer matrices (limited to one dimension) and was able to derive results equivalent to Dyson's, but easier to apply; he also derived results for the spectrum of a two-component system, and Agacy (1964) solved the appropriate functional equation exactly. Dean (1960) had previously obtained machine calculations for this case in very good agreement with Agacy's results. Again in the two-component disordered chain, Borland (1964) showed that at certain special frequencies, and for a mass ratio greater than 2.0, it was possible to find the integrated density of states exactly, again in good agreement with computations by Dean.

One other aspect of the spectra of disordered systems, which is seen most strongly in one dimension and has been derived from the transfer-matrix technique, has recently been reviewed by Hori (1968). Given certain conditions, it may be shown that there are gaps in the spectrum; this was demonstrated exactly in one dimension. It is unlikely that this behavior is general in three dimensions, but it may appear in special models. In his review Hori discusses his work with Matsuda and Fukushima on higher-dimensional systems, but the phase operator, which is a simple concept along a chain (ordered or disordered), must now become a tensor (matrix), and manipulation and integration become quite unmanageable in general. One other result for chains was obtained by Rosenstock and McGill (1962), who show that eigenfrequencies and eigenfunctions may be ordered so that the Kth mode has precisely $K - 1$ nodes.

One property of the disordered alloy on which there are exact theorems is the bounding limits of the spectrum of disordered systems (Saxon and Hunter, 1949; Luttinger, 1951; Lifshitz, 1964; Taylor, 1966, 1967; Velicky, Kirkpatrick, and Ehrenreich, 1968; Thouless, 1970). The result is that in a two-component, randomly occupied, regular lattice the gap between bands (if it exists) and the upper and lower spectral limits are determined by the common gap and band regions, respectively, of the two limiting crystalline species. (The results are valid only in the "model sense" in that, taking the electronic structure of a disordered alloy as an example, charge transfer and change of basis functions are not accounted for—which surely is a simplification of what happens in a real disordered alloy.) The arguments given by Lifshitz, Thouless, and Taylor are not restricted to one dimension.

We now turn to another successful approach to "exact results," computer modeling. Since Dean (1972) has reviewed this aspect of the subject extensively, we need only present the main features. The earliest computer experiments concerned electronic spectra of one-dimensional random chains by Landauer and Helland (1954), and were followed by Lax and Phillips (1958) and Frisch and Lloyd (1960). These provided information about the spectra and wave functions; they supported the Saxon–Hunter theorem and stimulated subsequent work on "tail-states."

The kind of calculations begun by Dean in 1959, and carried out on a much larger scale since, exhibit clear indications of two important new features in the spectra and modes of disordered systems. Although done for lattice vibrations it should be clear from our discussion of model Hamiltonians in Sec. IIA above that the results may be applied to electronic spectra. The feature in question is seen by reference to Fig. 6 from the work of Dean (1960), and in three dimensions by Payton and Visscher (1967, 1968), as shown in Fig. 7. The important feature referred to is that the character of the spectral density in the region outside of the main host band is extremely irregular (spiked) in character. As the concentration of defects is increased, this behavior persists until a critical concentration is reached (which never really happens in one-dimensional systems), at which point the structure smooths out to a form very similar to the in-band structure. Wave functions going with the spiky spectrum are spatially localized, in contrast to the in-band modes which, though irregular in amplitude, extend through the crystal. When Dean first obtained his results it was thought that they were a result of statistical fluctuations due to finite lattice size; it has long since become clear that in fact he was the first to show "experimentally" that localization of states and jagged spectral character are a new and general feature of disordered systems, which at this writing have only very recently been approximately reproduced (see Sec. IIIC1) by formal analytical models or methods.

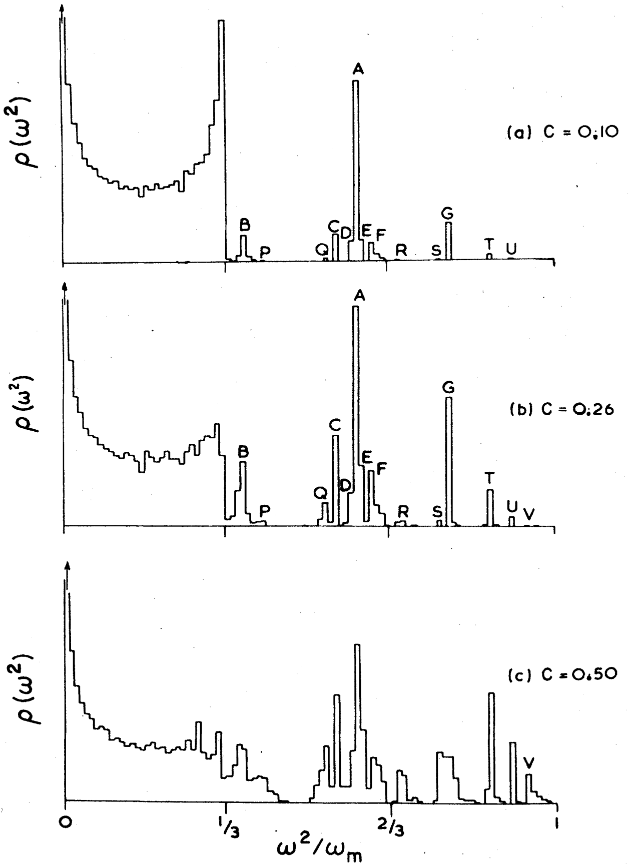

FIG. 6. The phonon density of states $\rho(\omega^2)$ versus $\omega^2/\omega_M{}^2$ for disordered linear chains of atoms of mass M_A and $M_B = M_A/3$ for concentrations c of B atoms of 10%, 26%, 50% [after Dean (1961)].

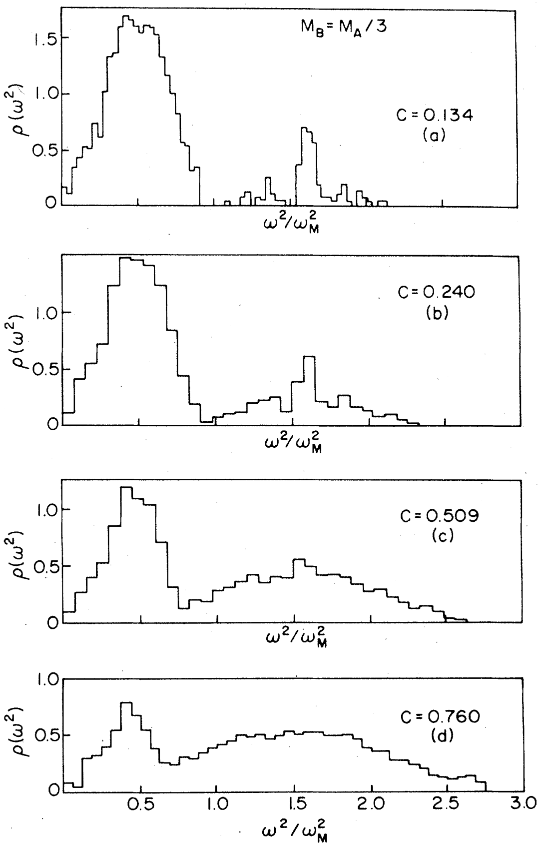

FIG. 7. The phonon density of states $\rho(\omega^2)$ versus $\omega^2/\omega_M{}^2$ for disordered simple cubic lattices of atoms of mass M_A and $M_B = M_A/3$ for concentrations c of B atoms of 13.4%, 24%, 50.9%, and 76% [after Payton and Visscher (1967)].

The computer calculations have, then, served as a basis for comparing formal approximate theories and experiment, as well as having been useful in pointing out the unique features of the exact results.

2. *Configuration averaging*

The experimental quantities discussed in Sec. IIC have an essential common feature—they all involve a sum over all sites in a macroscopic sample. For example, the neutron scattering cross section (2.69) is simply related to

$$\sum_{\boldsymbol{\delta}} \Big[\sum_{\boldsymbol{l}} G(\boldsymbol{l}, \boldsymbol{l}+\boldsymbol{\delta})\Big] \exp(i\mathbf{k}\cdot\boldsymbol{\delta}), \tag{2.123}$$

where we have written $\boldsymbol{l}$ for U(l) to condense the notation. The local property $G(\boldsymbol{l}, \boldsymbol{l}+\boldsymbol{\delta})$ will depend on the local conditions around $\boldsymbol{l}$ and $\boldsymbol{l}+\boldsymbol{\delta}$, which will differ from point to point across the crystal. But the sum will sample all possible local environments and hence is the same as that which would be calculated by fixing $\boldsymbol{l}$ and $\boldsymbol{\delta}$ but taking a configuration average over possible configurations of arbitrary but finite size. Lifshitz (1964) pointed out that such extensive properties involving a sum over all sites were effectively "self-averaging." In an actual scattering experiment this sample average is not quite as simple as a sum over all sites directly, but is more like a "Monte Carlo" evaluation of the sum, as the neutrons—or whatever the scattered particles may be—randomly sample different portions of the system.

Transport properties can be obtained by a configuration average of the two-particle Green's function. If the sample were too small, fluctuations due to different configurations would be important, since the sum over sites would not be large enough to ensure that representative configurations were present. The experimenter would see this as a random sample dependence of the measured quantity.

The local density of states is sometimes important for conceptual reasons even though inaccessible to most experiments; we define it at site $\boldsymbol{l}$ as

$$\rho(\boldsymbol{l}, E) = -2\,\mathrm{Im}\langle\langle a(\boldsymbol{l}); a^{+}(\boldsymbol{l}), E\rangle\rangle, \tag{2.124a}$$

so that $\rho(E)$ in Eq. (2.56) is

$$\rho(E) = N^{-1}\sum_{l} \rho(\boldsymbol{l}, E). \tag{2.124b}$$

We assumed above that such a quantity was local in that it depended only on the environment of $\boldsymbol{l}$. Butler and Kohn (1970) have recently discussed the question of how local such a quantity is in a weakly scattering disordered system.

They considered the effect of a small perturbation v, localized at point $\mathbf{r}'$, on the diagonal one-electron Green's function $G(\mathbf{r}, \mathbf{r}, E)$ at a general point $\mathbf{r}$. The quantity actually found was the configuration-averaged quantity

$$\begin{aligned}&\langle[\delta/\delta v(\mathbf{r}')]G(\mathbf{r}, \mathbf{r}; E+i\epsilon)\rangle\\ &\quad = \langle G(\mathbf{r}, \mathbf{r}'; E+i\epsilon)G(\mathbf{r}', \mathbf{r}; E+i\epsilon)\rangle_{v\to 0}.\end{aligned} \tag{2.125}$$

But for a system containing weak, random potentials the spatial behavior of the Green's function can be related to the mean free path $l(E)$,

$$\begin{aligned}&\langle G(\mathbf{r}, \mathbf{r}'; E+i\epsilon)\rangle_{v=0}\\ &\quad \sim \frac{1}{4\pi\,|\mathbf{r}-\mathbf{r}'|}\exp[i(E)^{1/2}\,|\mathbf{r}-\mathbf{r}'|]\\ &\quad \times \exp[-|\mathbf{r}-\mathbf{r}'|/2l(E)].\end{aligned} \tag{2.126a}$$

So, for weak scattering, from Eq. (2.126) it can be shown that

$$\begin{aligned}&|\langle[\delta/\delta v(\mathbf{r}')]G(\mathbf{r}, \mathbf{r}; E+i\epsilon)\rangle|\\ &\quad \sim \exp[-|\mathbf{r}-\mathbf{r}'|/l(E)].\end{aligned} \tag{2.126b}$$

Thus a scattering potential at $\mathbf{r}'$ has negligible effect on $G(\mathbf{r}, \mathbf{r}, E)$ and the local density of states at point $\mathbf{r}$, if $|r-r'| \gg l(E)$. A brief argument was also given to show that there was also a negligible effect if $|\mathbf{r}-\mathbf{r}'| \gg \Lambda_t$, where

$$\Lambda_t = \hbar/(2mk_BT)^{1/2} \tag{2.127}$$

is the thermal wavelength. In either case one can argue that the local density of states does not depend upon the configuration of atoms or defects outside of some radius ρ which must be much less than the size R of the experimental sample if the sample average is to be a configuration average. Although their argument strictly applied only in the weak scattering limit, equivalent arguments probably exist in the general case.

Even when all mean free paths are essentially infinite, the effects of atoms at very large distances should be unobservable; the arguments proceed like those made for neglecting surface effects on the bulk properties of crystals for any other than microcrystals. Any experiment measuring density of states has finite energy resolution, and this coarse graining wipes out the structure in energy spectra due to impurities at large distances. Matsuda (1964) discussed the problem for a harmonic linear chain with nearest-neighbor forces and arbitrary disorder; the method was strictly one-dimensional, using transfer matrices. Denoting the coarse graining due to experimental resolution by a width Γ, the final result was the rigorous inequality

$$\begin{aligned}|G(\mathbf{r}, \mathbf{r}'; E+i\Gamma)| &< (l_0/a)^{1/2}M\\ &\quad \times \exp(-|\mathbf{r}-\mathbf{r}'|/2\lambda_0),\end{aligned} \tag{2.128a}$$

where $\mathbf{a}$ is the spacing of atoms, and M is the lesser of $G(\mathbf{r}, \mathbf{r}, E+i\Gamma)$ and $G(\mathbf{r}', \mathbf{r}'; E+i\Gamma)$ while

$$\lambda_0 \le a\,\mathrm{Max}\{1+[\Phi(n, n-1)/\Gamma]^2\}, \tag{2.128b}$$

with $\mathrm{Max}\{X_n\}$ being the maximum element in the set $\{X_n\}$, for all sites n. But if there is some perturbation $V(n, n')$ the change in G is given by

$$\begin{aligned}\Delta G(l, l') &= G'(l, l') - G(l, l')\\ &= \sum_{n,n'} G(l, n)\Delta V(n, n')G'(n', l'),\end{aligned} \tag{2.129}$$

which follows immediately from the equations of motion. Clearly, for $\Delta V(n, n')$ to produce any significant change in $G(l, l')$, then n and n' must be within λ_0 of l and l', respectively. Thus a crystal of size $L \gg \lambda_0$ contains an ensemble of smaller crystals such that the sample average of the Green's function $G(l, l')$ is effectively the same as the configuration average. For an infinite crystal, $L \to \infty$ the configuration average is exact. To date no such theorem has been proven for higher-dimensional disordered systems. However, a theorem of this sort seems a likely conjecture (provided the interactions are of finite range), since it is true for translationally invariant systems, as follows easily by the usual arguments (Koster, 1954) by putting in a complex energy.

The above arguments, as stated, refer directly only to homogeneously disordered crystals, e.g., those with no concentration gradients. It there exists, say, a position-dependent concentration $c(r)$ of impurities, the sample average G could be found via an ensemble average providing this constraint were put into the theory. This can be done either directly in the expansion, where terms coming from the region of r_i will, on the average, be weighted with $c(r_i)$, or indirectly by Lagrange multiplier techniques. On the other hand, an experimentalist with data on a sample with a concentration gradient might want to compare his results to those predicted by the simple theories. The sample average can be related to the configuration-averaged $\langle G(c)\rangle$ at uniform concentration by

$$\langle \overline{\mathbf{G}} \rangle = V^{-1} \int_V d^3r\, \langle G[c(r)]\rangle, \tag{2.130}$$

where V is the volume of the sample, providing that the effective range λ_0, the mean free path $l(E)$, or the thermal wavelength Λ_t is small compared to the distance over which the concentration varies appreciably.

Finally, given that one desires to calculate $\langle G\rangle$, there are still computational problems remaining, as will be discussed below, in evaluating the individual terms in the expansion of $\langle G\rangle$ representing scattering by various order clusters of impurities. One is forced either to truncate the series somehow, or to perform a random-phase approximation which effectively treats terms involving large clusters of atoms as products of terms involving smaller clusters of atoms. The validity of these approximations is clearly related to the effective range λ_0, the mean free path $l(E)$, or the thermal wavelength Λ_t in that one makes negligible error in eliminating terms corresponding to clusters of atoms larger in size than λ_0, $l(E)$, or Λ_t.

3. Notation for average Green's functions

For a homogeneously random system the configurational average of $\mathbf{G}$, denoted by $\langle \mathbf{G}\rangle$, depends only on the relative position of the two sites,

$$\langle \mathbf{G}(\boldsymbol{\delta})\rangle = N^{-1}\sum_{l} \mathbf{G}(l, l+\boldsymbol{\delta}). \tag{2.131}$$

Hence $\langle \mathbf{G}\rangle$ has average translational symmetry like $\mathbf{P}$, and its Fourier transform is

$$\langle \mathbf{G}(\mathbf{k})\rangle = N^{-1}\sum_{\boldsymbol{\delta}} \langle \mathbf{G}(\boldsymbol{\delta})\rangle \exp(i\mathbf{k}\cdot\boldsymbol{\delta}). \tag{2.132}$$

By suitably collecting terms and averaging Eq. (2.98) we may write

$$\langle \mathbf{G}\rangle = \mathbf{P} + \mathbf{P}\boldsymbol{\Sigma}\langle \mathbf{G}\rangle, \tag{2.133}$$

where $\boldsymbol{\Sigma}$ may be called the self-energy. Using Eq. (2.44) for $\mathbf{P}$,

$$\langle G(\mathbf{k})\rangle = [E - E(\mathbf{k}) - \Sigma(\mathbf{k}, E)]^{-1}. \tag{2.134}$$

In general Σ depends on $\mathbf{k}$ and E, but in some approximations, particularly those arising from impurities with site-diagonal perturbations, the dependence on $\mathbf{k}$ may be negligible.

We may also obtain forms for certain useful conditionally averaged Green's functions from the self-energy matrix $\boldsymbol{\Sigma}$. Thus in the equation of motion of the Green's function, Eq. (2.97), the $G(i,j)$ on the right-hand side is preceded by a V_i and hence contributes only to the sum if its first index i is a defect site. Defining a conditional Green's function $G^d(l,l')$ which equals $G(l,l')$ if l is a defect site, and vanishes otherwise, we can rewrite Eq. (2.97) to obtain

$$\mathbf{G} = \mathbf{P} + V\mathbf{P}\mathbf{G}^d, \tag{2.135}$$

where V is now simply a number, and the restriction that $\mathbf{V}$ only contribute at defect sites has been transferred to $\mathbf{G}^d$. Comparing this with the Dyson equation for $\langle \mathbf{G}\rangle$ (2.133) and averaging over configurations of atoms gives the exact relationship

$$\langle \mathbf{G}^d\rangle = V^{-1}\boldsymbol{\Sigma}\langle \mathbf{G}\rangle. \tag{2.136}$$

For $G^h(i,j)$, which has a host site i as its first index,

$$\langle \mathbf{G}^h\rangle = \langle \mathbf{G}\rangle - \langle \mathbf{G}^d\rangle = (1 - V^{-1}\boldsymbol{\Sigma})\langle \mathbf{G}\rangle, \tag{2.137}$$

since each site must be either a host or defect site. A similar relation can be written for a double-conditional Green's function $G^{dd}(i,j)$ which equals $G(i,j)$ if both sites i and j are defect sites, and is zero otherwise. The relation for G^{dd}, obtained by iterating Eq. (2.97) just once, keeping G in the interior, is

$$\mathbf{G} = \mathbf{P} + \mathbf{PVP} + \mathbf{PVGVP}, \tag{2.138}$$

or

$$\mathbf{G} = \mathbf{P} + \mathbf{PVP} + V^2\mathbf{P}\mathbf{G}^{dd}\mathbf{P}, \tag{2.139}$$

which gives

$$\langle \mathbf{G}^{dd}\rangle = V^{-2}\boldsymbol{\Sigma}\langle G\rangle\boldsymbol{\Sigma} + V^{-2}(\boldsymbol{\Sigma} - cV\mathbf{1}), \tag{2.140}$$

$$\begin{aligned}\langle \mathbf{G}^{dh}\rangle &= \langle \mathbf{G}^d\rangle - \langle \mathbf{G}^{dd}\rangle\\ &= -(V^{-1}\boldsymbol{\Sigma} - \mathbf{1})\langle \mathbf{G}\rangle\boldsymbol{\Sigma}V^{-1} - V^{-2}(\boldsymbol{\Sigma} - cV\mathbf{1}),\end{aligned} \tag{2.141}$$

$$\begin{aligned}\langle \mathbf{G}^{hh}\rangle &= \langle G^h\rangle - \langle G^{hd}\rangle\\ &= (V^{-1}\boldsymbol{\Sigma} - \mathbf{1})\langle \mathbf{G}\rangle(V^{-1}\boldsymbol{\Sigma} - \mathbf{1}) + V^{-2}(\boldsymbol{\Sigma} - cV\mathbf{1}).\end{aligned} \tag{2.142}$$

These functions are the conditional averages of G suitably weighted, e.g., $-G^{hh}$ is weighted by $(1-c)^2$, G^{hd} by $c(1-c)$, G^d by c, etc. When $i = j$ on the diagonal, these Green's functions must satisfy special consistency relations

$$G^{hd}(l,l) = G^{dh}(l,l) = 0 \tag{2.143}$$

since site l cannot be both host and defect. Also, clearly,

$$G^d(l,l) = G^{dd}(l,l) \tag{2.144a}$$

and

$$G^h(l,l) = G^{hh}(l,l). \tag{2.144b}$$

Still another kind of averaging appears in the transport coefficients in a random alloy, which can most generally be calculated by means of a Kubo formula (2.78). This requires calculation of the two-particle Green's function (Velicky, 1969; Leath, 1970; Brouers and Vedyayev, 1972). For our case of a one-particle Hamiltonian (quadratic in annihilation and creation operators) the two-particle Green's function factors simplify into the product

$$G^{(2)}(l,m;n,p) = G(l,n)G(m,p), \tag{2.145}$$

or

$$\mathsf{G}^{(2)} = \mathsf{G} * \mathsf{G}. \tag{2.146}$$

The configuration-averaged two-particle Green's function, however, is the average of the product $\langle \mathsf{G} * \mathsf{G} \rangle$ and not the product of the averages $\langle \mathsf{G} \rangle \langle \mathsf{G} \rangle$, and this introduces diagrammatically irreducible four-point vertex parts.

We proceed first to iterate the average of Eq. (2.145) in powers of V to obtain

$$\langle \mathsf{G} * \mathsf{G} \rangle = \mathsf{P} * \mathsf{P} + \mathsf{P}\langle \mathsf{V} \rangle \mathsf{P} * \mathsf{P} + \mathsf{P} * \mathsf{P}\langle \mathsf{V} \rangle \mathsf{P} + \mathsf{P}\langle \mathsf{VP} * \mathsf{PV} \rangle \mathsf{P} + \cdots. \tag{2.147}$$

As is discussed, for example, by Leath (1970), there are self-energy corrections to the G on the left and on the right and also irreducible vertex parts which connect the two G's. The sum of all irreducible vertex parts, the four-point vertex function $\mathbf{\Lambda}$, can be related to $\langle \mathsf{G}^{(2)} \rangle$ by a Bethe–Salpeter equation,

$$\langle \mathsf{G}^{(2)} \rangle = \langle \mathsf{G} \rangle * \langle \mathsf{G} \rangle + [\langle \mathsf{G} \rangle * \langle \mathsf{G} \rangle]\mathbf{\Lambda}\langle \mathsf{G}^{(2)} \rangle. \tag{2.148}$$

In order to satisfy the usual conservation laws in self-consistent field calculations there is a Ward identity which relates the vertex function $\mathbf{\Lambda}$ to the self-energy. A simple derivation of this result follows from the work of Baym (1962), as discussed by Leath (1970). This formula is

$$\Lambda(lm,np) = \frac{\delta\Sigma(l,n)}{\delta\langle G(m,p)\rangle} = \frac{\delta\Sigma(m,p)}{\delta\langle G(l,n)\rangle}, \tag{2.149}$$

which, for the case of a site-diagonal self-energy gives the completely diagonal result

$$\Lambda = \delta\Sigma/\delta\langle G(0)\rangle. \tag{2.150}$$

So the second equality in Eq. (2.149) is trivially satisfied. This will not be the case when Σ is nonlocal by the inclusion of pair or cluster scattering, or when the defect is extended, and in these cases one must also be sure that Σ can be obtained from a certain sum of free energy diagrams as described by Baym (1962), in order for both equalities in Eq. (2.149) to be satisfied.

4. Localization

Although the averaged single-particle Green's functions give information about densities of states, they do not contain information about the localization or current carrying properties of the states [see, for example, Thouless (1970)]. In order to learn about the degree of localization one must study either averaged two-particle Green's functions (which give mean square single-particle properties) or the probability distribution of the single-particle properties (Anderson, 1958). There seems now to be general agreement on which quantities measure localization and, in particular, that the average single-particle properties do not measure localization, although this has not always been agreed upon [see Lloyd (1969), Ziman (1969), Brouers (1970)]. Thouless (1972b) has listed six criteria, some of which are equivalent, for localization of eigenstate s.

(1) Vanishing of the imaginary part of the locator self-energy, except on a set of measure zero (Anderson's criterion, see below).

(2) A vanishing dc conductivity (for a static lattice) and an ac conductivity of order ω^2 (Halperin, 1967; Mott, 1967).

(3) A finite value of $\int |\psi_s(r)|^4 d^3r$ (Thouless, 1970).

(4) A discrete (but dense) spectral density $\int |\psi_s(r)|^2 \delta(E - E_s)\, dE$, for any point r.

(5) A finite value of $\int |r - R_s|^2 |\psi_s(r)|^2 d^3r$, for some value of $\mathbf{R}_s$.

(6) The energy levels are shifted by an amount of order $\exp(-N^{1/3})$ rather than of order N^{-1}, upon a general change of boundary conditions, for a sample of N atoms (Edwards and Thouless, 1972).

In the case of a single defect (Sec. IID2) certain states may be localized if the scattering strength Δ is sufficiently large compared to the host bandwidth W. Are there localized states, however, when there is a finite concentration of such defects? The answer is not trivially obvious, and there has been a good deal of controversy on this issue in the past, although there now seems to be general agreement that in three dimensions either localized or extended states can exist, depending upon the ratio Δ/W. The details of just what values of Δ/W and at just what energies there are localized states has been a matter for considerable discussion.

In random one-dimensional lattices all states are localized in this sense (Borland, 1963; Mott, 1968; Hirota, 1973), and the resistivity increases exponentially with the number of impurities (Erdos, 1965; Landauer, 1970).

The question of localization was first raised by Anderson (1958) with regard to spin diffusion in random crystals. It is beyond the scope of this work to discuss localization to any great extent, since the subject is still rapidly developing. For enlightening commentary on the points raised here the reader is referred to Thouless (1970) or the book by Mott and Davis (1971).

We note briefly that Anderson (1958) studied the Green's function in the locator expansion [as named by Ziman (1969)], where the Green's function is written

$$G(l,l,E) = [E - E(l) - \Delta(l,E)]^{-1}, \tag{2.151}$$

where $E(l)$ is the single-site energy in Eq. (2.3), and where

$\Delta(l, E)$ is the (complex) single-site self-energy. The single-particle correlation function (not averaged over configurations),

$$\langle a(l, t)\, a^{+}(l, 0) \rangle_{T} \propto \operatorname{Im} \int \frac{dE \exp(-iEt/\hbar)}{[\exp(E/k_{B}T) + \eta][E - E(l) - \Delta(l, E)]}, \tag{2.152}$$

gives, as $t \rightarrow \infty$, information about localization. If Δ is real the correlation function simply oscillates, but if Δ is complex it damps out with time. Thus $\Delta(l, E + i\eta)$'s reality is a condition [condition (1), above] for localization. The averaging over configurations throws out the crucial phase information in Δ, so Anderson considered instead the most probable Δ. His technique was to examine convergence of the expansion for real Δ. Anderson found that the critical value of Δ/W for localization is five or ten times larger than a recent crude argument (Herbert and Jones, 1971; Economou and Cohen, 1972; Economou *et al.*, 1970, 1971, 1972) would suggest. He showed that the Lth order term in the perturbation series contained a number of paths of order K^{L} (where K is a number somewhat less than the coordination number z). A crude estimate of this order of magnitude for a typical term of order K^{L} in the expansion gives

$$(KW)^{L}(2e/\Delta)^{L-1}, \tag{2.153}$$

so that the crude estimate (Herbert and Jones, 1971; Economou and Cohen, 1972) would give convergence, and hence localization, for

$$\Delta/W > 2eK. \tag{2.154}$$

Anderson, however, assumed statistical independence of the K^{L} terms and showed that the probability distribution function had a sufficiently long tail that the sum of the K^{L} terms was dominated by the largest term, which effectively put a factor $\ln(\Delta/W)$ on the right side of (2.154), thereby increasing the critical value of Δ/W by a factor of 5 to 10. Herbert and Jones, and Economou and Cohen, on the other hand, argued that statistical independence was impossible and that very strong correlation was more likely, so that the crude estimate was better. There is still doubt as to the correct value, although recent numerical studies on two-dimensional systems (Khor and Smith, 1959; and Edwards and Thouless, 1972) seem to be in better agreement with the crude estimate, which gives localization more easily.

Economou and Cohen (1972) have developed an approximate theory of the critical energies E_{c} which divide the localized from the conducting states. They define a localization function $L(E)$ such that $L(E) \gtrless 1$ indicates extended (localized) states at E and $L(E_{c}) = 1$. This function, like Δ, is determined by approximate summation of a series. They find

$$L(E) \sim W \exp[-\langle \log | E - E_{c} | \rangle], \tag{2.155}$$

where the average is over the probability distribution of the $E(l)$. They further show that under the condition that the disorder leads to a site-diagonal self-energy $\Sigma(E)$ in the configuration average of G in Eq. (2.134), the condition $L(E_{c}) = 1$ can be replaced by the simple condition

$$f(E) = \tfrac{1}{2}W/[E - \Sigma(E)] = 1, \tag{2.156a}$$

when E is measured from the center of the unperturbed band. For the phonon problem the equivalent function is given in terms of W^{2}

$$f(\omega^{2}) = \omega^{2}/[\omega^{2} - \Sigma(\omega^{2})], \tag{2.156b}$$

where W^{2} is the bandwidth in ω^{2}.

These results are capable of a simple physical interpretation—in the perfect lattice limit they lead to extended states in the band and localized states outside, and in the general case give the same criterion in terms of the renormalized energy in the effective medium, $E - \Sigma(E)$.

Subsequently Bishop (1973) examined this criterion using the best available form for $\Sigma(E)$ obtained from the coherent potential approximation (see Sec. IIIA2) and found that it gave a very reasonable description with localized states in the band tails and extended states in the center of the band. In the case of severe disorder all the states became localized. More recently Abou-Chacra *et al.* (1973, 1974) have developed a self-consistent localization criterion which is exact on a Cayley tree. This gives qualitatively similar behavior to Bishop's evaluation of the Economou–Cohen criterion but it is different in some important respects. The differences are large for the Lloyd model (see Appendix B) where the distribution of $E(l)$ is Lorentzian. For a rectangular distribution of $E(l)$ of half-width Γ the results are fairly similar; the localization edge E_{c} lies fairly close to the band edge of $\Gamma < 1.5W$ (approx.) but then moves rapidly towards the band center to give completely localized states of $\Gamma > 2W$ (approx.).

The "Economou–Cohen localization criterion" as given in Eqs. (2.156) is clearly a way of estimating whether localization exists from the averaged one-particle Green's function. However, from the discussion of Thouless (1972) there would seem to be no such criterion. The answer must be that Eq. (2.156) is not a *criterion* or *condition* for localization in the same sense that, say, the vanishing of the conductivity is, but that it is an *estimate* of whether localization is likely. Often, in other contexts, similar estimation methods are used. For example, a neutron scatterer could see whether a particular phonon or magnon peak position ω_{k}, in his inelastic data, was roughly independent of k as would be expected for a localized state.

The existence of a definite mobility edge E_{c} where the states change character was only conjectured by Mott (1970) and by Cohen, Fritzche, and Ovshinsky (1969) on the basis of Anderson's ideas [see also Thouless (1972b)]. The physical properties associated with these edges are still under discussion. Edwards and Thouless (1972) have shown that the average density of states is analytic across such an edge. Mott (1972) has argued that the conductivity should drop abruptly to zero at the mobility edge, essentially because the mean free path can be no less than an interatomic spacing. On the other hand, Thouless (1972) feels that the many-body aspects of the problem can, through the phase of the wave function, conspire to produce a conductivity which is even lower than one would get if the mean free path were an interatomic distance. He sees, perhaps, something more like the conductivity in a classical percolation problem, which vanishes at the critical percolation but not abruptly. We have not intended that this topic, being outside the main scope of our paper, should be covered extensively here; we suggest that the reader consult the references for a complete discussion.

III. METHODS OF APPROXIMATION FOR $\langle \mathbf{G} \rangle$

A. Single-site approximations for $\langle \mathbf{G} \rangle$—formal methods

The perturbation expansion of the configuration-averaged Green's function is obtained formally by averaging, term by term, the expansion (2.98), which gives

$$\begin{aligned}\langle G(l,l')\rangle &= P(l,l') + \sum_m P(l,m)\langle V(m)\rangle P(m,l')\\ &\quad + \sum_{m,n} P(l,m)\langle V(m)P(m,n)V(n)\rangle\\ &\quad \times P(n,l) + \cdots,\end{aligned} \tag{3.1}$$

where, again, $\langle \cdots \rangle$ denotes the ensemble or configuration average. Unless otherwise specified we now consider the case of random occupancy of a structurally well-defined lattice. The unperturbed propagators P can be removed from the average since they are independent of the location of impurities, leaving only an average product $\langle V(1)V(2)\cdots V(n)\rangle$ in each term. This average product in a homogeneously disordered sample (no concentration gradients, as will be assumed throughout this paper) will depend, in general, upon the distances between the sites $1, 2, \cdots n$. For statistically independent site occupation probabilities the value of the product depends only upon whether some of the defect sites $1, 2, \cdots, n$ coincide. The problem that arises in evaluating Eq. (3.1) is not one of evaluating any particular term, but a kinematic one of keeping track of the sites connected by the propagators associated with $\langle V(1)V(2)\cdots V(n)\rangle$, and with then summing the resulting series. Let us consider first the case of very small perturbations, $V(m) \ll 1$, for all m. In this case, one might try viewing Eq. (3.1) as a series expansion in powers of V which could be truncated after some finite number of terms. For example, for extremely small $V(m)$, one might write

$$\begin{aligned}\langle G(l,l';E)\rangle &\cong P(l,l';E) + \sum_m P(l,m;E)\\ &\quad \times \langle V(m)\rangle P(m,l';E) + \cdots\\ &= P(l,l';E) + \langle V\rangle \sum_m P(l,m;E)\\ &\quad \times P(m,l';E) + \cdots,\end{aligned} \tag{3.2}$$

where $\langle V\rangle = \langle V(m)\rangle$ is independent of site m. The first term $P(l,l';E)$ is finite for three-dimensional systems but has discontinuous slopes at the unperturbed band edges and van Hove critical points, but the second term varies like

$$\sum_m P(l,m;E)P(m,l';E) \sim \sum_{\mathbf{k}} \frac{f(\mathbf{k};l,l')}{(E-E_{\mathbf{k}})^2}, \tag{3.3}$$

which diverges at the critical points. [For a discussion of such divergences, see Lifshitz (1956) and Lifshitz and Stepanova (1956).] The higher powers in V which were truncated in Eq. (3.2) diverge even more strongly, so that the perturbation expansion for the density of states seriously fails to converge near the band edges and critical points, and any truncation procedure will be plagued by this divergence. A common resolution of this difficulty is to approximately decouple, thus renormalizing away the divergence. After such a rearrangement the series can hopefully be rewritten in the form of a Dyson equation (2.133), and the self-energy Σ should now be free of divergences. In the following we review calculations of Σ in various approximation schemes.

For small perturbations V, one can simply decouple by a random phase approximation

$$\langle V(1)V(2)\cdots V(n)\rangle \cong \langle V(1)\rangle\langle V(2)\rangle\cdots\langle V(n)\rangle, \tag{3.4}$$

which in a random alloy neglects the coincidences of the sites $1, 2, \cdots, n$.

This approximation gives

$$\begin{aligned}\langle \mathbf{G}(E)\rangle &= \mathbf{P}(E)[\mathbf{1} - \langle V\rangle \mathbf{P}(E)]^{-1}\\ &= [E\mathbf{1} - \mathbf{H}_0 - \mathbf{1}\langle V\rangle]^{-1}.\end{aligned} \tag{3.5}$$

The Green's function looks like that for a perfect crystal with a simple shift $\langle V\rangle$. This approximation has become known as the virtual crystal approximation (VCA) which, since it is convergent at the band edges and is exact for small V, has been fairly successful in those cases of small perturbation (the rigid band limit) where the perturbed wave functions are quite extended in space so that each particle sees nearly the average perturbation (Nordheim, 1931; Muto, 1938; Parmenter, 1955). The virtual crystal approximation forms the crudest interpolation formula over the entire concentration range by simply scaling the position of the energy bands linearly with the concentration of each species.

In terms of the self-energy Σ, the virtual crystal approximation represents the lowest-order contribution,

$$\Sigma_V = \langle V\rangle. \tag{3.6}$$

If a fraction c of the sites are occupied by impurity atoms with potential Δ, then

$$\Sigma = c\Delta. \tag{3.7}$$

Since this approximation to Σ is real, the lifetime of the $\mathbf{k}$ states is infinite; and since it is independent of $\mathbf{k}$, $\mathbf{\Sigma}$ is a diagonal, local matrix. Some numerical results of calculations within the virtual crystal approximation are discussed in Sec. IV.

1. T *Matrix decoupling schemes*

When a few $V(m)$ are large, however, localized states can appear and the virtual crystal approximation must fail. $V(m)$ must be renormalized by summing more terms properly. If the concentrations of one species, say, B is low enough and V_B is large, one can sum the Born series at each site to obtain individual t-matrices. If the concentration of B atoms is small enough, the intersite scattering by clusters can be ignored as improbable. The single-site t-matrix method was developed by Watson (1956, 1957), J. Korringa (1958), Beeby and Edwards (1963), and Beeby (1964a, b), and extended by Aiyer *et al.* (1969). One re-sums directly from Eq. (3.1) by collecting together those terms involving repeated scattering by the same site, to obtain

$$\begin{aligned}\langle G(l,l')\rangle &= P(l,l') + \sum_m P(l,m)\langle t(m)\rangle P(m,l') \\ &\quad + \sum_{m,n}{}' P(l,m)\langle t(m)P(m,n)t(n)\rangle P(n,l') \\ &\quad + \sum_{m,n,p}{}' P(l,m)\langle t(m)P(m,n)t(n)P(n,p)t(p)\rangle \\ &\quad \times P(p,l') + \cdots, \end{aligned} \tag{3.8}$$

where the prime on the sum means that further successive scatterings at the same site are restricted, although return may occur after any intermediate scattering at other sites. Here $t(m)$ has the value defined in Eq. (2.99), where $\Delta = V_A - V_B$. Again, in calculating $\langle G\rangle$ and Σ we may not simply truncate Eq. (3.8) after the second term, due to the divergence at the band edges and critical points. Occasionally truncation at the first term is used when thermodynamic quantities or other integrals of $\langle G(\epsilon)\rangle$ over energy are desired which are not so sensitive to the details at critical points, i.e., the so-called isolated impurity approximation.

To assist in the evaluation of this decoupling scheme, we formally rewrite Eq. (3.8) in matrix notation

$$\langle \mathsf{G}\rangle = \mathsf{P} + \mathsf{P}\langle \mathsf{t}\rangle\mathsf{P} + \mathsf{P}\langle \mathsf{tP't}\rangle\mathsf{P} + \mathsf{P}\langle \mathsf{tP'tP't}\rangle\mathsf{P} + \cdots, \tag{3.9}$$

where

$$P'(n,m) = P(n,m) - P(0)\delta_{nm}, \tag{3.10}$$

where

$$t_{nm} = t(n)\eta(n)\delta_{nm}, \tag{3.11}$$

and $\eta(n) = 1(0)$ on B(A)-atom sites. The internal propagator P' has zero diagonal element in order to remove the restriction on the sums in Eq. (3.8). We then decouple here, as above, by a random phase approximation,

$$\langle t(1)t(2)\cdots t(n)\rangle \cong \langle t(1)\rangle\langle t(2)\rangle\cdots\langle t(n)\rangle, \tag{3.12}$$

which, in this case of a random alloy, is a better approximation than the decoupling in Eq. (3.2) because adjacent sites are restricted from coinciding. Thus we find the single-site decoupling approximation

$$\mathsf{G}^1 = \mathsf{P} + \mathsf{P}[\langle t\rangle(1 - \mathsf{P}'\langle t\rangle)^{-1}]\mathsf{P}. \tag{3.13}$$

This shows that $\langle t\rangle(1 - \mathsf{P}'\langle t\rangle)^{-1}$ is the approximation for the T-matrix of the system [Eq. (2.95)]. Thus the self-energy which is related to T by

$$\mathbf{\Sigma} = \mathsf{T}(1 + \mathsf{PT})^{-1} \tag{3.14}$$

becomes

$$\Sigma^{(1)} = \langle t\rangle/[1 + \langle t\rangle P(0)], \tag{3.15}$$

where $P(0)$ is the host-lattice Green's function. Using $\langle t\rangle = ct$ with Eq. (2.99), we write this in the form

$$\Sigma^1 = c\Delta/[1 - (1-c)\Delta P(0)]. \tag{3.16}$$

This single-site self-energy, first derived by Elliott and Taylor (1967), has also become known as the average t-matrix approximation (ATA), although the more common usage of ATA uses the virtual crystal propagator for P. This self-energy is local and complex, and has a pole near to the pole of t which gives the single-impurity state energy. Thus, from the form of the Green's function

$$G^1(E) = [E - H_0 - \Sigma^1(E)]^{-1}, \tag{3.17}$$

we see that the energy levels are shifted by an amount $\mathrm{Re}\{\Sigma^1(E)\}$ and broadened by a width $\mathrm{Im}\{\Sigma^1(E)\}$, which can be large near the impurity state energies. As Eq. (3.16) stands, with the $P(0)$ as the A-atom lattice Green's function, this formula and the resulting Green's function is not symmetric in the A- and B-atom types as was the virtual crystal approximation, and so cannot be used as an interpolation formula. Symmetry can be easily restored, however, by letting the unperturbed propagator P in Eq. (3.1) become that for the virtual crystal G_v. Then the perturbation is no longer $V(m)$ in Eq. (3.1) but $\phi(m) = V(m) - \langle V\rangle$ so that Eq. (3.15) becomes simply

$$\Sigma^1 = \langle t\rangle/[1 + G_v(0)\langle t\rangle], \tag{3.18}$$

where

$$\langle t\rangle = \frac{(1-c)(V_A - \langle V\rangle)}{1 - (V_A - \langle V\rangle)G_v(0)} + \frac{c(V_B - \langle V\rangle)}{1 - (V_B - \langle V\rangle)G_v(0)}. \tag{3.19}$$

This formula is now symmetric in A- and B-atom types and provides a useful interpolation formula (Leath and Goodman, 1969) over the entire concentration range except at the unperturbed band edges and at special frequencies corresponding to pairs and higher clusters. It is the commonly used form of the average t-matrix approximation (ATA). Detailed numerical results on Eqs. (3.16) and (3.19) are discussed in Secs. IIIB and IV. They are rederived using diagram techniques in Sec. IIIA3. The above decoupling procedure can also be used after further rearrangement of Eq. (3.1) to treat pairs and higher clusters of impurities (Sec. IIIC1).

2. The self-consistent field of coherent potential method (CPA)

The first attempt to do the single-site scattering problem with a self-consistent field was by Davies and Langer (1963) and Klauder (1961), who simply substituted the full Green's function $\langle G\rangle$ as the internal propagator in the single-site t matrix of Eq. (2.99). Their formula was thus

$$\Sigma_{\mathrm{DL}}{}^{1} = c\Delta/[1 - \Delta G(0)]. \tag{3.20}$$

The absence of $(1 - c)$ factor in the denominator as compared to Eq. (3.16) does not make a qualitative difference. Davies and Langer were able to solve this equation analytically for the Dyson equation (2.33) of an isotopically disordered, linear chain of atoms with nearest-neighbor forces. In the case when high-frequency localized states were present, the result was an extremely broad and structureless impurity band, which extended beyond the rigorously known upper bounds on the frequency spectrum. On the other hand, the host band edge moved slightly to lower frequency as states were pulled into the impurity band, as one would expect physically. Nevertheless, the numerical results were clearly unphysical, and quite unlike the high-frequency structure of Dean's calculations. These numerical results are discussed again below in Sec. IIIB.

An enormously improved result emerged from the essentially simultaneous calculations of Taylor (1967), who called the method "self-consistent," and of Soven (1967), who called the method "the coherent potential method" in the phonon and electron problems, respectively. They introduced a method based on multiple-scattering theory [see Lax (1951)], and also made use of the physical ideas expressed by Anderson and McMillan (1967). A recent review of the coherent potential method has been given by Yonezawa and Morigaki (1973). In this method one views the impurities as imbedded in an effective medium whose propagator $\mathbf{G}_0$ has a self-energy adjusted so that the t matrix for scattering off of a single impurity in this medium is zero on the average.

Specifically, one assumes an effective medium Green's function $\mathbf{G}_0$,

$$\mathbf{G}_0 = \mathbf{P} + \mathbf{P}\boldsymbol{\Sigma}\mathbf{G}_0. \tag{3.21}$$

However, the true Green's function $\mathbf{G}$ must satisfy its Dyson equation (2.97). Solving Eq. (3.21) for $\mathbf{P}$ and substituting into Eq. (2.97) eliminates $\mathbf{P}$ and gives the modified Dyson equation

$$\mathbf{G} = \mathbf{G}_0 + \mathbf{G}_0(\mathbf{V} - \boldsymbol{\Sigma})\mathbf{G}. \tag{3.22a}$$

The scattering perturbation now takes on the value $(\Delta - \Sigma)$ at impurity states and $(-\Sigma)$ at host sites. Now one finds the average single-site t-matrix, with internal propagator $G_0(0)$ instead of $P(0)$ and requires that it be zero:

$$\langle t\rangle = \frac{(1-c)(-\Sigma)}{1+\Sigma G_0(0)} + \frac{c(\Delta-\Sigma)}{1-(\Delta-\Sigma)G_0(0)} = 0. \tag{3.22b}$$

Multiplying through the equation by $[1 - (\Delta - \Sigma)G_0(0)]$ and collecting terms, one finds the implicit equation

$$\Sigma = c\Delta/\{1 - (1-c)\Delta G_0(0)/[1+\Sigma G_0(0)]\}, \tag{3.23}$$

which can also be written

$$\Sigma = c\Delta/[1 - (\Delta - \Sigma)G_0(0)]. \tag{3.24}$$

The physical reasoning here follows closely that of Anderson and McMillan (1967). If we could calculate explicitly the average $\mathbf{T}$-matrix $\langle\mathbf{T}\rangle$ for the entire scattering by all the sites in the medium we must get zero or

$$\langle\mathbf{T}\rangle\text{medium} = \mathbf{O} \tag{3.25}$$

since the medium is to represent the true system. However, we do not know how to calculate the entire T-matrix for the system, so that we approximate here by setting $\langle t(i)\rangle = 0$ in Eq. (3.22b), knowing full well that the scattering we are neglecting is that by pairs and higher clusters.

This formula, derived by Taylor and by Soven, has been rederived by a great variety of quite different techniques (Onodera and Toyozawa, 1968; Leath, 1968; Yonezawa, 1968; and Aiyer *et al.*, 1969). Several illuminating calculations of the effects of this approximation have been made by Velicky *et al.* (1968). Calculations as such are discussed in Sec. IIIB.

One of the most interesting and useful points about the coherent potential approximation (CPA) is its invariance with respect to the choice of host lattice and its correct limiting value in the perfect crystal and split band (or atomic) limits. That the CPA is invariant with respect to interchange of host A and impurity B was pointed out by Taylor (1967). This invariance extends even beyond his original argument. Let us consider for a moment the perturbation expansion about any medium (translationally invariant) with propagator $\mathbf{P}_M$ with energy $\mathbf{P}_M$ on each site. Then the Dyson equation for this expression is

$$\mathbf{G}_0 = \mathbf{P}_M + \mathbf{P}_M\boldsymbol{\Sigma}_M\mathbf{G}_0. \tag{3.26}$$

The perturbations now will be $(V_i - V_M)$ instead of $\Delta = (V_i - V_A)$ as above, and the Dyson equation (3.26) relating Σ_M to G_0 gives the relationship $\Sigma_M = \Sigma - (V_M - V_A)$ as the relationship between this new self-energy and that above. The CPA equation, analogous to Eq. (3.22) for the self-energy in this medium, will be

$$\langle t\rangle = \frac{(1-c)[(V_A - V_M) - \Sigma_M]}{1 - [(V_A - V_M) - \Sigma_M]G_0(0)} + \frac{c[(V_B - V_M) - \Sigma_M]}{1 - [(V_B - V_M) - \Sigma_M]G_0(0)} = 0. \tag{3.27}$$

Upon making the substitution $\Sigma_M = \Sigma - (V_M - V_A)$, we find this is exactly Eq. (3.22b), so that $G_0(0)$ is invariant with respect to the choice of unperturbed lattice, or to the value of V_M. This invariance means, in particular, that the coherent potential approximation is exact at either limit of the concentration, so it is useful as an interpolation formula. Furthermore, it means that the CPA can be considered as an expansion about the virtual crystal [since one could choose $V_M = \langle V(j)\rangle$] and thus that it is at least as good as the virtual crystal approximation at all concentrations. A comparison of virtual crystal, ATA, and CPA has been made by Schwartz, Brouers, Vedyayev, and Ehrenreich (1971).

Secondly, the CPA is exact in the atomic or split-band limit when the interatomic hopping is very weak. In fact it was this property which led to the CPA in the calculation of Onodera and Toyozawa (1968) in the excitonic problem [see also Kirkpatrick, Velicky, and Ehrenreich (1970)]. They began with the virtual crystal approximation $V_M = \langle V\rangle$, and looked for the diagonal self-energy $\Sigma(\omega)$ which gave the correct atomic limit. Their result was

$$\Sigma_{OT}(E) = \frac{c(1-c)\Delta^2 G(0)/[1+\Sigma_{OT}(E)G(0)]}{1-(1-2c)\Delta G(0)/[1+\Sigma_{OT}(E)G(0)]}. \tag{3.28}$$

Since $\Sigma_{OT}(E)$ is generally related to the self-energy Σ of the expansion about the A lattice by the formula

$$\Sigma_{OT}(E) = \Sigma - (\langle V\rangle - V_A) = \Sigma - c\Delta, \tag{3.29}$$

one sees immediately that Eq. (3.28) is indeed the same as the CPA equation (3.23).

Furthermore, the CPA always yields a properly analytic Green's function (Müller-Hartmann, 1973).

Finally, comparing the CPA self-energy (3.24) with the self-consistent calculation (3.20) of Davies and Langer (1963), it becomes apparent that the difference arises because CPA substitutes $(\Delta - \Sigma)G$ for ΔG in the single-site t-matrix. But, by Eq. (2.137) we see that

$$(\mathbf{V} - \mathbf{\Sigma})G = \mathbf{V}\mathbf{G}^h, \tag{3.30}$$

so that the CPA substitutes $\mathbf{G}^h$ rather than the full $\mathbf{G}$ into these scatterings. The difference between these propagators is that $G^h(i,j)$ has a host site as its first index. Therefore the diagonal element $G^h(0)$ has no scattering off of the explicit site of the t-matrix into which it is inserted. That is, between scattering off of site i, in t_i, one inserts self-consistently all scatterings off of the rest of the medium *excluding the site i* (which would constitute a double counting). The numerical difference between the two approaches is substantial.

3. *Diagram techniques*

Since the introduction by Edwards, in 1958, of diagrammatic notation for classifying and collecting the terms in the perturbation expansion of the electronic properties of liquid metals and alloys, many authors have extensively used such diagrams to help study many of the properties of disordered systems, and they have been useful in seeing physically what sort of scatterings are important. A large impetus to the use of this method was given by Langer (1960, 1961a, b), who developed a many-body theory for impurity resistance in metals and first applied the technique to the vibrational properties of a disordered lattice. Langer's technique correctly finds the coefficients of a series expansion of $\langle G\rangle$ in powers of c by making an Ursell–Mayer type cluster expansion. In this theory Langer recognized that a polynomial cumulant coefficient $P_n(c)$ was associated with each diagram part, and evaluated the linear c and quadratic c^2 terms in $P_n(c)$. Parallel diagrammatic formalisms were developed independently at about the same time by Klauder (1961) and by Matsubara and Toyozawa (1961). This early formalism was extended and completed for the lattice vibrational problem by Leath and Goodman (1966, 1968), who found a closed form for $P_n(c)$, and by Yonezawa and Matsubara (1966, 1967, 1968), who found a generating function for $P_n(c)$. These authors, however, discovered a serious lack of convergence of the expansion at special energies, extending to infinity, where spurious poles cropped up in the self-energy due to an overcorrection inherent in partial summations which used cluster expansions, as is discussed in Appendix A.

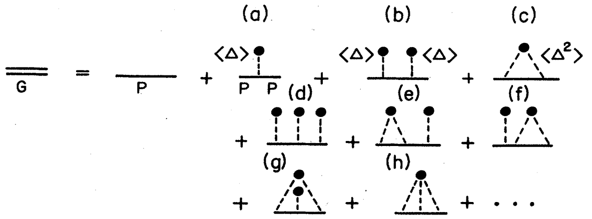

FIG. 8. The diagrams appearing in the expansion (3.32) of $\langle G\rangle$.

Meanwhile, the formula found by Elliott and Taylor (1967) for the single-site self-energy, which by inspection of the diagrams was accurate to all orders in concentration, eliminated the overcorrection inherent in the cluster expansion, and thus was free of the spurious poles. Recently Aiyer *et al.* (1969), corrected by Nickel and Krumhansl (1971) and Leath (1972), have found a self-consistent method for extending this kind of multiple-occupancy correction to arbitrary classes of diagrams.

We shall use this method to obtain the CPA equations as a self-consistent scattering problem, but shall begin our description by a rederivation of the formulas obtained by the t-matrix decoupling schemes of the previous section. For the binary alloy with the A-atom host lattice, the perturbation $V(m)$ as in Eq. (2.99) is Δ at defect sites and zero at host sites, which is expressed formally by

$$V_i = V\eta(i), \tag{3.31}$$

where η an indicator function is 0 (or 1) at A (or B) sites, respectively, so that Eq. (3.1) can be rewritten as

$$\begin{aligned}\langle G(l,l')\rangle &= P(l,l') + \Delta\sum_m P(l,m)\langle\eta(m)\rangle P(m,l')\\ &\quad + \Delta^2\sum_{m,n} P(l,m)\langle\eta(m)P(m,n)\eta(n)\rangle\\ &\quad \times P(n,l') + \cdots.\end{aligned} \tag{3.32}$$

We represent this equation diagrammatically in Fig. 8, where $\langle \mathbf{G}\rangle$ is represented by a double horizontal line. The diagram rules for a single defect were given in Sec. IID2; now each interaction point is weighted by the concentration c, its probability of being a defect site.

The *bare* contribution of each diagram is given by the product of its irreducible parts (any part of a diagram which

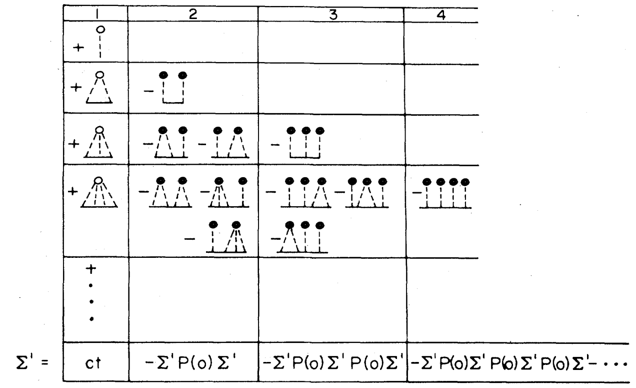

FIG. 9. The self-energy diagrams and multiple-occupancy corrections appearing in the single-site approximation (ATA). The first column contains the bare single-site diagrams which sum to ct, the higher nth column contains those multiple-occupancy correction diagrams with n irreducible parts whose sum is given at the bottom of the column.

cannot be severed into two bits by cutting a single, internal **P** line). The full contribution of each irreducible part is obtained by subtracting from the *bare* contribution the *full* contribution of each diagram that can be obtained by breaking lines away from the interaction points in the irreducible part, *providing that the resulting diagram is one found explicitly elsewhere in the partial summation one is performing.* [See Aiyer *et al.* (1969).] Finally, the diagrams are summed over all internal-site indices and summed to obtain $\langle \mathbf{G} \rangle$.

As an example of this kind of rearrangement we consider the Δ^2 term in the perturbation series (3.32) which is proportioned to $\langle \eta_{(i)}\eta_{(j)} \rangle$. For a random binary alloy, we have

$$\langle \eta_{(i)}\eta_{(j)} \rangle = c^2 + (c - c^2)\delta_{ij}. \tag{3.33}$$

The c^2 term gives the diagram in Fig. 8b; the second term, proportional to δ_{ij}, gives the diagram in Fig. 8(c). The $(c - c^2)$ factor in the latter term comes from the bare contribution c minus that from the diagram with the interaction lines broken apart [Fig. 8(b)]. This expansion differs from the usual cluster expansions only by the inclusion of the phrase underlined above which, though obviously empty if all diagrams are summed, makes considerable difference for the usual partial summations.

Fortunately, as is well known in principle, we can reduce the diagram summing problem to one of including only irreducible parts to obtain the self-energy $\mathbf{\Sigma}$ which is related to $\langle \mathbf{G} \rangle$ by the Dyson equation (2.133). The simplest irreducible part is Fig. 8(a), which gives

$$\Sigma_v = c\Delta = \langle V \rangle, \tag{3.34}$$

the virtual crystal approximation of Eq. (3.6). It is the lowest-order contribution in Δ, as might have been expected.

The terms linear in c can be summed to find the single-site t-matrix approximation; these bare diagrams are shown in the first column of Fig. 9. They add to the single-particle t-matrix simply related to that in Eq. (2.99). A sum of these gives the bare self-energy

$$\Sigma_{\text{bare}}{}^1 = ct = c\Delta/[1 - \Delta P(0)]. \tag{3.35}$$

The multiple-occupancy corrections are shown in the second and higher columns. The corrections in the nth column $(n \geq 2)$ can be summed vertically, since each such correction diagram has n irreducible parts, to obtain

$$-\Sigma^1[P(0)\Sigma^1]^{n-1}, \tag{3.36}$$

since the full contribution of these diagrams must be included. Thus Σ^1, the full, single-site self-energy, given by the sum of all the columns, is

$$\Sigma^1 = ct - \Sigma^1 P(0)\Sigma^1 - \Sigma^1 P(0)\Sigma^1 P(0)\Sigma^1 - \cdots, \tag{3.37}$$

a self-consistent relation for Σ^1, with the trivial solution

$$\Sigma^1 = ct/[1 + ctP(0)] = c\Delta/[1 - (1 - c)\Delta P(0)], \tag{3.38}$$

which agrees with that previously derived by the algebraic decoupling procedure in Eq. (3.16) above. The expression (3.38), first derived diagrammatically by Elliott and Taylor (1967), differs from that derived earlier by Langer (1961b) by the factor $(1 - c)$ in the denominator. Langer's formula was that for $\Sigma_{\text{bare}}{}^1$ of Eq. (3.35), which represents the uncorrected linear c contribution to Σ^1. Clearly the two formulas agree for small enough concentration. The differences are mainly three: first, exact sum rules for integrated optical absorption coefficients and neutron scattering in the phonon problem are obeyed precisely by the corrected formula (Elliott and Taylor, 1967), but are satisfied only to lowest order in concentration using the uncorrected version; second, when an impurity band is predicted the uncorrected version does not place it symmetrically about the local state energy as expected; third, the $(1 - c)$ tends to cut out the resonant denominator in Eq. (3.38) as concentration increases, so that the theory tends to the virtual crystal approximation as concentration increases, rather than keeping the impurity band.

Clearly, this single-site t-matrix approximation (or average t-matrix approximation) can also be made using an arbitrary unperturbed host lattice (with diagonal energies E_M on each site). This diagrammatic procedure leads immediately to the obvious generalization of Eq. (3.38):

$$\Sigma^1 = \langle t \rangle/[1 + P_M(0)\langle t \rangle], \tag{3.39}$$

where $P_M(0)$ is the effective host lattice propagator, and $\langle t \rangle$ is the average single-site t-matrix. If the host lattice is chosen to be the virtual crystal, i.e., $E_M = \langle V \rangle$, and $P_M(0) = G_r(0)$, then Eq. (3.30) gives the same result as that of Leath and Goodman (1969), as expressed in Eqs. (3.18) and (3.19) above, which is the ATA and is symmetric with respect to A and B atoms and constitutes an interpolation formula over the concentration range.

Next, the coherent potential approximation is obtained by summing the same single-site diagrams but with the full Green's function $\langle \mathbf{G} \rangle$ inserted self-consistently into the internal lines (Leath, 1968). These diagrams, looked at in terms of the unperturbed propagator **P**, correspond to all nested, single-site diagrams, i.e., between basic scatterings of off a single site the propagator is scattered off all other sites and in these scatterings the same propagator is inserted.

An example of a double-nested diagram is shown in Fig. 10. The sum of all the diagrams in the self-energy, shown in the first column of Fig. 11, is just

$$c\tau = c\Delta/[1 - \Delta G(0)], \tag{3.40}$$

which is the self-energy [Eq. (3.20)] of Davies and Langer. These bare diagrams are easily corrected for multiple counting using the technique of Aiyer *et al.* (1969) by subtracting those diagrams in the second and higher columns of Fig. 11 (Leath, 1968). The result for the second column is

$$-\{\Sigma[\gamma] - \Sigma[\langle G(0)\rangle]\}, \tag{3.41}$$

where Σ is treated as a functional of its internal propagator, and

$$\gamma = \langle G(0)\rangle/[1 - \Sigma[\gamma]\langle G(0)\rangle]. \tag{3.42}$$

The third and higher columns are similarly evaluated to obtain for the sum of all columns, and hence for Σ,

$$\Sigma[\langle G(0)\rangle] = c\tau + \Sigma[\langle G(0)\rangle] - \frac{\Sigma[\gamma]}{1 - \Sigma[\gamma]\langle G(0)\rangle},$$

which has the immediate solution

$$\Sigma[\gamma] = \frac{c\tau}{1 + c\tau\langle G(0)\rangle} = \frac{c\Delta}{1 - (1-c)\Delta\langle G(0)\rangle}$$

$$= \frac{c\Delta}{1 - (1-c)\Delta\gamma/[1 + \gamma\Sigma[\gamma]]}. \tag{3.44}$$

But since we want $\Sigma[\langle G(0)\rangle]$, we make the substitution

$$\gamma \to \langle G(0)\rangle \tag{3.45}$$

to obtain

$$\Sigma = \frac{c\Delta}{1 - (1-c)\Delta\langle G(0)\rangle/[1 + \Sigma\langle G(0)\rangle]}, \tag{3.46}$$

which is precisely the coherent potential approximation of Eq. (3.23).

To summarize this section, it has been found possible by diagrammatic techniques to obtain all results otherwise found from intuitive or decoupling approximations—thereby exhibiting just what the nature of the approximation is.

4. *The locator expansion*

A quite different, but as it turns out (for the CPA) equivalent, approach for the configurationally averaged Green's function was developed by Matsubara and Toyozawa (1961). Their use of this expansion seems obviously inspired by the earlier work of Anderson (1958). The formalism has been extended by Matsubara and Kaneyoshi (1966) and more recently by Leath (1970) and Matsubara (1970). The technique is to start with localized atomic states (Einstein oscillators) and expand in powers of the interatomic hopping $\mathbf{W}$, the second term of the Hamiltonian (2.3). It was hoped that by starting with purely localized states and then turning on the interatomic hopping, it might be possible to study the Anderson transition to conducting states. This approach begins by rewriting the equation of motion (2.43) [or the equivalents in the phonon or spin-wave problems, Eqs. (2.50) or (2.54)] in the form

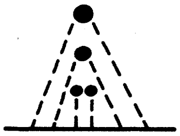

FIG. 10. An example of a double-nested diagram included in the coherent potential approximation.

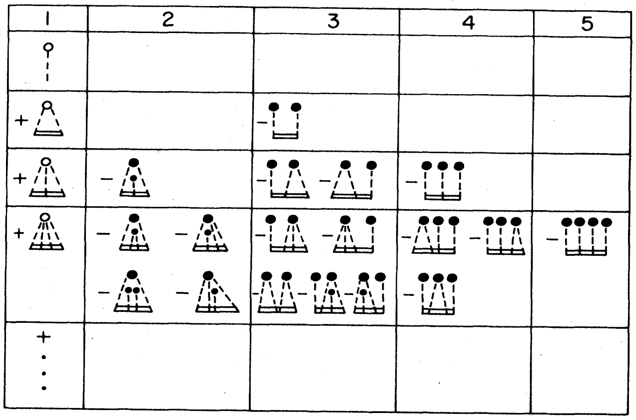

FIG. 11. The bare single-site, self-consistent, self-energy diagrams included in the coherent potential approximation (column 1) and their multiple-occupancy corrections (higher columns) after Leath (1968)].

$$[E - E(l)]G(l, l'; E)$$
$$= \delta_{ll'} + \sum_{l''} W(l, l'')G(l'', l', E), \tag{3.47}$$

which can be written in matrix notation as

$$\mathbf{G} = \mathbf{g} + \mathbf{gWG}, \tag{3.48}$$

where, in this "site-representation,"

$$g(n, m; E) = [E - E(n)]^{-1}\delta_{nm} = g(n)\delta_{nm} \tag{3.49}$$

is the Green's function for the localized states and takes on the values $(E - E_A)^{-1}$ and $(E - E_B)^{-1}$ on A- and B-atom sites, respectively, and where $W(n - m)$ represents interatomic hopping. In the locator expansion technique one then expands Eq. (3.48) in powers of $\mathbf{W}$, and averages, term by term, over all configurations of the atomic species to obtain the formal result

$$\langle G(n, m)\rangle = \langle g(n)\rangle\delta_{nm} + \langle g(n)W(n - m)g(m)\rangle$$
$$+ \langle \sum_l g(n)W(n - l)g(l)W(l - m)g(m)\rangle$$
$$+ \cdots. \tag{3.50}$$

Now it is the $g(n)$ which depend upon the configuration of the species. We can represent the terms in Eq. (3.50) by topologically the same diagrams as in the previous section, but with no external lines, as shown, for example, in Fig. 12. The transport from site to site (the solid line) is no longer by the propagator $\mathbf{g}$, which is local, but is by the interaction

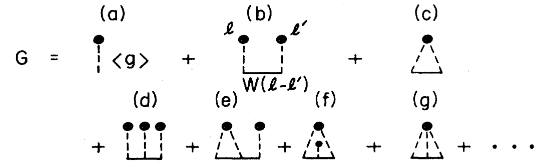

FIG. 12. The diagrams appearing in the locator expansion (3.50) of $\langle G\rangle$.

$W(n-m)$ which in this role is called the interactor, as suggested by Ziman (1969). The upright dashed line corresponds here to the localized-site Green's function g. Upon averaging, the rules become only slightly more complicated than before; a cluster of r localized-site g lines at the same site [as in Figs. 12(c), (g)] have the bare value $\langle (g_n)^r\rangle$. For example, the diagrams in Figs. 12(a) and 12(f) have the values

$$\langle g(n)\rangle = \frac{(1-c)}{E-E_A} + \frac{c}{E-E_B}, \tag{3.51}$$

and

$$\sum_m \langle g(n)^2\rangle\langle g(m)\rangle W(n-m)^2$$
$$= \left(\frac{(1-c)}{(E-E_A)^2} + \frac{c}{(E-E_B)^2}\right)\left(\frac{(1-c)}{E-E_A} + \frac{c}{E-E_B}\right) \times \sum_m W(n-m)^2. \tag{3.52}$$

Actually, no diagrams like Fig. 12(c) with a diagonal interactor appear, since $W(n-m) = 0$ for $n = m$, but we can include them formally to make the calculation parallel to that in the previous section even if their contribution is zero. Even for a perfect A-atom crystal, an infinite series must be summed, but in this case Eq. (3.50) is simply the geometric series

$$\mathsf{G} = \frac{1}{(E-E_A)} + \frac{1}{(E-E_A)^2}\mathsf{W} + \frac{1}{(E-E_A)^3}\mathsf{W}^2 + \cdots, \tag{3.53}$$

which gives immediately the standard result

$$\mathsf{G} = [E(-E_A)\mathsf{1} - \mathsf{W}]^{-1}. \tag{3.54}$$

By Fourier transforming to $\mathbf{k}$ representation, the usual band energies appear.

We can clearly define an irreducible part as we did before; the sum of all irreducible parts $\boldsymbol{\sigma}$ is called the locator (after Ziman, 1969), which represents the renormalization of the localized-state Green's function g. The pseudo-Dyson equation satisfied by $\boldsymbol{\sigma}$ is

$$\langle \mathsf{G}\rangle = \boldsymbol{\sigma} + \boldsymbol{\sigma}\mathsf{W}\langle \mathsf{G}\rangle, \tag{3.55}$$

so that

$$\langle \mathsf{G}\rangle = \boldsymbol{\sigma}/(1-\mathsf{W}\boldsymbol{\sigma}) = (\boldsymbol{\sigma}^{-1}-\mathsf{W})^{-1}. \tag{3.56}$$

The relationship between the exact locator $\boldsymbol{\sigma}$ and self-energy $\boldsymbol{\Sigma}$, according to Eqs. (2.133) and (3.56), is

$$\boldsymbol{\sigma}^{-1} = (E-E_A)\mathsf{1} - \boldsymbol{\Sigma}, \tag{3.57}$$

so that if $\boldsymbol{\Sigma}$ is site-diagonal so also will be $\boldsymbol{\sigma}$.

The multiple-counting corrections appear here just as they did in the self-energy expansion. Matsubara and Kaneyoshi (1966) considered the multiple-counting corrections and chose the full cumulant expansion technique, which, as noted earlier, led to spurious divergences. Therefore the multiple-occupancy corrections are again made self-consistently, using the diagram technique developed by Aiyer *et al.* (1969) as discussed in the previous section.

The single-site locator, which we evaluate here for illustration, consists of diagrams shown in the first column of Fig. 11 (in the calculation of the CPA) with the same multiple-occupancy corrections shown in the higher columns. The double internal interactor line here we denote as U, the fully renormalized interactor,

$$\mathsf{U} = \mathsf{W} + \mathsf{W}\langle \mathsf{G}\rangle\mathsf{W}. \tag{3.58}$$

Then we find for the bare value of the locator from the first column of Fig. 11,

$$\sigma_{\text{bare}} = \left\langle \frac{g(n)}{1-U(0)g(n)}\right\rangle = \frac{(1-c)g_{\text{A}}}{1-U(0)g_{\text{A}}} + \frac{cg_{\text{B}}}{1-U(0)g_{\text{B}}}, \tag{3.59}$$

where $g_{\text{A}} = (E-E_{\text{A}})^{-1}$ which is analogous to Eq. (3.40). The sum of all columns gives, in analogy to Eq. (3.43), the fully corrected σ,

$$\sigma = \sigma[U(0)] = \left\langle \frac{g(n)}{1-U(0)g(n)}\right\rangle + \sigma[U(0)] - \frac{\sigma[\phi]}{1-\sigma[\phi]U(0)}, \tag{3.60}$$

where $\phi(0) = U(0)/(1-\sigma[\phi]U_0)$. The solution of this equation is

$$\sigma = \left\langle \frac{g(n)}{1-U(0)g(n)/[1+\sigma U(0)]}\right\rangle \Bigg/ \left[1 + \left(\frac{U(0)}{1+\sigma U(0)}\right)\left\langle \frac{g(n)}{1-U(0)g(n)/[1+\sigma U(0)]}\right\rangle\right] \tag{3.61}$$

which can easily be written in the form

$$\sigma = \left\langle \frac{g(n)}{1-[g(n)-\sigma]U(0)}\right\rangle. \tag{3.62}$$

Then, according to Eqs. (3.55) and (3.58), we can make the substitution

$$U(0) = \sigma^{-2}\langle G(0)\rangle - \sigma^{-1}. \tag{3.63}$$

We also substitute for σ from Eq. (3.57) and identify $V(n) = E(n) - E_A$ to find that Eq. (3.62) becomes

$$1 = \left\langle \frac{1}{1 - [V(n) - \Sigma]\langle G(0)\rangle} \right\rangle, \tag{3.64}$$

which can be manipulated into the form

$$\Sigma = \left\langle \frac{V(n)}{1 - [V(n) - \Sigma]\langle G(0)\rangle} \right\rangle. \tag{3.65}$$

This formula is equivalent to Eq. (3.24), the CPA equation for the self-energy.

This establishes that the expansion in localized states agrees with the expansion in band states for the CPA treatment of single-site scattering (where topologically the same diagrams are included in each method). The generalization of this simple theorem to pair and cluster scattering gives surprising results as is discussed in Sec. IIIC1 below. This equivalence does not hold for just any class of diagrams; the multiple-counting corrections and self-consistency are essential. Perhaps one might have guessed the result earlier from the work of Onodera and Toyozawa (1968), who showed that single-site CPA reduced to either atomic or virtual crystal expressions in the appropriate limits.

In Sec. IIID below we briefly outline the calculation of two-particle Green's functions where it has been shown that the two approaches always agree if the one-particle Green's functions agree and if the Ward identity is satisfied.

Finally, the proof given here in Eqs. (3.61) to (3.65) is clearly not dependent upon the binary alloy model calculations, but would hold for any disordered system, including glasses. This point has been made by Matsubara (1970).

5. *Other approaches to the* CPA

There have been two derivations of the single-site CPA equation using the basic properties of G^h and G^d. The earliest was by Aiyer *et al.* (1969), who noted that diagonal elements of $\langle G^{dd}\rangle$ and $\langle G^d\rangle$ are identical in site representation. From Eqs. (2.136) and (2.140) this gives the matrix equation whose diagonal elements are

$$\langle V^{-1}\mathbf{\Sigma}\langle \mathsf{G}\rangle\rangle_{00} = (V^{-2}\mathbf{\Sigma}\langle \mathsf{G}\rangle\mathbf{\Sigma})_{00} + (V^{-2}[\mathbf{\Sigma} - cV\mathsf{1}])_{00}. \tag{3.66}$$

If, in addition, one requires that $\mathbf{\Sigma}$ be site-diagonal, i.e., a constant matrix, then the diagonal elements of Eq. (3.66) satisfy

$$\Delta\Sigma\langle G(0)\rangle = \Sigma^2\langle G(0)\rangle + \Sigma - c\Delta, \tag{3.67}$$

which has the CPA equation (3.24) as its immediate solution. Likewise, either of the other similar equations, $\langle G^{hh}(0)\rangle = \langle G^h(0)\rangle$ or $\langle G^{dh}(0)\rangle = \langle G^{hd}(0)\rangle = 0$, can be used to derive the same result. Thus, the CPA self-energy is the only single-site diagonal self-energy which is consistent with these requirements of the host- and defect-sites Green's functions.

Recently Butler (1972) and Brouers *et al.* (1973a) have demonstrated a derivation of the CPA equations using the consistency equation from Eq. (2.137) that

$$\langle \mathsf{G}\rangle = \langle \mathsf{G}^h\rangle + \langle \mathsf{G}^d\rangle, \tag{3.68}$$

plus knowledge obtained from the locator expansion. Their method can be generalized to include some of the important effects of pairs and larger clusters. The technique is as follows: From the locator expansion, as developed by Anderson (1958), the site-diagonal Green's function $G(l,l)$ can be written exactly as

$$G(l,l) = [E - E(l) - \Delta(l)]^{-1}, \tag{3.69}$$

where $\Delta(l)$ is a renormalization of the site energy $E(l)$ at site l and consists of the terms

$$\Delta(l) = \sum_n{}' \frac{W(l-n)^2}{E - E(n)} + \sum_{n,m}{}' \frac{W(l-n)W(n-m)W(m-l)}{[E - E(n)][E - E(m)]} + \cdots, \tag{3.70}$$

where the summations are restricted not to return to the original site l. This site self-energy $\Delta(l)$ is then a term involving all hops leaving from l and back to site l with no intermediate returns to l; thus, for example, $\Delta(l)$ is independent of $E(l)$ in this model. Butler and Brouers then average $G(l,l)$ over the occupation of site l to obtain

$$\langle G(l,l)\rangle_l = \langle G^h(l,l)\rangle_l + \langle G^d(l,l)\rangle_l = \frac{(1-c)}{E - E_A - \Delta(l)} + \frac{c}{E - E_B - \Delta(l)}, \tag{3.71}$$

which is exact. They then assume that $\Delta(l)$ is the same for each site, i.e., each site l is sitting in the same medium as specified by $\Delta(l) = \Delta$. Then, equating this $\langle G(0)\rangle$ to the one for a medium with the coherent potential Σ on each site, they obtain

$$\langle G(0)\rangle = \frac{1}{E - \Sigma - \Delta} = \frac{(1-c)}{E - E_A - \Delta} + \frac{c}{E - E_B - \Delta}, \tag{3.72}$$

from which Δ can be eliminated, with the result

$$\langle G(0)\rangle = \frac{(1-c)}{\Sigma - E_A + \langle G(0)\rangle^{-1}} + \frac{c}{\Sigma - E_B + \langle G(0)\rangle^{-1}}, \tag{3.73a}$$

or

$$1 = \frac{(1-c)}{1 - (E_A - \Sigma)\langle G(0)\rangle} + \frac{c}{1 - (E_B - \Sigma)\langle G(0)\rangle}, \tag{3.73}$$

which is precisely Eq. (3.64) and gives the usual CPA equations. This technique has been generalized by both

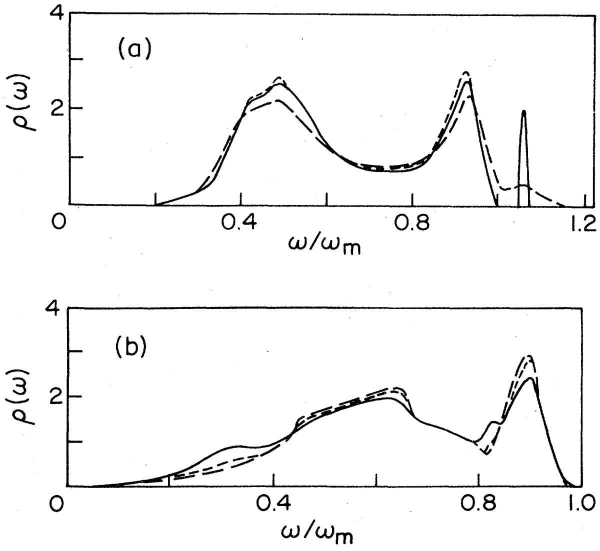

FIG. 13. The phonon density of states $\rho(\omega)$ versus ω/ω_M in the average t-matrix approximation (with the host lattice as the unperturbed lattice) for (a) 3% In in Pb ($\epsilon = 0.446$) solid line is theory, dashed line is experiment (Rowell *et al.*, 1965) and dotted line is experiment (McMillan and Rowell, 1965) for pure Pb; (b) theoretical curves for 3% Au in Cu (dotted line), 10% Au in Cu (solid line), pure Cu [dashed line (Sinha, 1966)] [after Elliott and Taylor (1967)].

Brouers *et al.* (1972) and by Butler (1972) to study larger clusters as is discussed in Sec. IIIC1 below.

Finally, there is the continued fraction technique of Matsubara and Yonezawa (1967), who showed from the full cumulant expansion (Appendix A) that the infinite series resulting for the single-site t-matrix could be put into the form of a continued fraction. This continued fraction, if evaluated exactly, would have contained the spurious poles discussed in Appendix A. However, they were able to approximate the continued fraction in a way giving the coherent potential approximation, and in fact a systematic analysis by Yonezawa (1968) demonstrated diagrammatically that the effect of this approximation was just to remove the unwanted multiple-occupancy corrections, as in the ordinary diagram technique.

B. Single-site approximations for $\langle G\rangle$—model calculations

In this section we evaluate the usefulness of the various single-site formal approximations to the density of states and to $\langle G(k,\omega)\rangle$ by comparing them with numerical results of some model calculations for the phonon, electron, and exciton problems. The similar features of these various problems becomes much clearer in the graphical comparison of the results.

For the dilute, strong-scattering alloy where the isolated impurities are capable of producing localized out-of-band or resonant in-band states, the average t matrix approximation [Eqs. (3.16) and (3.38)] is a good approximation (Sec. IIIA1). Since the self-energy Σ is site-diagonal [Eq. (3.16)] then, by Eq. (3.17), the Green's function is given by

$$\langle \mathsf{G}^1(E)\rangle = \mathsf{P}[E - \Sigma^1(E)]. \tag{3.74}$$

That is, the average Green's function $\langle \mathsf{G}(E)\rangle$ for the disordered system is given by that of the unperturbed perfect lattice $\mathsf{P}(z)$ evaluated at the complex point $z = E - \Sigma^1(E)$. For a linear chain this analytic continuation is trivial, since the analytic form of $\mathsf{P}(z)$ is known exactly. For higher-dimensional systems, the analytic form of $\mathsf{P}(z)$ is not generally known, although its numerical value on the real E axis is known either from a model calculation of the density of states or directly from experiment. Using Hilbert transforms [Eq. (2.36)] to relate the real part at one complex point z to the imaginary part at some other z', one can numerically continue $\mathsf{P}(z)$ into the complex plane quite simply, on a computer. A review of such calculations in the very dilute limit for the phonon problem is given by Maradudin (1966). We give only one example from the phonon calculations of Elliott and Taylor (1967) in Fig. 13, which shows two distinct cases. In Fig. 13(a) is shown their calculation within the simplest average t matrix approximation (assuming only isotopic defects) for 3% In in Pb which is compared with the superconducting tunneling experiments of Rowell *et al.* (1965). The only numerical input into the calculation was the phonon spectrum of pure Pb taken from a similar experiment and the known mass ratio of Pb to In. At this mass ratio there is predicted a high-frequency band of localized vibrational states about the lighter In atoms which is seen unresolved in the experiment. In Fig. 13(b) the same calculation is made for 3% and 10% Au in Cu to demonstrate the appearance of low-frequency in-band resonant modes about the heavy Au atoms. As the concentration increases, this theory simply lets the impurity

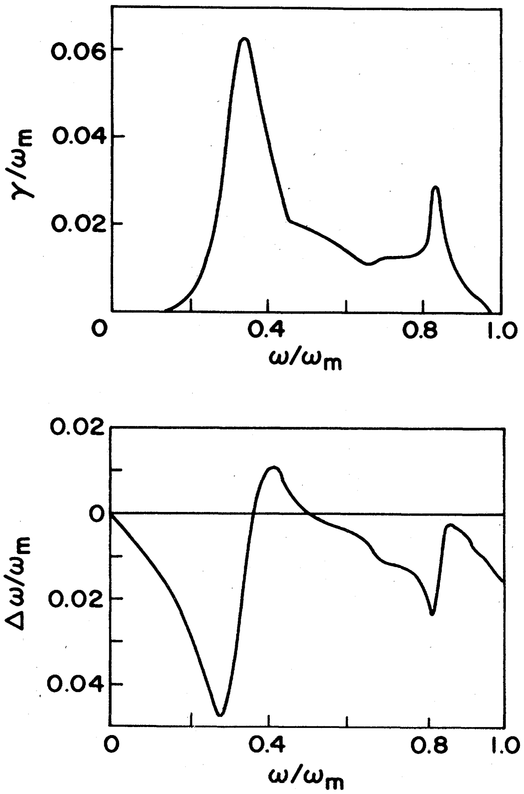

FIG. 14. Typical phonon frequency shifts and widths in the ATA for in-band resonant modes, for 10% Au in Cu (after Elliott and Taylor (1967)].

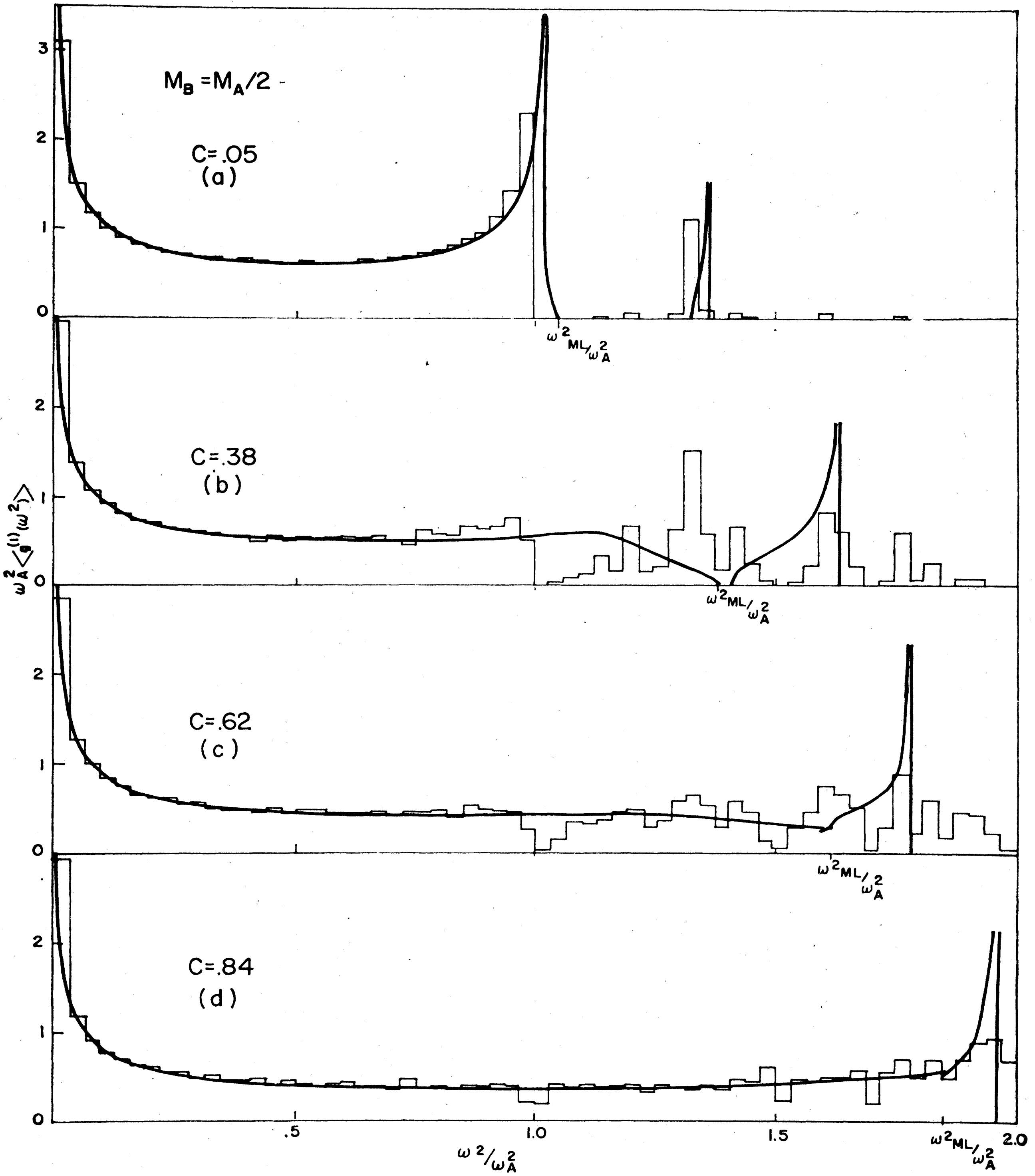

FIG. 15. The phonon density of states $\rho(\omega^2)$ versus ω^2/ω_M^2 for disordered linear chains in the ATA with the virtual crystal as the unperturbed crystal (solid line) and the machine calculations (histogram) of Dean (1961) for $M_B = M_A/2$ at four concentrations c of B atoms [after Leath and Goodman (1969)].

band broaden, merge with the host band, and finally melt away. At high concentrations it is no better than the virtual crystal approximation. The effect of the $(1-c)$ factor in the denominator of Eq. (3.16) is to make the impurity band broaden more or less symmetrically about the isolated defect-mode frequency, in contrast to the earlier formulae without this factor (Langer, 1961b; Takeno, 1962; and Maradudin, 1963), which broaden on one side only.

The self-energy $\Sigma^1(E)$ has both large real and imaginary parts near in-band resonant modes which represent large shifts and widths, respectively, of the corresponding perfect

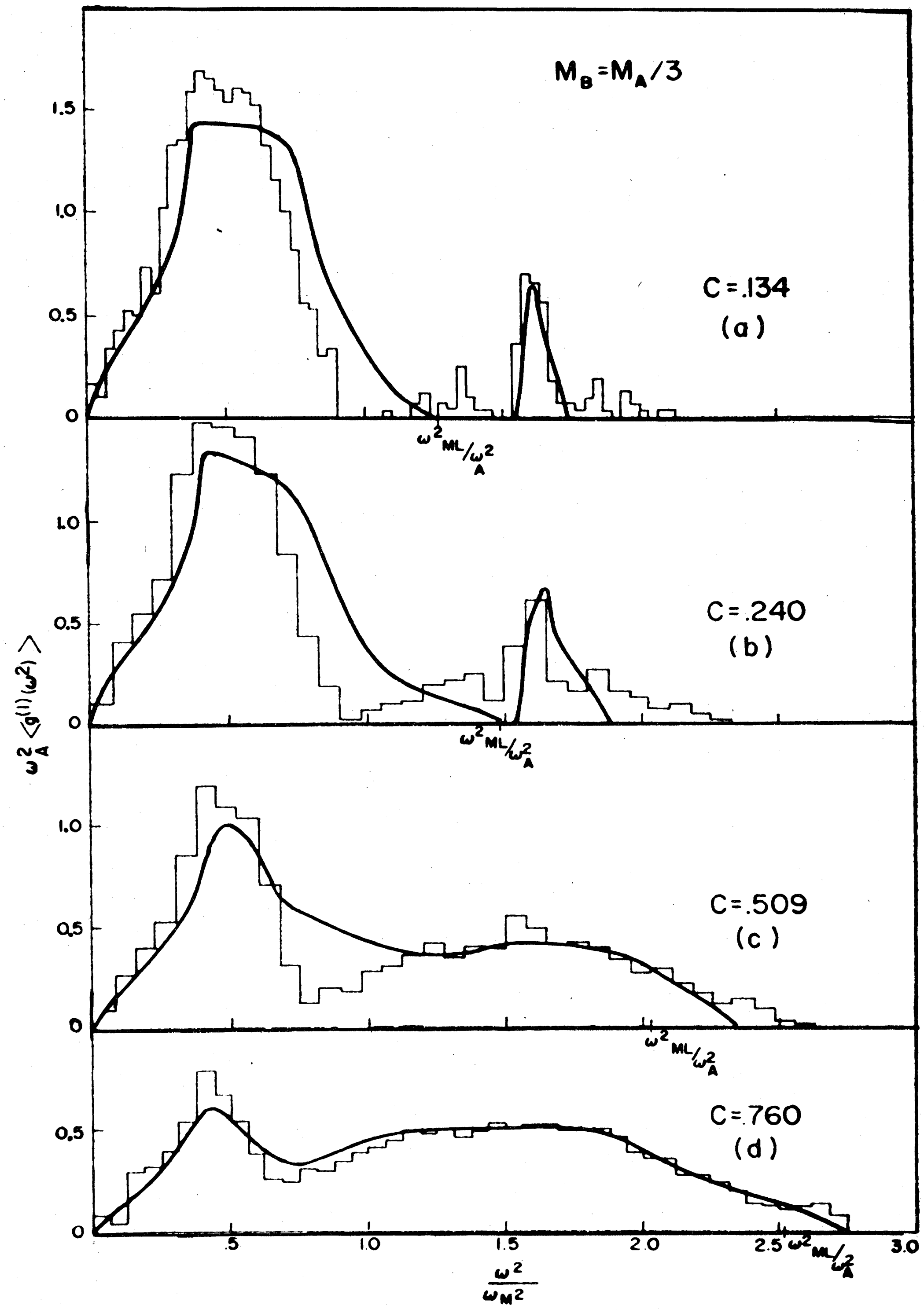

FIG. 16. The phonon density of states $\rho(\omega^2)$ versus ω^2/ω_M^2 for disordered simple cubic lattices in the ATA with the virtual crystal as the unperturbed crystal (solid line) and the machine calculations (histogram) of Payton and Visscher (1967) for $M_B = M_A/3$ at four concentrations c of B atoms [after Leath and Goodman (1969)].

crystal states. The appropriate shifts and widths from the phonon calculation of Elliott and Taylor (1967) are shown in Fig. 14. These curves agree qualitatively with results seen in some similar cases from inelastic neutron scattering, although force constants changes generally produce considerable extra effects and must be included in the model.

One can substantially improve the behavior of the average t matrix approximation (at least in three-dimensional systems) by taking the virtual crystal as the perfect host crystal, as in formula (3.18) above. This approximation was developed for the phonon problem by Leath and Goodman (1969) and has recently been taken over to the electronic case by Schwartz *et al.* (1971). Results from the phonon problem, taken from the work of Leath and Goodman (1969), are shown (solid lines) in Figs. 15 and 16 for a linear chain of atoms and for a simple cubic lattice, respectively, with only nearest-neighbor forces in each case. The various samples taken span the entire concentration range. They show graphically how this average $\langle t \rangle$-matrix approximation correctly produces a band of high-frequency localized states at low concentrations of the lighter atoms, how this impurity band merges with the host band at intermediate concentrations, and how a resonant impurity band is pulled out at low frequencies when the concentration of heavier atoms become small.

The calculations are to be compared with the computer experiments of Dean (1961) for the linear chain and those of Payton and Visscher (1967) for the simple cubic lattice, which have been discussed in Sec. IIE1 above. For the linear chain, the comparison is good only at the extremes of concentration, since fluctuations in concentration play a dominant role in the spiky high-frequency structure. This structure is due to modes localized about various clusters of A and B atoms and will only be produced in higher orders in perturbation theory when the scattering by such clusters is included.

In the three-dimensional example, the agreement is substantially better with, perhaps, surprisingly good agreement even at 50% concentration. Thus must be because a site in the three-dimensional system has a larger number of nearest neighbors and more nearly sees an average, and fluctuations are less important.

The weakest point of the formal approximation, as is obvious from Fig. 16, is its failure to correctly reproduce the band edges, This failure is due to the overly simple analytic properties of the self-energy, which has the analytic behavior of the host-lattice Green's function plus a simple pole. This pole is positioned so that $E - \Sigma^1(E)$ sweeps through the energy region of the host band to produce the impurity band in the right place, but is unable to move the unperturbed band edge from its value in the host crystal. To shift the band edges with concentration, a self-consistent field is required, where the self-energy and Green's function have similar analytic behavior.

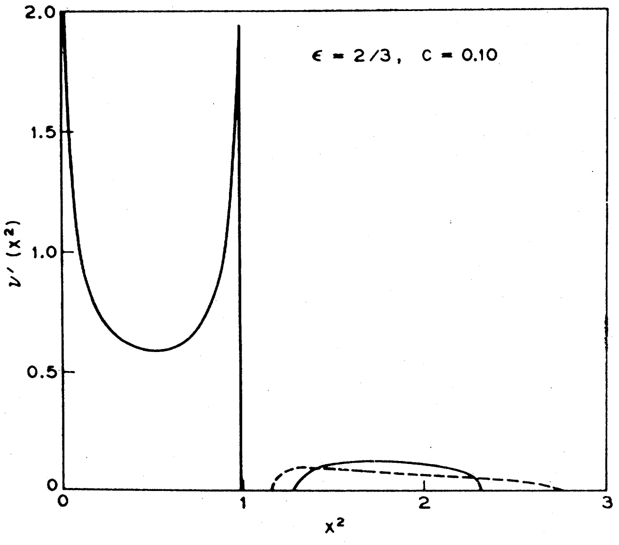

FIG. 17. The phonon density of states $\rho(\omega^2)$ versus $x^2 = \omega^2/\omega_M^2$ for a disordered linear chain with $M_B = M_A/3$ and $c = 0.1$. A comparison of the CPA (solid line) with the self-consistent formula witout multiple-occupancy corrections from Davies and Langer (1963) [after Taylor (1967)].

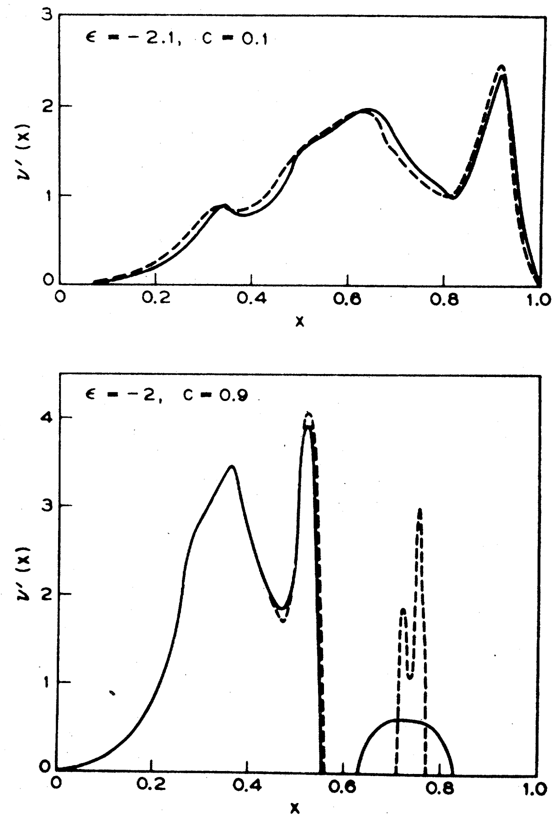

FIG. 18. Comparison between the ATA (dashed line) and CPA (solid line) densities of states for the cases where resonant, in-band states and localized states exist, respectively [after Taylor (1967)].

We proceed to the single-site, self-consistent approximation, i.e., CPA [Eqs. (3.23), (3.24), or (3.46)]. We begin by comparing the CPA with the early self-consistent field approximation of Davies and Langer (1963). Figure 17 shows the calculation of the CPA by Taylor (1967) (solid line) for a linear chain, compared with Davies and Langer's calculation (dashed line). The high-frequency impurity band is compressed in the CPA. This compression is essential because the extended impurity band of Davies and Langer for some values of c and E extended beyond the maximum frequency of the purely light atom lattice; this is forbidden by the Saxon–Hutner localization theorem (Thouless, 1970). The CPA is compared [also from Taylor (1967)] with the average t-matrix approximation in Fig. 18 in the dilute, strong scattering limit. The impurity band is broader in the CPA and the band edges are shifted. The comparison [taken from Taylor (1967)] in Figs. 19 and 20 of the CPA (solid line) with computer experiments (histograms) from the same work as in Figs. 15 and 16 above show the effect of the CPA.

The agreement with the computer experiments for the linear chain, Fig. 19, is not good. In the dilute limit the CPA fails to reproduce the sharp band of states due to isolated light atoms as satisfactorily as the average t-matrix approximation, but instead it gives a smooth impurity band which represents a mean of all the impurity cluster bands. In Fig. 20 for three dimensions, by contrast, the CPA

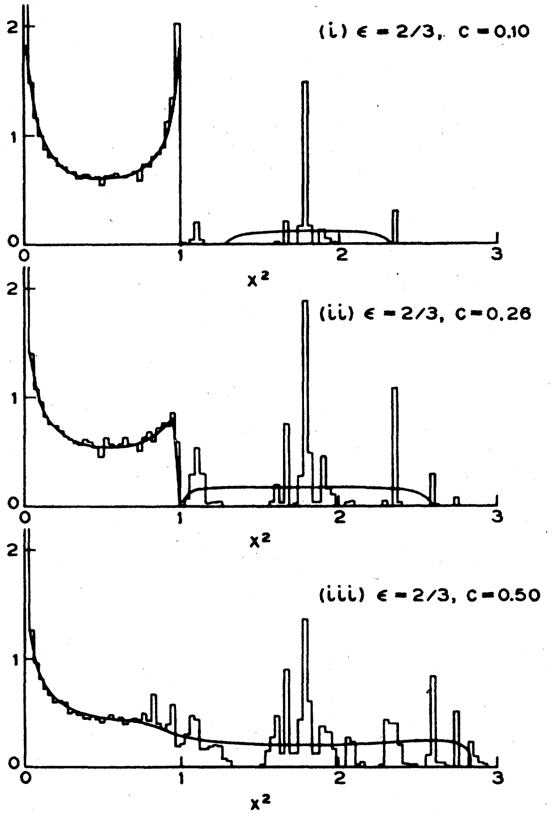

FIG. 19. The phonon density of states $\rho(\omega^2)$ versus $x^2 = \omega^2/\omega_M{}^2$ for disordered linear chains with $M_B = M_A/3$ at three concentrations c of B atoms. A comparison between the CPA (solid line) and the machine calculations of Dean, 1961 (histogram) [after Taylor (1967)].

works miraculously well at all concentrations (or at least at all concentrations of light atoms above a critical concentration $c_0 \simeq 0.28$ in the simple cubic lattice, where the high-frequency structure disappears). Even the band edges are nearly right, although the CPA, missing band-tailing effects, tends to produce split bands a little too easily. The divergence difficulty seen at low frequencies in these calculations are not fundamental to CPA (which is essentially exact at low frequencies), but were due to Taylor's numerical procedure. In order to reproduce the high-frequency structure that occurs for concentrations below c_0 properly, the scattering by pairs and larger clusters must be included.

This critical concentration c_0 is related to the so-called percolation limit. In a randomly occupied lattice, atoms of one type will occur in clusters in which they are nearest neighbors of each other. At very low c the most likely configuration is an isolated atom, but as c increases the average cluster size increases. This size diverges at $c = c_0$ when an infinite cluster spanning the whole crystal is formed. There are still some small isolated clusters at $c > c_0$ but the number diminishes rapidly with c. [For a recent review of this theory see Shante and Kirkpatrick (1971), Kirkpatrick (1973) and the brief discussion below in Sec. IVE.] In the impurity band, isolated atoms have localized states and these have a small residual interaction over large distances. However $P(0, l)$ falls off rapidly with distance in this energy range so the main interactions between localized states occur for nearest-neighbor defects, and hence the structure is largely determined by the occurance of isolated clusters at neighboring atoms. Once the infinite cluster is formed at $c > c_0$ this structure is largely broadened away. No structure occurs for small concentrations of heavy atoms since they produce a broad resonance and not strongly localized states.

The CPA density of states integrated over the impurity band, when it is split away from the host band, gives c, the appropriate weight for the sum of all impurity modes. The energy width of the impurity band is proportional to $c^{1/2}$ (Taylor, 1967).

The analytic properties of the single-site CPA result are that $\langle G_{\mathrm{CPA}} \rangle$ is analytic everywhere except for branch cuts on the real axis corresponding to the host and impurity bands. There is a pole in $\Sigma_{\mathrm{CPA}}(\omega)$ on the real axis in the gap between the host and impurity bands for sufficiently split bands [see Velický *et al.* (1968)], but this merely produces a zero in $\mathrm{Re}G(\omega)$ at this point. The disappearance

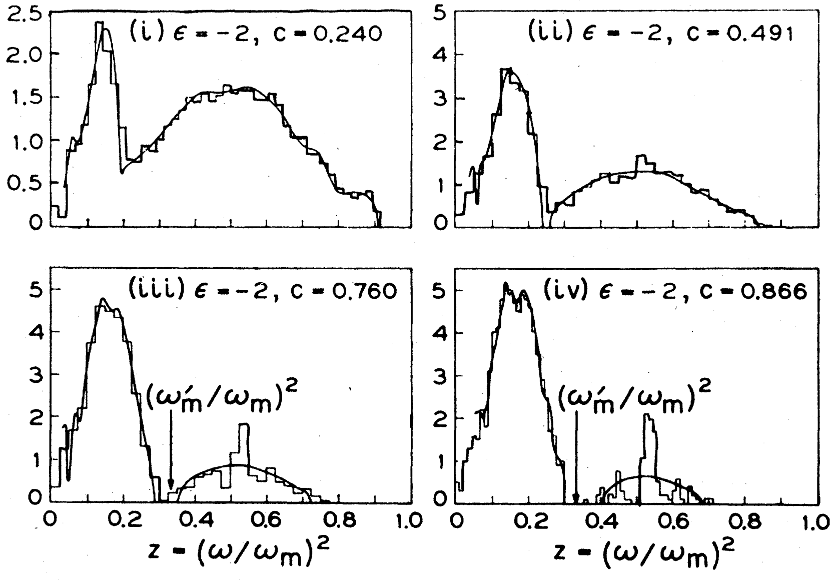

FIG. 20. The phonon density of states $\rho(\omega^2)$ versus $\omega^2/\omega_M{}^2$ for disordered simple cubic lattices with $M_B = 3M_A$ at four concentrations c of B atoms. A comparison between the CPA (solid line) and the machine calculations of Payton and Visscher (1967) [after Taylor (1967)].

in the CPA of the Van Hove singularities of the perfect crystal with the addition of disorder has been discussed by Halpern (1972).

In the electronic problem very illustrative calculations of Soven's CPA formulas were carried out by Velický *et al.* (1968), and by Schwartz *et al.* (1971). In Fig. 21 from Schwartz *et al.* we show their comparison of the effect of the average t-matrix approximation [Eqs. (3.15) or (3.39)] and the coherent potential approximation [Eqs. (3.24) or (3.46)] at a concentration $c = 0.15$ for a variety of scattering strengths $\delta = \Delta/W$. The calculations are made for the simple model unperturbed density of states [of Hubbard (1964)]

$$\rho^0(E) = \begin{cases} (2/W^2)(W^2 - E^2)^{1/2} & |E| \leq W \\ 0 & |E| > W. \end{cases} \tag{3.75}$$

The virtual crystal approximation always produces a single band which is a uniformly stretched version of the unperturbed density of states and gives the mean energy correctly. The coherent potential approximation shows nicely the splitting of the bands into host and impurity bands at about $\delta = 1.0$. The average t-matrix approximation keeps the host and impurity bands split for much too low values of δ, but produces the sharp spike for the band of states corresponding to the isolated defects quite well.

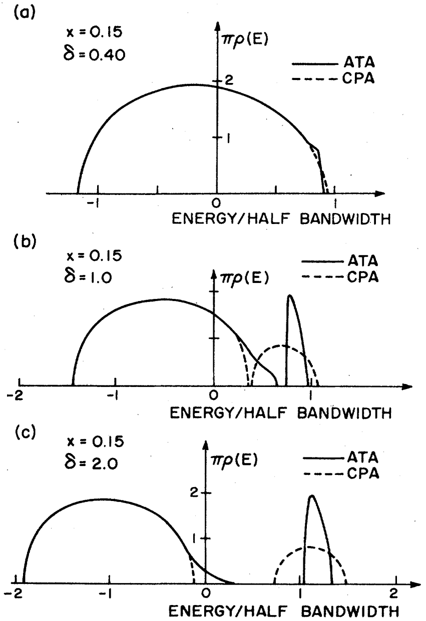

FIG. 21. A comparison of the model electronic density of states as calculated in the ATA and CPA approximations. The concentrations are x and $1 - x$. The site energy difference determines $\delta = [(\epsilon^A - \epsilon^B)/W]$ in units of the bandwidth W [after Schwartz *et al.* (1971)].

Although the CPA nicely and smoothly moves from the single-band to the split-band regime at $\delta \sim 1$, the exact value for splitting from the Saxon–Hunter localization theorem [see Thouless (1970)] is at $\delta = 2$, when there are no states from either perfect A- or B-atom crystal at $E = 0$. A general comparison of the band gaps of the CPA with the exact band gaps (Fig. 22) was given by Velický (1969). The gap appears too readily in the CPA because it does not include band-tailing effects. A discussion of these effects for a square distribution of site energies (Anderson's model) has been given by Brouers (1971).

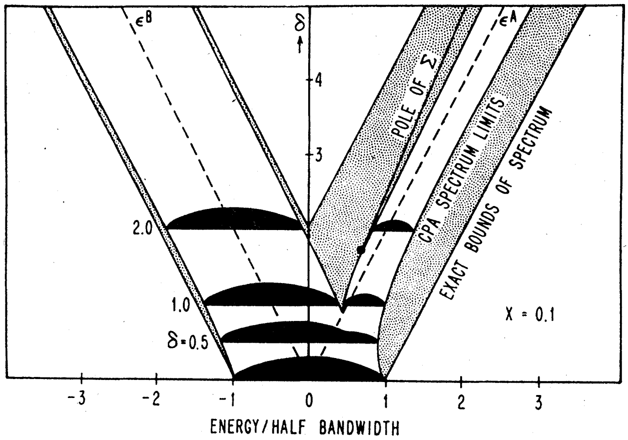

FIG. 22. The exact and CPA limits of the model electronic spectrum for a binary alloy versus $\delta = \Delta/W$. The CPA limits are more restrictive, always producing split bands before the exact splitting. The black profile is the CPA density of states [after Velický (1969)].

We have chosen here to illustrate the CPA primarily with the relatively simple mass defect phonon case. An extensive comparison of ATA and CPA model calculations has been carried out by Schwartz *et al.* (1971), including two band models for transition metals.

It is interesting to observe within the CPA the shape of the density of states for various **k** values; several such calculations have been performed. First, Onodera and Toyozawa (1968) demonstrated clearly that both the single-band behavior and split-band behavior were general features of the CPA in their calculation of $\langle G(k = 0, E) \rangle$ for the excitonic optical absorption spectrum in mixed crystals. Some of their results are shown in Figs. 23 and 24. In Fig. 23 is shown the density of states, the imaginary

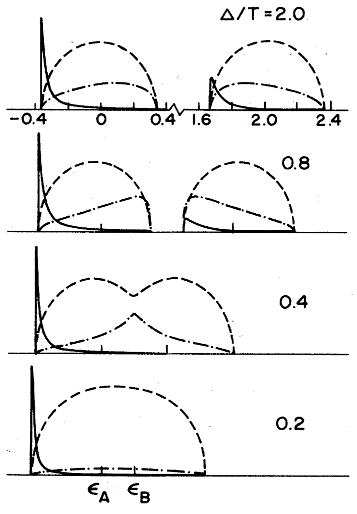

FIG. 23. The density of states (dashed line), imaginary part of the self-energy $\mathrm{Im}[\Sigma(E)]$ (dot-dash line), and the optical absorption spectrum $\mathrm{Im}\langle G(k = 0, E)\rangle$ (solid line) in the CPA, for $c = 0.5$, and $\delta = \Delta/W = 2.0$, 0.8, 0.4, and 0.2, respectively [after Onodera and Toyozawa (1968)].

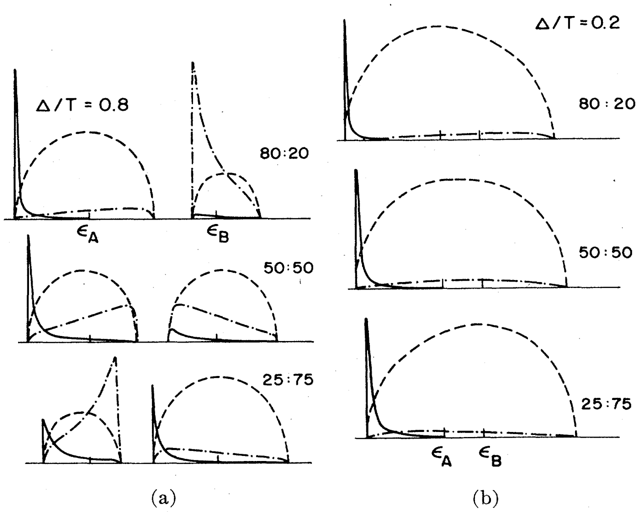

FIG. 24. The density of states (dashed line), imaginary part of the self-energy $\mathrm{Im}[\Sigma(E)]$ (dot-dash line), and the optical absorption spectrum $\mathrm{Im}\langle G(k=0,E)\rangle$ (solid line) in the CPA, for (a) $\delta = \Delta/W = 0.8$ (two-mode behavior), and (b) $\delta = 0.2$ (one-mode behavior), for $c = 0.2$, 0.5, and 0.75 [after Onodera and Toyozawa (1968)].

part of the self-energy, and the optical absorption spectrum versus energy for $c = 0.5$ and for several values of $\delta = \Delta/W$, while the unperturbed density of states was just that of Eq. (3.67) above. One notes immediately how the $k = 0$ response shifts from one-mode to two-mode behavior as the bands split. In Fig. 24 the concentration dependence is given. In the split-band limit (a) there are two optical peaks whose weight is proportional to the concentrations of the two species; and in the weak scattering limit (b) the single peak shifts linearly with concentration, as would be predicted by the virtual crystal approximation. Similar features occur in the optical absorption by defect phonon states in mixed crystals, except that there are many polarization branches and optical and acoustic modes to make the picture somewhat more cloudy.

In the electronic problem, Soven (1969) gave a useful plot of the energies and widths versus **k** within the CPA, which we show in Fig. 25. He defines the energy difference between the half-maxima in $\langle G(k,E)\rangle$ versus E as the width for the value **k**. The model host density of states again is that in Eq. (3.67). The curve is broadest at the center where the gap is about to appear in the density of states.

Finally, for completeness, we show plots, Fig. 26, of $\langle G^h(E)\rangle$ and $\langle G^d(E)\rangle$ as in Eq. (2.136) and (2.137) versus energy taken from the calculations of Velický *et al.* (1968). This calculation demonstrates quite directly how, in the split-band limit, the two subbands are associated almost entirely with states localized on each species of atom.

C. Extensions for $\langle G\rangle$

So far we have discussed diagonal, substitutional disorder with only single-site scattering included self-consistently. There have been several extensions to pair and cluster scattering, to off-diagonal disorder, and to structural disorder, with some limited success.

1. *Pairs and clusters*

The first attempt to calculate the irreducible scattering of pairs of defects was by Langer (1961b), who found, in the 2×2 notation of Eq. (2.122), the bare scattering by pairs of defects separated by a distance $\mathbf{R} = \mathbf{R}_{ij}$,

$$\Sigma^{(2)}(\mathbf{R},\omega) = ct_1 + \frac{c^2 t_1^3 P_2(\mathbf{R})}{1 - t_1 P_2(\mathbf{R})}, \tag{3.76}$$

where

$$P_2(\mathbf{R}_{ij}) = P(i,j)\sigma^x. \tag{3.77}$$

The actual formula written by Langer for the total self-energy in **k** representation is obtained by separating $\Sigma^{(2)}$ into diagonal and off-diagonal elements, which are defined by

$$\Sigma^{(2)}(\mathbf{R}) = \begin{pmatrix} \Sigma^{(2)d}(\mathbf{R}) & \Sigma^{(2)n}(\mathbf{R}) \\ \Sigma^{(2)n}(\mathbf{R}) & \Sigma^{(2)d}(\mathbf{R}) \end{pmatrix}, \tag{3.78}$$

and writing

$$\Sigma^{(2)}(\mathbf{k},\omega) = \sum_{\mathbf{R}} \{\Sigma^{(2)d}(\mathbf{R}) + \exp[i\mathbf{k}\cdot\mathbf{R}]\Sigma^{(2)n}(\mathbf{R})\}. \tag{3.79}$$

The poles of this self-energy are at the zeroes of Eq. (2.120), which are at the defect-pair state frequencies. The theory will produce, at low concentration, narrow impurity bands corresponding to the isolated defect states and to the bonding and antibonding pair states. Unfortunately no numerical evaluation of this formula exists in the literature.

The first attempts to include multiple-counting corrections into this pair formula were by Yonezawa and Matsubara (1966) and by Leath and Goodman (1968), who used the full cumulants $P_n(c)$ (Appendix A). The two formulae are the same; that of Matsubara and Yonezawa

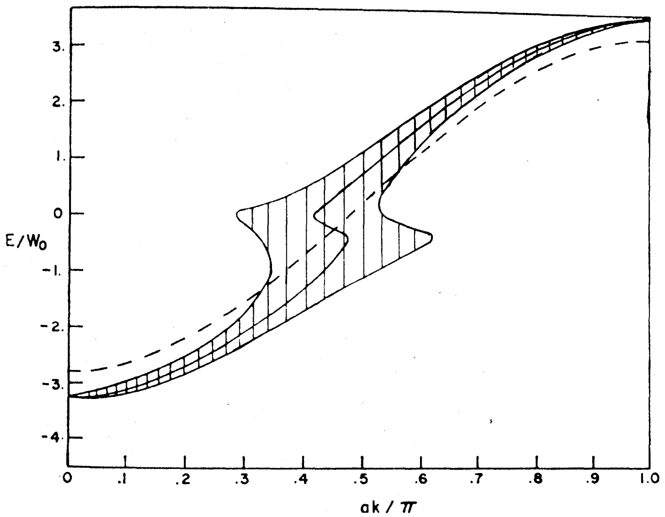

FIG. 25. Locus of the maximum of the CPA spectral density $\mathrm{Im}G_k(\omega)$ versus $[k,k,k]$ for $c = 0.4$, and $\delta = \Delta/W = 1$. The boundaries of the shaded region define the half-height position of the spectral peak. The dotted line is $E(k)$ for the virtual crystal approximation [after Soven (1969)].

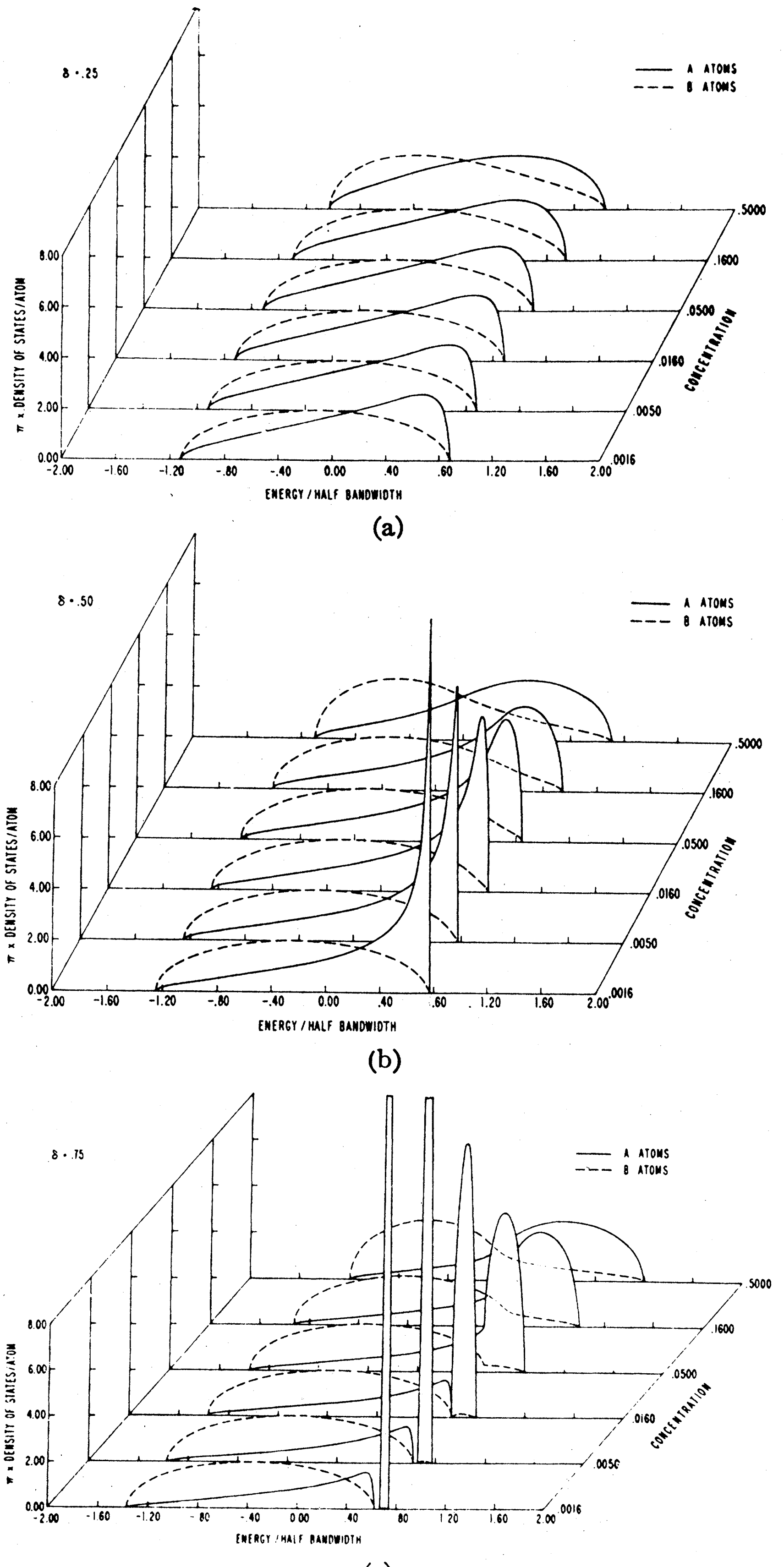

FIG. 26. Average local densities of states about A atoms $\rho_A(\omega)$ (solid lines) and B atoms $\rho_B(\omega)$ (dashed lines) for concentrations of A atoms as given and for $\delta = \Delta/W = 0.25, 0.50$, and 0.75, respectively [after Velický *et al.* (1968)].

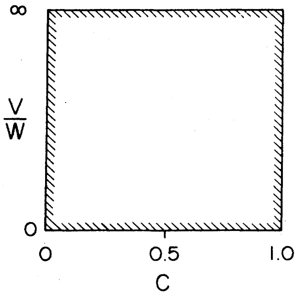

FIG. 27. The left and right sides of the square represent the two extremes of concentration (the dilute limits); the top and bottom sides correspond to the atomic (split band) limit and the weak scattering (virtual crystal) limit, respectively. The ordinary CPA is a perturbation theory in an expansion about each of these limits (the shaded regions) [after Leath (1973)].

is a very difficult integral formula and has never been studied fully, although from the work of Leath and Goodman it is clearly an integral representation of a generalized hypergeometric function. The full cumulant method, as in the single-site case, has generally been abandoned because it introduces spurious poles.

The first pair formula with multiple-counting corrections or corrected cumulants was produced by Aiyer *et al.* (1969). This formula (the extension of the average *t*-matrix approximation to pairs of defects) was derived both by a *t*-matrix decoupling scheme, like that in Sec. IIIA1 above, and by a diagrammatic summation (as in Sec. IIIA3). The result was

$$\Sigma^{(2)}(\mathbf{R},\omega) = ct_1\Big/\left[1 + ct_1P(0) - \frac{c(1-c)t_1^2P_2(\mathbf{R})^2}{1-(1-c)t_1P_2(\mathbf{R})}\right], \tag{3.80}$$

which is to be compared with Eq. (3.68), the bare formula (of course, neither formula is self-consistent). This ATA result with appropriate multiple-occupancy corrections should have the property that the impurity bands are centered at proper frequencies. Again, no numerical calculations exist in the literature, although the formula should be appropriate for studying pair modes at low concentration ($\simeq$10%) of defects.

The primary interest in pair and cluster scattering to date has been in trying to find a generalization of the coherent potential approximation, a kind of Bethe–Peierls approximation, which is useful at all concentrations and scattering strengths. This requires cluster scattering in a self-consistent medium. Let us recall the range of validity of the ordinary CPA. Clearly it is useful at very low concentrations and at very small scattering strengths V/W, since it can be viewed as a renormalized perturbation theory about these limits. But Taylor (1967) showed that the CPA was symmetric in the two atom types so that it is also useful for very high concentrations or very small values of $(1-c)$, the concentration of host atoms. Finally, Leath (1970) showed that the CPA was also obtainable from perturbation theory, and thus useful, in the extreme split band limit where W/V is very small. Therefore the CPA is useful at each extreme of concentration and scattering strength, as shown in Fig. 27, and forms an analytic interpolation formula in the interior between these limits. As such, the CPA succeeded far beyond what one would expect of a perturbation theory. Nevertheless, the CPA has other nonphysical features such as a **k**-independent self-energy and an impurity band with no structure. Thus generalizations of the CPA were sought with the hope of maintaining the symmetries of the CPA while improving the **k** dependence of the self-energy and the impurity band structure. Aiyer *et al.* (1969) attempted a self-consistent pair calculation. However, it was discovered by Nickel and Krumhansl (1971) that a simple error had been made in the evaluation of the pair formula. When this is corrected the result can be written in the form

$$\langle t_2\rangle = \left\langle \frac{V_2-\Sigma_2}{1_2-(V_2-\Sigma_2)G_2}\right\rangle = 0. \tag{3.81}$$

This is a two-site generalization of CPA, where now Σ_2 is a 2×2 matrix as in Eq. (3.70), and where V_2 and G_2 are the $2\times 2(i,j)$ subspace of the full V and G matrices:

$$V_2 = \begin{pmatrix} V_i & 0 \\ 0 & V_j \end{pmatrix}, \tag{3.82a}$$

$$G_2 = \begin{pmatrix} G(i,i) & G(i,j) \\ G(j,i) & G(j,j) \end{pmatrix}. \tag{3.82b}$$

Leath (1972) showed that this result corresponded to the self-energy formula

$$\Sigma^{(2)}(\mathbf{R},\omega) = c\tau_1\Big/\left[1 + c\tau_1\Gamma(0) - \frac{c(1-c)\tau_1^2\Gamma_2(\mathbf{R})^2}{1-(1-c)\tau_1\Gamma_2(\mathbf{R})}\right], \tag{3.83}$$

which is just the direct perturbation theory pair formula (3.80) with the unperturbed propagator replaced everywhere by a self-consistently determined propagator Γ. The Γ propagators, as in Eq. (3.23), are a 2×2 version of $G/(1+\Sigma G)$ with all intermediate scattering by the sites i and j in the t-matrix pair removed. This result could also have been obtained from the t-matrix decoupling method.

There is, however, a subtle difference between the diagrammatic and the CPA methods. Namely, the CPA, a rather more physical or intuitive approach, would lead one to use the *full* self-energy or coherent potential (with all possible internal scattering) in Eq. (3.81) for Σ_2; but the diagrammatic method quite unambiguously shows that Σ_2 contains only the pair diagrams for scattering by that particular pair of sites (i,j).

Finally, numerical calculations have been carried out on this corrected formula (3.81) by Butler and Nickel (1973), with disturbing results. Although useable at small scattering strengths V/W, in the strong scattering regime (where pair modes are important) the formula developed serious nonanalyticities (branch points) off the real axis in the complex energy plane and on the physical Riemann sheet (see Fig. 28). The formula is apparently not suitable

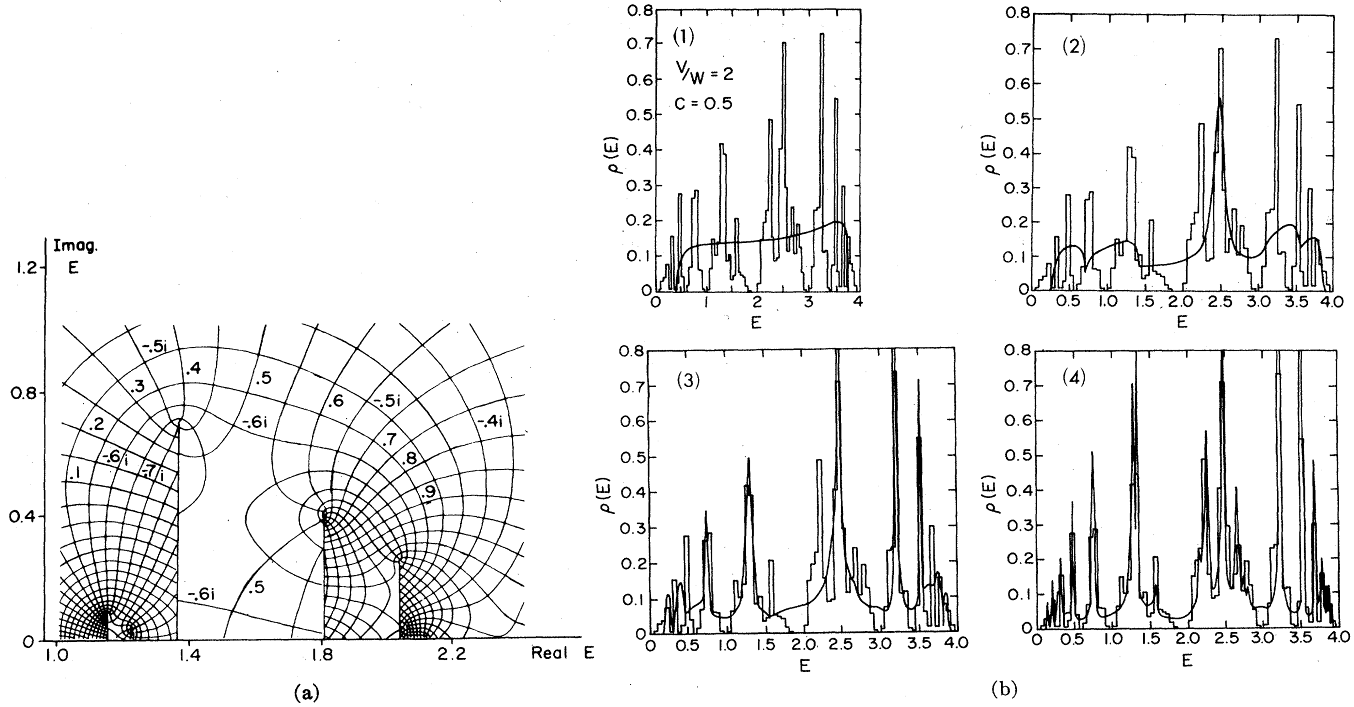

FIG. 28. (a) The contours of constant Im$\langle G(E)\rangle$ (dotted lines) and Re$\langle G(E)\rangle$ (solid lines) on the first quadrant of the physical sheet in the complex-energy plane, in the CPA for pairs without cluster diagonality [after Butler and Nickel (1973)]. (b) The density of states $\rho(E)$ versus $(E - E_{\max})$ in units of $E_{\max}$ in the region of the localized impurity bands for $c = 0.5$ and $\delta = \Delta/W = 2$. The cluster-diagonal CCPA (or the equivalent boundary-site boundary condition approach) (solid lines) is compared with that of the mode counting numerical method of Dean (histograms) for clusters of size (1) one (the ordinary CPA), (2) three, (3) five, and (4) seven [after Butler (1973)].

in the strong scattering or split-band regime. It should be pointed out that non-analyticities had previously been reported in a somewhat similar calculation by Čapek (1971).

In 1971, Ducastelle demonstrated that indeed the formula as calculated by Butler and Nickel does not reduce to the proper value in the split-band limit. Recently Leath (1973) has shown that it is possible to maintain this CPA formula (3.81) and obtain the correct split band limit if and only if the self-energy is cluster-diagonal, as in a model Tsukada (1968, 1972) had used earlier. In this CPA calculation the full self-energy, limited on its external indices to the pair of sites (i,j), is put into Eq. (3.81) and cluster diagonality in this sense requires that the full self-energy Σ does not have any nonzero off-diagonal elements connecting either site i or j to the other sites in the system. The proof applies generally to clusters of arbitrary size, with the CPA formula [see Nickel and Krumhansl (1971)]

$$\langle t_n\rangle = \left\langle \frac{V_n - \Sigma_n}{1 - (V_n - \Sigma_n)G_n} \right\rangle = 0. \tag{3.84}$$

The nonanalyticity seems also to disappear when the cluster diagonality is imposed. At least Butler (1973) has found this true for one-dimensional systems. That is, the forcing of the weak scattering perturbation theory to have the correct split-band limit apparently maintains the proper analyticity in that regime. Furthermore, if Σ is cluster-diagonal the subtle difference (mentioned above) between the diagrammatic and the CPA approaches clearly disappears, since the difference was due only to the off-diagonal contributions.

Ducastelle (1972) not only showed that the formula of Nickel and Krumhansl (1971) did not have the appropriate split-band limit, but also identified the diagrams where expansions in localized states and in Bloch states first began to disagree for the higher-order CPA. Although he was unable to find a resolution of the difference, his paper was instrumental in pinpointing the difficulty with the various generalizations of the CPA.

A separate approach in the literature was the multiple scattering technique of Cyrot-Lackmann and Ducastelle (1971), who set to zero not the average $n \times n$ t_n-matrix, but the sum of such average t-matrices over all n-cluster scatterings which began on the same site. Not only is this computationally intractable, but, as originally stated, Ducastelle (1972) also found that the formula was wrong in the extreme split-band limit. Nevertheless, if Σ is cluster-diagonal these differences completely disappear and their formula merges with the CPA.

Another cluster approach of some complexity has been introduced by Freed and Cohen (1972). They rediscovered the technique that Taylor (1967) had used for deriving the CPA for phonons and the suggestions made in that paper for generalizations to clusters. Thereafter they make several complicated approximations, which seem to contain difficulties, since the results are not correct even to lowest appropriate orders in concentration (Ducastelle, 1972).

A very simple cluster theory has been studied recently by several groups (Butler, 1972; Čapek, 1972; Tsukada, 1972; Brouers *et al.*, 1973a), which has been discussed in Sec. IIIA5 above. They calculate the average t-matrix for scattering by a cluster in a medium [as in Eq. (3.84)] with a diagonal coherent potential but, in contrast to Eq.

(3.84), they set not the entire average t-matrix to zero, but only the diagonal element on a single site in the center of the cluster. This may be carried out in a manner similar to that in Sec. IIIA5 by insisting that $\langle G(l,l)\rangle$ at the center of the cluster be the average of the cluster over all occupations of site l and its nearest neighbors. Numerical calculation is easy since Σ is diagonal, and reasonable results were obtained for weak scattering [$V/W \sim 0.5$, see Butler (1972) or Brouers *et al.* (1972)]. Unfortunately, Ĉapek (1972) and Butler and Nickel (1973) found that this method also suffers from nonanalytic behavior of a very similar sort to that in Fig. 28(a) when the band splitting is taken too large ($V/W \sim 1.0$).

Butler (1973) has recently revived interest in this numerically appealing approach, however, by noting that all the nonanalyticities disappear when, instead of the central site of the cluster, the boundary site of the cluster is chosen for the effective medium equations. He further was able to show in one dimension that this boundary site condition was precisely the full CPA with cluster-diagonal self-energy as discussed above. His results are shown in Fig. 28(b) for the difficult energy region beyond the edge of the host band and are compared with the exact computer results. As his cluster size increases from one to seven, the spiked structure of the exact result (like that in Dean's calculation) is clearly reproduced. Thus, it now seems, if one is interested in approximately reproducing the highly structural density of states found by Dean so long ago, the CPA is now up to that task.

Very recently, Mills (1974) has explicitly demonstrated a condition for the proper analyticity of the average Green's function as given by a partial summation of diagrams, with translational symmetry assumed. His criterion is for a certain left–right symmetry in the sum of self-energy graphs which is satisfied by the ordinary CPA but not by the pair formula of Butler and Nickel (1973). He suggested a "pair" formula consisting of *all graphs* that could be drawn on a Cayley tree (i.e., those without closed loops of three or more sites) but did not carry out the calculation. Perhaps his suggested calculation would be equivalent to that recently performed by Abou-Chacra *et al.* (1973).

Finally, we note the self-consistent pair calculation of Schwartz and Siggia (1972). They apply functional derivative techniques which reproduce the full cumulant coefficients $P_n(c)$ for each diagram. Then they consider each term in the perturbation expansion in powers of z^{-1}, where z is the number of nearest neighbors. They first sum all zeroth-order diagrams in the expansion (i.e., all site-diagonal diagrams plus all other diagrams for the case when all the sites coincide); this summation reproduces the single-site CPA. The result could have been expected since, diagrammatically, the CPA is just the sum of site-diagonal diagrams with the corrected cumulants $Q_n(c)$. They were also able to show that there were no contributions to the resulting perturbation expansion of order z^{-1} so that the CPA was exact to order z^{-2}. Then they proceeded to include all diagrams of order z^{-2} and z^{-3}, which meant pair diagrams and which also would then be correct to order c^2. In this order, however, they were unable to carry through the equations exactly [which presumably would have reproduced the CPA2 formulas of Nickel and Krumhansl (1971)] and approximated $P_n(c)$ according to

$$P_n(c) \simeq c(1-c)(1-2c)^{n-2} \qquad n \geq 3 \tag{3.85}$$

in order to carry through the calculation; the motivation behind the approximation is not clear except that it is appropriately symmetric in the two atom types [i.e., in c and $(1-c)$]. In any event the approximation (3.85) clearly removes any spurious poles from the self-energy and, in fact, produced pair state bands in the split-band regime, although no comparisons with exact calculations were made. Considerable discussion of this result appears in a later paper by Schwartz and Ehrenreich (1972b).

Since the calculations of Butler (1973), it now seems that the cluster-diagonal CPA is clearly the most satisfactory theory to date for producing the general features of the density of states (with the exclusion of impurity band tails, which must require contributions from clusters of arbitrary size). Nevertheless, the theory is in a rather unsatisfactory state, in spite of the progress, because the cluster-diagonal CPA and the equivalent boundary-site effective medium theory are inconsistent with the translational invariance of $\langle \mathbf{G}\rangle$. That is, both of these theories give improper behavior for the spatial dependence of $\langle G(n,m)\rangle$ although $\langle G(n,n)\rangle$ gives a good density of states. In a sense, the perturbation theory has broken down because the assumption of a translationally invariant $\langle \mathbf{G}\rangle$ or $\mathbf{\Sigma}$ is inconsistent with selecting only finite sized clusters. It would seem that, to remove these difficulties, one must sum the contribution from clusters of all sizes.

The outstanding test for any analytic theory of clusters is that it reproduces the essentially exact computer results [like those of Dean (1961) or Payton and Visscher (1967)]. Most of the recent work on the electronic problem has been for simple models appropriate to the electronic problem, and therefore has ignored these exact calculations of phonon spectra. Authors would be well advised to simply evaluate their approximations for a common set of parameters where exact computer results exist (like those of the simple phonon problem) to test the usefulness of their formulas. It was just these sorts of test which put the CPA on a firmer footing, and it will be similar tests versus exact results which will make or break any generalization.

2. *Extended defects* (*off-diagonal disorder*)

The attempted generalizations, in the literature, of the perturbation theory to extended defects or off-diagonal disorder have been mostly unsuccessful. A rather common misfortune has been the failure to agree with known formulae in the dilute (low concentration) limit. Therefore we begin with a discussion of that dilute limit.

In the extreme dilute limit all overlap effects between defects can be neglected. If one can calculate the t-matrix $\mathbf{t}_l$ for scattering by a single defect at site l in an otherwise perfect crystal, as outlined in Sec. IID above, then one can write, for the self-energy

$$\mathbf{\Sigma}_{\text{dilute}} = \langle \mathbf{t}_l \rangle. \tag{3.86}$$

Since $\mathbf{t}_l$ is no longer diagonal in site representation, $\langle t_l(\mathbf{k})\rangle$

will vary with **k**. In order to discuss this **k** dependence, we shall consider, for definiteness, the case of a single defect at the origin in a simple cubic lattice, where the perturbation $V(l, l')$ in the vicinity of the defect is given, for example, by Eq. (2.116).

$$V(0,0) = \epsilon, \qquad V(0,1) = -\gamma, \qquad \text{and } V(1,1) = \rho, \tag{3.87}$$

where the site 1 is a nearest neighbor to the defect at the origin. Using the symmetry transformation discussed in Appendix C, this matrix can be block-diagonalized into s-, p-, and d-wave parts

$$\tilde{V}_s = \begin{pmatrix} \epsilon & -\gamma(6)^{1/2} \\ -\gamma(6)^{1/2} & \rho \end{pmatrix},$$

$$\tilde{V}_p = \rho \begin{pmatrix} 1 & 0 & 0 \\ 0 & 1 & 0 \\ 0 & 0 & 1 \end{pmatrix}, \qquad \tilde{V}_d = \rho \begin{pmatrix} 1 & 0 \\ 0 & 1 \end{pmatrix}, \tag{3.88}$$

as in Eq. (2.118), so that, according to Appendix C, the Fourier components $\langle V(\mathbf{k})\rangle$ are

$$\langle V(\mathbf{k})\rangle = \sum_{l,l'} \langle V(l,l')\rangle \exp\{i\mathbf{k}\cdot[\mathbf{R}(l) - \mathbf{R}(l')]\} \tag{3.89a}$$

$$\langle V(\mathbf{k})\rangle = c[V_s(\mathbf{k}) + V_p(\mathbf{k}) + V_d(\mathbf{k})], \tag{3.89b}$$

where

$$\begin{aligned} V_s(\mathbf{k}) &= \epsilon - 12\gamma\gamma_{\mathbf{k}} + 6\rho\gamma_{\mathbf{k}}^2, \\ V_p(\mathbf{k}) &= \rho(1 - \gamma_{2\mathbf{k}}), \\ V_d(\mathbf{k}) &= (3/2)\rho(1 + \gamma_{2\mathbf{k}} - 2\gamma_{\mathbf{k}}^2). \end{aligned} \tag{3.89c}$$

The sum of all scatterings by the perturbation about a single defect at site l, of course, gives

$$\mathbf{t}_l = \mathbf{V}_l/(\mathbf{1} - \mathbf{V}_l\mathbf{P}_l), \tag{3.90}$$

where $\mathbf{P}_l$ is the 7×7 matrix representing the host lattice Green's function about site l, which can also be block-diagonalized into s-, p-, and d-wave parts by the same symmetry transformation. Therefore $\mathbf{t}_l$ can be broken into the orthogonal s-, p-, and d-wave parts

$$\tilde{t}_s = \frac{\tilde{V}_s}{1 - \tilde{V}_s\tilde{P}_s}, \qquad \tilde{t}_p = \frac{\tilde{V}_p}{1 - \tilde{V}_p\tilde{P}_p}, \qquad \tilde{t}_d = \frac{\tilde{V}_d}{1 - \tilde{V}_d\tilde{P}_d}, \tag{3.91}$$

as given by Eqs. (2.117) and (2.118). The **k** components of the average t-matrix are then calculated, with the result that in the dilute limit

$$\Sigma_{\text{dilute}}(\mathbf{k}) = c[\langle t_s(\mathbf{k})\rangle + \langle t_p(\mathbf{k})\rangle + \langle t_d(\mathbf{k})\rangle]. \tag{3.92}$$

For higher concentrations, overlap and multiple-occupancy effects enter, and Eq. (3.92) is generally no longer accurate.

An example of a correct treatment of the dilute limit with such off-diagonal disorder is the calculation of Izyumov (1966) in the case of disordered Heisenberg ferromagnets.

In the case of electrons in metals, the perturbing atomic potentials $V(l, l')$ must often be chosen self-consistently to satisfy the Friedel sum rule, as has been pointed out by Dawber and Turner (1966) and emphasized more recently by Stern (1971). To date, it seems that no CPA calculation exists for electrons in metals which also gives the correct dilute limit. As Dawber and Turner, and Stern have pointed out, the diagonal-disorder model contains, necessarily, only s-wave scattering by each defect, and hence has only a single phase shift to satisfy the sum rule; thus it is satisfied (if at all) only for very special values of the scattering parameters and Fermi energy. However, although the off-diagonal disorder is necessary for proper screening, it is clear from Eqs. (3.88)–(3.92) that the mere existence of some off-diagonal disorder ($\gamma \neq 0$) is not sufficient for p- and d-wave scattering by a defect to occur. Rather it is clearly required that the perturbing potential on the neighboring sites also be nonzero. For example, $\rho \neq 0$ is sufficient. Thus the standard model of off-diagonal disorder which has been in common use in various generalizations of the CPA for the electronic problem (Shiba, 1971; Foo *et al.*, 1971; Blackman *et al.*, 1971a, b; Brouers, 1972; Brouers and Van der Rest, 1972; Brouers *et al.*, 1973b; Schwartz *et al.*, 1973), namely,

$$\begin{aligned} V(l,l) &= V_{\text{A}} \text{ or } V_{\text{B}} \\ V(l,l+\delta) &= V_{\text{AA}}, \qquad V_{\text{BB}}, \qquad \text{or } V_{\text{AB}}, \end{aligned} \tag{3.93}$$

depending upon occupancy of sites l and $l + \delta$ by A and B atoms, clearly fails to produce more than simply s-wave scattering and hence also does not allow enough flexibility to include the effect of self-consistent screening. In an argument related to the one given here, Rudnick and Stern (1973) have come to a similar conclusion. An adequate model should at least allow ρ to be nonzero in Eq. (3.87) (even though that leads to some mathematical complications at high concentrations), so that the charge around a defect site can be adjusted self-consistently. Rudnick and Stern (1973) have recently, in fact, proposed that if $\rho \neq 0$, then it is adequate to allow $\gamma = 0$ (no disorder in the interatomic hopping) for the purposes of self-consistent screening. Within this model they show that such screening effects are quantitatively important. Finally, the discussion here has been only for a single cubic lattice, but the results are clearly true for any crystal structure since p, d, and higher angular momentum wave functions do not overlap the origin (Bass and Leath, 1974).

Since no further progress has been made, to date, on such self-consistently chosen atomic potentials, we turn now to those off-diagonal approaches and models for ferromagnets which have at least begun to handle overlap and multiple-occupancy problems correctly at high concentration. The calculations of this sort where progress has been made are the two special cases of additive and separable perturbations, and the binary alloy problem with random values for the two site energies and the nearest-neighbor hopping elements.

In the first model, that of additive perturbations, one assumes that the perturbation $V_n(l,l')$ due to a defect located at site n is additive with that due to all other defects,

$$\mathcal{H} = \mathcal{H}_0 + \sum_n \sum_{l,l'} V_n(l,l') a_l^+ a_{l'}, \tag{3.94}$$

where the sum $\sum_n$ is over all defect sites. This general model was suggested by Takeno (1968), who essentially showed that the CPA calculation for this model goes through as in the case of only diagonal disorder except that the CPA equations (3.22) are now matrix equations with matrices of dimension equal to the number of sites, about site n, which are perturbed by the presence of a defect at site n. A special case has been considered by Schwartz *et al.* (1973), who assume $\rho = 0$ and a special relation

$$V^{\mathrm{AB}} = (1/2)(V^{\mathrm{AA}} + V^{\mathrm{BB}}) \tag{3.95}$$

between hopping elements.

The only physical case known to the authors where the off-diagonal perturbations are rigorously additive is that of dilute magnets. The Heisenberg ferromagnet with nearest-neighbor interactions has recently been studied by Elliott and Pepper (1973) and in great detail by Harris *et al.* (1974), using the CPA. In this special case $\epsilon = 6\rho = 6\gamma = -6$ in the perturbation (2.116) corresponds to the removal of a single magnetic site from the simple cubic lattice. In this case, $\mathbf{V}$ is singular which indicates that the system still has the zero energy excitation corresponding to the uniform rotation of all the spins. The perturbation is strictly additive if one neglects the incorrect exchange integral thus introduced between neighboring magnetic vacancies. To remove this inaccuracy, as well as the mode associated with excitations on the defect site itself, Harris *et al.* (1974) have recently suggested the non-Hermitian perturbation

$$\tilde{V}_\tau = A \begin{pmatrix} -6\tau & \tau & \tau & \tau & \tau & \tau & \tau \\ 1 & -1 & 0 & 0 & 0 & 0 & 0 \\ 1 & 0 & -1 & 0 & 0 & 0 & 0 \\ 1 & 0 & 0 & -1 & 0 & 0 & 0 \\ 1 & 0 & 0 & 0 & -1 & 0 & 0 \\ 1 & 0 & 0 & 0 & 0 & -1 & 0 \\ 1 & 0 & 0 & 0 & 0 & 0 & -1 \end{pmatrix} \tag{3.96}$$

where the limit is taken in the calculation as $\tau \to \infty$. This hard core, on the defect site and in hopping from the defect site, rigorously removes all spin excitations from the defect site, makes the additivity of the perturbation rigorous, and guarantees the absence of a gap in the spin-wave spectrum by preserving the singular nature of the perturbation. The non-Hermiticity does not lead to serious problems. Their calculated results for $\mathrm{Im}G(k,\omega)$ at $c = 0.3$ nonmagnetic sites are shown in Fig. 29 and compared with the results obtained from a Padé approximant approach by Nickel (1974). Edwards and Jones (1971) proposed a model potential like Eq. (3.96) with $\tau = 0$ and constructed a low c expansion. Their model when put into a CPA calculation (Harris *et al.*, 1974) gives results quite similar to those in Fig. 29, but with a very weak spurious resonance in the middle of the energy band.

Tahir-Kheli (1972) has proposed another model of a dilute magnet in which bonds are removed between pairs of sites at random. The perturbing potential again is additive and is given by Eq. (2.114) with $\Lambda = -2JS$. His method is equivalent to the CPA and gives, for the spin-wave Green's functions (2.53) a simple form,

$$G(\mathbf{k},E) = \{E - [2JS - \Sigma'(E)] \times \sum_{\boldsymbol{\delta}} [1 - \exp(i\mathbf{k}\cdot\boldsymbol{\delta})]\}^{-1}, \tag{3.97}$$

where the self-energy Σ' depends only on E. At low concentrations, Σ' has a spurious resonance at low E related to that given by Eq. (2.114) (Elliott and Pepper, 1973). In addition, he finds that in the limit $E \to 0$, $\Sigma' \to 2JScz/(z-2)$, where z is the number of nearest neighbors $\boldsymbol{\delta}$, and c the concentration of missing bonds. Thus the spin-wave stiffness D in the limit of low $\mathbf{k}[E(\mathbf{k}) = Dk^2]$ varies linearly with c at all concentrations. If the concentration of bonds is interpreted as the concentration of magnetic sites, the spin-wave curve is in good agreement with the computer calculations of Kirkpatrick (1973), although this does not seem to be a valid theoretical procedure. Clearly this bond model gives the wrong dilute limit, since it neglects the correlations between the bonds removed around a missing magnetic site. Nevertheless, the approximation appears to be quantitatively fair at higher concentrations where all CPA treatments have difficulties.

The most successful approach using additive perturbations in the electronic problem is by Soven (1970). He considers a system of muffin-tin potentials which are zero everywhere except within a radius R of each site, where they take on the values $V_{\mathrm{A}}(r)$ and $V_{\mathrm{B}}(r)$, depending upon the

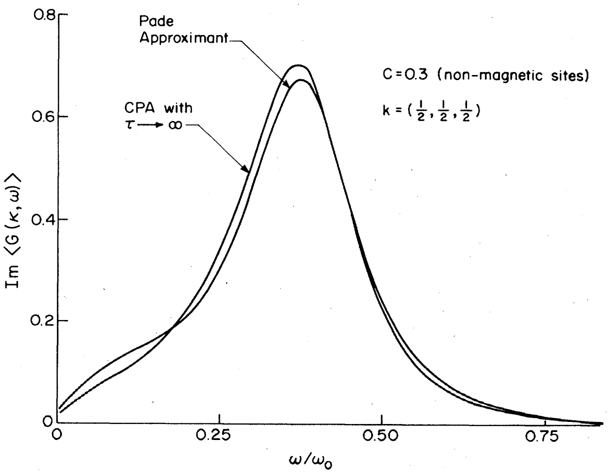

FIG. 29. The spectral density Im $\langle G_k(\omega)\rangle$ versus ω/ω_M of spin waves in a dilute, simple cubic Heisenberg ferromagnet for 30% missing magnetic sites and $k = \pi/a(1/2, 1/2, 1/2)$ as calculated by Padé approximants on a moment expansion (solid line, from Nickel, 1973) and within the CPA (dashed line) with $\tau \to \infty$ in Eq. (3.96) [after Harris *et al.* (1974)].

occupation of the particular site by an A or B atom. Clearly the perturbations are additive.

Soven first notes that the Green's function for this system $G(\mathbf{r}, \mathbf{r}')$ can be decomposed into partial waves

$$G(\mathbf{r}, \mathbf{r}') = \sum_L Y_L(\mathbf{r}) G_{LL} Y_{L'}(\mathbf{r}'), \qquad \text{for } |\mathbf{r}| = |\mathbf{r}'| = R, \tag{3.98a}$$

where $Y_L(\mathbf{r})$ are the real spherical harmonics of angular momentum L, and from the work of Anderson and McMillan (1967) notes that the local density of states on an A-atom site is given by

$$\pi\langle\rho_{\mathrm{A}}(E)\rangle = -R^2 \operatorname{Im} \sum_L \langle G_{LL}\rangle_{\mathrm{A}} d\gamma_{L,\mathrm{A}}/dE, \tag{3.98b}$$

where $\langle G_{LL}\rangle_{\mathrm{A}}$ is the angular momentum decomposition Eq. (3.98a) of $G(\mathbf{r}, \mathbf{r}')$ between A-atom sites, and where $\gamma_{L,\mathrm{A}}(E)$ is the logarithmic derivative at energy E and radius R of the regular solutions, of angular momentum L, of the Schrödinger equation involving the muffin-tin potential $V_{\mathrm{A}}(\mathbf{r})$. His expansion was not in terms of the physical $V_{\mathrm{A}}(\mathbf{r})$, however, but in terms of a very special shell potential

$$V_{\mathrm{A}}'(\mathbf{r}, \mathbf{r}') = \sum_L Y_L(\mathbf{r})[\delta(|\mathbf{r}| - R)/R^2] W_{L,\mathrm{A}}(E) \times [\delta(|\mathbf{r}'| - R)/R^2] Y_L(\mathbf{r}'), \tag{3.98c}$$

where $W_{L,\mathrm{A}}(E)$ was chosen to give $V_{\mathrm{A}}'(\mathbf{r}, \mathbf{r}')$ the same phase shifts as $V_{\mathrm{A}}(\mathbf{r})$. Then he was able to show that the physical density of states $\langle\rho(E)\rangle$ was given by

$$\pi\langle\rho(E)\rangle = \operatorname{Im}\{\operatorname{Tr}\langle \mathbf{G}'\rangle - N \sum_L [(1 - c)\langle G_{LL}'\rangle_{\mathrm{A}}(dW_{L,\mathrm{A}}/dE) + c\langle G_{LL}'\rangle_{\mathrm{B}}(dW_{L,\mathrm{B}}/dE)]\}, \tag{3.99}$$

where $\mathbf{G}'$ is the Green's function for the systems with the shell muffin-tin potentials V_{A}' and V_{B}' at the sites where the real system had potentials V_{A} and V_{B}, respectively. The rest of his calculation was the application of the CPA method to this simpler model with the shell muffin-tin potentials. Essentially the CPA equations reduce after transformation to the angular momentum representations to matrix equations coupling the various channels L, L' of scattering by a single site.

Numerical calculations were performed only for a very simple model consisting of s-wave scattering only. The results with this s-wave model (Fig. 30) first demonstrated qualitatively how the nature of the bands might depend upon the bandwidths of the two species. Since the potential and the self-energy (or coherent potential) are cell-localized in this model, it is clear that exact dilute, weak scattering, and strong scattering limits are obtained (Leath, 1973). Soven (1970), in fact, demonstrated the correctness in the

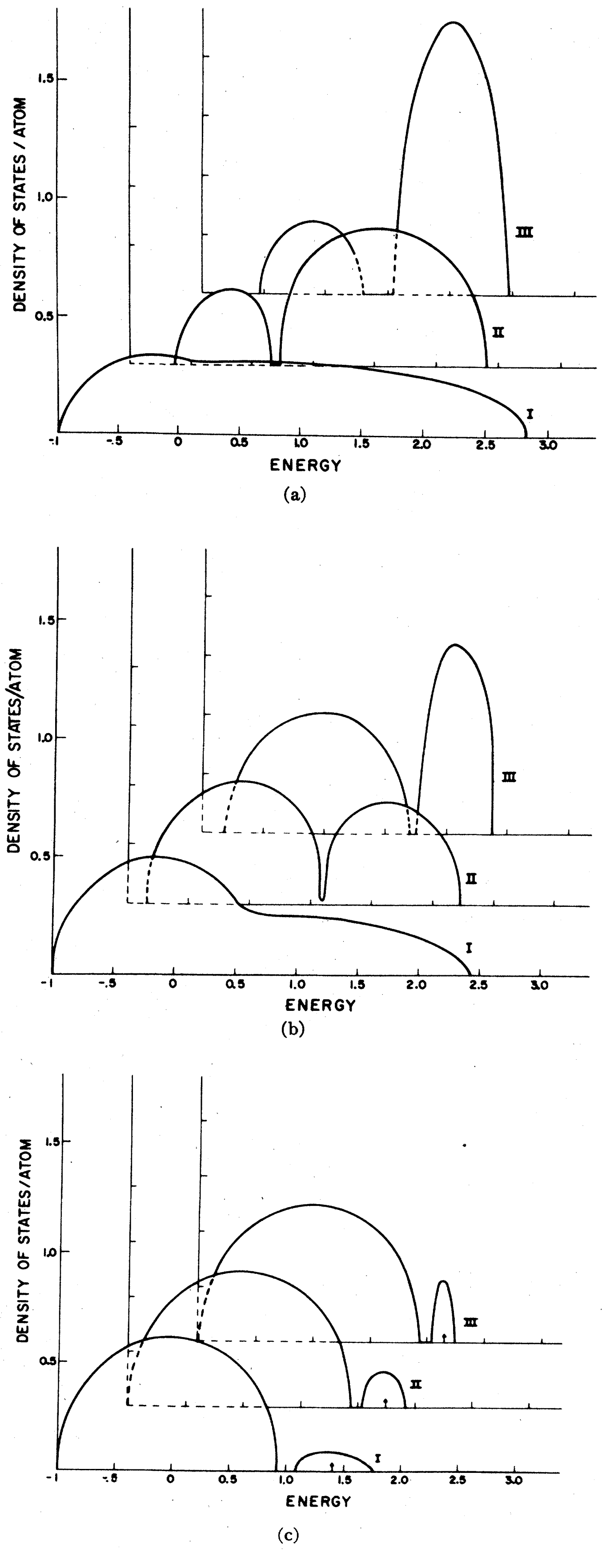

FIG. 30. The CPA densities of states for three alloy systems with muffin-tin potentials and only s-wave scattering included. The pure A material has a half-bandwidth of 1, while the pure B has half-bandwidths of 2, 1, and 0.5 for cases I, II, and III, respectively, for concentrations c_{B} = (a) 0.05, (b) 0.40, (c) 0.80 [after Soven (1970)].

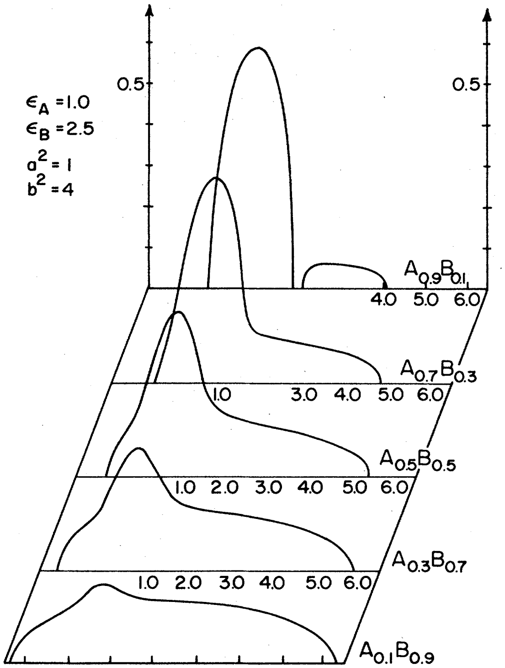

FIG. 31. Typical CPA densities of states $\rho(\omega)$ versus ω for random hopping integrals of the separable form [Eq. (3.100)]; the bandwidth of the pure B material is 4 times that of pure A material [after Shiba (1971)].

dilute and weak scattering limits. It now remains to be seen whether these results can be improved by allowing $V_{A(B)}(r)$ to vary self-consistently with the occupation of the neighboring sites in order to include screening effects.

The second, successful, special model is the model of the *separable* perturbation introduced by Shiba (1971) into the electronic problem. Although his model also does not generally allow for self-consistent screening, the concept of a separable perturbation is sufficiently useful to deserve review. His model, which has since been incorrectly adopted by other authors (Brouers, 1972; Brouers and Van der Rest, 1972; and Brouers *et al.*, 1973b), is that the diagonal site energies take on the two values ϵ_A or ϵ_B and that the off-diagonal interatomic hopping elements V^{AA}, V^{AB}, and V^{BB} between nearest-neighbor atoms are given by the separable form

$$V(i,j) = \alpha(i) W \alpha(j), \tag{3.100}$$

where $\alpha(i)$ takes on the values α_A and α_B depending upon the occupation of site i by an A or B atom, respectively. With this separable perturbation one can see that the locator expansion (3.50) becomes especially simple,

$$\langle G(l,m)\rangle = \left\langle \frac{1}{\epsilon-\epsilon(l)} \right\rangle \delta_{lm} + \left\langle \frac{\alpha(l)}{\epsilon-\epsilon(l)} W \frac{\alpha(m)}{\epsilon-\epsilon(m)} \right\rangle + \sum_n \left\langle \frac{\alpha(l)}{\epsilon-\epsilon(l)} W \frac{\alpha(n)}{\epsilon-\epsilon(n)} W \frac{\alpha(m)}{\epsilon-\epsilon(m)} \right\rangle + \cdots. \tag{3.101}$$

The rest of the calculation then proceeds precisely as that for the ordinary CPA locator technique (Sec. IIIA4) except that the unperturbed locator $g(n) = [\epsilon - \epsilon(n)]^{-1}$ is replaced throughout by the weighted locator

$$g'(n) = \alpha(n)/[\epsilon - \epsilon(n)]. \tag{3.102}$$

Clearly this result reduces to that of the ordinary CPA for the case of diagonal disorder, since in that case $\alpha(n)$ is independent of n. Typical density of states curves obtained by Shiba (1971), the case of bandwidths of the pure A and B materials differing by a factor of four, are shown in Fig. 31 for the entire concentration range of the two species.

This simple theory, based on the locator expansion, clearly reduces to the ordinary CPA in the case of only diagonal disorder, and gives qualitatively useful answers at all concentrations. The correct dilute limit is surprisingly obtained even when there is off-diagonal disorder, in contrast to the claim of Schwartz *et al.* (1973).

This correctness of the dilute limit of the theory is discussed by Bass and Leath (1974). The adaptations of the theory by Brouers (1972), Brouers and Van der Rest (1972), and Brouers *et al.* (1973b) fail to give $\Sigma(\mathbf{k})$ properly in the dilute limit because they assume incorrectly that Σ is of the general form

$$\Sigma = \Sigma_1(E) \sum_n |n\rangle\langle n| + \Sigma_2(E) \sum_{m,n}{}' |n\rangle\langle m|, \tag{3.103}$$

which in the dilute limit neglects the $\gamma(\mathbf{k})^2$ term in $\langle t_s(\mathbf{k})\rangle$ in Eq. (3.92) (see Appendix C).

For the case of a binary alloy, Blackman *et al.* (1973) have shown that the locator CPA method can be carried out for the Hamiltonian (3.92) discussed above, in general without the separability or additivity, by going to a 2 × 2 matrix notation,

$$V = \begin{pmatrix} V^{AA} & V^{AB} \\ V^{BA} & V^{BB} \end{pmatrix}. \tag{3.104}$$

Clearly, for an n component alloy, the theory becomes an $n \times n$ matrix theory. They produce a great many interesting density-of-states curves which qualitatively are very much like those of Fig. 31. For the case of a separable Hamiltonian this result reduces to that of Shiba (1971), as is discussed by Blackman (1973). Again it is important to note that this theory is correct in general in the dilute limit (in contrast to the statement of Schwartz *et al.*, 1973), as has also been discussed by Bass and Leath (1974).

A very interesting and unique approach to the problems of off-diagonal disorder has been found in the spin-wave problem in disordered Heisenberg antiferromagnets by Buyers *et al.* (1972, 1973), although it is difficult to analyze the size of their omitted terms. For a given concentration of A and B magnetic atoms they calculated the fractions of A and B atoms surrounded by each possible configuration of nearest neighbors, and hence found the fraction with each possible value (out of n possible values) of the exchange field on a site. They did a CPA calculation on the diagonal part of the disorder by assuming an n-component system and finally scaled the off-diagonal part so that no gap was produced in the spin-wave spectrum. The numerical results gave quite good agreement with dispersion waves obtained from neutron scattering experiments. Clearly, this technique also will not give the proper dilute limit since the correlations about a single site are not properly included. This calculation is discussed further in Sec. IVC below.

Another example from the literature is that of Foo *et al.* (1971), who have included the off-diagonal disorder not in the single-site scattering, but only between the two-sites-in-a-pair scattering calculation. Clearly this calculation also does not have the correct dilute limit because the self-energy is of the form (3.103), which does not properly handle the coherent scattering by the changed hopping around a defect site.

There remains much work to be done in the field of off-diagonal disorder if a qualitative understanding of experiments in disordered systems is to be achieved. An appropriate theory must be correct in the dilute, weak scattering, and strong scattering limits and include the partial-wave scatterings in such a way that screening processes can be included self-consistently.

3. Systems with short-range order

The discussion so far has been concerned exclusively with systems which have long-range structural order, but where the impurities are distributed at random over the lattice sites. There are many important situations where the scattering centers are not distributed at random, but in a way which shows short-range order. It is natural to consider whether the methods which have proved successful for the completely random case can be generalized to deal with this situation. The problem is in fact much more complicated, and only limited progress has so far been possible.

Short-range order systems can be divided into two types. The first is a straightforward extension of the case already treated—impurities placed substitutionally on a definite lattice but with correlated position. CuAu alloys are a well-known example of a metal showing appreciable short-range order. We shall treat this situation first because it is a straightforward generalization of the random case already treated.

More generally, there are amorphous solids, glasses, and liquids where there is no long-range order at all, but short-range order is present, and indeed can frequently be determined experimentally. There is no obvious unperturbed basis system from which to start a theory of these materials, so that it is not immediately obvious how they can be related to the earlier description. One exception to this is the case of electrons in liquid metals, where the free electron approximation can be used as a starting point [see for example Ziman (1966)]. As a result there has been some advance in the theory of liquid metals as discussed below. However, in either case the essential feature of short-range order leads to conceptually similar modifications of the methods discussed in Sec. IIIA. The relationship between the alloy and the liquid case has been discussed in detail by Schwartz and Ehrenreich (1971) and Schwartz (1973). We shall only summarize some aspects of this work in the present review.

The best approximation for the random case, the CPA described in Sec. IIIA, was obtained in a variety of ways based on (successively more sophisticated) truncation procedures of a hierarchy of equations obtained in a multiple scattering theory as developed by Lax (1951, 1952), Edwards (1962), Beeby and Edwards (1962), Beeby (1964a, b). In the present context various authors have tried to generalize by including short-range order at various stages in the process. As a result there are a variety of equations available, but it is by no means clear in some cases which approximation is the more valid.

a. Alloys with short-range order

As stressed in the treatment of the random case in Sec. IIIA1 and the extensions in IIIC1, a full treatment of the alloy would include a discussion of the scattering of all defect clusters. The probability of finding a cluster of n atoms at sites 1, 2, $\cdots$, n in the random case is proportional to c^n. If there is short-range order, it will be given by

$$c^n \alpha_n(1, 2, \cdots n), \tag{3.105}$$

where $(\alpha_n - 1)$ is the correction to purely random site occupancy. The various decoupling schemes and the cumulant expansion discussed in Appendix A provide a way in which the interference part of the cluster scattering is separated from that due to n single sites and smaller clusters.

Even the simplest t-matrix decoupling scheme includes some correlation, in that $\alpha = 0$ when $1 = 2$ or $2 = 3$ etc. as given in Eq. (3.10). For pairs of sites in an alloy it is convenient to define a "hole" distribution function $\beta_2(n, m) = \alpha_2(n, m) - 1$. For purely random, but single, occupancy of sites $\beta_2 = -\delta_{n,m}$. This "hole" distribution function is similar to that occuring in the description of liquids (Egelstaff, 1967), i.e., $\bar{g}(R, R') = g(R, R') - \rho(R')$, where $g(R, R')$ is the pair distribution function which vanishes when $R = R'$. Here $\beta \equiv \bar{g}$, and $\alpha \equiv g$.

In the single-site CPA method it was shown that in multiple scattering at a defect one must correct the total propagator P (or G) by some modified propagator which involves the rest of the medium. The simplest way to approximate this is to make the replacement

$$\mathsf{P} \rightarrow \mathsf{P}' = (1 + \boldsymbol{\beta})\mathsf{P} \tag{3.106}$$

which for the totally random case is simply Eq. (3.10). Using this more generally for short-range order, with the random phase approximation (3.12) leads to the generalization of Eq. (3.15),

$$\Sigma(\mathbf{k}) = \langle t \rangle / [1 - \langle t \rangle \langle \beta P(\mathbf{k}) \rangle_{\mathrm{Av}}], \tag{3.107}$$

where

$$\begin{aligned} \langle \beta P(\mathbf{k}) \rangle_{\mathrm{Av}} &= \sum_m \beta(n, m)\, P(n, m) \exp\{i\mathbf{k}\cdot[\mathbf{R}(n) - \mathbf{R}(m)]\} \\ &= \sum_{\mathbf{k}'} \beta(\mathbf{k} - \mathbf{k}') P(\mathbf{k}'). \end{aligned} \tag{3.108}$$

Since P appears in this approximation, the result is not self-consistent. This form for $\boldsymbol{\Sigma}$ was first derived by Gyorffy (1970), although the first-order terms at low c had been considered by Hartmann (1968). Gyorffy went on to improve this approximation by including self-consistency, and his method has been subsequently elucidated in a paper of Korringa and Mills (1972). They suggested replacing P in Σ and t by the full propagator G. However, as Schwartz (1973) has stressed, this does not reduce to the CPA in the random limit and leads, like Eq. (3.20), to some unsatisfactory features.

Schwartz and Ehrenreich (1971) proposed another generalization which does reduce to the CPA. This replaces $\langle t\rangle P$ by ΣG and writes t as a function of Γ as used in Eqs. (3.44) and (3.23). The resulting expression is

$$\Sigma(\mathbf{k})[1 - \langle\beta G(\mathbf{k})\rangle_{\mathrm{Av}}] = ct(\Gamma) = cV + V\sum_{\mathbf{q}}\Sigma(\mathbf{q})G(\mathbf{q}). \tag{3.109}$$

Other generalizations of Eq. (3.109) have been given by Takeno (1971) and Towers (1971). They suggest that an appropriate expression may be obtained by substituting the usual CPA value of Σ_0 for the single-site scattering and writing

$$\Sigma(\mathbf{k}) = \Sigma_0/[1 - \Sigma_0\beta_2{}^1G(\mathbf{k})], \tag{3.110}$$

where $\beta_2{}^1(n, m) = \delta_{n,m} + \beta_2(n, m)$. Towers has also suggested a slightly different formula, but which also reduces to CPA is $\beta^1 \to 0$. He has made some calculations in the linear chain with this approximation.

None of these generalizations is 'correct,' and it is difficult to find a criterion for their relative applicability. Schwartz (1973) has shown that the moments given by Eq. (3.109) are correct to higher order than those given by the Gyorffy formula.

An alternative approach is via the cluster approximations discussed in Sec. IIIC1. If a correct procedure is found for dealing with clusters, it should be straightforward to introduce short-range order by including the appropriate α_n for each cluster. Unfortunately, as we have seen, no completely satisfactory self-consistent cluster theory yet exists. Several authors have suggested generalizing the approximate cluster theories discussed above. Cyrot-Lackmann and Cyrot (1972) suggest that the pair CPA result (3.73) could be modified to read

$$\left\langle\alpha_2\left[\frac{V_2 - \Sigma_2}{1 - (V_2 - \Sigma_2)G_2}\right]\right\rangle = 0. \tag{3.111}$$

Elliott and Leath (unpublished) have made a similar conjecture using Nickel and Krumhansl's form of the pair $\Sigma^{(2)}$ given by Eq. (3.83). This can be manipulated into the form

$$\begin{aligned}\Sigma_2(\mathbf{R})/[1 - \Sigma_2(\mathbf{R})G_2]\\ = ct + c^2t^2(\Gamma)\Gamma(\mathbf{R})[1 + \beta_2(\mathbf{R})]/[1 - t(\Gamma)\Gamma(\mathbf{R})]\end{aligned} \tag{3.112}$$

and $\Gamma = G_2/(1 + \Sigma_2G_2)$. Towers (1973) has also used this formula to make some calculations in the one-dimensional case. However, only the single-site terms are treated self-consistently. The pair effects are then given as

$$\Sigma_2(\mathbf{R}) = \Sigma_0 + \Sigma_0{}^2G_0(\mathbf{R})[1 + \beta_2(\mathbf{R})]/[1 - \Sigma_0G_0(\mathbf{R})]. \tag{3.113}$$

This does appear to give results which are physically reasonable.

When the defects take up positions with some incomplete long-range order, the CPA may also be used to predict the excitation spectrum. This problem has been considered by Foo and Amar (1970), Towers (1973), and Plischke and Mattis (1971).

b Liquid metals

The theory of liquid metals can be developed in a manner parallel to the alloy theory just discussed [see Schwartz and Ehrenreich (1971); Schwartz (1973)], as has already been indicated.

The input ingredients in the theory are the distribution of the scatterers (ion cores), the effective potential for scattering of the electrons, and the choice of unperturbed Hamiltonian and basis. The usual density operator for the scatters is $\rho(\mathbf{R}) = \sum_i n_i = \sum_i \delta(\mathbf{R} - \mathbf{R}_i)$. As to potential, Ziman has shown that the "muffin-tin" potential facilitates calculation of a number of properties; for the ith scatterer $v(\mathbf{r} - \mathbf{R}_i)$ then is taken to be spherically symmetric and to vanish for $|\mathbf{r} - \mathbf{R}_i| > R_m$ where R_m is a screening length. It is also not unreasonable to require that the scatterers (potentials) do not overlap. The unperturbed Hamiltonian is usually taken to be that for free electrons $\mathcal{H}_0 = P^2/2m$, although this choice may lead to formal difficulties in calculating energy moments of the density of states unless some upper cutoff factor is introduced. In principle, this problem can then be followed through, considering $\mathcal{H} = \mathcal{H}_0 + V$ with $V = \sum_i v(\mathbf{r} - \mathbf{R}_i)$, in a manner similar to that for the alloy problem [Eq. (3.113)], except that now the $\mathbf{R}_i$ are randomly distributed continuous variables. In developing the multiple scattering description it has been noted that there is a natural order of approximation involving single sites, pairs of sites, and n clusters generally; but beyond the various single-site approximations it has not yet been possible to obtain a clearly best approximation—the same is true in the case of liquids.

There is one important difference from the alloy which will become apparent in the results to be quoted, namely, the lattice in the random alloy is replaced in the liquid by pair and higher density distribution functions, which do include a specification of short-range order. [The recent note by Korringa and Mills (1972) is informative in comparing with the alloy methodology.]

When the terms of various order in the multiple scattering series are configurationally averaged, the weighting depends on the distributions of scatterers. Thus the average of the site distribution function $\langle n_i\rangle = \int n(\mathbf{R})\, d\mathbf{R}$ is just the analog of the impurity concentration c in the alloy case. The distribution of pairs of atoms is

$$\langle n_in_j\rangle = c^2\alpha_2(\mathbf{R}_i - \mathbf{R}_j) + c\delta(\mathbf{R}_i - \mathbf{R}_j), \tag{3.114}$$

where α_2 is the analogue of α defined in Eq. (3.105). At large $(\mathbf{R}_i - \mathbf{R}_j)$, $\alpha_2 \to 1$ as in the random case. The residual pair scattering is proportional to

$$\beta_2(\mathbf{R}_i - \mathbf{R}_j) = \alpha_2(\mathbf{R}_i - \mathbf{R}_j) - 1. \tag{3.115}$$

α_2 is the usual pair distribution function, which may be determined by x-ray or neutron scattering; indeed for a uniform liquid $\beta = (\bar{g}/\rho_0)$, where $\bar{g}$ is the "hole" pair function. Higher-order correlations, α_3 etc., in liquids cannot be determined directly from experiment. It is usual to resort to some approximation such as the Kirkwood superposition approximation (Egelstaff, 1967) to express α_3 etc. in terms of α_2.

Schwartz and Ehrenreich (1971) discuss the various single-site approximations in terms of a coordinate dependent self-energy $\sigma_i = \sigma(\mathbf{r} - \mathbf{r}' - \mathbf{R}_i)$ so that

$$\Sigma(\mathbf{r} - \mathbf{r}') = c \int \sigma(\mathbf{r} - \mathbf{r}' - \mathbf{R}_i)\, dR_i. \tag{3.116}$$

The ATA equation (3.16) can be written [with propagator $P(\mathbf{R}_i - \mathbf{R}_j)$]

$$\sigma_i = t_i + ct_i \int P(\mathbf{R}_i - \mathbf{R}_j)\beta_2(\mathbf{R}_i - \mathbf{R}_j)\sigma_j\, d\mathbf{R}_j \tag{3.117}$$

where t_i is the t-matrix for the potential $v(\mathbf{r})$ centered at $\mathbf{R}_i$,

$$t(\mathbf{r},\mathbf{r}') = v(\mathbf{r})\delta(\mathbf{r} - \mathbf{r}') + v(\mathbf{r}) \times \int P(\mathbf{r} - \mathbf{r}'')t(\mathbf{r}'',\mathbf{r}')\, d\mathbf{r}''. \tag{3.118}$$

When Fourier transformed, they approximate σ_j by t, for $\beta \ll 1$, to obtain

$$\Sigma(\mathbf{k}) = c[t(\mathbf{k},\mathbf{k}) + c \int t(\mathbf{k},\mathbf{k}')(E - \hbar^2 k'^2/2m)^{-1} \times t(\mathbf{k}',\mathbf{k})\beta_2(\mathbf{k}',\mathbf{k})\, d\mathbf{k}']. \tag{3.119}$$

This is essentially Gyorffy's result, which can be made self-consistent by inserting $\Sigma(\mathbf{k})$ into the propagator.

Ehrenreich and Schwartz's result includes further terms in the interaction. For $v(\mathbf{r}) = v\delta(\mathbf{r})$ so that the Fourier transforms of t are independent of $\mathbf{k}$ and $\mathbf{k}'$ they give

$$\Sigma(\mathbf{k}) = cv + v \int \Sigma(\mathbf{q})G(\mathbf{q})\, d\mathbf{q} + \Sigma(\mathbf{k}) \int \beta_2(\mathbf{k} - \mathbf{q})\Sigma(\mathbf{q})G(\mathbf{q})\, d\mathbf{q} \tag{3.120}$$

which is similar to Eq. (3.109). Roth (1973) has compared various methods from alloys in the context of liquid metals and amorphous systems. Part of this work is simply another demonstration that ATA, CPA, and the like can be carried out in either locator or Bloch basis, as discussed in Sec. IIIA4, and various authors referred to there. However, the work also includes consideration of a nonorthogonal basis set, and particularly for the liquid discusses the details in averaging the particle distribution function in the evaluation of various moments of the spectrum. Calculations of densities of states were made to compare ATA and CPA (in our terminology) approximations, for both a purely random liquid and for a Percus–Yevick model of a hard sphere liquid. It is concluded that the non-self-consistent approximations are inadequate, and that including nonorthogonality has an important effect on results.

Realistic calculations are difficult, not only because of the short-range order, but because it is necessary to obtain an adequate treatment of the t-matrix to represent atomic scattering of free electrons. Ziman (1966) looks at the complex values of $\mathbf{k}$ which gives poles in the t-matrix at a given E using muffin-tin potentials. The real and imaginary part of this $\mathbf{k}_E$ then gives the width and shift of the excitation for weak scattering. Anderson and MacMillan (1967) give a self-consistent version of the theory using the CPA idea of finding an effective potential which gives the correct average scattering. They applied the method to liquid Fe. Schwartz and Ehrenreich (1971) use their improved self-consistent theory to calculate the electronic states of liquid Cu.

4. *Amorphous systems*

In an amorphous material, as in a static model of a liquid, the structural disorder is fundamental—no basis lattice exists. It is not obvious how to apply the methods discussed so far, but some progress has been made.

One might say that in the binary alloy we have discussed there is one limiting case of disorder—definite structure, but random physical parameters in the governing Hamiltonian (due to composition randomness). The other limiting case seems to be closely approximated by amorphous Si and Ge, whose structure is such that short-range coordination is tetrahedral, with nearly constant nearest-neighbor bond length and interaction energy, but the extended atomic network is random (Polk, 1971).

Thorpe *et al.* (1971, 1973) have examined the properties deriving from the totally topological disorder of a simple valence band model Hamiltonian for Si and Ge, in which only nearest-neighbor interactions occur without variation in magnitude, in a tight binding representation. The objective was to try to isolate the effect of topological disorder alone. The energy spectrum and wave functions for limiting states may be obtained. The methods used do not make explicit contact with the main techniques which we are discussing, so we only summarize the results. The formulation is similar to the "locator" representation of Section IIIA4; a one-electron Green's function is written at each site in tight binding representation. The overlap with nearest neighbors leads to a perturbation series, which when represented diagrammatically shows explicitly how various paths in the topologically disordered network determine the renormalization, and the single-site self-energy. In the actual case the calculation is complicated by the need to use a two-band Hamiltonian; but thanks to a theorem which Weaire (1971) proved, it was possible to reduce the problem to a single orbital at each site, from which the actual energy spectrum could be generated.

The two main features of the analysis were the use of theorems on the eigenstates of infinite materials to bound the spectrum, and diagrammatic methods to relate the renormalization to the amorphous structure. Calculations were done for various "lattices": Diamond, Bethe lattice, Husimi Cacti. These studies demonstrated that various properties of the density of states are independent of details of structure, provided that each atom is tetrahedrally coordinated with the same overlaps; the density of states, existence of gaps, and the bounds on the energy spectrum are alike for crystalline and structurally disordered systems. In particular, gaps remain in the energy spectrum, and tail states are not found in this model. Other proofs have been given (Schwartz and Ehrenreich, 1972a, b). Of course, tail states will appear and gaps will be partially filled if there is disorder in the overlaps due to bond bending, which was not included in these models.

Kramer (1970) had developed a theory for nearly free electrons in an amorphous semiconductor based on a pseudopotential approach. He used a Gaussian distribution function about the usual lattice sites to give a particle correlation function with quasi-crystalline order (Kramer, 1971). The self-energy is taken only to first order in V, which is essentially nondiagonal, but a many-band formalism is adopted and a matrix $G_{nn'}(\mathbf{k})$ is evaluated, for bands n and n' connected by the pseudopotential. The method has been used to calculate densities of states in amorphous III–V semiconductors (Kramer *et al.*, 1971).

In contrast to this detailed study of the spectrum, other studies of the dynamics of amorphous disordered systems have addressed the configuration-averaged response function. Hubbard and Beeby (1969) and Takeno and Goda (1971) have essentially adopted liquid theories to obtain (up to pair distributions, but not higher-order) approximate expressions for electron energy spectra

$$E(\mathbf{k}) = E_0 + \int W(\mathbf{R})\alpha_2(\mathbf{R}) \exp(i\mathbf{k}\cdot\mathbf{R})\, d\mathbf{R} \qquad (3.121)$$

or phonons

$$\begin{aligned} M\omega_{\text{long}}^2(\mathbf{k}) &= \frac{1}{k^2}\int d\mathbf{R}\, \alpha_2(\mathbf{R}) \\ &\quad \times [1 - \exp(i\mathbf{k}\cdot\mathbf{R})](\mathbf{k}\cdot\nabla)^2 V(\mathbf{R}) \\ M\omega_{\text{trans}}^2(\mathbf{k}) &= \frac{1}{k^2}\int d\mathbf{R}\, \alpha_2(\mathbf{R}) \\ &\quad \times [1 - \exp(i\mathbf{k}\cdot\mathbf{R})](\mathbf{k}\times\nabla)^2 V(\mathbf{R}), \end{aligned} \qquad (3.122)$$

where $\alpha_2(\mathbf{R}, 0)$ is the pair distribution function and W or V are interaction energies. Clearly these are low-order approximations, being neither self-consistent nor allowing for higher-order structural randomness as appears in models for amorphous germanium, e.g., five- versus six-membered rings. However, Takeno and Goda apply the method to liquid argon, and Takeno (1971) suggests that this approach can be generalized to give a CPA-like description.

The work on amorphous materials which is most closely related to the random alloy methods is that of Taylor and Wu (1970), Dy and Wu (1971), and Wang, Dy, and Wu (1973). They first develop a transformation of basis from the structurally disordered lattice so that most of the methods for cellular disorder can be carried over, as follows. Starting with a standard Hamiltonian in site representation they observe that the usual transformation to $\mathbf{k}$ representation, whose $\mathbf{k}$, $\mathbf{l}$ element is

$$S_{\mathbf{k}}(\mathbf{l}) = N^{-1/2} \exp(-i\mathbf{k}\cdot\mathbf{l}), \qquad (3.123)$$

will not have the simple inverse

$$A_{\mathbf{k}}(\mathbf{l}) = N^{-1/2} \exp(i\mathbf{k}\cdot\mathbf{l}) \qquad (3.124)$$

nor a well-defined Brillouin zone, if the sites $\mathbf{l}$ do not lie on a periodic lattice. Therefore, Wu and Taylor define an additional quantity R such that

$$(1 + \mathsf{R})\mathsf{S}^{-1} = \mathsf{A} \qquad (3.125)$$

from which R is found to be

$$R_{\mathbf{kk'}} = \{N^{-1}\sum_{\mathbf{l}} \exp[i'(\mathbf{k} - \mathbf{k'})\cdot\mathbf{l}]\} - \delta_{\mathbf{kk'}}. \qquad (3.126)$$

It is simply related to the structure factor of the solid. They then write the equation for the Green's function in the form

$$\tilde{\mathsf{G}} = \mathsf{G}_0 + \mathsf{G}_0(\tilde{\mathsf{V}} + \tilde{\mathsf{W}})\tilde{\mathsf{G}}, \qquad (3.127)$$

where $\mathsf{G}_0 = z^{-1}\mathsf{1}$ (or E^{-1}), and $\tilde{\mathsf{G}} = \mathsf{S}^{-1}\mathsf{G}\mathsf{S}$.

Here

$$\begin{aligned} \tilde{V}_{\mathbf{kk'}} &= \delta_{\mathbf{kk'}} N^{-1}\sum_{\mathbf{l}} \int d\mathbf{L}\, g(\mathbf{L}) \\ &\quad \times \exp(i\mathbf{k}\cdot\mathbf{L})\, V(\mathbf{l}, \mathbf{l} - \mathbf{L}), \end{aligned} \qquad (3.128)$$

with $g(\mathbf{L})$ the pair correlation function and $V(\mathbf{l}, \mathbf{l}')$ the potential energy, and

$$\begin{aligned} \tilde{W}_{\mathbf{kk'}} &= (1/N)\sum_{\mathbf{k''}}\{(1 + \mathsf{R})_{\mathbf{kk''}}^{-1}\sum_{\mathbf{l}} \\ &\quad \times \exp[i(\mathbf{k''} - \mathbf{k'})\cdot\mathbf{l}]U_{\mathbf{k'}}(\mathbf{l})\} \end{aligned} \qquad (3.129)$$

with

$$\begin{aligned} U_{\mathbf{k'}}(\mathbf{l}) &= -\tilde{V}_{\mathbf{kk'}}\delta_{\mathbf{kk'}} + \sum_{\mathbf{L}} V(\mathbf{l}, \mathbf{l} - \mathbf{L}) \\ &\quad \times \exp(i\mathbf{k'}\cdot\mathbf{L}). \end{aligned} \qquad (3.130)$$

It will be recognized that $\tilde{V}_{\mathbf{kk'}}$, which is diagonal in $\mathbf{k}$, is just the average spectrum determined from the short-range order (of pairs), so that $\tilde{V}$ may be included in a new starting Green's function G_{SR}, whence the new Dyson equation

$$\tilde{G} = G_{\text{SR}} + G_{\text{SR}}\tilde{W}\tilde{G} \qquad (3.131)$$

involves only the "structural disorder correction" $\tilde{W}$. Dy and Wu (1971) then apply the CPA method to this equation in a straightforward manner.

It is not altogether clear how to regard the method. Of course, mathematically speaking, it is necessary to have a proper inverse S^{-1} in order to make unitary transformations consistently. On the other hand, one can only argue for a $\mathbf{k}$ basis to index the eigenstates in the long wave limit for a homogeneously random amorphous solid; at short wavelengths, or if details of connectivity or localization in rings or bonds play an essential role, it is hard to see why one should attempt to use such a basis. Beyond that, however, it can be said that for optical or neutron scattering experiments a $\mathbf{k}$ basis is just what is probed by the measurements, so one would want to calculate it anyhow.

In practice, as demonstrated in computations by these authors on various examples of amorphous systems, the factor $(1 + \mathsf{R})_{\mathbf{kk''}}^{-1}$ seems to provide an automatic cutoff in $\mathbf{k}$ space. For a one-dimensional example, Wang, Dy, and Wu (1973) found good agreement of their results with exact calculations based on the node counting method. The practicality in three dimensions remains to be demonstrated. See Fig. 32.

In closing this section, we comment that as in the case of alloys all of the above methods are well suited to finding the spectral and correlation function in regions where the perturbation theory does not break down. The details near band edges (tail states), bound states of clusters, and questions of localization remain beyond the scope of these methods. But for a variety of optical, thermal, and electrical properties, good descriptions are possible using configuration-averaged Green's functions.

5. The Hubbard model

In a classic series of papers, Hubbard (1963, 1964) made one of the earliest applications of many-electron theory to the metal–nonmetal transition. Our purpose in commenting on the Hubbard model is to call attention to the fact, noted by Velický *et al.* (1968), that Hubbard developed the CPA method in the course of that work, which has often gone unnoticed by many workers on the random alloy problem.

Using a model Hamiltonian which included a spin-dependent correlation energy, he developed a Green's description which was good in the opposite limits of strongly and of weakly interacting electrons. In site representation the Hubbard Hamiltonian is

$$\mathcal{H} = E_0 \sum_{i,\sigma} n_{i,\sigma} + \sum_{ij} W_{ij} c_{i,\sigma}^{+} c_{j,\sigma} + I \sum_{i,\sigma} n_{i,\sigma} n_{i,-\sigma}. \quad (3.132)$$

Here σ is the spin index; i, j are lattice sites; E_0 is a site binding energy for one electron; W_{ij} is the inter-site hopping energy; and the many-body correlation energy is measured by I, taken to be local in the sense of depending only on interactions of two electrons on the same site. This interaction is spin dependent, and the probabilities that site does or does not have a "$-\sigma$" spin present are $n_{i,-\sigma}$ and $(1 - n_{i,-\sigma})$, respectively.

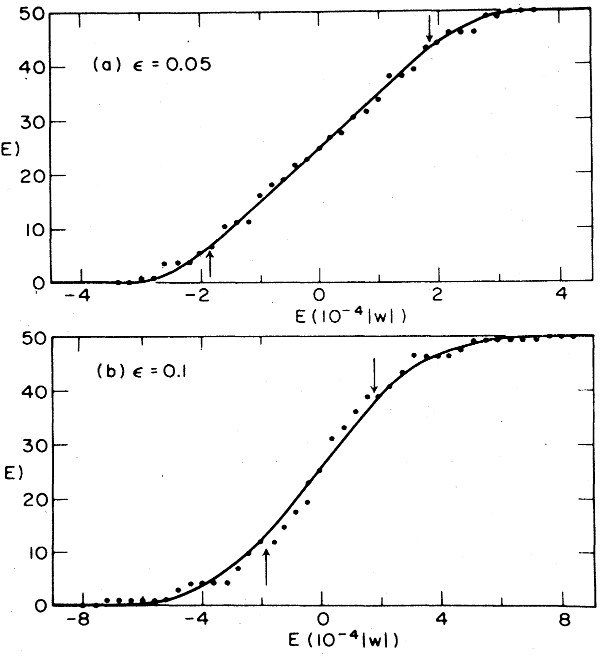

FIG. 32. Integrated density of states versus E calculated by the Dy–Wu method (solid line) and the node counting method (dots) for 30 δ-function potentials with $A = 10$ and (a) $\epsilon = 0.05$ and (b) $\epsilon = 0.1$. The arrows indicate the band edges for the perfectly ordered system [after Wang, Dy, and Wu (1973)].

The analogy with the random alloy is then as follows: The Hamiltonian describes propagation of an electron with spin σ as though it were moving in an alloy consisting of two species, in concentrations $n_{-\sigma}: 1 - n_{-\sigma}$ for which the binding energies are $E_0 + I$ and E_0, respectively. The analogy would be exact if indeed the $n_{i,-\sigma}$ were fixed during the motion of the $n_{i,\sigma}$. This is not literally so, but the motion found by neglecting resonant energy transfer between opposite spins gives the leading behavior, and was treated by self-consistent single-site multiple scattering, that is by CPA, though not called that in Hubbard's work.

Perhaps a few more details may be of interest. The earliest Hubbard work led to the expression for the spin Green's function

$$G^{\sigma}(\mathbf{k}, E) = \frac{1}{2\pi} \frac{1}{F_0^{\sigma}(E) - [E(\mathbf{k}) - E_0]}, \quad (3.133)$$

where

$$\frac{1}{F_0^{\sigma}(E)} = \frac{1 - n_{-\sigma}}{E - E_0} + \frac{n_{-\sigma}}{E - (E_0 + I)} \quad (3.134)$$

and

$$W_{i,j} = N^{-1} \sum_{k} (E(\mathbf{k}) - E_0) \exp[i\mathbf{k}\cdot(\mathbf{R}_i - \mathbf{R}_j)]. \quad (3.135)$$

It is easy to see that $[F_0^{\sigma}(E)]^{-1}$ is just the lowest virtual crystal approximation to the locator representation, Sec. IIIA4, with the interactor being $W_{i,j}$ and the whole expression then transformed to k space. In his third paper Hubbard noted several inadequacies of this approximation, among them that the poles of $G^{\sigma}(\mathbf{k}, E)$ occurred at purely real E, so that the quasiparticle states were not damped. He therefore, considered scattering by the spin fluctuations specifically (in Sec. 4 of Hubbard III). Using the Zubarev notation

$$G_{ij}^{\sigma}(E) = \langle\langle c_{i\sigma}; c_{j\sigma}^{+}\rangle\rangle, \qquad (\eta = -1) \quad (3.136)$$

and projection operators $n_{i,\sigma}^{+} = n_{i,\sigma}$, $n_{i,\sigma}^{-} = (1 - n_{i,\sigma})$, the equation of motion for one type of Green's function is

$$\begin{aligned} E\langle\langle n_{i-\sigma}^{\alpha} c_{i\sigma}; c_{j\sigma}^{+}\rangle\rangle_E &= n_{-\sigma}^{\alpha}\left\{\frac{1}{2\pi}\delta_{ij} + \sum_{k} W_{ik}\langle\langle c_{k\sigma}; c_{j\sigma}^{+}\rangle\rangle\right\} \\ &\quad + \epsilon_{\alpha}\langle\langle n_{i,-\sigma}^{\alpha} c_{i\sigma}; c_{j\sigma}^{+}\rangle\rangle_E \\ &\quad + \sum_{k} W_{ik}\langle\langle (n_{i,-\sigma}^{\alpha} - n_{-\sigma}^{\alpha}) c_{k\sigma}; c_{j\sigma}^{+}\rangle\rangle \\ &\quad + \text{“resonance broadening terms”}. \end{aligned} \quad (3.137)$$

The scattering by spin fluctuations from the average $n_{-\sigma}^{\alpha}$

appears in the term containing $(n_{i,-\sigma}{}^{\alpha} - n_{-\sigma}{}^{\alpha})$, being the ith site fluctuation from the average $n_{-\sigma}$. This is just the binary alloy problem. We need not repeat the details; it suffices to say that Hubbard proceeded to solve this scattering problem by the CPA method; the detailed correspondence to more recent work is given by Velický *et al.* (1968). The equivalence is rather apparent, in the same spirit that single-site CPA may be obtained from the bare propagator by insertion of a self-energy, plus an auxiliary condition (on the t-matrix) which determines this self-energy. Thus, Hubbard's CPA result is that

$$G^{\sigma}(\mathbf{k}, E) = \frac{1}{2\pi} \frac{1}{F_s{}^{\sigma}(E) - (E(\mathbf{k}) - E_0)} \tag{3.138}$$

as before, but now $F_s{}^{\sigma}(E)$ is

$$\frac{1}{F_s{}^{\sigma}(E)} = \frac{E - (n_{\sigma}{}^{+}\epsilon_{-} + n_{-\sigma}{}^{-}\epsilon_{+}) - \Omega_{\sigma}{}'(E)}{[E - \epsilon_{-} - n_{-\sigma}{}^{+}\Omega_{\sigma}{}'(E)][E - \epsilon_{+} - n_{-\sigma}{}^{-}\Omega_{\sigma}{}'(E)] - n_{-\sigma}{}^{+}n_{-\sigma}{}^{-}[\Omega_{\sigma}{}'(E)]^2}, \tag{3.139}$$

where

$$\Omega_{\sigma}{}'(E) = F_s{}^{\sigma}(E) - [2\pi G_{ii}{}^{\sigma}(E)]^{-1}. \tag{3.140}$$

Here $\epsilon_{+} = E_0 + I$, $\epsilon_{-} = I$, and $G_{ii}{}^{\sigma}(E)$ is obtained by Fourier transforming $G^{\sigma}(\mathbf{k}, E)$. With the simple changes to our notation $F_s{}^{\sigma}(E) \equiv E - \Sigma(E)$, and $G_{ii}{}^{\sigma}(E) = G(0)$, and other obvious equivalents, these equations become completely equivalent to our Eqs. (3.24) and (3.27). From the physics viewpoint it should also be noted that Hubbard found both amalgamated and split-band regimes, as has been developed in detail by Velicky *et al.* (1968).

Recently Cyrot (1972), also noting that the Hubbard scattering correction is equivalent to CPA, went on to study the resonant broadening correction by adapting functional integral methods which are well adapted to handle fluctuations from the CPA averages. Other related recent works are those of Fukuyama and Ehrenreich (1973) and Gobsch and Weller (1973).

9. CPA *as an intermediate step in miscellaneous calculations: metal–nonmetal transitions, amorphous magnetism*

In closing this section, we give two examples of how the CPA frequently is useful as an intermediate step in other calculations—particularly for interpolating over ranges of composition or degrees of disorder. Both the metal–nonmetal transition and amorphous ferromagnetism have a large and evolving literature, from which we have selected two examples to show how the averaging methods for random alloys may be employed.

The earliest substantial formal studies of the metal–nonmetal transition using modern methods began with Hubbard in the work just discussed. As in the case of alloys he found two regimes of behavior, depending on whether the overlap term W_{ij} is large or small compared to the difference in electron binding energy (spin-dependent) from site to site. In the former case one has broad overlapping bands, in the latter split bands which can lead to insulators with the appropriate number of electrons present. In 1969, Falicov and Kimball proposed that the metal–nonmetal transition could be described by a self-consistent method, if electron correlations are included in a mean field manner. Subsequently, Plischke (1972) and Goncalves DaSilva and Falicov (1972) extended the method using the CPA, as follows:

Assume two sets of levels, (a) localized nonconducting, (b) a conduction band separated by a gap Δ from (a) and having width W. The Hamiltonian is of the form

$$\mathcal{H} = \sum_{\mathbf{k},\sigma} [E_c(\mathbf{k}) + \Delta + \tfrac{1}{2}W] c_{\mathbf{k}\sigma}{}^{+} c_{\mathbf{k}\sigma} + E_v \sum_{i,\sigma} b_{i\sigma}{}^{+} b_{i\sigma} - G \sum_{i,\sigma,\sigma'} b_{i\sigma}{}^{+} c_{i\sigma'}{}^{+} c_{i\sigma'} b_{i\sigma}, \tag{3.141}$$

where the operators $c_{\mathbf{k}\sigma}$ refer to band states, and $b_{i\sigma}$ to holes in the localized states, and G is the electron–hole interaction strength.

In mean field approximation, replace the operator $\Sigma_{\sigma} b_{i\sigma}{}^{+} b_{i\sigma}$ by n_T, where n_T is the fraction of ionized nonconducting states at temperature T. Then the spectrum of the band states is simply given by the poles of $[E_c(\mathbf{k}) + \Delta + \frac{1}{2}W - Gn_T]^{-1}$, i.e., dependent on n_T.

The question of metal vs nonmetal then follows from the thermodynamically consistently calculated n_T

$$n_T = 2 \int_{-\infty}^{\infty} d\omega\, \rho_0(\omega) n(\omega) \tag{3.142}$$

while at the same time

$$n(\omega) = \left(\frac{n_T}{2(1 - n_T)} \exp\beta(\omega + \Delta + \tfrac{1}{2}W - Gn_T) + 1 \right)^{-1} \tag{3.143}$$

leading to an implicit equation for n_T; if $n_T = 0$, insulator, and vice versa.

The nature of the solutions depends on (Δ/W) and on temperature. Both smooth and first-order transitions from insulating to metallic states have been found by this method.

Now it is apparent that the mean field approximation made above is the simplest virtual crystal approximation to the spectrum. Noting that fact, it is immediately suggested that an improvement would result by regarding $b_{i\sigma}{}^{+} b_{i\sigma}$ as a c number with values 1 or 0, varying randomly from site to site with probability n_T and $1 - n_T$, respectively.

This becomes the site-diagonal random alloy problem, to which CPA is applied directly. The states now have energies $E_c(k) + \Delta + \frac{1}{2}W + \Sigma(n_T E)$, where the self-energy Σ is determined by the CPA condition. Finally, there must be thermodynamic consistency,

$$n_T = \int d\omega\, \rho[\omega, \Sigma(\omega, n_T)] n(\omega), \tag{3.144}$$

where $\rho(\omega) = -\pi^{-1} \operatorname{Im}[\operatorname{Tr} G_k(\omega, n_T)]$.

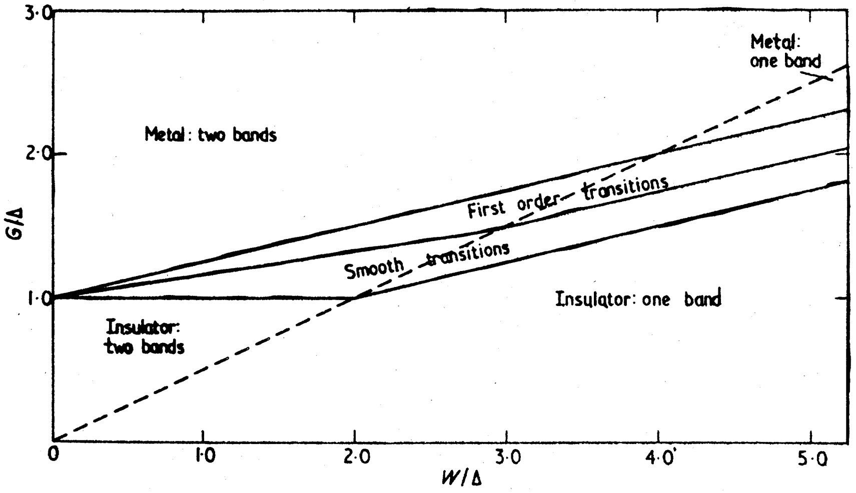

FIG. 33. Metal–nonmetal transitions in the model of Goncalves da Silva and Falicov (1972); the parameters in the "G-W plane" refer to the electron-hole interaction strength G, and bandwidth W, both in units of the gap Δ.

Goncalves da Silva and Falicov (1972) have solved the equation for a rectangular density of states model. They find a phase diagram for the metal–excitonic and metal–nonmetal configurations as determined by (ω/Δ) and the Coulomb interaction G. (See Fig. 33.) The CPA analysis by Plischke (1972), which uses a simple cubic density of states, does not seem to be correct in detail but does follow the same idea. We see that CPA can be used to improve intermediate approximations in the theory of the metal–nonmetal transition.

The first investigation of amorphous magnetism was developed by Gubanov (1961), using mean field theory. His calculation prompted other mean field calculations for both amorphous ferromagnetism and antiferromagnetism, as found, for example, in the work of Handrich (1969) and Simpson (1970). More recently, numerous investigators have used as a starting point the CPA or other self-consistent approaches. Principal activity in this regard is discussed in the text *Amorphous Magnetism* [edited by Hooper and de Graaf (1973)].[2] In one way or another the calculations therein all make use of double-time, temperature-dependent, spin–spin Green's functions, as developed by Tyablikov (1967) for ferromagnetism.

As in the theory of metal–nonmetal transitions, there also is a thermodynamically self-consistent argument, as follows:

(1) First, the spin-wave Hamiltonian is linearized in terms of the average $\langle S_z\rangle$, and the Green's functions for spin deviations $\langle\langle S_f{}^+; S_g{}^-\rangle\rangle$ are found—to some approximation.

(2) On the other hand, the expectation density of spin deviations $\langle n\rangle$ is related to the magnetization $\sigma = \langle S_z\rangle/S$ by

$$\sigma = 1 - 2\langle n\rangle. \tag{3.145}$$

(3) But from the theory of Green's function we have

$$\tfrac{1}{2}(1-\sigma) = \langle n\rangle = -\pi^{-1}\int d\omega\,\mathrm{Tr}\,\mathrm{Im}G(\omega) \times [\exp(\beta\omega)-1]^{-1} \tag{3.146}$$

and since $G(\omega)$ depends on the linearization to $\langle S_z\rangle$ this becomes an implicit temperature-dependent condition on $\langle S_z\rangle$. There are several possible choices of approximations for evaluating the spin Green's function.

In most Green's function calculations of amorphous magnetism the magnet is not truly amorphous, as Bravais lattices exist for the model systems. The "amorphous" nature of the system is simulated either by a disordered alloy with nonmagnetic scattering sites or by a randomly fluctuating exchange interaction. Various random alloy methods, including the CPA, are then employed to obtain the spin-wave Green's functions. Only the series of studies by Gubernatis and Taylor (1973), using methods developed by Taylor and Wu for phonons in amorphous materials (Sec. IIIC3), incorporate the actual amorphous structure to any degree.

D. Two-particle Green's functions

The techniques developed in the previous section can also be used to obtain averages of two-particle Green's functions in order to evaluate the disorder contribution to the transport coefficients, such as electrical conductivity [Eq. (2.82)] and lattice thermal conductivity [Eq. (2.83)]. In this section we shall review briefly the application of the CPA to such transport coefficients and show how, for weak scattering, these formulas reduce to the well-known linearized Boltzmann equation results.

The first formulation of a transport coefficient problem within the framework of the CPA was that for the electrical conductivity of high concentration alloys by Velický (1969). The starting point for his calculations was essentially Eq. (2.81) above which, when averaged over the ensemble of configurations, becomes

$$\langle\sigma\rangle = \frac{2\pi e^2}{\hbar^2 V k_B T}\int_{-\infty}^{\infty}\frac{dE\exp[(E-\mu)/k_BT]}{\{\exp[(E-\mu)/k_BT]+1\}^2} \times \mathrm{Tr}\langle B_\alpha\,\mathrm{Im}\mathbf{G}(E)B_\alpha\,\mathrm{Im}\mathbf{G}(E)\rangle, \tag{3.147}$$

where μ is the chemical potential and

$$\mathbf{B}(l,l') = [\mathbf{R}(l)-\mathbf{R}(l')]W(l,l'). \tag{3.148}$$

---

[2] See F. Brouers *et al.*; M. Cyrot; D. J. Kim; R. Harris and M. J. Zuckermann; Licciardello *et al.*; R. A. Tahir-Kheli and D. M. Esterling; R. A. Tahir-Kheli; Bose *et al.*; J. E. Gubernatis and P. L. Taylor; R. M. Stubbs and C. G. Montgomery. All but the last two calculations are CPA.

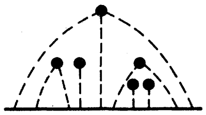

FIG. 34. A typical diagram included in the decoupling scheme of Eq. (3.152).

The quantity to be calculated is

$$\mathrm{Tr}\langle \mathbf{B}\,\mathrm{Im}\mathbf{G}(E)\,\mathbf{B}\,\mathrm{Im}\mathbf{G}(E)\rangle = 1/4i\,\mathrm{Tr}\langle \mathbf{B}(\mathbf{G}(E)-\mathbf{G}^*(E)\mathbf{B}(\mathbf{G}(E)-\mathbf{G}^*(E)))\rangle, \tag{3.149}$$

where $\mathbf{G}^*(E)$ is the complex conjugate or advanced Green's function. This requires averages of two Green's functions, such as

$$\mathrm{Tr}\langle \mathbf{B}\mathbf{G}(E)\mathbf{B}\mathbf{G}^*(E)\rangle. \tag{3.150}$$

These average quantities are calculated by inserting into Eq. (3.150) an expansion [like (3.9)] of G in terms of G^0 and the single-particle t-matrices

$$\begin{aligned}\mathrm{Tr}\langle \mathbf{BGBG}\rangle &= \sum_l \langle B(l,n)[G^0(n,m)+\sum_1 G^0(n,1)t_1G^0(1,m)\\ &\quad+\sum_{1\neq2} G^0(n,1)t_1G^0(1,2)t_2G^0(2,m)+\cdots]B(m,p)\\ &\quad\times[G^0(p,l)+\sum_{1'} G^0(p,1')t_{1'}G^0(1',l)\\ &\quad+\sum_{1\neq2} G^0(n,1')t_{1'}G^0(1',2')t_{2'}G^0(2',l)+\cdots]\rangle,\end{aligned} \tag{3.151}$$

where $\mathbf{G}^0$ is the effective medium propagator of Eq. (3.21) and where, in the CPA, the average value of a single $\langle t\rangle$ is zero. Thus, in the same spirit, and consistent with the Ward identity (2.150), only terms with an even number of t's survive the average and then only the average $\langle t_n{}^2\rangle$ is kept, so that the averages in Eq. (3.151) decouple pairwise in a nested fashion:

$$\begin{aligned}&\langle t_1t_2t_3\cdots t_{n-2}t_{n-1}t_n\rangle\\ &\quad\cong\langle t_1\langle t_2\langle t_3\langle\cdots\rangle t_{n-2}\rangle t_{n-1}\rangle t_n\rangle\\ &\quad=\langle t_n{}^2\rangle^{n/2}\delta_{1,n}\delta_{2,n-1}\delta_{3,n-2}\cdots.\end{aligned} \tag{3.152}$$

A typical decoupling of this sort corresponds, in Eq. (3.151), to the diagram shown in Fig. 34, where the solid interaction lines represent single-particle t's. This decoupling is equivalent to having summed the irreducible vertex part shown in Fig. 35 and corresponds to a vertex function

$$\Lambda_{\mathrm{CPA}}=\frac{\delta\Sigma_{\mathrm{CPA}}}{\delta G_0}=\frac{\Sigma_{\mathrm{CPA}}(V-\Sigma_{\mathrm{CPA}})}{1-(V-2\Sigma_{\mathrm{CPA}})G_0}. \tag{3.153}$$

When this decoupling is performed throughout Eq. (3.151) there is left in the middle average term a quantity of the form

$$\langle t_n{}^2\rangle\sum_m G^0(n,m)B(m,p)G^{0*}(p,n). \tag{3.154}$$

But this quantity is zero in any crystal with inversion symmetry, since then $\mathbf{G}^0$ and $\mathbf{G}^{0*}$ are even under inversion and B is, by definition (3.149), odd. Thus all of the CPA vertex contributions vanish in the electrical conductivity, and the only remaining part of Eq. (3.150) is the factorized average $\mathrm{Tr}[\mathbf{B}\langle\mathbf{G}(\omega)\rangle\mathbf{B}\langle\mathbf{G}(\omega)\rangle]$.[1] Therefore the average conductivity (3.147) becomes

$$\langle\sigma\rangle=\frac{2\pi e^2}{\hbar Vk_BT}\int_{-\infty}^{\infty}\frac{dE\exp[(E-\mu)/k_BT]}{\{\exp[(E-\mu)/k_BT]+1\}^2}\times\mathrm{Tr}[\mathbf{B}\langle\mathrm{Im}\mathbf{G}(E)\rangle\mathbf{B}\langle\mathrm{Im}\mathbf{G}(E)\rangle]. \tag{3.155}$$

Using the relation

$$\frac{\exp[(E-\mu)/k_BT]}{\{\exp[(E-\mu)/k_BT]+1\}^2}=-kT\left(\frac{\partial f(E)}{\partial E}\right), \tag{3.156}$$

where $f(E)$ is the Fermi function, together with the definition in Sec. IIID2, we get

$$\langle\sigma\rangle=\frac{2e^2\hbar}{\pi V}\int_{-\infty}^{\infty}dE\left(\frac{-df}{\partial E}\right)\sum_{\mathbf{k}}v(\mathbf{k})^2[\mathrm{Im}\langle G(\mathbf{k},E)\rangle]^2, \tag{3.157}$$

where $v(\mathbf{k})$ is the group velocity of the electron of wave vector $\mathbf{k}$. This formula was evaluated numerically by Velický (1969) for the simple model of elliptic bands discussed in Sec. IIIB above. His calculation was at $T=0$ where the only contribution to the integral is at the Fermi level $E=\mu$. In addition, one unnecessary approximation was made that

$$\sum_{\mathbf{k}}v(\mathbf{k})^2\delta[E-\epsilon(\mathbf{k})]\propto(1-E^2)^{3/2}, \tag{3.158}$$

which eliminates the necessity for having to do the $\mathbf{k}$ sum and yet still gives the correct behavior at the band edge. His results for σ shown in Fig. (36), are for $c=0.1$ and for values of $\delta=V/W=0.005$, 0.5, and 2.0, and are plotted versus the occupied fraction of the host band. For small δ, the Nordheim rule, as discussed below, is valid and the curve is symmetric. For the intermediate $\delta=0.5$, the curve becomes assymmetric, indicating the reduced mobility of the strongly scattered states at the Fermi level when more than 90% of the band is filled. In the split-band regime, $\delta=2$, the conductivity drops by two orders of magnitude when the band is 90% filled. In this situation, however, we expect truly localized states at the Fermi energy and hence $\langle\sigma\rangle\equiv0$, which indicates that the CPA cannot be trusted in this region.

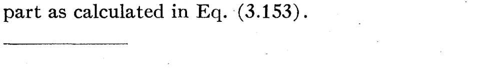

FIG. 35. The single-site, self-consistent (CPA) irreducible vertex part as calculated in Eq. (3.153).

---

[1] The contributions of the vertex corrections to the conductivity will quite generally vanish in any theory containing only s-wave scattering. For example, even with off-diagonal perturbations of the sort described in Eq. (3.93) there will be no vertex contributions to the conductivity.

The reduction of this formula to the usual linearized Boltzmann equation result was discussed in some detail by Velický (1969). We shall not repeat his arguments here, but merely show how the familiar conductivity formulas are reproduced in the limit of weak scattering.

First, we rewrite the **k** sum in Eq. (3.157) as

$$\sum_{\mathbf{k}} v(\mathbf{k})^2[\mathrm{Im}G(\mathbf{k},\epsilon)]^2$$

$$= \int_{-\infty}^{\infty} \rho(E')\, dE'\, v^2(E') \left[\frac{\Gamma}{(E-E'-\Delta)^2+\Gamma^2}\right]^2, \tag{3.159}$$

where $\rho(E')$ is the density of states, $\Delta(E)$ and $\Gamma(E)$ are the **k**-independent values of the real and imaginary parts of $\Sigma(E)$ in the CPA, and spherical energy bands have been assumed so that v can be written as a function only of E (otherwise a more complicated, weighted density of states must be defined). As Δ and Γ go to zero, the most divergent part of Eq. (3.159) is

$$2\pi\rho(E)v^2(E)/\Gamma(E). \tag{3.160}$$

Thus Eq. (3.157) becomes, at $T = 0$,

$$\langle\sigma\rangle = \frac{4e^2\hbar}{V}\frac{\rho(E_F)v^2(E_F)}{\Gamma(E_F)}. \tag{3.161}$$

If in addition $\delta = V/W$ is small, then $\Gamma = \mathrm{Im}\Sigma(\epsilon)$ is given by the optical theorem or by expanding Eq. (3.16) to lowest order in V. The result is

$$\Gamma(E) = c(1-c)V^2\,\mathrm{Im}P(E) + O(V^3). \tag{3.162}$$

This result is symmetric about $c = 0.5$ and leads immediately, via Eq. (3.161), to a conductivity which is symmetric about $c = 0.5$. This is Nordheim's rule, which was first derived from a Boltzmann equation approach (Nordheim, 1931).

For free electrons, Eq. (3.161) reduces still further upon substituting for the group velocity and the density of states at the Fermi level to

$$\langle\sigma\rangle = ne^2\tau(E_F)/m^\star, \tag{3.163}$$

where n is the electron density and $m^\star$ is the electronic effective mass.

It should be pointed out that the development of these formulas in the literature relied heavily on the early work of Edwards (1958, 1959) in the weak scattering limit, and Langer (1960) in the dilute (low c) limit, and was followed by the later calculation of the third- and fourth-order terms in the scattering potential by Verboven (1960) and Moore (1967), respectively.

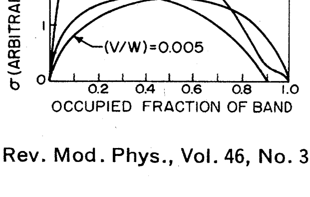

FIG. 36. The CPA dc electrical conductivity versus the occupied fraction of the energy band as given by Eqs. (3.157) and (3.158) for $c = 0.1$ and $\delta = \Delta/W = 2$, 0.5, and 0.005 [after Velický (1969)].

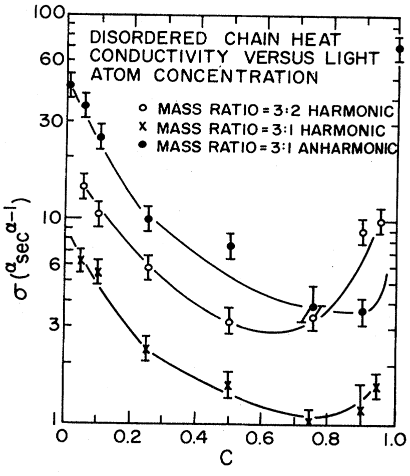

FIG. 37. Lattice thermal conductivity κ for disordered binary linear chains of atoms versus concentration of the two species as obtained by a computer experiment.The error bars are estimates of the accuracy of reading the thermal gradients [after Payton *et al.* (1967)].

The calculation of the contribution to the lattice thermal conductivity in mixed crystals due to impurity or disorder scattering follows quite closely that for the electrical conductivity above. In addition, there exist computer experiments for simple models, so that a detailed evaluation is possible. We begin with a discussion of the computer experiments.

In 1967, Payton *et al.* reported the results of computer experiments to measure the lattice thermal conductivity in harmonic one- and two-dimensional systems. Their one-dimensional experiment was performed for a classical, harmonic linear chain of 100 atoms with only nearest-neighbor forces. They assumed each end of the chain was free of constraint but was struck at random by a Maxwellian distribution of particles at different temperatures. Then the classical equations of motion were followed, and after a steady state was reached the local temperature was measured along the chain, as well as the heat flow through each end. They used the resulting bulk internal temperature gradient, which turned out to be considerably less than the applied temperature gradient due to a large surface resistance, to calculate the thermal conductivity. Their results are shown in Fig. 37 at all concentrations for harmonic chains of mass ratio 3:1 and 3:2. Also shown in Fig. 37 are their results for an anharmonic linear chain of mass ratio 3:1. Surprisingly they found that the thermal conductivity went up as the anharmonicity was added, a gross violation of Mattheisen's rule. Since clearly localized modes are present, this is presumably due to a transport mechanism whereby phonons hop from localized state to localized state via intermediate decay into two band state phonons, but no analytic theory has given a detailed explanation to date.

The CPA evaluation (Flicker and Leath, 1973) of Eq. (2.83) follows quite parallel to that for the electrical conductivity. The vertex corrections again vanish for crystals with inversion symmetry when only mass defect scattering

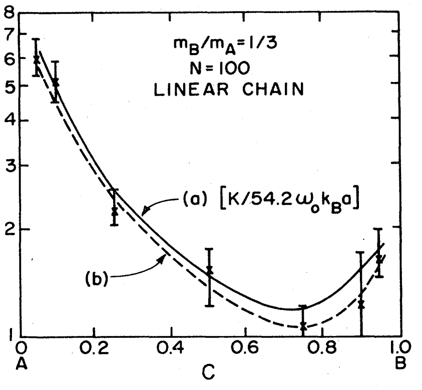

FIG. 38. Lattice thermal condctivity κ versus concentration for disordered binary linear chains. A comparison of the CPA results (solid line) with the computer experiments of Payton *et al.* (1967) as in Fig. 38 (dashed line). The CPA formula has been divided by 10.8 for this comparison [after Flicker and Leath (1973)].

is included and no off-diagonal diagrams are included in $\Sigma(\omega)$. Thus one finds that Eq. (2.83) reduces to

$$\langle\kappa\rangle = \frac{-2\hbar^2}{\pi V k_B T^2}\int_{-\infty}^{\infty} d\omega\, \frac{\omega^2 \exp(\hbar\omega/k_BT)}{[\exp(\hbar\omega/k_BT) - 1]^2} \times \mathrm{Tr}[A^\alpha\langle \mathrm{Im}G(\omega)\rangle A^\alpha \langle \mathrm{Im}G(\omega)\rangle], \qquad (3.164)$$

where V is the volume of the sample. This formula was studied by Flicker and Leath (1973) who noted an infrared divergence, so that $\langle\kappa\rangle$ as given by Sec. IIID14 is infinite. This arises because $A(\mathbf{k})$ is proportional to $v(\mathbf{k})$ and $v(\mathbf{k})$ goes to the speed of sound as $\mathbf{k} \to 0$, rather than vanishing. The result is that the integrand of Eq. (3.164) diverges as ω^{-2} for small ω so that $\langle\mathbf{k}\rangle$ diverges linearly with N (the number of atoms in the chain) for large N. This divergence does not occur in the electronic problem, since the low energy electrons move slowly. The low-frequency phonons have a mean free path which diverges at low $\mathbf{k}$ and yet they move at the speed of sound, so that they do not come into thermal equilibrium with each other unless there are scattering mechanisms which allow them to dissipate energy into other modes.

The addition of another scattering mechanism such as boundary scattering or anharmonic phonon–phonon scattering removes this divergence so that the effect of disorder can be calculated. The approach developed by Woll (1965), in the dilute limit, is to cut off the integral [Eq. (3.161)] at $\omega_{\min}$ the lowest-frequency phonon allowed in a finite crystal of size N. This procedure can only be approximate, since in a finite crystal the discrete nature of all the mode frequencies should be included. The CPA results using this approximation (Flicker and Leath, 1973) are shown in Fig. 38 in comparison with the harmonic chain results of Payton *et al.* (1967), discussed above. Numerically, the overall magnitude is off by a factor of about 10 (which depends upon the exact boundary conditions), but the concentration dependence is quite good. In particular, the assymmetry about $c = 0.5$, due to the effective scattering by low-frequency resonant phonon modes about isolated heavy atoms, is quite well reproduced.

Similar results were obtained by Flicker and Leath (1973) for a simple cubic lattice, although the assymmetry is a bit less (Fig. 39). In this three-dimensional case they also considered the additions of a phonon–phonon-like scattering term, via an assumed Mattheisen's rule, to the impurity scattering. The resulting, reduced value of $\langle\kappa\rangle$, shown also in Fig. 39, illustrates that the effect of this anharmonic contribution is to flatten and make more symmetric the $\langle\kappa(c)\rangle$ curve.

It is useful at this point to also verify that the formulae developed here reduce to that previously derived by many authors using a Boltzmann equation approach. We begin by evaluating the trace in the integrand of Eq. (3.164) in the normal mode representation of the perfect lattice, where it becomes

$$\sum_{\mathbf{k}j} A^\alpha(\mathbf{k},j)^2\langle \mathrm{Im}G(\mathbf{k},j)\rangle^2 = \sum_{\mathbf{k}j}\omega_j(\mathbf{k})v_j^\alpha(\mathbf{k}) \times \left[\frac{\mathrm{Im}\Sigma(\omega)}{[M(\omega^2 - \omega_j^2(\mathbf{k}) - \mathrm{Re}\Sigma(\omega)]^2 + [\mathrm{Im}\Sigma(\omega)]^2}\right]^2. \qquad (3.165)$$

Upon interchanging the order of the resulting $\mathbf{k}$ summation and ω integration in Eq. (3.164) the ω integral can be done by contour integration in the weak scattering limit [$\mathrm{Re}\Sigma(\omega)$ and $\mathrm{Im}\Sigma(\omega)$ small compared to $M\omega_j^2(\mathbf{k})$ at resonance]. In this limit the dominant residue gives, for Eq. (3.164),

$$\kappa = \frac{M_0\hbar\beta}{VT}\sum_{\mathbf{k}j}\frac{\omega_j^2\exp\{\hbar\omega_j(\mathbf{k})/k_BT\}[v_j^\alpha(\mathbf{k})]^2}{\{\exp[\hbar\omega_j(\mathbf{k})/k_BT] - 1\}^2[\mathrm{Im}\Sigma(\omega)]}, \qquad (3.166)$$

which can be written in the form

$$\kappa = \frac{1}{V}\sum_{\mathbf{k}j} C_{\mathrm{ph}}[\omega_j(\mathbf{k})]\tau_j(\mathbf{k})\,|\,v_j(\mathbf{k})\,|^2\cos^2\theta, \qquad (3.167)$$

where

$$C_{\mathrm{ph}}(\omega) = \hbar^2\omega^2\exp(\hbar\omega/k_BT)/\{k_BT^2[\exp(\hbar\omega/k_BT) - 1]^2\}$$

is the specific heat contribution of a phonon of frequency ω,

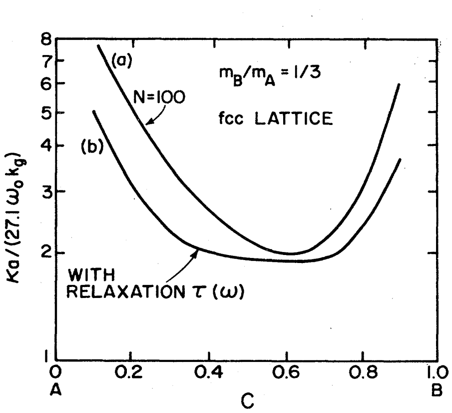

FIG. 39. (a) The CPA thermal conductivity of a $100 \times 100 \times 100$ atom harmonic fcc lattice versus concentration; (b) the same theory but with an added umklapp scattering term in the self-energy [after Flicker and Leath (1973)].

and if the relaxation time $\tau_{\mathbf{k}j}$ for phonon $(\mathbf{k}, j)$ is identified as

$$\tau_j(\mathbf{k}) = M\omega_j(\mathbf{k})/\{\mathrm{Im}\Sigma[\omega_j(\mathbf{k})]\}. \tag{3.168}$$

This result (3.167) is identical with the usual result derived by kinetic theory or via the Boltzmann equation (Carruthers, 1961).

With regard to the divergence of $\langle\kappa\rangle$ for large N, it should be pointed out that some analytic progress has been made on the exact form of $\langle\kappa\rangle$ for linear chains. In particular, Casher and Liebowitz (1971) have proven that, for disordered harmonic linear chains, the thermal conductivity κ diverges as N with probability one if the spectral density $\rho(\omega)$ has an absolutely continuous part as a function of ω. Matsuda and Ishii (1971) had previously shown (using a transfer matrix technique) that κ diverges as $\kappa^{1/2}$ for binary, mass-disordered linear chains and this led Casher and Liebowitz to conclude that the spectral density in this case has no absolutely continuous part. Apparently also [see Visscher (1971)] the form of the divergence depends strongly on the form of the boundary conditions at the ends of the chain. Finally, there remains the problem of fundamental divergences in the cluster expansion (Langer and Neal, 1966) arising from higher-order terms which are well known in the general theory of virial expansions of transport coefficients in statistical mechanics. Clearly much work remains to be done on transport coefficient in highly disordered systems.

IV. COMPARISON WITH EXPERIMENT

A. Electrons

In addition to the model calculations described in Secs. IIIB, and C there have been a number of attempts to derive the electron energy levels in alloys using realistic band structures, and to compare the results with experiment.

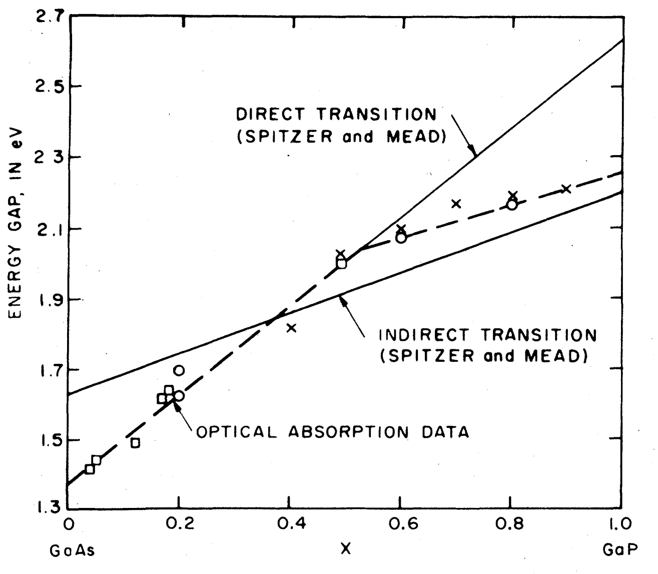

FIG. 40. The variation of energy gap in $\mathrm{GaAs}_{1-x}\mathrm{P}_x$. The abrupt change is due to a crossing of the conduction bands. At the As rich end the lowest conduction band is at the point Γ which at the P rich end it is at Δ. Each band moves linearly in the VCA. The points are the results of optical experiments. [after Long (1966)].

1. *Energy bands*

The virtual crystal approximation is widely used in interpreting band structures of mixed crystals. It is fairly satisfactory for s and p bands in simple metals and in semiconductors like alloys of Si–Ge or of III–V compound (Herman *et al.* 1957; Long, 1966). The predicted linear shift of the bands with concentration is often borne out by optical experiments. The width of the $\mathbf{k}$ states is usually small, indicating that changes in potential are small compared to bandwidths. See Fig. 40.

Stroud and Ehrenreich (1970) examined the application of the CPA method to Ge–Si alloys, using pseudopotentials and projecting out core states. To place it in context of a diagonal disorder potential they took the local potential difference

$$\Delta = \tfrac{1}{3}[(V_{111} + V_{220} + V_{311})_{\mathrm{Si}} - (V_{111} + V_{220} + V_{311})_{\mathrm{Ge}}], \tag{4.1}$$

where the subscripts refer to reciprocal lattice points. Using parameters obtained by Brust (1964) to fit the perfect materials, Δ is found to be 0.023 Ry. The relative changes vary with band, but are less than 0.1 Ry, and the broadening is only 0.01 Ry. Since typical bandwidths are $\sim$0.5 Ry it is not surprising that the CPA and VCA descriptions differ little overall. The virtual crystal and CPA are compared in Fig. 41 for an $\mathrm{Si}_{0.37}\mathrm{Ge}_{0.63}$ alloy.

A substantial series of applications to transition metal alloys have developed following the work of Soven, particularly by Velický *et al.* (1968, 1970), who established a useful model Hamiltonian to discuss Cu–Ni alloys, for example, and also derived theorems on the moments of the energy spectrum, and bounds for certain models. A more complete treatment has been given for the Cu–Ni system by Stocks *et al.* (1971), who calculated density of states and electronic specific heat. In all cases one is dealing with a "two-band" system and $H = H_{ss} + H_{sd} + H_{dd}$ where the s and d subscripts have obvious meaning; the s band is wide, while the d band is narrow, or even assumed to have zero width for some purposes. Assuming a site-diagonal energy difference for d states $\Delta^{dd}(\text{Cu–Ni}) = -0.134$ Ry, but the same s parameters for Cu and Ni, it was possible to carry through the CPA. With the assumed Δ, the resulting density of states is not quite separated into two peaks [rather like the model calculations in Figs. 21 and 22 with δ slightly less than 1.0]. The density of Cu and Ni states, defined by $G^d(0)$ or $G^h(0)$ in Sec. IE3, show two peaks separated by about 0.2 Ry [Fig. (42)]. Comparison has been made to the optical density of states from photoemission data (Seib and Spicer, 1970; Eastman and Krolikowski, 1968) by making simple assumptions about the photoemission process (see Sec. IIC6). Considering experimental and model potential uncertainties, the agreement is satisfactory. In addition, comparison may be made to soft x-ray data (Farineau and Morland, 1938; Freedman and Beeman, 1940; Azaroff and Das, 1964; Kunz and Gudat, 1972), where a weighted average of the Green's function is required (Sec. IIC6) which was not studied; but Stocks *et al.* (1971) conclude that the gross features agree with the CPA calculations.

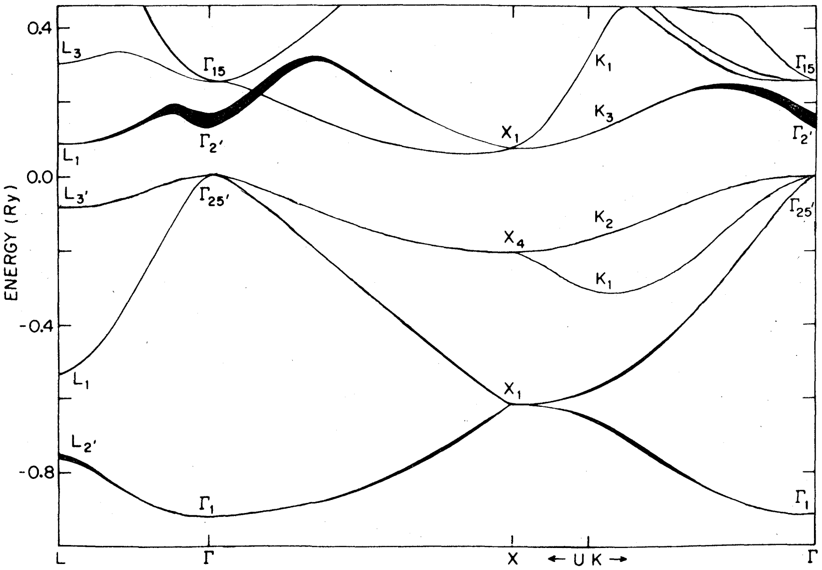

FIG. 41. The energy bands of $Si_{0.37}Ge_{0.63}$ as calculated by Stroud and Ehrenreich (1970) using the CPA. The width of the lines (given by IMΣ) is small compared to the bandwidths.

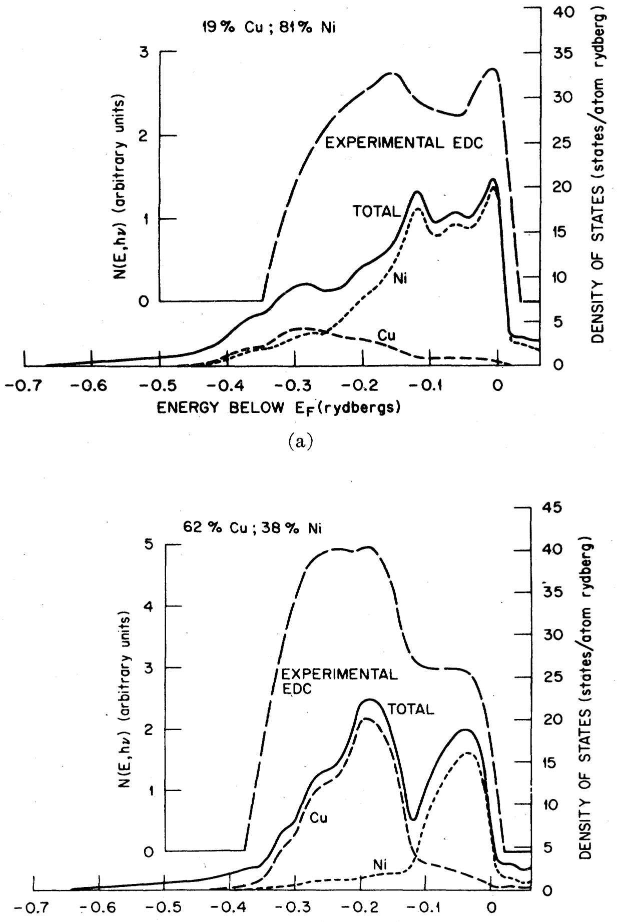

(a)

(b)

FIG. 42. Density of states in $Cu_{0.19}Ni_{0.81}$ and $Cu_{0.62}Ni_{0.38}$ as calculated by Stocks *et al.* (1971). The weighted densities of states associated with each constituent are also shown. The results are compared with the photoemitted electron distribution measured by Seib and Spicer (1970).

A similar CPA calculation has been performed for the d bands in AuAg alloys by Levin and Ehrenreich (1971), and compared with the ATA by Schwartz *et al.* (1971). The CPA was used on a diagonal d-band energy $\Delta^{dd}(\text{Au–Ag}) \sim 1.6$ eV. Thus the Green's function takes the form

$$G(\mathbf{k}, E) = \begin{pmatrix} G_{ss} & G_{sd} \\ G_{ds} & G_{dd} \end{pmatrix} = \begin{pmatrix} E - E_s(\mathbf{k}) & \bar{\gamma} \\ \bar{\gamma} & E - E_d(\mathbf{k}) - \Sigma_d \end{pmatrix}^{-1}, \tag{4.2}$$

where $E_s(\mathbf{k})$ is the s-band energy and $\bar{\gamma}$ is the s–d hybridization matrix element which is assumed independent of $\mathbf{k}$. Both are taken in the virtual crystal approximation. The CPA equation is

$$\Sigma_d = c\Delta / [1 - (\Delta - \Sigma_d) G_{dd}(0)]. \tag{4.3}$$

The resulting doubly peaked density of states agrees well with optical absorption (Beaglehole and Erlbach 1970). Schwartz *et al.* (1971) made a critical comparison between ATA and CPA for this case and show that there is little quantitative difference.

2. *Specific heat*

A considerable number of experimental results are available on the low-temperature specific heat γ of alloys, particularly its variation with concentration. Since γ depends only on $\rho(E_F)$ (except for many electron effects), it is a property which is not sensitive to the full details of the band structure as discussed above. For this reason even the VCA may be satisfactory. This is useful in systems like Ag Pd alloys since Ag and Pd are adjacent in the periodic table. However, even here d-band effects become important as the Pd concentration increases. A detailed discussion has been given by Lee and Lewis (1969).

On the other hand, when the constituents are quite dissimilar, particularly in valence, the scattering potential is large and the VCA fails. Dawber and Turner (1966) have given a low concentration theory of the effect using $\Sigma^{(1)} = ct$, where t is the single defect t-matrix. They show that to first order in c the change in density of states is (P as defined in Sec. IID)

$$\Delta\rho = \mathrm{Im}[\Sigma^{(1)}(\partial P/\partial E)]. \tag{4.4}$$

If a phase shift η is defined by

$$\tan\tfrac{1}{2}\eta = \frac{\Delta\pi\rho(E)}{|1-\Delta P(0)|}, \tag{4.5}$$

then

$$\Delta\rho(E_F) = \frac{C}{2\rho(E_F)}\left[\sin 2\eta\left(\frac{\partial\rho}{\partial E_F}\right) - 2\sin^2\eta\,\frac{\partial P_R}{\partial E_F}\right]. \tag{4.6}$$

If only a diagonal change is assumed in V, only the s-wave phase shift is affected, and the Friedel sum rule (to accomodate one electron) requires $\sin\eta = 1$ whence $1 - \Delta P_R(E_F) = 0$ and a resonance right at E_F is always required. To get around this they propose use of an effective charge Z', to be screened by the s-wave charge density, so that $\eta = \pi Z'$. By suitable choice of Z' they can account for specific heat γ observed.

This difficulty with charge conservation and the Friedel sum rule has been discussed more recently by Stern (1971), who shows that this problem is unavoidable with the choice of zero range scattering forces. A more physical description of the alloy requires extended, or "off-diagonal" potentials; even so, charge conservation is a real issue, which must be attended to by adjustment of the potential parameters, as was discussed in more detail in Sec. IIIC2. Clark and Dawber (1972) have also proposed a pseudopotential model for dealing with alloys whose constituents have different bandwidths.

The CPA calculation of Stocks *et al.* (1971) for Cu–Ni alloys discussed above was used to compute the electronic specific heat from the density of states at the Fermi level. Comparison with experiment is shown in Fig. 43; the structure appearing in the experimental curve is probably due to the fact that the alloys become ferromagnetic for Cu concentrations less than 56%.

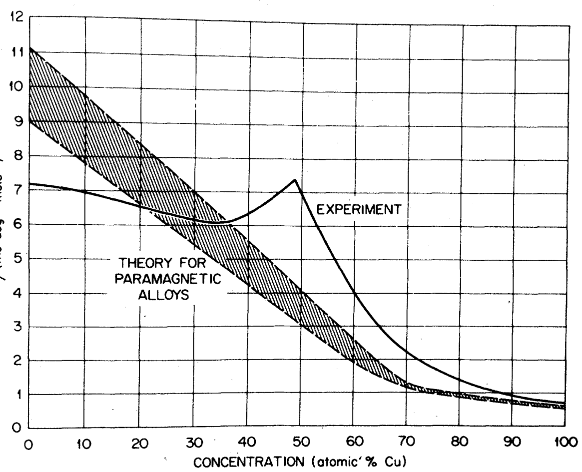

FIG. 43. The low T specific heat γ in Cu–Ni alloys. The shaded area gives the range of results predicted by Stocks *et al.* (1971) using the CPA. The experimental curve is by Dixon *et al.* (1968).

3. *Magnetic susceptibility*

The Pauli spin susceptibility is, in a simple model, also proportional to the density of states at E_F. In static experiments it is often difficult to separate this contribution from the diamagnetic component. The knight shift measures the s component of electron spin moment at the nucleus and hence a weighted susceptibility at particular atomic sites, proportional to $\rho_s{}^d(E_F)$ or $\rho_s{}^h(E_F)$. It is this s-electron density at the nucleus which is studied in the resonance experiment. Some discussion of this matter is given by Blackman and Elliott (1970), using simple band models. There is little experimental work or comparison with theory to date [for a review see Drain (1967), p. 211].

Recently there has been a considerable amount of work on the magnetic susceptibility of transition metal alloys where exchange enhancement is important and the simple Pauli idea is inappropriate (Levin *et al.*, 1972; Harris and Zuckerman, 1972; and Hasegawa and Kanemori, 1970). All these authors use the Hubbard model (see Sec. IIIC5) where the effective Hamiltonian is

$$\mathcal{H} = \sum_{l\sigma} E_\sigma(l)a_\sigma{}^+(l)a_\sigma(l) + \sum_{\sigma ll'} W(l,l')a_\sigma{}^+(l)a_\sigma(l') + \sum_l I(l)n_\pm(l)n_\mp(l) \tag{4.7}$$

for a single band with two spin orientations. The last term is taken to give an effective field, and the effective site energy

$$E_\pm(l) = E(l) \pm \beta H + I(l)n_\mp(l) \tag{4.8}$$

which depends on the number of electrons at this site—to be determined self-consistently. For low T

$$n_\mp(l) = \int_0^{E_F} \rho_\mp(l,E)\,dE \tag{4.9}$$

and again $\rho_\pm(l)$ is defined by a trace of an appropriately projected Green's function [Eq. (2.56)]. Fixing the total number of electrons determines E_F.

In the CPA n is calculated from the weighted average density of states appropriate to the atom involved. Thus $E(l)$, $I(l)$, and $n(l)$ will depend on the type of occupation of site l. In the paramagnetic state the static spin susceptibility is

$$\chi = \lim_{H\to 0}\frac{\beta}{H}[n_{+\sigma}(H) - n_{-\sigma}(H)] \tag{4.10}$$

and for a binary alloy $\chi = c\chi^{\mathrm{A}} + (1-c)\chi^{\mathrm{B}}$. After considerable manipulation the CPA yields

$$\chi^{\mathrm{A}} = 2\beta^2\left[\frac{\rho^{\mathrm{A}}(E_F)(1+I^{\mathrm{B}}f^{\mathrm{BB}}) - \rho^{\mathrm{B}}(E_F)I^{\mathrm{B}}f^{\mathrm{AB}}}{(1+I^{\mathrm{A}}f^{\mathrm{AA}})(1+I^{\mathrm{B}}f^{\mathrm{BB}}) - I^{\mathrm{A}}I^{\mathrm{B}}f^{\mathrm{AB}}f^{\mathrm{BA}}}\right] \tag{4.11}$$

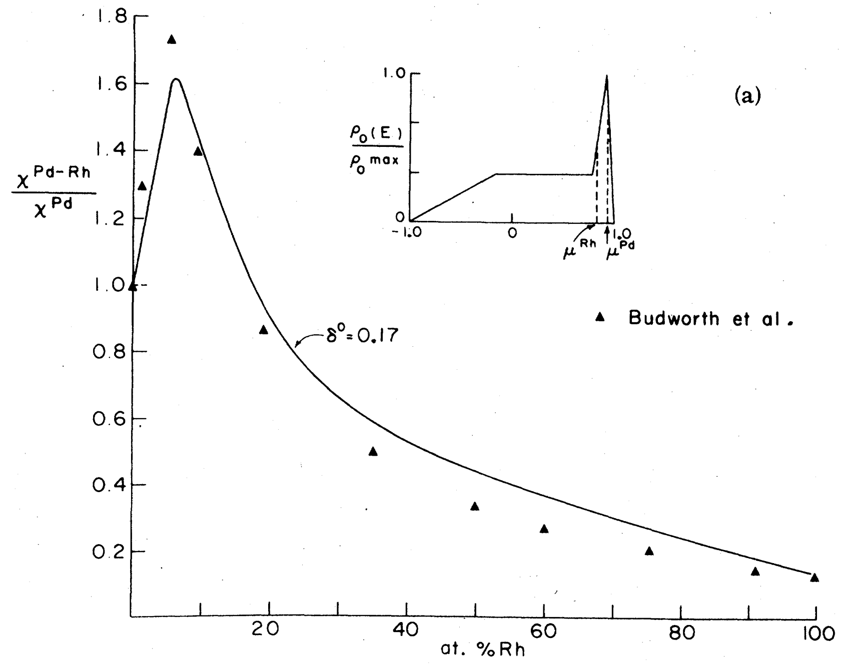

FIG. 44. Susceptibility of Pd–Rh alloys calculated by Levin, Bass and Bennemann (1972) using the CPA with the model density of states shown. $\delta = \Delta/W$ (in units of the half bandwidth) was taken as 0.17. The experimental points are Budworth *et al.* (1960).

and a similar expression for χ^B; here $f^{ij} = \partial n_\sigma{}^i/\partial E_\sigma(j)$. These equations, together with charge conservation, may be solved self-consistently in the limit $H \rightarrow 0$. Note that exchange enhancement now appears in such a way as to involve the parameters of both atoms. Both the weak scattering limit and the dilute alloy case are discussed by Levin *et al.*, and the expressions reduced somewhat. In particular, the condition (for dilute alloys) for the formation of local magnetic moments reduces to $(1 + I^A f_0{}^{AA}) = 0$, the zero subscript referring to the host. The theory, with computations, was applied by Levin *et al.* (1972) to several Ni, Rh, and Pd alloys, giving satisfactory agreement with the concentration dependence of χ (Fig. 44). Despite the fact that s electrons were neglected and only a simplified d-band model was used, it appears that the relative electron density, and therefore exchange enhancement, is well estimated by CPA. Several extensions to ferromagnetic systems have also been made. Hasegawa and Kanemori (1972) have calculated magnetic moments in Fe and Ni alloys (Fig. 45). Apparently the alloy Green's function methods are a useful basis for computing magnetic properties of random alloys.

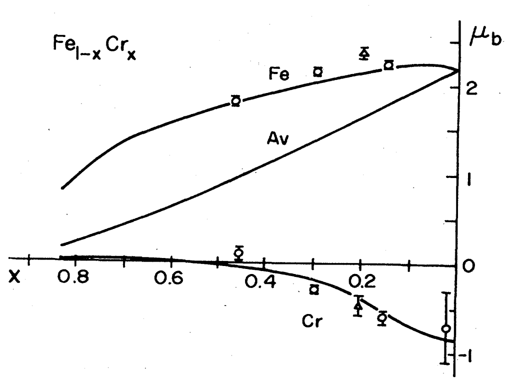

FIG. 45. The magnetic moments in Fe–Cr alloys as calculated from a model density of states using the CPA compared with experimental results on the average moments, and on the constituent moments determined by neutron diffraction [after Hasegawa and Kanemori (1972)].

4. *Resistivity*

As discussed in Sec. IIC5, the electrical conductivity of a metal is related to the two-particle Green's function, although, if many-body effects are neglected, it can be reduced [Eq. (2.82)] to the product of single-particle G's. In Sec. IIID the application of the CPA to the average of this product is discussed. It was shown that under certain further approximations the expression for σ can be reduced to the familiar expression of kinetic theory $\sigma = (Ne^2\tau/M^*)$ where τ, the relaxation time, is related to the width of $G(\mathbf{k}, E)$ for states with $E(\mathbf{k}) = E_F$.

The results expected on this model were set out by Nordheim in 1931 [see Mott and Jones (1958)]. If Δ is small, the VCA gives a shift of the energy levels by $c\Delta$. The fluctuations around this mean give, in Born approximation,

$$1/\tau = (2\pi/\hbar)c(1-c)\Delta^2\rho(E_F) \tag{4.12}$$

and a resistivity proportional to $c(1-c)$. This gives a satisfactory description of the residual resistivity of alloys like $Au_{1-c}Cu_c$. When Δ is larger, the ATA gives a reasonable approximation. In this case,

$$\hbar/\tau = \mathrm{Im}\langle t\rangle = \mathrm{Im}[c(1-c)\Delta^2 G^v/(1-\Delta G^v)] \tag{4.13}$$

using Eq. (3.19), where G^v is the Green's function in the virtual crystal. Equation (4.12) is obtained for this by neglecting the denominator. Dawber and Turner (1966) have used this expression in a low c theory when $G^v = G^h$. Using the phase shift defined in Eq. (4.5)

$$\hbar/\tau = \tfrac{1}{2}\Delta c(1-c)\sin\eta. \tag{4.14}$$

The results of this theory suffer from the difficulty described in the last section, arising from the fact that the diagonal form of V gives only one phase shift which should be chosen according to the Friedel sum rule to be $\pi/2$.

The most complete theory of the conductivity of alloys has been given by Brouers and Vedyayev (1972), using the *s–d* band model for transition metal alloys introduced by Ehrenreich and Levin and discussed above. Only weak scattering is introduced into the s band, but the large self-energy in the d band is calculated by the CPA. This gives a large contribution to the resistivity through the *s–d* mixing, and the resulting total ρ depends strongly on the amount of d-mixing which occurs in states with $E\sim E_F$. This can result in large deviations from Nordheim's rule (Fig. 46).

The special case of the resistivity of ferromagnetic transition metal alloys has recently been considered by Harris and Zuckerman (1972), who used the ATA and applied their results to Pd–Ni alloys, and by Brouers *et al.* (1973c), who used the CPA and applied the theory to Cu–Ni alloys. Both used the Hubbard Hamiltonian (4.7). This theory involves the self-consistent calculation of G_s and G_d for spin-up and spin-down bands. This gives rise to a spontaneous anisotropy of the resistance relative to the magnetization direction.

In addition to the resistivity caused by static defects, some consideration has been given to the effect of them on dynamics. Kagan *et al.* have considered the way in which phonon (1966) and magnon (1968) scattering of electrons is affected by the change in the excitation spectrum of these quasiparticles. This is entirely a low c theory and shows that a strong resonance in the spectrum at low energies can give an anomalous temperature dependence to the resistivity.

B. Phonons

Phonons are the form of elementary excitation which have been most extensively studied in mixed crystals. However, because of the complexity of the calculations, detailed comparison between theory and experiment on the basis of realistic models has not been extensive. There are always several branches to a phonon spectrum, and force-constant changes are often important. Nevertheless model calculations have been mainly on mass changes and fairly simple phonon spectra have been compared quite successfully in some cases. The most detailed information about phonons comes from inelastic neutron scattering, but relatively few experiments have yet been performed. Much more attention has been given to the optical properties of mixed ionic crystals, and there are some results on thermal properties.

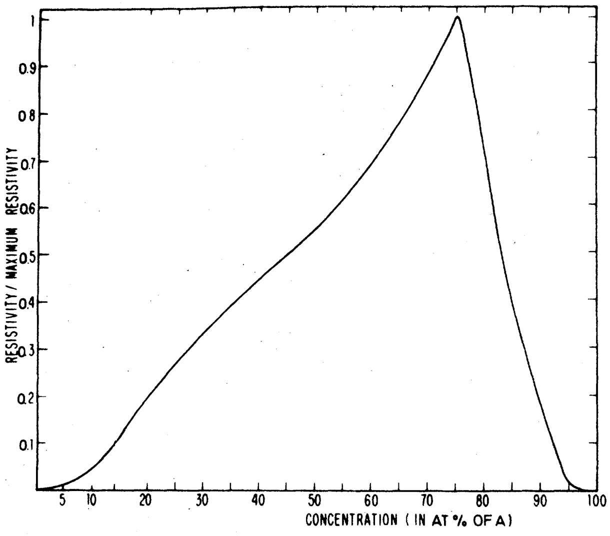

FIG. 46. The residual electrical resistivity of an alloy calculated by Brouers and Vedyayev (1972) using the *s-d* hydridization model and the CPA. The asymmetry is caused by an increase in the *s-d* mixing at the Fermi level. The Nordheim theory would give a symmetric parabolic curve.

1. Inelastic neutron scattering

As discussed in Sec. IIC3, inelastic neutron scattering consists of a coherent and incoherent part, because of the isotopic and spin dependence of the nuclear scattering. Each cross section [Eqs. (2.68) and (2.69)] depends on the averaged and weighted Green's functions defined in Sec. IIE3. Specifically, the incoherent part depends on the Green's function at a single site,

$$\frac{d^2\sigma}{d\Omega dE}=\frac{1}{\pi}\frac{K'}{K}\sum_{\alpha\mathrm{A}}\beta_\alpha{}^{\mathrm{A}^2}q_\alpha{}^2\,\mathrm{Im}\langle G_{\alpha\alpha}{}^{\mathrm{AA}}(0,0,E)\rangle, \tag{4.15}$$

where A defines the atomic species at site α. For a binary alloy A will be host h or defect d, so that the result can be written in terms of the unweighted average $\mathbf{G}$ by using Eqs. (2.136) and (2.137). The sum becomes

$$V^{-1}[\beta^{h2}(V-\Sigma)+\beta^{d2}\Sigma]\,\mathrm{Im}\langle G(0,0,E)\rangle. \tag{4.16}$$

The coherent cross section (2.69) becomes

$$\frac{d^2\sigma}{d\Omega dE}=\frac{1}{\pi}\frac{K'}{K}\sum_{\alpha\alpha',\mathrm{AA}'}B_\alpha{}^{\mathrm{A}}B_{\alpha'}{}^{\mathrm{A}'}q_\alpha q_{\alpha'}\,\mathrm{Im}\langle G_{\alpha\alpha'}{}^{\mathrm{AA}'}(\mathbf{q},E)\rangle \tag{4.17}$$

which depends on weighted averages of $G(\mathbf{q},E)$. For the binary case this can be written using Eqs. (2.140)–(2.142) as

$$\begin{aligned}&\mathrm{Im}[B^h-(B^h-B^d)(\Sigma/V)]^2\langle G(\mathbf{q},E)\rangle\\&\quad+(B^h-B^d)^2(\Sigma-cV)/V^2.\end{aligned} \tag{4.18}$$

The last term comes from the correction terms in Eqs. (2.140)–(2.142), which arise from the different weighting of the $\langle G(0,0,E)\rangle$ terms. It can be regarded in some sense as an incoherent component arising from the random distribution of coherent scatterings. The first factor gives the coherent scattering with an effective scattering length $[B^h-(B^h-B^d)\Sigma/V]$. However this divison is somewhat arbitrary. If we use the CPA approximation for Σ and $\langle\mathbf{G}\rangle$, Eq. (4.18) can also be written, after some manipulation, as

$$[B^h-(B^h-B^d)/VP(\mathbf{q},E)]^2\,\mathrm{Im}\langle G(\mathbf{q},E)\rangle \tag{4.19}$$

with a different effective scattering length and no extra term. For a complex crystal with several phonon branches j, and eigenvectors $\sigma_j(\mathbf{q})$ as defined by Eq. (2.14), the general

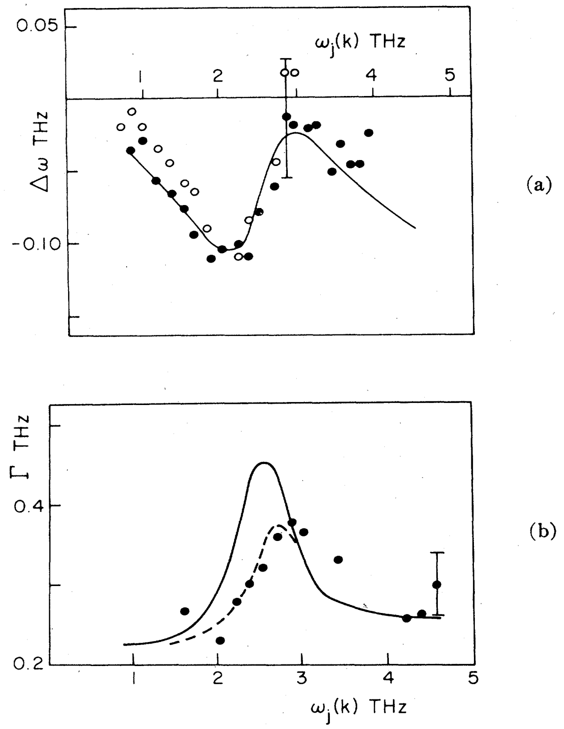

FIG. 47. (a) The frequency shift in $Cu_{0.97}Au_{0.03}$ along the (110) direction as measured by Svensson and Kamitakahara (1971) compared with the theory of Bruno and Taylor (1971) using the ATA. The difference from Fig. 14 is mainly due to a shift due to lattice dilation using the Gruneisen constant. Force-constant changes are also included. (b) The mode width in the (100) direction for the same alloy. The full line is due to mass change only (as in Fig. 14), the dashed curve includes force-constant changes.

expansion is

$$\sum_{\alpha,\beta j} [q^{\alpha}\sigma_j^{\alpha}(\mathbf{q})][q^{\beta}\sigma_j^{\beta}(\mathbf{q})] \times [B^h - (B^h - B^d)/VP_j(\mathbf{q}, E)]^2 \,\mathrm{Im}\langle G_j(\mathbf{q}, E)\rangle. \tag{4.19a}$$

Experimental observations have been mainly concerned with the coherent cross section which contains the most information. There have been two extensive investigations of the effect on a relatively small concentration of heavy defects in a simple crystal of light atoms, where a well-defined low-frequency resonance is expected. The first is on $Cu_{1-x}Au_x$, $x < 10\%$ by Svensson and Kamitakahara (1971) [see also Svensson *et al.* (1965, 1969)]. The shift and width of the phonons are predicted by Elliott and Taylor (1967) using the ATA to show a well-defined resonance (see Fig. 14). The experimentally observed resonance is much broader and depends in detail on the direction of **k** (Fig. 47). This indicates that force-constant changes are important, and recently Bruno and Taylor (1971) have made a detailed analysis of this by extending the theory of Lakatos and Krumhansl (1969). They conclude that anharmonic effects arising from lattice dilation are also important in inducing shifts. The effect of short-range order, as discussed by Hartmann (1968), is not important.

The other system of this type which has been studied in detail is $Cr_{1-x}W_x$ by Mackintosh and Moller (1968) and Cunningham *et al.* (1970). This also shows a well-defined resonant effect on the shifts and widths, and the detailed form does not agree precisely with the prediction of the mass defect in the ATA. Cohen and Gilat (1972) have shown that this is due to force-constant changes and have proposed a simplified theory to include these effects.

Another class of experiments involves low concentrations of light mass defects where a sharp impurity band is to be expected. The most detailed experiments to date are on

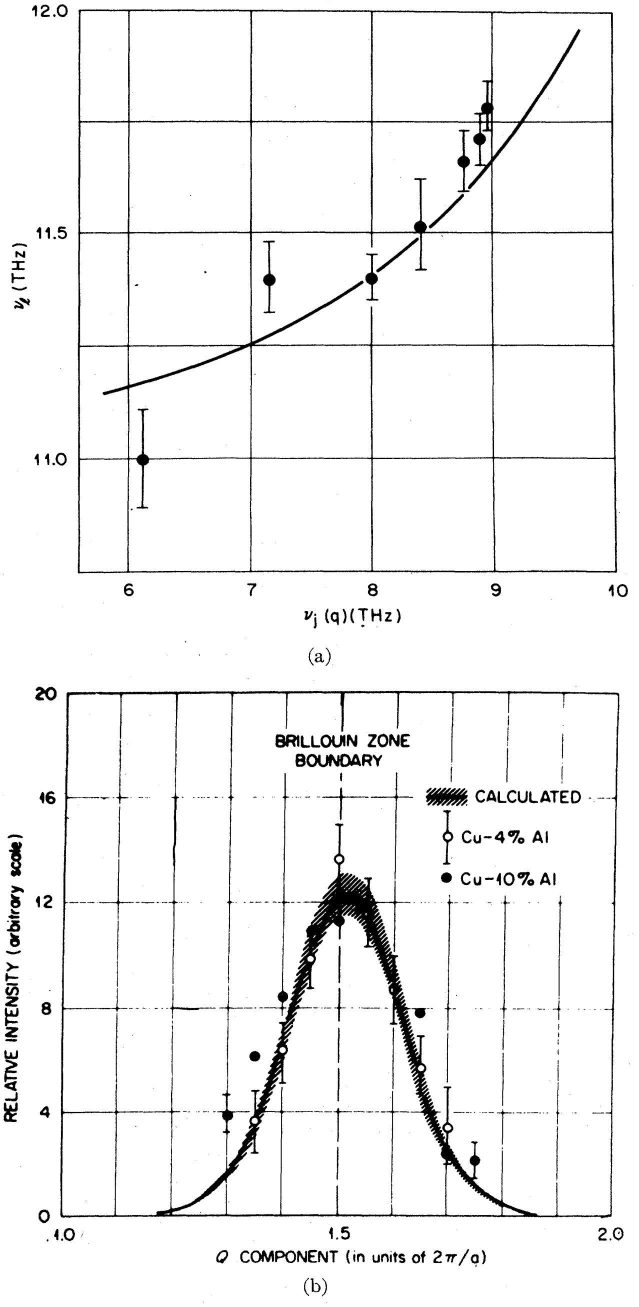

FIG. 48. (a) The peak frequency of the impurity band in $Ge_{0.91}Si_{0.09}$ as a function of **q** [after Wakabayashi *et al.* (1971)]. (b) The intensity of impurity band scattering in $Cu_{1-x}Al_x$ as a function of **q** [after Nicklow *et al.* (1968)].

$Cu_{1-x}Al_x$ at $x < 10\%$ by Nicklow *et al.* (1968) and $Ge_{1-x}Si_x$ by Wakabayashi, Nicklow, and Smith (1971). They compare the scattering with the prediction of the ATA. They show that in the Si–Ge case there is an apparent dispersion in the impurity band which is predicted by the pole of Eq. (3.17) in this region using Eq. (3.16) for Σ where $\Delta = M\epsilon\omega^2$ from Eq. (2.18) and

$$P(0) = \frac{1}{M}\sum_j \int \frac{d\mathbf{q}}{\omega^2 - \omega_j^2(\mathbf{q})}$$

from Eq. (2.51). If ω_l is the isolated localized mode frequency given by Eq. (2.100), the dispersion is

$$\delta\omega_l(\mathbf{q}) = c\left[1 - \frac{\epsilon\omega_l^2}{\omega_l^2 - \omega_j(\mathbf{q})^2}\right] \Big/ \left[\frac{d}{d\omega}\,\epsilon\omega^2 P(0,\omega)\right]_{\omega=\omega_l}. \tag{4.20}$$

The results of this approximation are compared with experiment in Fig. 48. The intensity of the impurity band scattering also depends strongly on $\mathbf{q}$, as was observed in the CuAl case. From Eq. (4.19) we see that this is proportional to

$$\left[\frac{B_h}{\omega_l^2 - \omega_j^2(\mathbf{q})} - \frac{(B_h - B_d)}{\epsilon\omega_l^2}\right]^2 \Big/ \left[\frac{d}{d\omega}\,\epsilon\omega^2 P(0,\omega)\right]_{\omega=\omega_l} \tag{4.21}$$

and the strong variation of the first term is reflected in the results shown in Fig. 48. The shift of the band modes was also studied in their experiments. Experiments on incoherent scattering of dilute vanadium alloys have been reported by Mozer (1968). He has found structure in the impurity band of Be_xV_{1-x} at $x = 3\%$ which is expected in the ATA. He also obtained information on the density of modes in Cr_xV_{1-x} $x = 25\%$, where the mass difference is very small $\epsilon \sim 0.04$.

There have also been measurements on various metal alloys, notably NbMo (Woods and Powell, 1965), Bl–Pb–Tl (Ng and Brockhouse, 1967; Brockhouse and Roy, 1970) TaNb (Als-Nielsen, 1968). Here the difference in masses is small but the force constants change considerably as the Fermi surface changes with valence. In particular, the Kohn anomalies move. Since these are all long-range effects, an average force constant and hence the VCA is a good approximation, and this has been used to interpret the data. More recently Kamitakahara and Brockhouse (1972) have reported a detailed study of Ni_xPd_{1-x} $x = 55\%$. The mass defect is fairly large $\epsilon \sim 0.81$, and a detailed analysis of the dispersion curves shows that the larger near-neighbor force constants change very little between Ni and Pd, although there are large relative changes in the smaller distant-neighbor force constants. The results were compared with a CPA calculation. The predicted widths are similar to those observed, but some of the structure is different. The corresponding shifts are not reported, but the results observed agree closely with VCA with average mass.

Experiments have also been performed by Cowley and Buyers (1968) on $K_{1-x}Rb_xBr$ $x = 22\%$ and 45%. The resulting spectra are found to be broad, and no detailed investigation has been attempted. In view of the interest in the optical properties of mixed alkali halides discussed below, a more detailed study of such systems by neutron scattering would be an important next step in the understanding of mixed crystals.

2. *Optical properties*

A great deal of experimental information has been collected on the optical properties of mixed crystals, particularly alkali halides, alkaline earth fluorides, III–V and II–VI compounds. Much of this information has been reviewed by Chang and Mitra (1971). Further details can be found in the recent article of Harada and Narita (1971) and the forthcoming review of Barker and Sievers. It is therefore unnecessary to repeat a catalog of results and references here. We shall mainly concern ourselves with a general outline of the results with specific examples and a discussion of the theoretical interpretation.

In Sec. IIC4 it was pointed out that the optical properties of a medium are largely determined by the polarizability, which is related to a weighted displacement Green's function by Eq. (2.75). In a simple ionic crystal this has a real part $1/M[\omega^2 - \omega_0^2(0)]$ arising from the $\mathbf{k} = 0$ optic mode. As a result, the dielectric constant $\epsilon = 1 + 4\pi\chi$ becomes negative over a frequency region $\omega_T < \omega < \omega_L$ where the longitudinal and transverse mode frequencies are related by the LST relation (Born and Huang, 1954)

$$\omega_L^2/\omega_T^2 = \epsilon(0)/\epsilon(\infty). \tag{4.22}$$

In the imperfect lattice χ has a real and an imaginary part, but the properties of the system will still be determined by the frequency regions where $\mathrm{Re}\chi$ is large and negative. The simplest experiments usually measure the reflectivity which is largest in these regions. Detailed analysis of the results to obtain ϵ_R and ϵ_I is often difficult, and most interpretation rests on the assumption of one or more Lorentzian oscillators. This leads to a crude classification of the spectra of mixed crystals into those which show only one reflectivity or absorption peak and those which show two, for a given active optical branch of the pure crystal. In Fig. 49 we show typical results for KClBr, a good example of a one-mode system, and for GaAsP, a good example of a two-mode system.

There has been a great deal of discussion in the literature about the criteria for these two types of behavior. The most important necessary condition for two-mode behavior to occur at a low concentration x of some element is that there be a local mode at the isolated defect (Chang and Mitra, 1968; Brodsky *et al.*, 1970). On a mass criterion this requires that the substituted element be lighter than the host which is replaced. At the other end of the substitution range $x \sim 1$, there will then be a small concentration of heavy defects. These will tend to produce a response below the optic branch, but unless this is well separated from the acoustic branches it will only give a resonance in the acoustic band and not a localized gap mode. The detailed criteria for the existence of localized and gap modes depend on the actual spectrum, and in this respect the linear chain models commonly used may be misleading. It is always easier to satisfy the criteria for localized modes in one dimension than in three. Moreover

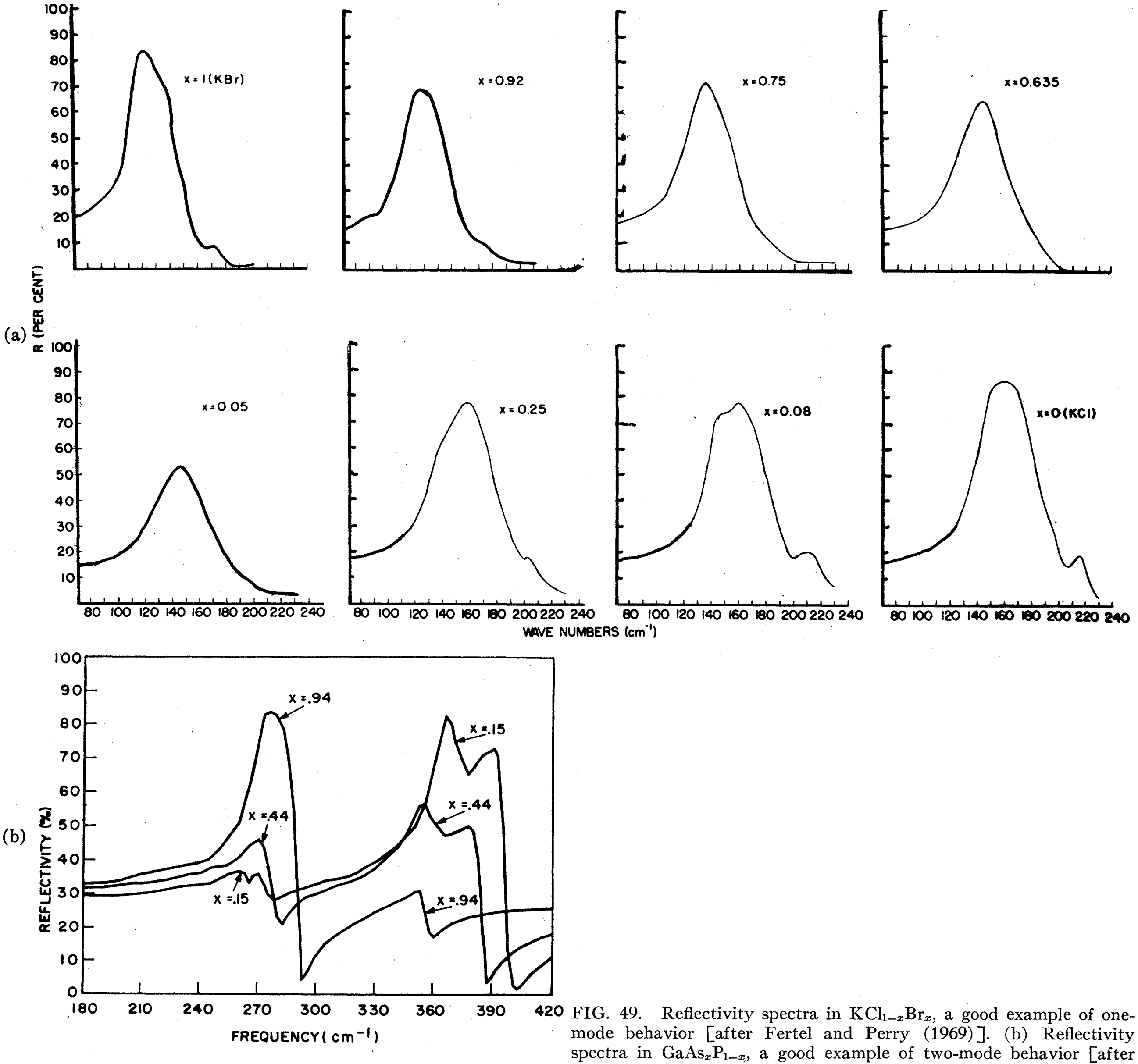

FIG. 49. Reflectivity spectra in $KCl_{1-x}Br_x$, a good example of one-mode behavior [after Fertel and Perry (1969)]. (b) Reflectivity spectra in $GaAs_xP_{1-x}$, a good example of two-mode behavior [after Verleur and Barker (1966)].

these models fail to account for the full width of the phonon branches; in particular, they neglect the width of the optic branch arising from the splitting of ω_L from ω_T by the electrical forces. Some attempt to include this width has been made by Fertel and Perry (1969), Harada and Narita (1971), and others. The former suggested that for two-mode behavior the reststrahl bands of the two constituted crystals must not overlap. This is too strong a condition, but certainly if the overlap is large, one-mode behavior is always found. In this situation the perturbation introduced by mixing is small and the VCA is an adequate description.

For the case of large perturbations, none of these theories attempts to deal with the large concentration case in any detail. Attempts in this direction have been confined to special models which are not physically realistic. For example, Verleur and Barker (1966) calculate the spectra from finite clusters of atoms. Other authors have assumed a regular atomic arrangement in the random crystal, and some detailed comparison has been done with a theory (Chen *et al.*, 1966; Chang and Mitra, 1968) which determines $\mathbf{k} = 0$ optical modes by assuming that all atoms of a given type oscillate in phase.

It is surprising that comparatively little detailed theoretical work has been done using Green's function techniques, which have proved so valuable elsewhere in this field. Important exceptions to this are found in the work of Pershan and Lacina (1970) and Beserman and Balkanski (1970), who essentially used the ATA on $Ca_{1-x}Sr_xF_2$ and $CdS_{1-x}Se_x$, respectively. An early attempt at this type of calculation was made by Elliott and Taylor (1964) for $LiH_{1-x}D_x$. The CPA was used by Taylor (1967) in his original paper to study the vibrations of Ge–Si alloys, but there is no comparable work on ionic crystals. This is probably due to the fact that such calculations are harder in a diatomic crystal with important electric forces, and because it is known from local mode studies that force-constant changes are important for defects in alkali halides, although less so in III–V and II–VI compounds. Nevertheless we feel that such calculations could and should now be undertaken to confront the mass of experimental data. Very recently Taylor (unpublished) has applied the CPA to calculate the reflectance in a one-mode system $KBr_{1-x}Cl_x$ and a two-mode system $K_{1-x}Rb_xI$ (Fig. 50).

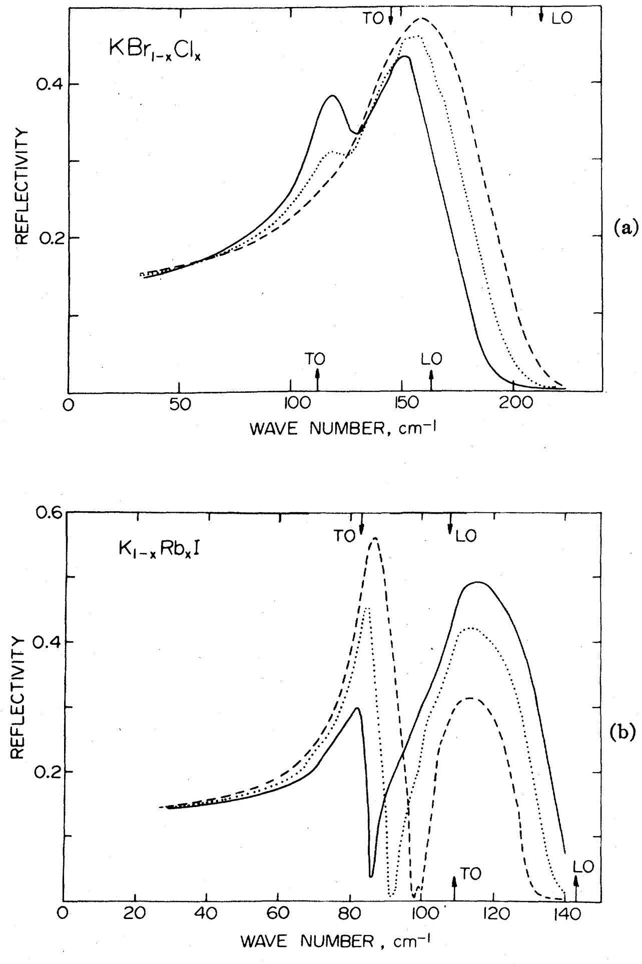

FIG. 50. Calculated reflectivities using the CPA by Taylor (unpublished) for KCl_xBr_{1-x} and $K_{1-x}Rb_xI$. Full line $x = 0.25$, dotted line $x = 0.50$, dashed line $x = 0.75$. The lower (upper) arrows indicated ω_{TO} and ω_{LO} for $x = 0(1)$.

TABLE I.[a] One- and two-mode behavior of mixed ionic crystals.

Crystal	x	$\lvert 1-\mu/\mu'\rvert$	$\dfrac{\epsilon_0-\epsilon_\infty}{\epsilon_0+\epsilon_\infty}$	Expt
$Na_xK_{1-x}Cl$	1	0.26	0.45	I
	0	0.35	0.39	I
$K_xRb_{1-x}Cl$	1	0.25	0.39	I
	0	0.33	0.39	I
$K_xTl_{1-x}Cl$	1	0.38	0.39	I
	0	0.61	0.72	I
$Ca_xSr_{1-x}F_2$	1	0.26	0.61	I
	0	0.36	0.57	I
$Ba_xSr_{1-x}F_2$	1	0.12	0.55	I
	0	0.11	0.57	I
$Cd_xZn_{1-x}S$	1	0.15	0.23	I
	0	0.13	0.24	I
KCl_xBr_{1-x}	1	0.29	0.39	I
	0	0.40	0.39	I
$GaAs_{1-x}Sb_x$	1	0.22	0.05	II
	0	0.18	0.08	I
$ZnSe_xTe_{1-x}$	1	0.14	0.19	I
	0	0.16	0.14	I
$Ni_xCo_{1-x}O$	1	0.002	0.30	I
	0	0.002	0.42	I
$K_{1-x}Rb_xI$	1	0.72	0.35	II
	0	0.41	0.30	II
$Zn_xCd_{1-x}Te$	1	0.30	0.14	II
	0	0.43	0.18	II
GaP_xAs_{1-x}	1	0.40	0.09	II
	0	0.68	0.08	II
InP_xAs_{1-x}	1	0.46	0.09	II
	0	0.85	0.09	II
$Ga_{1-x}In_xAs$	1	0.25	0.09	II
	0	0.20	0.08	II
$Ga_{1-x}In_xSb$	1	0.36	0.04	II
	0	0.27	0.05	II
$InAs_{1-x}Sb_x$	1	0.29	0.04	II
	0	0.22	0.09	II
CdS_xSe_{1-x}	1	0.46	0.23	II
	0	0.88	0.18	II
ZuS_xSe_{1-x}	1	0.40	0.24	II
	0	0.68	0.19	II
$Ga_{1-x}Al_xAs$	1	0.45	0.09	II
	0	0.82	0.08	II
$Na_xRb_{1-x}I$	1	0.65	0.37	?
	0	1.61	0.35	?

[a] We are grateful to Julia Martinez for assistance in compiling this table.

The general features of one- and two-mode spectra are predicated by the CPA calculations of Onodera and Toyozawa (1968). Using a parabolic density of states they show that $\mathbf{k} = 0$ response has two sharp peaks in the split-band limit, but only one peak if the bands are not split (cf. Figs. 23 and 24). We can use their theory to give a crude criterion for two-mode behavior in a crystal with constituents $AB_{1-x}B_x'$. To do this we neglect the acoustic branches and assume a parabolic density of states in $E = \omega^2$ for the optic branch. Thus the model will work best if the mass difference between the constant constitutent A and the mean mass of the mixed constituents B, B′ is large. The center of the host crystal band is determined by a characteristic force constant Φ and the reduced mass μ

$$\omega_0^2 = \Phi\left(\frac{1}{M_A} + \frac{1}{M_B}\right) = \frac{\Phi}{\mu}. \tag{4.23}$$

We assume that the extrema of the band are ω_T^2 and ω_L^2 so that the width is dominated by the electrical forces. Because of the LST relation (4.22), the width W is given by

$$\frac{W}{\omega_0^2} = \frac{\epsilon(0) - \epsilon(\infty)}{\epsilon(0) + \epsilon(\infty)}. \tag{4.24}$$

The condition for a localized mode at small x can be found to be

$$\left|1 - \frac{\mu}{\mu'}\right| > \frac{1}{2}\frac{\epsilon(0) - \epsilon(\infty)}{\epsilon(0) + \epsilon(\infty)}. \tag{4.25}$$

At $x \sim 1$ the condition has μ and μ' reversed. For the two bands to be separated over the whole concentration range,

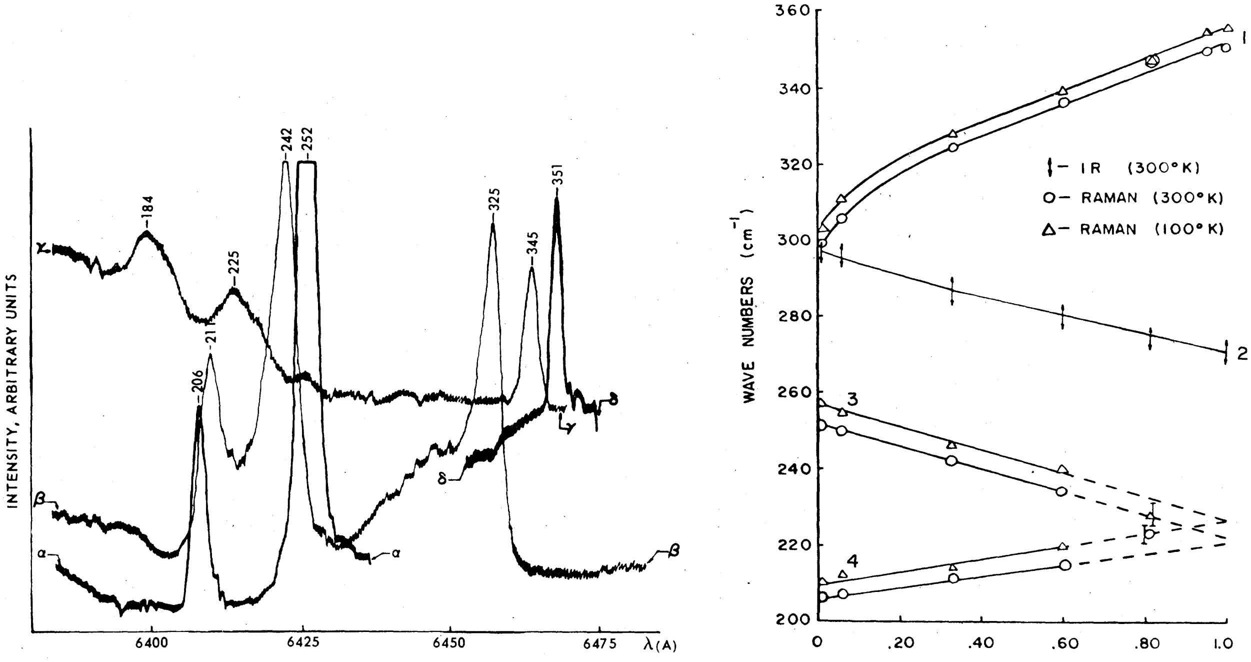

(a) (b)

FIG 51. (a) Raman spectra in ZnS_xSe_{1-x}. (b) Frequencies of $q = 0$ response observed in ZnS_xSe_{1-x} by Raman and infrared measurements. 1. LO(ZnS), 2. TO(ZnS), 3. LO(ZnSe), 4. TO(AnSe) [after Brafman *et al.* (1968)].

the CPA calculations require a stronger condition

$$1 - \frac{\mu}{\mu'} > \frac{\epsilon(0) - \epsilon(\infty)}{\epsilon(0) + \epsilon(\infty)} . \tag{4.26}$$

This is tested in Table I. We see that it accounts reasonably well for the observed behavior. In the strongly ionic alkali halides the reststrahl bands are strong and the condition is harder to satisfy than in the III–V compounds, which are weakly ionic. The only serious discrepancy is GaAsSb, but this is just the situation where the gap is known to be small ($M_{\text{Ga}} \sim M_{\text{As}}$) and the Sb will give an acoustic resonance rather than a gap mode.

This model is extremely crude, but no more crude than those employed by other workers in the field. In particular, it neglects force-constant changes and the effect of the acoustic branches. It does, however, include the random structure in the best available way by using the CPA. Its comparative success strengthens our view that more realistic CPA calculations would be worthwhile.

There are infrared experiments on other crystals which are more complex than the binary compounds above and may have several optically active branches. Some of these may show one-mode and others two-mode behavior within the same crystal, as for example in $KMg_{1-x}Ni_xF_4$ (Barker *et al.*, 1968). A more extensive discussion is to be found in the review article of Barker and Sievers (to be published).

The optical absorption by Ge_xSi_{1-x} alloys has also been studied by Braunstein (1963) and by Cosand and Spitzer (1971). In this case there is no optically active mode in the pure crystal, and the weak absorption process depends on the atomic polarizability. This process has been studied using a detailed shell model in the case of small concentrations of impurities in rare gas crystals (Elliott and Hartmann, 1967; Martin, 1967). Keeler and Batchelder (1972) have recently observed far infrared absorption due to Kr and Ne in A. In the mixed crystal the optical absorption will be proportional to an expression like (4.18), where B is now the effective induced charge; that is, we are interested in the response to an effectively uniform field, appropriate to the uniform mode

$$\langle G(\mathbf{k}, E) \rangle = 1/(M\omega^2 + \Sigma). \tag{4.27}$$

The absorption coefficient is given by

$$\propto (\bar{B}^h - \bar{B}^d)^2 \Sigma_I / [(M\omega^2 + \Sigma_R)^2 + \Sigma_I^2]. \tag{4.28}$$

At low c it is equivalent to the result of Elliott and Hartmann, who also suggested that B, which depends on the relative neighbor displacements, would be roughly proportional to ω^2. No detailed comparison between theory and experiment has been made except at low c, although Taylor (1967) did calculate some aspects of the phonon spectra of Si–Ge using the CPA.

Raman scattering has also been observed from a variety of mixed crystals. These results have also been reviewed by Chang and Mitra and by Barker and Sievers. In mixed crystals where the pure components have Raman-active optical modes, the spectrum usually consists of a few relatively narrow lines. Si and Ge have a single active mode, and the alloys show two lines corresponding to the split-band case (Feldman *et al.*, 1966). In the III–V and II–VI compounds both the LO and TO $\mathbf{k} = 0$ phonons are active, so that there are two lines in the pure crystal spectra. In mixed crystals like $ZnS_{1-x}Se_x$ which show split-band behavior four lines are observed (see Fig. 51) (Chang and Mitra, 1968).

The theoretical form of the Raman cross section [Eq. (2.77)] depends on a weighted average of $\mathrm{Im}\langle G(\mathbf{k}, E)\rangle$ similar to the neutron cross section [Eq. (4.18)] except that $\mathbf{k} \sim 0$, and B is replaced by the Raman polarizability C defined in Eq. (2.77). There have been no detailed attempts to calculate the appropriate average in any realistic case.

In the alkali halides the optical phonons are not Raman-active and there is no first-order Raman spectrum. In the mixed crystals, however, a broad spectrum is expected, and this has recently been observed by Nair and Walker (1971) in $\mathrm{KCl}_{1-x}\mathrm{Br}_x$. The peaks in the spectrum are correlated with peaks in the density of states and resonant modes. The theoretical expression for the cross section is similar to Eq. (4.28) with appropriate Raman polarizabilities.

3. *Other experiments*

The thermal properties of crystals which arise through the lattice vibrations reflect to some extent the spectrum of excitations. However, because they always involve an average over part of the spectrum, they are less sensitive than optical and neutron measurements. Low-lying resonance modes arising from small impurity concentrations can have a marked effect on the low-T specific heat, as was predicted by Kagan and Iosilveski (1965) and Lehmann and DeWames (1963). A recent example of this effect is seen in the work of Hartmann *et al.* (1970) on $\mathrm{Al}_{1-x}\mathrm{Au}_x$. The only work on high-concentration mixed crystals is that of Karlsson (1970), who measured $\mathrm{K}_{1-x}\mathrm{Tl}_x\mathrm{Cl}$, $x < 5\%$ and $\mathrm{KCl}_{1-x}\mathrm{Br}_x$ over the whole range of x. He finds that the Debye temperature of the mixed crystal is that expected from averaging the inverse square frequency

$$\theta_D(x)^{-2} = (1 - x)\theta_D(1)^{-2} + x\theta_D(0)^{-2}. \tag{4.29}$$

A similar situation holds in the case of thermal conductivity experiments. There has been a great deal of work on systems containing small concentrations of defects with low-lying resonances which give an anomaly at low T [see for example Pohl (1968)], but nothing on high-concentration mixed systems.

One other type of experiment has given important information about the phonon spectra of mixed crystals. Superconducting tunneling can be used to give the density of states weighted by some unknown (but slowly varying) coupling constant. The most studied system is $\mathrm{Pb}_{1-x}\mathrm{In}_x$ at low x by Rowell *et al.* (1965) [see Fig. 13] and large x by Adler *et al.* (1966).

C. Excitons

As pointed out in Sec. IIA4, Frenkel excitons provide another example of elementary excitations which can be studied in a disordered lattice. In the extremely tightly bound case, where the exciton is well described as an excited atom, the disordered system can be simply described as one of diagonal disorder. Here

$$\Delta(l) = E_{\mathrm{A}}(l) - E_{\mathrm{B}}(l) \tag{4.30}$$

is the difference in atomic excitation energies. At low concentrations, localized excitons will occur if Δ is sufficiently large compared to the exciton bandwidth. In the Frenkel case this may be relatively small.

In semiconductors excitons are better described by the Wannier model (Knox, 1966), and are large entities covering several atoms. The energy states consist of several overlapping exciton bands with relatively weak binding energy, and the simple models discussed in this review are not applicable. Although localized excitons occur at very low defect concentrations, exciton effects are normally not distinguishable at higher concentrations.

After preliminary work by Mahr (1961), the Japanese school has had a monopoly on the study of excitons in mixed ionic crystals. This work has been influenced by the CPA calculation of Onodera and Toyozawa (1968), and largely interpreted in these terms. The salient feature of the optical absorption is that it shows one- or two-band behavior like the optical phonons discussed in Sec. IVB2. In general, mixtures of alkali ions in alkali halides lead to one-mode behavior. This is well demonstrated in $\mathrm{K}_x\mathrm{Rb}_{1-x}\mathrm{Cl}$, $\mathrm{K}_x\mathrm{Na}_{1-x}\mathrm{Cl}$ (Nakai *et al.*, 1965), $\mathrm{K}_x\mathrm{Rb}_{1-x}\mathrm{I}$ (Nakamura, 1967), $\mathrm{K}_x\mathrm{Rb}_{1-x}\mathrm{I}$ (Nakamura and Nakai, 1967). The peaks shift smoothly by $\Delta \sim 0.1$ eV across the series (see Fig. 51). The small value of Δ is due to the fact that the exciton is largely confined to the halogen. Mixed crystals which vary the halide show a tendency toward two-mode behavior, for example, $\mathrm{KCl}_x\mathrm{Br}_{1-x}$ (Murata and Nakai, 1967) and $\mathrm{KCl}_x\mathrm{I}_{1-x}$ (Nagasawa *et al.*, 1968), where $\Delta \sim 1$ eV.

Other systems which have been studied include $\mathrm{Ar}_{1-x}\mathrm{Xe}_x$ (Nagasawa *et al.*, 1972) which shows one-mode behavior though the shift suggests $\Delta \sim 1$ eV, which must indicate a relatively broad exciton bandwidth. The mixed crystals $\mathrm{CuCl}_x\mathrm{Br}_{1-x}$ have more extensive excitons which are not well described by the Frenkel model. The system shows one-mode behavior (Goto *et al.*, 1968, 1970) and the line is so sharp, even at intermediate x, that Zeeman studies have been performed (Mabuchi *et al.*, 1971). Sen (1973) has recently proposed that the CPA can be used to understand these results.

Some very interesting experiments have been carried out on organic crystals with hydrogenous components following the work of Sheka (1961), on naphthalenes, and Broude and Rashba (1962) on benzenes. In this situation deuteration of the molecule changes the zero-point energy. Although this is relatively small [in naphthalene with 8 protons (h_8), 4 protons and 4 deuterons (d_4), or 8 deuterons (d_8); $E(h_8) - E(d_4) \sim 50\ \mathrm{cm}^{-1}$, $E(h_8) - E(d_8) \sim 115\ \mathrm{cm}^{-1}$] the exciton bandwidth is also small $\sim 100\ \mathrm{cm}^{-1}$. The most detailed results of Robinson and Hong (1971) show two-band behavior in the h_8–d_8 mixtures and one-band behavior in the h_8–d_4 mixtures (Fig. 52).

Broude and Rashba gave a simplified theory, but more recently Dubrovskii and Konobeev (1970) suggested the use of the CPA for this system. Detailed applications of the CPA have now been made by Robinson and Hong (1970) and especially Kopleman and Hong (1971). The latter give an extensive analysis of the CPA and compare the results with moment calculations and computer model calculations.

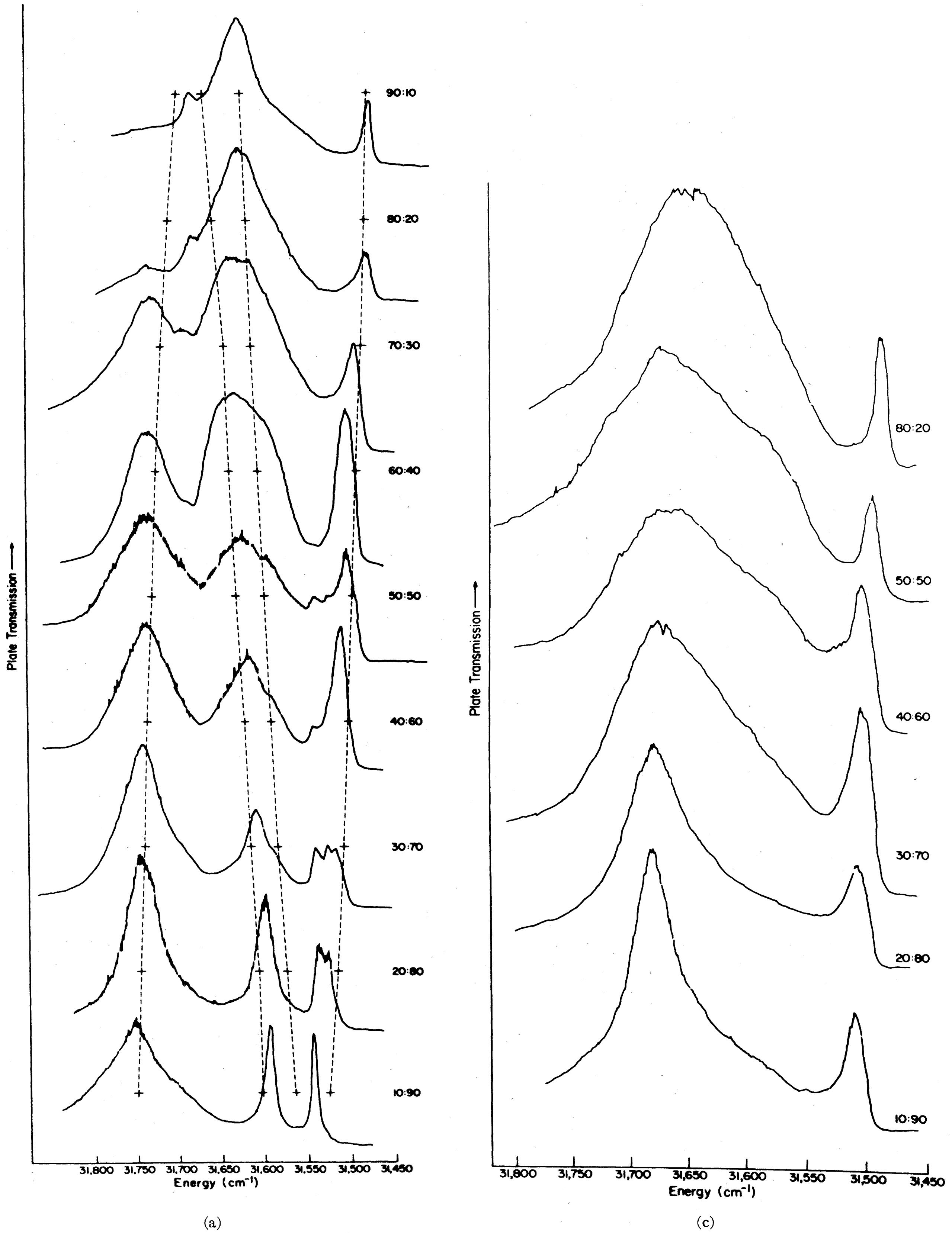
Plate Transmission
90:10
80:20
70:30
60:40
50:50
40:60
30:70
20:80
10:90
31,800 31,750 31,700 31,650 31,600 31,550 31,500 31,450
Energy (cm^{-1})
Plate Transmission
80:20
50:50
40:60
30:70
20:80
10:90
31,800 31,750 31,700 31,650 31,600 31,550 31,500 31,450
Energy (cm^{-1})

(a)

(c)

D. Magnons

Although, in some ways, magnons are a more esoteric elementary excitation than electrons or phonons, they promise to be very convenient systems for comparing theory and experiment. The main reason is that in a simple magnet there is only one branch to the magnon spectrum and that in insulators the exchange interactions are short range. By making detailed measurements on the pure materials these exchange interactions may be determined so that there are no unknown parameters in the random crystal. On the other hand, as discussed in Secs. IIA5 and IIIC2, the modification of the exchange interaction always gives an extended defect matrix V. In addition, the simplest systems with short-range interactions are usually antiferromagnets. Metallic ferromagnets normally show a long-range interaction via conduction electron polarization. Some aspects of their properties have been considered in Sec. IVA3.

1. Inelastic neutron scattering

The most detailed experimental observations come from inelastic neutron scattering measurements, although some optical work has also been done. Until recently most of this was directed towards the observation of local modes and resonances induced by low concentrations of defects. This work has recently been extensively reviewed by Cowley and Buyers (1972) and we shall not repeat it here. The systems studied in detail are $KMnF_3$ with Co, Ni, and Zn impurities and MnF_2 with Fe, Co, Ni, and Zn. Relatively little has been done on more concentrated samples, but recent studies by neutron scattering on $Mn_{1-x}Co_xF_2$ and $KMn_{1-x}Co_xF_3$ (Buyers *et al.*, 1971) and on $Mn_{1-x}Zn_xF_2$ (Coombs *et al.*, 1973), represent a fairly complete study of a relatively simple system. In addition, Enders *et al.* (1973) have studied the antiferromagnetic resonance in $Mn_{1-x}Co_xF_2$ and $Mn_{1-x}Fe_xF_2$. In Raman scattering it turns out that two-magnon processes are comparatively strong. Effectively a weighted density of magnon states is measured in this type of experiment. This has been studied in $Mn_{1-x}Zn_xF_2$ by Mitlehner *et al.* (1971) at low x, and Buchanan *et al.* (1972) over a wide range of x. Similar experiments have been performed by Parisot *et al.* (1971) on low concentrations $c < 2\%$ Ni in $RbMnF_3$ and $KMnF_3$. They examined the localized modes which broadened rapidly as c was increased.

A comparison between theory and experiment requires an extension of the theory to a two-sublattice antiferromagnet. There are two atoms per unit cell, so it is necessary to extend the definition [Eq. (2.53)] by specifying the sublattice of the sites.

$$G^{\alpha\beta}(l, l', E) = (-1)^{1+\alpha} \times \langle\langle S_-^{\alpha}(l), S_+^{\beta}(l')\rangle\rangle / 2[S(l)S(l')]^{1/2}, \tag{4.31}$$

where $\alpha = 1, 2$ for the up (down) sublattice. In the perfect crystal this gives

$$P(\mathbf{k}, E) = \begin{pmatrix} P^{11}(\mathbf{k}, E) & P^{12}(\mathbf{k}, E) \\ P^{21}(\mathbf{k}, E) & P^{22}(\mathbf{k}, E) \end{pmatrix} = \begin{pmatrix} E - 2sI(0) & 2sJ(\mathbf{k}) \\ -2sJ(\mathbf{k}) & E + 2sI(1) \end{pmatrix}^{-1} \tag{4.32}$$

with poles at the energies given by Eq. (2.29). Since interchange of the sublattices leads to reversal of all the spins, it is equivalent to time reversal. This gives some simplification to the Green's function in the general case. Writing, for a given $\mathbf{k}$,

$$G = \mathbf{P} + \mathbf{P\Sigma G} \tag{4.33}$$

$\mathbf{\Sigma}$ takes the form

$$\mathbf{\Sigma} = \begin{pmatrix} \Sigma_1(\mathbf{k}, E) & \Sigma_2(\mathbf{k}, E) \\ -\Sigma_2(\mathbf{k}, -E) & -\Sigma_1(\mathbf{k}, -E) \end{pmatrix}. \tag{4.34}$$

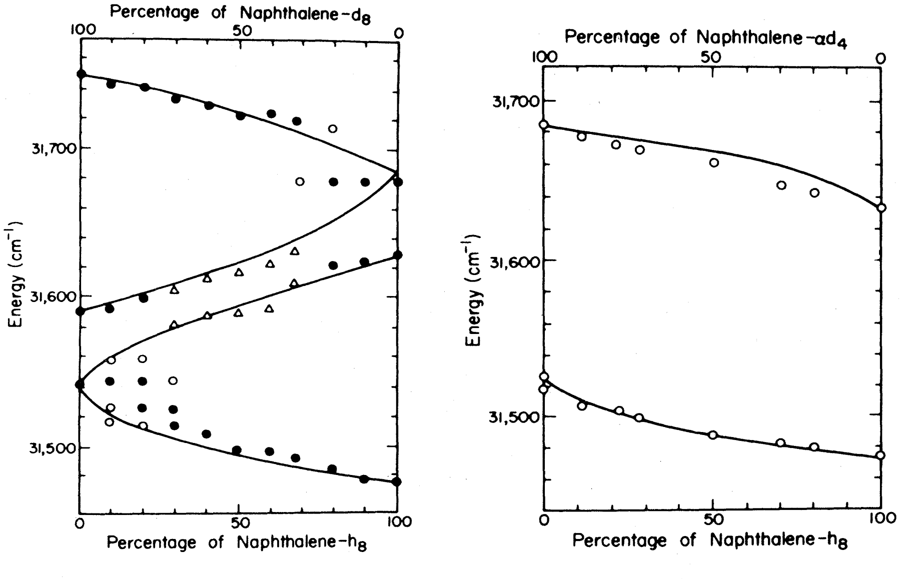

(b) (d)

FIG. 52. (a) Absorption spectra of mixed crystals of naphthalene h_8 and d_8. (b) Positions of the observed Davydov components; the solid curves represent CPA calculations. (c) and (d) As (a) and (b) for mixed crystals of naphthalene h_8 and d_4 [after Robinson and Hong (1971)].

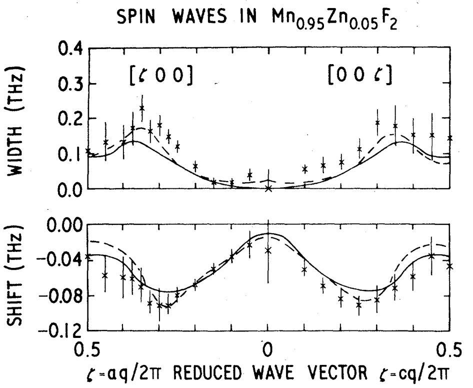

FIG. 53. The shift and width of the magnon modes in $Mn_{0.95}Zn_{0.05}F_2$ measured by Svensson *et al.* (1969). The results of the low c ATA theory are shown dashed, and the approximate CPA theory as the full line [after Buyers *et al.* (1972)].

2. Dilute antiferromagnet

At low defect concentrations $\Sigma(l,l')=ct(l,l')$ where the t-matrix is, say, a 7×7 matrix in real space, as in Eqs. (2.116)–(2.118). For that situation t^p, t^d and the diagonal parts of $\mathbf{t}^s$ contribute to Σ_2. Detailed calculations have been made for the antiferromagnet by Tonegawa (1968), Shiles and Hone (1970), and particularly Lovesey (1968). The poles of t give the local modes, while in the band Σ gives rise to a shift and width to the response, given by

$$\begin{aligned}\Delta(\mathbf{k},E)&+i\pi\Gamma(\mathbf{k},E)\\ &=\{I(0)[\Sigma_1(\mathbf{k},E)+\Sigma_1(\mathbf{k},-E)]\\ &\quad+E[\Sigma_1(\mathbf{k},E)-\Sigma_1(\mathbf{k},-E)]\\ &\quad+J(k)[\Sigma_2(\mathbf{k},E)+\Sigma_2(\mathbf{k},-E)]\}/2E(\mathbf{k}) \qquad (4.35)\end{aligned}$$

evaluated at $E=E(\mathbf{k})$. Such a calculation has been compared with neutron scattering experiments in $Mn_{1-x}Zn_xF_2$ $x=0.05$ by Svensson *et al.* (1969), as shown in Fig. 53. Similar results on $Mn_{1-x}Co_xF_2$ ($x=0.05$) by Buyers *et al.* (1968) and $KCo_{1-x}Mn_xF_2$ ($x=0.05$) are discussed in Cowley and Buyers (1972).

The CPA for high concentrations of these extended defects has not yet been performed. However Buyers *et al.* (1972, 1973) have proposed an approximate theory where only the site-diagonal parts of the perturbation are treated by the CPA. These are taken to depend on the neighboring atoms so that for a host ion with r defect neighbors

$$V_H(r)=\pm 2r(I'S'-IS), \qquad (4.36a)$$

while a defect atom with r defect neighbors has

$$\pm V_D(r)=2z(I'S-IS)+2r(I''S'-I'S) \qquad (4.36b)$$

where the Ising coupling between defect and defect is I''. This gives only $\Sigma_1(E)$. The off-diagonal parts of V are treated more approximately by assuming

$$\Sigma_2(\mathbf{k},E)=\Sigma_1(\mathbf{k},E)\sum_{\boldsymbol{\delta}}\exp(i\mathbf{k}\cdot\boldsymbol{\delta}), \qquad (4.37)$$

which assures that $\omega(\mathbf{k})\to 0$ as $\mathbf{k}\to 0$ in the isotropic case, as required by the Goldstone theorem. Results for the line shapes in $Mn_{0.3}Co_{0.7}F_2$ and the dispersion in $KMn_{0.29}Co_{0.71}F_3$ are compared with experiment in Figs. 54 and 55. A similar theory for $Mn_{1-c}Zn_cF_2$ also requires the addition of large τ as in Eq. (3.96) to prevent the appearance of a spurious low-frequency resonance. Results for some line shapes in $Mn_{0.78}Zn_{0.22}F_2$ are shown in Fig. 56. In addition, the results of this approximation are compared with the low c theory in Fig. 53.

The success of this approximate theory is in large part due to the fact that the Ising interactions are treated properly and clustering effects included. In an antiferromagnet the Ising part of the interaction dominates the excitation spectrum. In the pure crystal the density of states has a sharp divergence at $E=2I(0)S$. For this reason localized states and resonances are predicted quite accurately using only the Ising terms. Some attempts have also been made to consider the impure antiferromagnets by considering only isolated changed bonds (Tahir-Kheli, 1972; Parkinson, 1973). In the dilute case this appears to give a different line shape (Elliott and Pepper, 1973) which agrees less well with experiment.

The question of localization of spin waves has been considered recently by Economou (1972), using the theory of Cohen and Economou (1972), and by Lyo (1972), who extended Anderson's (1958) theory. Since the experiments are all concerned with single-particle Green's functions, there is no direct evidence to compare with the predictions.

All these results have been considered effectively at

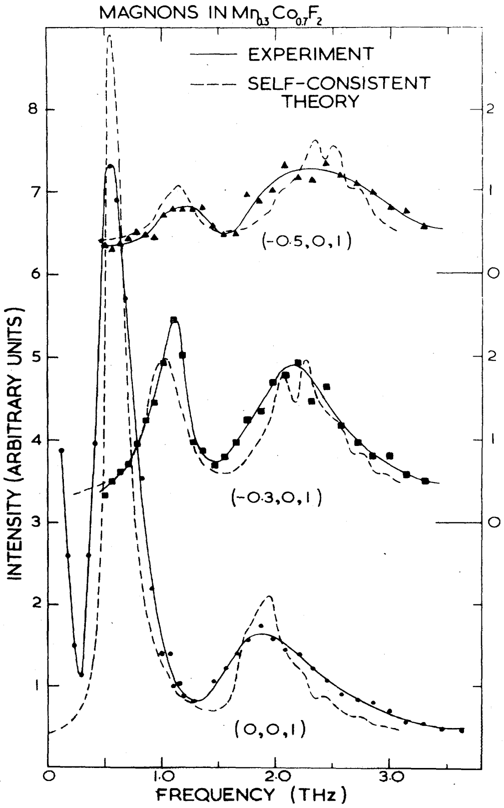

FIG. 54. Neutron scattering line shapes measured by Buyers *et al.* (1971) in $Mn_{0.3}Co_{0.7}F_2$ compared with the CPA theory of Buyers *et al.* (1972).

$T = 0$°K. At finite T it is necessary to make further approximations to study the spin-wave spectrum theoretically, and this has only been done in the low-concentration limit (Cowley and Buyers, 1972). One exception is the work of Foo and Wu (1972). They used the CPA for isolated bonds, as discussed in Sec. III2, and used the random phase approximation to determine the transition temperature T_c. They compare the theory with experiments on $\mathrm{GdN}_{1-x}\mathrm{O}_x$ by Gambino *et al.* (1970).

E. Percolation and conduction

If one continues to remove resistors from an infinite network, at some concentration (fraction) c_0 of removed resistors the conduction across the network ceases as the last connecting path across the network is broken. Such critical percolation concentrations or percolation thresholds were first studied by Broadbent and Hammersley (1957) [and Hammersley (1957)], who introduced lattice models for fluid flow through a random medium and showed that no fluid will flow below the critical percolation concentration of the active medium. They also introduced the idea of the percolation probability $P(c)$ which is the probability that any active region of the medium is contained in an infinite cluster of active material and hence available for conduction. There are a number of good reviews on the subject [for example, Frisch and Hammersley (1963); Fisher (1964); Shante and Kirkpatrick (1971); Essam (1973); and Kirkpatrick (1973a)]. Recently a number of experiments and computer experiments have been reported on random networks [e.g., Last and Thouless (1971); Kirkpatrick (1971) and (1973b); Adler *et al.* (1973); and Watson and Leath (1974)].

A major interest in this field has been in the suggestion (Miller and Abrahams, 1960) that the problem of hopping conduction in doped semiconductors is closely related to conduction through a resistor network and hence to the percolation problem. Similar suggestions have been made (see the review by Shante and Kirkpatrick, 1971) that percolation effects play an important role in metal–semiconductor transitions and in conductivity in certain amorphous materials.

In the critical region about the percolation threshold where the fluctuations in the size of the clusters are large compared to the size of the clusters, such properties as the percolation probability, the conductivity, and the mean cluster size apparently exhibit power law behavior $(c - c_P)^\gamma$ about the critical percolation concentration c_p. Presumably a scaling or renormalization group argument would be necessary to analytically obtain exponents.

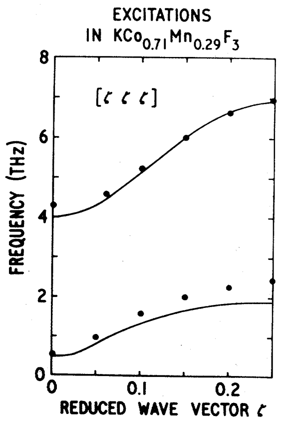

FIG. 55. The dispersion curves for the peak response in the neutron scattering experiments of Buyers *et al.* (1971) on $\mathrm{KCo_{0.71}Mn_{0.29}F_3}$ compared to the CPA calculations [after Buyers *et al.* (1972)].

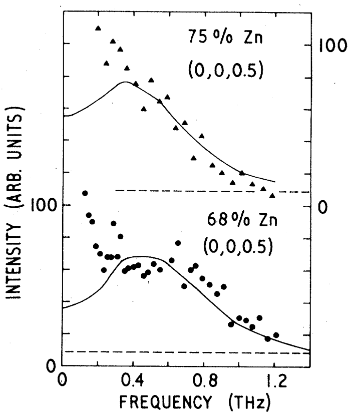

FIG. 56. Neutron scattering by short wavelength magnons in $\mathrm{Mn}_{1-x}\mathrm{Zn}_x\mathrm{F}_2$ measured by Coombs *et al.* (to be published) near the critical concentration. The solid lines are the CPA predictions of Buyers *et al.* (1973) showing a broad response which does not change very much with concentration.

However, outside of the critical region one can obtain remarkably accurate analytic calculations of σ using a classical theory of conduction through mixtures known today as effective medium theory [see Bruggeman (1935), Landauer (1952), Brown (1956), Kerner (1956), Krumhansl (1973), Kirkpatrick (1973a)]. The effective medium theory is entirely equivalent to the coherent potential approximation, as has been discussed formally in detail by Kirkpatrick (1973a).

We shall limit our discussion of effective medium theory here, for simplicity, to that of simple bond and site percolation problems on a simple square resistor network to illustrate its usefulness and its similarity to the coherent potential approximation.

Let us consider first the bond problem [see Kirkpatrick (1973a)] where we shall try to evaluate the conductivity of a simple square lattice filled with resistors of resistance R_A and R_B, randomly placed. We imagine first a perfect square lattice of resistors of magnitude R_m with an external voltage applied across the sample inducing current I_0 through each resistor along one of the principal axes. When a single resistor R_m, directed along the direction of this current I_0, is replaced by either physical resistance R_A or R_B there will be an additional voltage ΔV_A or ΔV_B appearing across that bond. The magnitude of this extra voltage can easily be seen to be

$$\Delta V_{\mathrm{A,B}} = I_0 R_m [1 - 2R_m/(R_m + R_{\mathrm{A,B}})]. \tag{4.38}$$

The effective medium theory approach is to require $\langle \Delta V \rangle = 0$ or

$$(1-c)\Delta V_\mathrm{A} + c\Delta V_\mathrm{B} = 0, \tag{4.39a}$$

which gives

$$R_m^2 + (1-2c)(R_\mathrm{B} - R_\mathrm{A})R_m - R_\mathrm{A}R_\mathrm{B} - 0. \tag{4.39b}$$

In the limit, $R_\mathrm{B} \to \infty$, the solution of this equation is

$$R_m = R_\mathrm{A}(1-2c)^{-1}, \tag{4.40a}$$

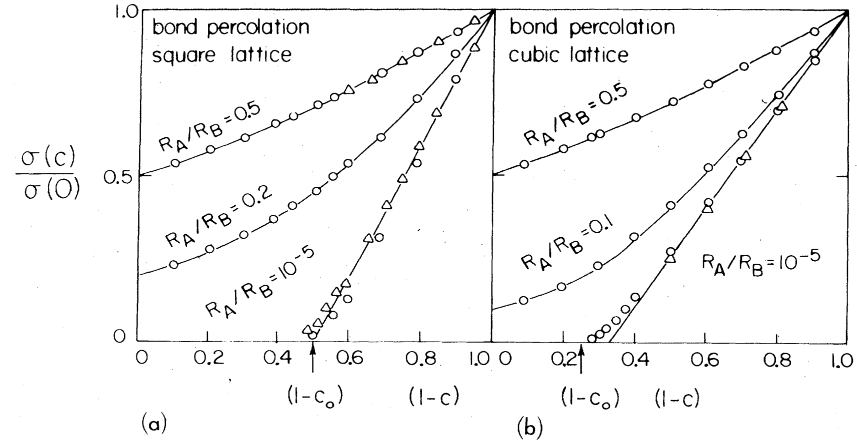

FIG. 57. (a) The conductivity of a simple-square lattice of randomly placed resistors of value R_A and R_B vs the fraction $(1-c)$ of resistors R_A, as determined by the effective medium theory (solid line) of Eq. (4.39) and by monte carlo computer experiments on a 25×30 resistor sample (data points), from Kirkpatrick (1971); (b) A similar plot for the conductivity of a disordered simple-cubic lattice, also from Kirkpatrick (1971).

or

$$\sigma(c) = \sigma_A(1-2c), \tag{4.40b}$$

where $\sigma(c)$ is the conductivity of the disordered network as approximated by the effective medium, and where $\sigma_A = \sigma(0)$. The solution of this equation for the simple square network and the analogous equation for a simple cubic lattice were carried out by Kirkpatrick (1971) and are shown in Fig. 57, where they have been compared to computer experiments carried out on finite samples. The agreement is excellent except within the critical region about c_0 for the case $R_A/R_B = 0$ where fluctuations play a dominant role. The effective medium theory as presented here always gives a straight line versus concentration

$$\sigma(c) = \sigma(0)(1-\alpha c), \tag{4.41}$$

as $R_B \to \infty$, where α is a constant that can be determined from the low concentration behavior. Clearly the effective medium theory is like the coherent potential approximation, with R_m filling the role of the coherent potential and $\langle \Delta V \rangle$ replacing $\langle t \rangle$. In fact, the relationship can be made formally analogous by construction of a Green's function theory for $\sigma(c)$ [see Kirkpatrick (1973a)].

The effective medium theory can also be extended to the site percolation problem with equal success, if care is taken, as has recently been shown by Watson and Leath (1974). In the site percolation problem bonds are not removed randomly, but rather sites (nodes) are chosen randomly and all bonds connecting that site to the lattice are then removed at once.

A naïve application of effective medium theory to this problem would be to calculate $\Delta V_{A,B}$ *across the entire cluster* of bonds (each of value R_A or R_B) about a particular A or B site imbedded in an effective medium, and require

$$(1-x)\Delta V_A + x\Delta V_B = 0, \tag{4.42}$$

where x is the concentration of B sites. This, however, as $R_B \to \infty$, always gives a straight line for $\sigma(x)$ versus x which does not agree with experiment [see Kirkpatrick (1973a)]. The method of Watson and Leath (1974), however, which does work, is to calculate the extra voltage $\Delta V_{\text{bond}}{}^{A,B}$ induced *across a single bond* in the cluster and to require

$$(1-b)\Delta V_{\text{bond}}{}^{A} + b\Delta V_{\text{bond}}{}^{B} = 0, \tag{4.43}$$

where b, the concentration of removed bonds, is the probability that the site on *either* end of the bond is a B site and hence that ΔV_{bond} takes on the value $\Delta V_{\text{bond}}{}^{B}$. But there is an exact relationship between the fraction of altered bonds and the fraction of altered sites in any such infinite lattice, namely,

$$(1-b) = (1-x)^2, \tag{4.44}$$

since a bond is changed if the site on either end is changed. For the case $R_B \to \infty$, this theory always gives

$$\sigma(x) = \sigma(0)(1-2\alpha x + \alpha x^2), \tag{4.45}$$

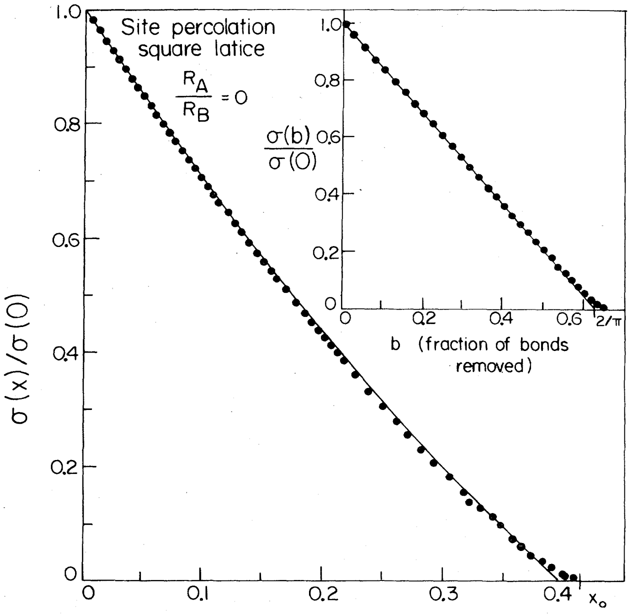

FIG. 58. The conductivity of a simple-square lattice of resistors vs. fraction x of randomly removed sites (or nodes) as determined directly by experiment on a 137×137 mesh (data points) and by the effective medium theory (solid line) of Eq. (4.44). A plot of the same theory (Eq. 4.43) and the same experimental data vs fraction of removed bonds (inset), from Watson and Leath (1974).

where α is determined from the low concentration behavior. As an example, the results for a simple square lattice, where $\alpha = \pi/2$, were compared with experiment by Watson and Leath (1974) and are showed in Fig. 58. The results are in excellent agreement (the slight disagreement apparent at $x \sim 0.2$–0.3 can be explained by the finite size of the experimental sample).

V. EPILOGUE

As this review is being completed there are numerous new pieces of work appearing almost daily in which the methods we have reviewed are being applied. It is satisfying to see that there now are available to physicists methods for systematically describing many properties of random materials, proceeding from plausible model Hamiltonian descriptions. Substantial improvements on virtual crystal approximations have been made for realistic random alloy models, and comparison can be made with experiments. So it is not necessary to try to patch up descriptions based on conventional band theory, and we hope that such attempts will be forgotten; even experimentalists need not find Green's function methods to be impractical. Indeed, with loss of lattice periodicity and symmetry there is as yet no other honest analytical choice so generally applicable.

The applications are not restricted to the electronic and lattice-dynamic properties we have concentrated on here; parallel concepts have developed in other fields (Krumhansl, 1973).

It is frequently possible to divide the physical problem in a random system into two parts—an average behavior, plus the fluctuations from it. An exact treatment must keep both, and when the latter becomes comparable to the former the separation is meaningless. Fortunately, there are many situations in which the separation is both useful and meaningful. In this case the "self-consistent local field theory" is quite useful for describing the average field; however, to complete sum rules (energy conservation, for example) the fluctuations must be included in principle.

Many field theories have usually been invented as needed for the application at hand. The essence of the standard problem is simply stated. The field (electromagnetic, elastic, Schrödinger, etc.), denoted by u, obeys a linear equations of motion characterized by an operator L, which in turn is parameterized by specification of the properties of the medium. In a homogeneous medium, L depends only on a few parameters, while in a random medium these parameters (conductivity, potential, index) vary from place to place according to some probability distribution; for brevity we denote the random parameter as ϵ in $L(\epsilon)$. The equation of motion is

$$L(\epsilon)u = 0. \tag{5.1}$$

The operator L may also depend on other important parameters which are not random (e.g., E in H–E for Schrödinger waves, ω^2 in acoustic and electromagnetic waves). The essence of the averaging methods is to define $L = \langle L\rangle + L_1$, and attempt to calculate $\langle u\rangle$ or other quantities such as $\langle \epsilon u\rangle$, and from them effective parameters $\epsilon^* = [\langle \epsilon u\rangle/\langle u\rangle]$. This may be done in various approximations, self-consistent or not. It is feasible to obtain the "self-consistent local field theory" as the best low-order local approximation to a resummed perturbation series; it also can be obtained by choosing a local field such that scattering vanishes to first order in the "concentration" of defects, i.e., all repeated scatterings by L_1 at a particular position. One may then compute an average ϵ^*, as above, to obtain an effective medium parameter. All this is similar to ATA and CPA.

Neither time nor space allow a detailed comparison of applications to be made here, but we may illustrate by the calculation of the dielectric constant of a composite medium consisting of nonoverlapping, randomly located small spheres of dielectric ϵ_2 imbedded in ϵ_1. The "equation of motion" is

$$\{[\nabla\cdot\epsilon(\mathbf{r})]\mathbf{E}(\mathbf{r})\} = 0, \tag{5.2}$$

in the absence of free charges. The field $u \rightarrow \mathbf{E}(\mathbf{r})$ and $L \rightarrow \nabla\cdot\epsilon(\mathbf{r})$. If an applied charge $\rho(r)$ is imposed, then it is useful in solving the problem to have the Green's function $G = [\nabla\cdot\epsilon(\mathbf{r})]^{-1}$ which satisfies $LG = \delta(\mathbf{r} - \mathbf{r}')$. Indeed, a systematic method for solving may now be based on writing $L = \langle L\rangle + L_1 = L_0 + L_1$, whence the operator relation holds that

$$G = G_0 + G_0L_1G. \tag{5.3}$$

There is also an exact scattering representation for fields

$$\mathbf{E} = \mathbf{E}_0 - GL_1\mathbf{E}_0 = \mathbf{E}_0 + \mathbf{E}_{\text{scatt}}, \tag{5.4}$$

where $\mathbf{E}_0$ is any field which satisfies $\langle L\rangle\mathbf{E}_0 = 0$. Equation (5.4) can be used to define an ϵ^*. In the example at hand $L_1 = \epsilon_2$ within the spheres, ϵ_1 in the host; thus $L_1 = \Sigma_i(\epsilon_2 - \epsilon_1)\nabla$, i running over spheres.

The specific practical problem for a dielectric is to compute the average dielectric function for some direction, say x: $\epsilon_{xx}{}^* = [\langle \epsilon E_x\rangle/\langle E_x\rangle]$. Here, the averaging is volume averaging, i.e., the $(k, \omega) = (0, 0)$ limit.

The basic scattering problem is to compute the scattering around a sphere in the presence of some local field. It is tedious but not difficult to solve this problem using a Green's function G_0; on the other hand, the exact fields around a single sphere or ellipsoid can easily be calculated using spherical harmonics:

$$\begin{aligned}\frac{E_x}{E_{x0}} &= 1 + \frac{\epsilon_1 - \epsilon_2}{2\epsilon_1 + \epsilon_2}\frac{a^2}{r^3}(1 - 3\cos^2\theta), \text{ outside a sphere.}\\ &= 1 + \frac{\epsilon_1 - \epsilon_2}{2\epsilon_1 + \epsilon_2}, \text{ inside a sphere.}\\ &= 1 + (E_{\text{scatt}}/E_{0x}).\end{aligned} \tag{5.5}$$

If a volume average of $\langle \epsilon E_x\rangle/\langle E_x\rangle$ is taken, assuming spheres to scatter independently, and f_2 is the volume fraction occupied by ϵ_2, the integrations yield

$$\epsilon_{xx}{}^* = \frac{\langle\epsilon\rangle + f_2\epsilon_2[(\epsilon_1 - \epsilon_2)/(2\epsilon_1 + \epsilon_2)]}{1 + f_1[(\epsilon_1 - \epsilon_2)/(2\epsilon_1 + \epsilon_2)]}. \tag{5.6}$$

This expression is not self-consistent, since the field incident on the spheres was assumed to be E_0 in a medium of $\epsilon = \epsilon_1$. For the moment, however, expanding Eq. (5.6) to lowest order of $\epsilon_2 - \epsilon_1$, which would apply to small dielectric fluctuations, one obtains an expression obtained by various other means (W. F. Brown, 1955; L. D. Landau and E. M. Lifshitz, 1960)

$$\epsilon_{xx}^* \simeq \langle\epsilon\rangle - \frac{f_2(\epsilon_1 - \langle\epsilon\rangle)^2}{3\langle\epsilon\rangle}. \tag{5.7}$$

A study of the methods shows that Eq. (5.6) is equivalent to the "average T matrix approximation, ATA," used in random alloys, while Eq. (5.7) is a low-order correction to the virtual crystal approximation.

In order to make the method totally symmetric in ϵ_1 and ϵ_2, as well as self-consistent, we take the medium to be describable by an average ϵ^* and then when in medium 1 scatter by $(\epsilon_1 - \epsilon^*)$, when in 2 by $(\epsilon_2 - \epsilon^*)$. With the assumptions of statistical independence and volume averaging one obtains the implicit equation for ϵ_{xx}^* (after much algebra):

$$1 = \sum_i \frac{3f_i}{2 + (\epsilon_i/\epsilon_{xx}^*)}. \tag{5.8}$$

On the other hand, taking volume average x components only, the scattering problem (neglecting interparticle scatterings) in an effective medium ϵ_{xx}^* looks like:

$$\langle E_x\rangle = \langle E_{0x}\rangle + \left(\sum_i \frac{\epsilon_{xx}^* - \epsilon_i}{2\epsilon^* + \epsilon_i} f_i\right)\langle E_{0x}\rangle + \cdots. \tag{5.9}$$

If we impose the condition that the first-order scattering shall vanish on the average, we obtain

$$\sum_i \left(\frac{\epsilon_{xx}^* - \epsilon_i}{2\epsilon^* + \epsilon_i}\right) f_i = 0. \tag{5.10}$$

But since $\Sigma_i f_i = 1$ it may be found that Eqs. (5.10) and (5.8) are exactly the same. Thus the self-consistent local field is equivalent to the choice of an active medium such that the averaged single-site scattering vanishes. This is identical to the CPA method in alloys. The essence of the method is to solve for the exact field around a representative element of the medium, which is taken to be imbedded in an effective medium determined in turn by requiring that the mean of the scattering by the random elements taken as statistically independent shall vanish.

There is a history of parallel developments in a variety of contexts. Landauer (1952) analyzed the conductivity of a random mixture of different materials, and derived an expression which is simply Eq. (5.10) above, with conductivities σ substituted for ϵ. Comparisons were made with experiment as in Sec. IVE above.

The thermal properties of random composities have received considerable theoretical and experimental attention. Important contributions to the subject were made by Kerner (1956) and more recently by Budiansky (1970).

The understanding of elastic properties of a random (polycrystalline) aggregate is a longstanding subject of concern in many subjects—geology, agronomy, civil engineering, continuum mechanics, and ceramics, to mention a few. Here again the "self-consistent" method developed, with original contributions to the subject by Budiansky (1970), by Hill (1967), and by Kröner (1967); indeed the similarity of Kröner's formalism to that developed for studying electronic properties of alloys is remarkable.

One should, of course, recognize that the elastic fields are tensor quantities, so the problem is considerably more complicated than that of Schrödinger scalar waves in random systems, and thus the idealizations of the self-consistent method may be more serious. Nonetheless, Thomsen (1972) has recently applied Kröner's method to the elasticity of polycrystals and rocks, with some success in comparison with experiment.

It might also be mentioned in passing that an entirely different approach to the properties of heterogeneous materials uses variational methods (Hashin, 1964; Beran, 1968) to set bounds on effective parameters; to the extent that we have checked several cases, the self-consistent results fall between the expected upper and lower bounds (e.g., $\langle\epsilon\rangle$ vs $\langle\epsilon^{-1}\rangle^{-1}$ for ϵ^* in the case of dielectrics).

While the essence of ATA or CPA approximations appeared in these studies, to our knowledge the systematic and diagrammatic analysis which we have reviewed for alloys has not been carried over, and could usefully serve in estimating the limitations of the approximations.

Finally, we repeat one important disclaimer—there are special questions of localization, dynamics of clusters, transport, and special spectral structure whose description lies beyond the methods which we have reviewed. Why this is so is now pretty well documented; when these special problems are solved, it may be said that over-all description of the physics of random systems will be nearly as complete as that for crystalline matter.

ACKNOWLEDGMENTS

We appreciate the advice and interest in this work on the part of many colleagues, but particular thanks go to Dr. B. G. Nickel and to Dr. J. E. Gubernatis for their critical reading and contributions to several sections of the manuscript. Thanks also go to Jean Fuchs and to Cindy Baran for their efforts in the preparation of the manuscript.

APPENDIX A. CUMULANT EXPANSIONS

The cluster expansion described above in Sec. IIIA3 is not the usual Ursell–Mayer cluster expansion, involving the cumulants of the random variable η_i, but is rather a self-consistent *partial* cumulant technique as has been emphasized by Yonezawa (1968). The difference in the analytic properties produced is substantial, due to spurious features that occur inherently in the cumulant expansion which are removed by the self-consistent technique. Nevertheless, the problem of a binary alloy presents a simple enough form for the cumulant coefficients that they can be found in closed form and summed, for certain classes of diagrams, to all orders. This infinite summation of cumulant coefficients has been done in no other problem to our knowledge, and its accomplishment here has pointed out the serious divergence difficulties which can arise in cumulant expansions.

The cumulant expansion technique has been carried out by Yonezawa and Matsubara (1966a, b) for the electronic problem, by Leath and Goodman (1966, 1968) for the phonon problem, and by Matsubara and Kaneyoshi (1966) for the localized state expansion of the electronic problem. Basically, Matsubara and his co-workers have used a generating function for the cumulants, whereas Leath and Goodman found a closed form for the cumulant coefficients.

The essential difference between the cumulant expansion and the self-consistent diagram rules of Sec. IIIA is that in the cumulant expansion each interaction point receives a coefficient $P_n(c)$ which is obtained by subtracting from c the coefficient of all diagrams that can be gotten by breaking the interaction lines away from the interaction point *regardless of whether the resulting diagrams are included in the particular approximation that is being made at the time.* For example, let us consider the third-order diagram shown in Fig. 59(a). The multiple-occupancy corrections which are included in the cumulant expansion to this diagram are shown in Figs. 59(b), (c), (d), (e), whereas Fig. 59(d) is not included via the self-consistent method when only single-site irreducible parts are summed (as one can see from the third row of Fig. 9). Thus, we find

$$P_3(c) = c - 3c^2(1-c) - c^3 = c - 3c^2 + 2c^3. \tag{A1}$$

However, the contribution from the method described by Fig. 9 would give the coefficient

$$c - 2c^2(1-c) - c^3 = c - 2c^2 + c^3 = c(1-c)^2 \tag{A2}$$

to this diagram. This difference, Fig. 59(d), and other such correction diagrams lead to the spurious behavior.

Leath and Goodman (1966) gave an elaborate inductive argument for the closed form of $P_n(c)$ for all n and subsequently (1968) rederived this form directly. They proved that $P_n(c)$ was of the form

$$P_n(c) = \sum_{m=1}^{n} (-1)^{m-1}(m-1)!c^m S(n,m), \tag{A3}$$

where $S(n,m)$ is a Stirling number of the second kind and represents the number of ways of partitioning a set of n objects into m nonempty subsets. In terms of the random variable η_i which may be chosen to denote site occupancy by a B atom, the cumulants or semi-invariants $P_n(c)$ are given by

$$\begin{aligned} P_1(c) &= \langle \eta_i \rangle = c \\ P_2(c) &= \langle \eta_i^2 \rangle - \langle \eta_i \rangle^2 = c - c^2 \\ P_3(c) &= \langle \eta_i^3 \rangle - 3\langle \eta_i^2 \rangle \langle \eta_i \rangle + 2\langle \eta_i \rangle^3 = c - 3c^2 + 2c^3. \end{aligned} \tag{A4}$$

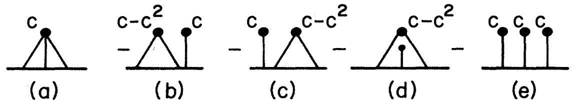

FIG. 59. (a) A third-order diagram and the correction diagrams (b)–(e) whose vertex confluence determines $P_3(c)$.

This closed form is useful for any random occupancy variable which takes on only two values, as in a binary alloy, or a spin-$\frac{1}{2}$ system.

The sum of the single-site self-energy diagrams shown in column 1 of Fig. 9 is then easily performed via the well known sum rules for Stirling numbers. (These sum rules can be found, for example, in the National Bureau of Standards, *Handbook of Mathematical Functions*, edited by Abramowitz and Stegun, 1964.) The result is

$$\Sigma^1(\epsilon) = \sum_{n=1}^{\infty} P_n(c) V^n P_0^{n-1}(\epsilon) \tag{A5}$$

which becomes

$$\Sigma^1(\epsilon) = \frac{cV}{1-VP_0(\epsilon)} \, {}_2F_1\{1, 1, 2 - [VP_0(\epsilon)]^{-1}; c\}, \tag{A6}$$

where ${}_2F_1$ is the hypergeometric function which has poles at all nonpositive integral values of its third argument, i.e., at $[1 - nVP(\epsilon)] = 0$ for $n = 2, 3, 4, \cdots$. These poles would correspond to 2, 3, 4, $\cdots$ perturbations V located on one site, i.e., "multiple-occupancy" of a single site. They are completely spurious and represent the overcorrection inherent in this cumulant expansion method.

The results of Matsubara and Yonezawa (1966) and of Matsubara and Kaneyoshi (1966) for the localized state expansion may appear to be different but they are identical.

The essential ingredient discovered by Matsubara and Yonezawa (1966a) is the generating function for the $P_n(c)$, which follows directly from the definition of cumulant coefficients. The cumulants of a single random variable X are defined by

$$\langle \exp(\alpha X) \rangle \equiv \exp\left(\sum_{n=1}^{\infty} \frac{\alpha^n P_n(X)}{n!} \right). \tag{A7}$$

In our case, $\langle X^n \rangle = \langle \eta_i^n \rangle = c$, so that

$$\langle \exp(\alpha X) \rangle = 1 + \alpha c + \frac{\alpha^2}{2!} c + \frac{\alpha^3}{3!} c + \cdots \tag{A8}$$

or

$$g(\alpha; c) = \sum_{n=1}^{\infty} \frac{\alpha^n P_n(c)}{n!} = \ln(1 - c + ce^{\alpha}) \tag{A9}$$

from which it follows that

$$P_n(c) = \left. \frac{d^n[g(\alpha; c)]}{(d\alpha)^n} \right|_{\alpha=0}. \tag{A10}$$

Then, we find for Eq. (A5) that

$$\Sigma^1(\epsilon) = V \int_0^{\infty} dt \exp(-t) [P_1(c) + P_2(c)(VP_0 t) + \frac{P_3(c)}{2!}(VP_0 t)^2 + \cdots], \tag{A11}$$

$$\Sigma^1(\epsilon) = V \int_0^{\infty} dt \exp(-t) \frac{d[g(VP_0 t; c)]}{d(VP_0 t)}, \tag{A12}$$

$$\Sigma^1(\epsilon) = V\int_0^\infty dt\,\frac{\exp(-t)c\exp(VP_0t)}{1-c+c\exp(VP_0t)}\,, \tag{A13}$$

which is an integral representation of the hypergeometric function in Eq. (A6) and thus also contains the spurious poles.

Matsubara and Yonezawa (1966b) and Leath and Goodman (1968) have also extended this work to include scattering by pairs of defects. Leath and Goodman (1968) showed that the pair self-energy so calculated not only contained terms with the spurious poles in the single-site self-energy corresponding to more than two defects on the same site, but also produced a new, infinite set of spurious poles corresponding to the multiple occupancy of pairs of sites by any number of defects.

It would seem that the lesson to be learned from these calculations is that one must be very careful in making a cumulant expansion approximation, especially when one is trying to renormalize divergences, because the cumulant expansion can inherently produce spurious new divergences which are echoes of the physical divergences.

APPENDIX B. LLOYD'S EXACTLY SOLVABLE MODEL

In 1969, Lloyd demonstrated a model of disorder which allows for an exact solution of the configuration-averaged one-particle Green's function. His model is such that the site-diagonal perturbations $V(n)$ at each site are statistically independent,

$$\mathcal{P}(\{V(n)\}) = \prod_n \mathcal{P}(V(n)), \tag{B1}$$

where the individual $V(n)$ are distributed according to the Lorentzian probability distribution

$$\mathcal{P}(V) = \frac{1}{\pi}\frac{\Gamma}{V^2+\Gamma^2} = \frac{1}{2\pi i}\left[\frac{1}{V-i\Gamma} - \frac{1}{V+i\Gamma}\right], \tag{B2}$$

where Γ is the width of the Lorentzian distribution centered at $V = 0$. (It is trivial to center the distribution at any other value.) By the configurational ensemble average of $\langle \mathbf{G}\rangle$ Lloyd means

$$\langle G_{nm}(E)\rangle = \int\cdots\int G_{nm}(E)\pi_r\mathcal{P}(V(r))\,dV(r). \tag{B3}$$

We shall see below that this coincides with the definition used above of the configuration average. The trick performed by Lloyd at this point is to use the properties of the Lorentzian distribution to evaluate the multiple (about 10^{23}-fold) integral (B3) exactly.

From the solution (2.99) above for the case of a single impurity, we note that the one-particle Green's function $G_{nm}(E, V(1)V(2)\cdots)$, where $V(r)$ is the value of the perturbations on site r, can be written in the form

$$G_{nm}(E, V(r)) = G_{nm}(E, V(r)=0) + G_{rr}(E,0) \times \frac{V(r)}{1-V(r)G_{rr}(E,0)}G_{rr}(E,0), \tag{B4}$$

where $G_{nm}(E;\ \cdots 0\cdots)$ differs from $G_{nm}(E;\ \cdots V(r)\cdots)$ only in that the perturbation on site r is different. In this form, the integral on $dV(r)$ in (B3) can be performed exactly. This integral is

$$\langle G_{nm}\rangle_r = \frac{1}{2\pi i}\int_{-\infty}^{\infty} dV(r)\left[\frac{1}{V(r)-i\Gamma} - \frac{1}{V(r)+i\Gamma}\right] \times G_{nm}(E, \cdot\cdot V(r)\cdots). \tag{B5}$$

The only $V(r)$ dependence in Eq. (B4) is in the last term, so that one need only evaluate the integral

$$\langle t(r)\rangle = \frac{1}{2\pi i}\int_{-\infty}^{\infty} dV(r)\left[\frac{1}{V(r)-i\Gamma} - \frac{1}{V(r)+i\Gamma}\right] \times \frac{V(r)}{1-V(r)G_{rr}(E,0)}\,. \tag{B6}$$

But G_{rr} is the retarded Green's function in our formalism and has a small negative imaginary part. Thus $V(r)/(1-V(r)G_{rr})$ as a complex function of $V(r)$ has a pole in the upper half-plane. Therefore we evaluate (B6) by closing the contour about the lower half-plane. This closing of the contour gives no additional contribution, since the Lorentzian vanishes at infinity. Thus the integral along the real axis has its only contribution from the residue of the pole at $V(r) = -i\Gamma$ which gives

$$\langle t(r)\rangle = -i\Gamma/[1+i\Gamma G_{rr}(E,0)] \tag{B7}$$

for the integral (B6). Thus formula (B5) becomes

$$G_{nm}(E, -i\Gamma). \tag{B8}$$

Likewise, the remaining 10^{23} integrals in (B3) are trivially done with the result

$$\langle G_{nm}(E)\rangle = G_{nm}(E, -i\Gamma, -i\Gamma\cdots) = G_{nm}(E+i\Gamma, 0) = P_{nm}(E+i\Gamma), \tag{B9}$$

which is the perfect crystal Green's function in which each state is coarse-grained or smeared with a resolution width Γ. This model very neatly shows the coarse-graining effect of the configuration-averaging process.

It is interesting to note what happens if one uses Lloyd's method of averaging [Eq. (B3)] on the binary alloy where the distribution function is

$$\mathcal{P}(V(r)) = (1-c)\delta(V(r)-V_{\mathrm{A}}) + c\delta(V(r)-V_{\mathrm{B}}). \tag{B10}$$

The average $\langle G_{nm}(E)\rangle_r$ on $V(r)$ becomes simply

$$\langle G_{nm}(E)\rangle_r = (1-c)G_{nm}(E, V(1), V(2), \cdots V_{\mathrm{A}}\cdots) + cG_{nm}(E, V(1), V(2), \cdots V_{\mathrm{B}}\cdots), \tag{B11}$$

where V_A and V_B appear in the rth position. Likewise, the remaining 10^{23} integrals can be done again with the final result

$$\begin{aligned}\langle G_{nm}(E)\rangle = {} & (1-c)^N G_{nm}(E, V_A, V_A\cdots) \\ & + c(1-c)^{N-1}G_{nm}(E, V_A, V_A, \cdots V_B, \cdots) \\ & + \cdots + c^N G_{nm}(E, V_B, V_B\cdots),\end{aligned} \tag{B12}$$

where the first term contains the Green's function for the perfect A-atom lattice (of N sites), the second term sums over N possible positions of a single B atom in the A-atom lattice, the third term sums over all possible configurations of two B atoms, etc. For large N the central limit theorem clearly applies, and essentially the term with the actual concentration of B atoms dominates, namely, the term

$$\begin{aligned}\langle G_{nm}(E)\rangle_N \to {} & c^{cN}(1-c)^{(1-c)N} \\ & \times \sum G_{nm}(E, E_A, E_A, \cdots\cdot E_B, E_B\cdots).\end{aligned} \tag{B13}$$

But in the limit of large N we find, using Stirling's formula,

$$c^{cN}(1-c)^{(1-c)N} = \left(\frac{N_B}{N}\right)^{N_B}\left(\frac{N_A}{N}\right)^{N_A} \to \frac{N_B!N_A!}{N!} \tag{B14}$$

which is the inverse of the binomial coefficient giving the number of terms in the sum (B13). Therefore Lloyd's method, as applied to the binary alloy, clearly establishes the formal equivalence of integrating over the distribution of $V(n)$ at each site and using ensemble configuration averaging which has more generally been in use. It also justifies the use of the grand ensemble average (exact conservation of the numbers of atoms of each species is not necessary) in disordered systems. Unfortunately Lloyd's method gives nothing more than this identity for the binary alloy, in marked contrast to the case of the Lorentzian distribution of Lloyd's model.

A primary purpose of Lloyd's paper seems to have been to show, from his exact calculation of the configuration-averaged one-particle Green's function, that no localized states exist. This proof is wrong, as was discussed above, in Sec. IIE4, since the averaging of the one-particle Green's function averages away the information on localization contained in the phase of the Green's function. On the other hand, a calculation of the conductivity which involves $\langle G(E+)G(E-)\rangle$, as had recently been attempted by Saitoh (1971), can yield this information. Unfortunately Lloyd's model is not so easily solved for this two-particle Green's function since $G(E+)$ and $G(E-)$ have their poles in opposite halves of the complex plane, so that closing the contour in either half plane encloses a real physical pole (corresponding to the real vertex function) so that all 10^{23} integrals are not so easily done. Thus Saitoh was only able to reach very limited conclusions about the conductivity.

APPENDIX C. SYMMETRY TRANSFORMATION IN SIMPLE CUBIC CRYSTALS

In this appendix, we show how the 7 × 7 matrices encountered in the treatment of the simple cubic lattice may be reduced to block-diagonal form (Wolfram and Callaway, 1963; Pepper, 1972). The matrices we are concerned with all have the following form:

$$\mathbf{A} = \begin{pmatrix} A_{00} & A_{01} & A_{01} & A_{01} & A_{01} & A_{01} & A_{01} \\ A_{01} & A_{11} & A_{12} & A_{13} & A_{13} & A_{13} & A_{13} \\ A_{01} & A_{12} & A_{11} & A_{13} & A_{13} & A_{12} & A_{13} \\ A_{01} & A_{13} & A_{13} & A_{11} & A_{12} & A_{13} & A_{13} \\ A_{01} & A_{13} & A_{13} & A_{12} & A_{11} & A_{13} & A_{13} \\ A_{01} & A_{13} & A_{12} & A_{13} & A_{13} & A_{11} & A_{12} \\ A_{01} & A_{13} & A_{13} & A_{13} & A_{13} & A_{12} & A_{11} \end{pmatrix}, \tag{C1}$$

where 0 signifies the central atom and 1 a neighbor; A_{12} is the element between a pair of opposite neighbors, and A_{13} between nearest neighbors on the first coordination sphere.

Any matrix like $\mathbf{A}$ may be block-diagonalized by a unitary transformation $\mathbf{S}$:

$$\mathbf{S} = \left(\begin{array}{cc|ccc|cc} 1 & 0 & 0 & 0 & 0 & 0 & 0 \\ 0 & a & b & 0 & 0 & 0 & d \\ 0 & a & -b & 0 & 0 & 0 & d \\ 0 & a & 0 & b & 0 & c & e \\ 0 & a & 0 & -b & 0 & c & e \\ 0 & a & 0 & 0 & b & -c & e \\ 0 & a & 0 & 0 & -b & -c & e \end{array}\right), \tag{C2a}$$

where

$$\begin{aligned} a &= 1/(6)^{1/2} & b &= 1/\sqrt{2} \\ c &= 1/2 & d &= 1/\sqrt{3}. \end{aligned} \tag{C2b}$$

The first two such symmetrized modes are s-like, the next two are p-like modes, and the last two are d modes. The effect of transforming $\mathbf{A}$ by $\mathbf{S}$ is as follows:

$$\mathbf{S}^T\mathbf{A}\mathbf{S} = \left(\begin{array}{cc|ccc|cc} A_{00} & (6)^{1/2}A_{01} & & & & & \\ (6)^{1/2}A_{01} & A_s' & & & & & \\ \hline & & A_p & 0 & 0 & & \\ & & 0 & A_p & 0 & & \\ & & 0 & 0 & A_p & & \\ \hline & & & & & A_d & 0 \\ & & & & & 0 & A_d \end{array}\right), \tag{C3}$$

with

$$\begin{aligned} A_s' &= A_{11} + A_{12} + 4A_{13} \\ A_p &= A_{11} - A_{12} \\ A_d &= A_{11} + A_{12} - 2A_{13}. \end{aligned} \tag{C4}$$

It is also necessary to be able to construct the Fourier transform $A(\mathbf{k})$ from the s, p, and d components of A. If we write the s block as

$$A_s = \begin{pmatrix} A_{00}{}^s & A_{01}{}^s \\ A_{01}{}^s & A_{11}{}^s \end{pmatrix} \tag{C5}$$

then we may invert (C3) and (C4) to obtain the ordinary space components A_{00}, A_{11}, etc. in terms of A_s, A_p, A_d, and so produce the Fourier transform:

$$\begin{aligned} A(\mathbf{k}) &= A_{00} + 6A_{11} + 12A_{01}\gamma_{\mathbf{k}} + 6A_{12}\gamma_{2\mathbf{k}} + 24A_{13}\Gamma_{\mathbf{k}} \\ &= [A_{00}{}^s + 2(6)^{1/2}A_{01}{}^s\gamma_{\mathbf{k}} + A_{11}{}^s(1 + \gamma_{2\mathbf{k}} + 4\Gamma_{\mathbf{k}})] \\ &\quad + 3A_p(1 - \gamma_{2\mathbf{k}}) + 2A_d(1 + \gamma_{2\mathbf{k}} - 2\Gamma_{\mathbf{k}}) \\ &= A_s(\mathbf{k}) + 3A_p(\mathbf{k}) + 2A_d(\mathbf{k}), \end{aligned} \tag{C6}$$

where

$$\begin{aligned} \gamma_{2\mathbf{k}} &= (1/6) \sum_{\Delta_{12}} \exp(i\mathbf{k}\cdot\mathbf{\Delta}_{12}) \\ \Gamma_{\mathbf{k}} &= (1/24) \sum_{\Delta_{13}} \exp(i\mathbf{k}\cdot\mathbf{\Delta}_{13}). \end{aligned} \tag{C7}$$

It will be useful to express the quantity $\Gamma_{\mathbf{k}}$ in terms of $\gamma_{2\mathbf{k}}$ and $\gamma_{\mathbf{k}}$. Squaring $\gamma_{\mathbf{k}}$ we obtain:

$$\begin{aligned} \gamma_{\mathbf{k}}{}^2 = \tfrac{1}{9}\{&\cos(2k_xa) + \cos(2k_ya) + \cos(2k_za) \\ &+ 2[\cos(k_xa)\cos(k_ya) + \cdots]\}. \end{aligned} \tag{C8}$$

Now Γ_k may be written as a sum of terms like

$$\cos(k_xa)\cos(k_ya),$$

and so Eq. (C8) may be rearranged as

$$\begin{aligned} \gamma_{\mathbf{k}}{}^2 = (1/18)&\{\cos(2k_xa) + \cos(2k_ya) + \cos(2k_za)\} \\ &+ \tfrac{1}{6} + \tfrac{2}{3}\Gamma_{\mathbf{k}}, \end{aligned} \tag{C9}$$

whence

$$\Gamma_{\mathbf{k}} = \tfrac{3}{2}\gamma_{\mathbf{k}}{}^2 - \tfrac{1}{4}(\gamma_{2\mathbf{k}} + 1). \tag{C10}$$

Using this in Eq. (C6), we obtain

$$\begin{aligned} A_s(\mathbf{k}) &= A_{00}{}^s + 2(6)^{1/2}A_{01}{}^s\gamma_{\mathbf{k}} + A_{11}{}^s\cdot 6\gamma_{\mathbf{k}}{}^2 \\ A_p(\mathbf{k}) &= A_p\cdot(1 - \gamma_{2\mathbf{k}}) \\ A_d(\mathbf{k}) &= A_d\cdot\tfrac{3}{2}(1 + \gamma_{2\mathbf{k}} - 2\gamma_{\mathbf{k}}{}^2). \end{aligned} \tag{C11}$$

REFERENCES

Abou-Chacra, R., P. W. Anderson, and D. J. Thouless, 1973, J. Phys. C **6**, 1934.

Abou-Chacra, R., P. W. Anderson, and D. J. Thouless, 1974, J. Phys. C **7**, 65.

Adler, D., 1971, CRC Crit. Rev. Solid State Sci. **2**, 317.

Adler, D., L. P. Flora, and S. D. Senturia, 1973, Solid State Commun. **12**, 9.

Adler, J. G., and B. S. Chandrashekar, 1968, in *Localized Excitations in Solids*, edited by R. F. Wallis (Plenum, New York), p. 694.

Agacy, R. L., 1964, Proc. Phys. Soc. Lond. **83**, 591.

Aiyer, R. N., R. J. Elliott, J. A. Krumhansl, and P. L. Leath, 1969, Phys. Rev. **181**, 1006.

Als-Nielson, J., 1968, in *Neutron Inelastic Scattering: Proceedings of a Symposium on Neutron Inelastic Scattering held by the International Atomic Energy Agency in Copenhagen, May 20–25, 1968* (IAEA, Vienna), p. 60.

Anderson, P. W., 1958, Phys. Rev. **109**, 1492.

Anderson, P. W., 1970, Comments Solid State Phys. **2**, 193.

Anderson, P. W., 1972, Proc. Natl. Acad. Sci. (US) **69**, 5, 1097.

Anderson, P. W., and W. L. McMillan, 1967, in "Theory of Magnetism in Transition Metals," *Proceedings of the International School of Physics 'Enrico Fermi'*, edited by H. Suhl (Academic, New York).

Azaroff, L. V., and B. N. Das, 1964, Phys. Rev. **134**, A747.

Baym, G., 1962, Phys. Rev. **127**, 1391.

Barker, A. S., and A. Sievers (to be published).

Barker, A. S., and R. Loudon, 1972, Rev. Mod. Phys. **44**, 18.

Barker, A. S., J. A. Ditzenberger, and H. J. Guggenheim, 1968, Phys. Rev. **175**, 1180.

Beaglehold, D., and E. Erlbach, 1970, Solid State Commun. **8**, 255.

Beeby, J., 1964a, Proc. R. Soc. Lond. A **279**, 82.

Beeby, J., 1964b, Phys. Rev. **135**, A130.

Beeby, J., and S. F. Edwards, 1962, Proc. R. Soc. Lond. A **274**, 395.

Bell, R., 1972, Rep. Prog. Phys. **35**, 1315.

Beran, M. J., 1968, *Statistical Continuum Theories* (Interscience, New York).

Beran, M. J., 1971, Phys. Status Solidi **6**, 365.

Beserman, R., and M. Balkanski, 1970, Phys. Rev. B **1**, 608.

Bishop, A. R., 1973, Phil. Mag. **27**, 651, 1489.

Blackman, J. A., 1973, J. Phys. F **3**, L31.

Blackman, J. A., D. M. Esterling, and N. F. Berk, 1971a, Phys. Lett. A **35**, 205.

Blackman, J. A., D. M. Esterling, and N. F. Berk, 1971b, Phys. Rev. B **4**, 2412.

Blackman, J. A., and R. J. Elliott, 1970, J. Phys. C **3**, 2066.

Borland, R. E., 1963, Proc. R. Soc. A **274**, 529.

Borland, R. E., 1964, Proc. Phys. Soc. Lond. **83**, 1027.

Born, M., and K. Huang, 1954, *Dynamical Theory of Crystal Lattices* (Oxford U. P., London).

Brafman, O., I. F. Chang, G. Lengyel, S. S. Mitra, and E. Carnall, Jr., 1968, in *Localized Excitations in Solids*, edited by R. F. Wallis (Plenum, New York), p. 602.

Braunstein, R., 1963, Phys. Rev. **130**, 869, 879.

Broadbent, S. R., and J. M. Hammersley, 1957, Proc. Camb. Philos. Soc. **53**, 629.

Brockhouse, B. N., and A. P. Roy, 1970, Can. J. Phys. **48**, 1781.

Brodsky, M. H., G. Lucovsky, M. F. Chen, and T. S. Plaskett, 1970, Phys. Rev. B **2**, 3303.

Broude, V. L., and E. Rashba, 1962, Sov. Phys.—Solid State **3**, 1415.

Brouers, F., 1970, J. Non-Cryst. Solids **4**, 428.

Brouers, F., 1971, J. Phys. C **4**, 773.

Brouers, F., 1972, Solid State Commun. **10**, 757.

Brouers, F., M. Cyrot, and F. Cyrot-Lackmann, 1973a, Phys. Rev. B **7**, 4370.

Brouers, F., F. Ducastelle, F. Gautier, and J. Van Der Rest, 1973b J. Phys. F **3**, 2120.

Brouers, F., and J. Van Der Rest, 1972, J. Phys. F **2**, 1070.

Brouers, F., and A. V. Vedyayev, 1972, Phys. Rev. B **5**, 349.

Brouers, F., A. V. Vedyayev, and M. Giorgino, 1973c, Phys. Rev. B **7**, 380.

Brown, W. F., 1955, J. Chem. Phys. **23**, 1514 (reviews much previous work).

Brown, W. F., 1956, Handb. Phys. **17**, 104.

Bruggeman, D. A. G., 1935, Ann. Phys. (Leipz.) **24**, 636.

Bruno, R., and D. W. Taylor, 1971, Can. J. Phys. **49**, 3201.

Brust, D., 1964, Phys. Rev. **134**, A1337.

Buchanan, M., W. J. L. Buyers, R. J. Elliott, R. T. Hayes, A. M. Perry, and I. D. Saville, 1972, J. Phys. C **5**, 2011.
Budiansky, B., 1970, J. Compos. Mater. **4**, 286.
Budworth, D. W., F. E. Hoare, and J. Preston, 1960, Proc. R. Soc. A **257**, 250.
Butler, W. H., 1972, Phys. Lett A **39**, 203.
Butler, W. H., 1973, Phys. Rev. B **8**, 4499.
Butler, W. H., and B. G. Nickel, 1973, Phys. Rev. Lett. **30**, 373.
Butler, W. H., and W. Kohn, 1970, J. Res. Natl. Bur. Stand. (US) A **74**, 443.
Buyers, W. J. L., D. E. Pepper, and R. J. Elliott, 1972, J. Phys. C **5**, 2611.
Buyers, W. J. L., D. E. Pepper, and R. J. Elliott, 1973, J. Phys. C **6**, 1933.
Buyers, W. J. L., T. M. Holden, E. C. Sversson, R. A. Cowley, M. T. Hutchings, D. Hukin, and R. W. H. Stevenson, 1971a, Phys. Rev. Lett. **27**, 1442.
Buyers, W. J. L., T. M. Holden, E. C. Svensson, R. A. Cowley, and M. T. Hutchings, 1971b, J. Phys. C **4**, 2139.
Buyers, W. J. L., R. A. Cowley, T. M. Holden, and R. W. H. Stevenson, 1968, J. Appl. Phys. Phys. **39**, 1118.
Callaway, J., 1964, J. Math. Phys. **5**, 783.
Čapek, V., 1971a, Phys. Status Solidi B **43**, 61.
Čapek, V., 1971b, Czech. J. Phys. B **21**, 997.
Čapek, V., 1972, Phys. Status Solidi B **52**, 399.
Carruthers, P., 1961, Rev. Mod. Phys. **33**, 92.
Casher, A., and J. L. Liebowtiz, 1971, J. Math. Phys. **12**, 1701.
Chang, I. F., 1968, Ph.D. dissertation, University of Rhode Island.
Chang, I. F., and S. S. Mitra, 1968, Phys. Rev. **172**, 924.
Chang, I. F., and S. S. Mitra, 1971, Adv. Phys. **20**, 359.
Chen, Y. S., W. Shockley, and G. L. Pearson, 1966, Phys. Rev. **151**, 648.
Clark, J. A., and P. G. Dawber, 1972, J. Phys. F **2**, 930.
Cohen, M. H. and J. Jortner, 1973, Phys. Rev. Lett. **30**, 699.
Cohen, M. H., H. Fritzsche, and S. R. Ovshinsky, 1969, Phys. Rev. Lett. **22**, 1065.
Cohen, S. S., and G. Gilat, 1972, Solid State Commun. **11**, 1269.
Coombs, G. J., R. A. Cowley, W. J. L. Buyers, E. C. Svensson, and T. M. Holden, 1973 (to be published).
Cosand, A. E., and W. G. Spitzer, 1971, J. Appl. Phys. **42**, 5241.
Cowley, R. A., and W. J. L. Buyers, 1968, in *Neutron Inelastic Scattering: Proceedings of a Symposium on Neutron Inelastic Scattering held by the International Atomic Energy Agency in Copenhagen, May 20–25, 1968* (IAEA, Vienna), p. 43.
Cowley, R. A., and W. J. L. Buyers, 1972, Rev. Mod. Phys. **44**, 406.
Cunningham, R. M., L. D. Muhlestein, W. M. Shaw, and C. W. Tompson, 1970, Phys. Rev. B **2**, 4864.
Cyrot, M., 1972, Phil. Mag. **25**, 1031.
Cyrot-Lackmann, F., and F. Ducastelle, 1971, Phys. Rev. Lett. **27**, 429.
Cyrot-Lackmann, F., and M. Cyrot, 1972, J. Phys. C **5**, L209
Das, M. P., and S. K. Joshi, 1972, Can. J. Phys. **50**, 2856.
Davies, R. W., and J. S. Langer, 1963, Phys. Rev. **131**, 163.
Dawber, P. G., and R. J. Elliott, 1963, Proc. R. Soc. Lond. A **273**, 222.
Dawber, P. G., and R. E. Turner, 1966, Proc. Phys. Soc. Lond. **88**, 217.
Dean, P., 1959, Proc. Phys. Soc. Lond. **73**, 413.
Dean, P., 1960, Proc. R. Soc. Lond. A **254**, 507.
Dean, P. 1961, Proc. R. Soc. Lond. A **260**, 263.
Dean. P., 1967, J. Inst. Math. Appl. **3**, 98.
Dean. P., 1972, Rev. Mod. Phys. **44**, 127.
Dixon, M., F. E. Hoare, and T. M. Holden, 1968, Proc. R. Soc. Lond. A **303**, 339.
Drain, L. E., 1967, Metall. Rev. **119**, 195.
Dubrovskii, O. A., and Y. V. Konoveev, 1970, Sov. Phys.—Solid State **12**, 321.
Ducastelle, F., 1971, J. Phys. C **4**, L75.
Ducastelle, F., 1972, J. Phys. F **2**, 468.
Ducastelle, F., 1973, in *Proceedings of the Conference on Disordered Materials, Strasbourg, 1974*, to be published in J. Phys. (Paris).
Dy, K. S., and Shi-Yu Wu, 1971, Phys. Rev. B **3**, 1173.
Dyson, F. J., 1953, Phys. Rev. **92**, 1331.
Eastman, D. E., and W. F. Krolikowski, 1968, Phys. Rev. Lett. **21**, 623.
Economou, E. N., 1971, Solid State Commun., **9**, 1317.
Economou, E. N., 1972, Phys. Rev. Lett. **28**, 1206.
Economou, E. N., and M. H. Cohen, 1970, Phys. Rev. Lett. **25**, 1445.
Economou, E. N., and M. H. Cohen, 1972, Phys. Rev. B **5**, 2931.
Economou, E. N., and C. Papatriantafillou, 1972, Solid State Commun. **11**, 197.
Economou, E. N., M. H. Cohen, K. F. Freed, and E. S. Kirkpatrick, 1971, in *Amorphous and Liquid Semiconductors*, edited by J. Tauc (Plenum, New York).
Economou, E. N., S. Kirkpatrick, M. H. Cohen, and T. P. Eggarter, 1970, Phys. Rev. Lett. **25**, 520.
Economou, E. N., D. C. Licciardello, and K. L. Ngai, Bull. Mater. Res. (to be published).
Edwards, J. T., and D. J. Thouless, 1971, J. Phys. C **4**, 453.
Edwards, J. T., and D. J. Thouless, 1972, J. Phys. C **5**, 807.
Edwards, S. F., 1958, Phil. Mag. **3**, 1020.
Edwards, S. F., 1959, Phil. Mag. **4**, 1171.
Edwards, S. F., and R. C. Jones, 1971, J. Phys. C **4**, 2109.
Eggelstaff, P. A., 1967, *An Introduction to the Liquid State* (Academic, New York).
Ehrenreich, H., *et al.*, 1971, "Fundamentals of Amorphous Semiconductors," publication NMAB-284 National Academy of Sciences-National Academy of Engineering, Washington, D.C.
Einstein, A., 1906, *Investigations on the Theory of Brownian Motion* (Dover Reprint, New York, 1956).
Elliott, R. J., and D. W. Taylor 1964, Proc. Phys. Soc. Lond. **83**, 189.
Elliott, R. J., and D. W. Taylor, 1967, Proc. R. Soc. Lond. A **296**, 161.
Elliott, R. J., and W. Hartmann, 1967, Proc. Phys. Soc. Lond. **91**, 187
Elliott, R. J., and D. E. Pepper, 1973, Phys. Rev. B **8**, 2374.
Enders, B., P. L. Richards, W. E. Tennant, and E. Catalano, 1973, in Proceedings of the American Institute of Physics Conference (to be published).
Erdos, P., 1965a, Phys. Rev. **138**, A1200.
Erdos, P., 1965b, Phys. Rev. **139**, A1249.
Essam, J. W., 1973, in *Phase Transitions and Critical Phenomena*, edited by C. Domb and M. S. Green (Academic, New York).
Falicov, L. M., and J. C. Kimball, 1969, Phys. Rev. Lett. **22**, 997.
Farineau, J., and M. Morland, 1938, J. Phys. Radium **10**, 447.
Feldman, D. W., M. Ashkin, and J. H. Parker, 1966, Phys. Rev. Lett. **17**, 1209.
Fertel, J. H., and C. H. Perry, 1969, Phys. Rev. **184**, 874.
Fisher, M. E., 1964, in *Proceedings of the IBM Scientific Computing Symposium on Combinatorial Problems* (IBM, New York).
Flicker, J. K., and P. L. Leath, 1973, Phys. Rev. B **7**, 2296.
Foldy, L. L., 1945, Phys. Rev. **67**, 107.
Foo, E-Ni, A. Amar, and M. Austloos, 1971, Phys. Rev. B **4**, 3350.
Foo, E-Ni, and D. H. Wu, 1972, Phys. Rev. B **5**, 98.
Foo, E-Ni, and H. Amar, 1970, Phys. Rev. Lett. **25**, 1748.
Freed, K. F., 1972, Phys. Rev. B **5**, 4802.
Freed, K. F., and M. H. Cohen, 1971, Phys. Rev. B **3**, 3400.
Friedman, H., and W. W. Beeman, 1940, Phys. Rev. **58**, 400.
Frisch, H. L., and J. M. Hammersley, 1963, J. Soc. Ind. Appl. Math. **11**, 894.
Frisch, H. L., and S. P. Lloyd, 1960, Phys. Rev. **120**, 1175.
Frisch, U., 1968, in *Probabilistic Methods in Applied Mathematics*, edited by A. T. Bharuch-Reid (Academic, New York).
Fukuyama, H., and H. Ehrenreich, 1973, Phys. Rev. B **7**, 3266.
Gambino, R. J., T. R. McGuire, H. A. Alperin, and S. J. Pickart, 1970, J. Appl. Phys. **41**, 933.
Gobsch, G., and W. Weller, 1973, Phys. Status Solidi B **57**, 593.
Goncalves Da Silva, C. E. T., and L. M. Falicov, 1972, J. Phys. C **5**, 906.
Goto, T., Y. Kato, and C. I. Yu, 1970, J. Phys. Soc. Jap. **28**, 104.
Goto, T., and T. Takahashi, 1968, J. Phys. Soc. Jap. **25**, 461.
Gubanov, A. I., 1960, Fiz. Tverd. Tela **2**, 502 [Sov. Phys.—Solid State **2**, 468 (1961)].
Gubernatis, J. E., and P. L. Taylor, 1973a, Phys. Lett. A **43**, 211.
Gubernatis, J. E., and P. L. Taylor, 1973b, in *Amorphous Magnetism*, edited by H. O. Hooper and A. M. deGraaf (Plenum, New York).
Gubernatis, J. E., and P. L. Taylor, 1973c, J. Phys. C **6**, 1889.
Gyorffy, B. L., 1970, Phys. Rev. B **1**, 3290.
Halperin, B. I., 1967, Adv. Chem. Phys. **13**, 123.
Halpern, V., 1972, J. Phys. C **5**, 3322.
Hammersley, J. M., 1957, Proc. Camb. Philos. Soc. **53**, 642.
Handrich, K., 1969, Phys. Status Solidi B **32**, K55.
Harada, H., and S. Narita, 1971, J. Phys. Soc. Jap. **30**, 1628.
Harris, A. B., P. L. Leath, B. Nickel, R. J. Elliott, and D. E. Pepper, 1974 J. Phys. C (to be published).
Harris, R., M. Plischke, and M. J. Zuckermann, 1973, Phys. Rev. Lett. **31**, 160.
Harris, R., and M. J. Zuckermann, 1972, Phys. Rev. B **5**, 101.
Hartmann, W. M., 1968, Phys. Rev. **172**, 677.

Hartmann, W. M., H. V. Culbert, and R. P. Huebener, 1970, Phys. Rev. B **1**, 1486.

Hasegawa, H., and K. Kanemori, 1970a, J. Phys. Soc. Jap. **31**, 382.

Hasegawa, H., and K. Kanemori, 1970b, J. Phys. Soc. Jap. **33**, 1599, 1607.

Hasegawa, H., and K. Kanemori, 1972, J. Phys. Soc. Jap. **33**, 1599, 1607.

Hashin, Z., 1964, Appl. Mech. Rev. **17**, 1.

Haydock, R., and A. Mookerjee (to be published).

Herbert, D., and R. Jones, 1971, J. Phys. C **4**, 1145.

Herman, F., M. Glicksman, and R. H. Parmenter, 1957, Prog. Semicond. **2**, 1.

Hill, R., 1967, J. Mech. Phys. Solids **15**, 79.

Hirota, T., 1973, Prog. Theor. Phys. **50**, 1240.

Holden, T. M., W. J. L. Buyers, E. C. Svensson, R. A. Cowley, and M. T. Hutchings, 1971, J. Phys. C **4**, 2127.

Hooper, H. O., and A. M. de Graaf, 1973, editors, *Amorphous Magnetism* (Plenum, New York).

Hori, J., 1968, *Spectral Properties of Disordered Chains and Lattices* (Pergamon, London).

Hubbard, J., 1963, Proc. R. Soc. Lond. A **276**, 238.

Hubbard, J., 1964a, Proc. R. Soc. Lond. A **277**, 237.

Hubbard, J., 1964b, Proc. R. Soc. Lond. A **281**, 401.

Hubbard, J., and J. L. Beeby, 1969, J. Phys. C **2**, 556.

Izyumov, Y., 1966, Proc. Phys. Soc. Lond. **87**, 505.

Joshi, S. K., 1972, Physica (Netherlands) **57**, 483.

Kagan, Y. M., and Y. A. Iosilveski, 1964, Sov. Phys.—JETP **18**, 562.

Kagan, Y., and A. P. Zhernov, 1966, Zh. Eksp. Teor. Fiz. **50**, 1107.

Kagan, Y., A. P. Zhernov, and H. Pashaev, 1968, in *Localized Excitations in Solids* (Plenum, New York).

Kamitakahara, W. A., and B. N. Brockhouse, 1972, in *Proceedings of a Symposium on Neutron Inelastic Scattering, Grenoble, 1972* (IAEA, to be published).

Karlsson, A. V., 1970, Phys. Rev. B **2**, 3332.

Keeler, G. J., and D. N. Batchelder, 1972, J. Phys. C **5**, 3264.

Keffer, F., 1966, Handbook Phys. **18/2**, 1.

Keller, J. B., and F. C. Karal, 1964, J. Math. Phys. **5**, 537.

Keller, J. B., and F. C. Karal, 1966, J. Math. Phys. **7**, 661.

Kerner, E. H., 1956, Proc. Phys. Soc. Lond. B **69**, 802, 808.

Khor, K. E., and P. V. Smith, 1971, J. Phys. C **4**, 2029.

Kikuchi, M., 1970, J. Phys. Soc. Jap. **29**, 296.

Kirkpatrick, S., 1971, Phys. Rev. Lett. **27**, 1722.

Kirkpatrick, S., 1973a, Rev. Mod. Phys. **45**, 574.

Kirkpatrick, S. 1973b, Solid State Commun. **12**, 1279.

Kirkpatrick, S., B. Velický, and H. Ehrenreich, 1970, Phys. Rev. B **1**, 3250.

Klauder, R., 1961, Ann. Phys. (N.Y.) **14**, 43.

Knox, R., 1966, *Theory of Excitons* (Academic, New York).

Kopelman, M., and H.-K. Hong, 1971, J. Chem. Phys. **55**, 3491, 5380.

Korringa, J., 1958, J. Phys. Chem. Solids **7**, 252.

Korringa, J., and R. L. Mills, 1972, Phys. Rev. B **5**, 1654.

Koster, G. F., 1954, Phys. Rev. **95**, 1436.

Koster, G. F., and J. C. Slater, 1954, Phys. Rev. **95**, 1167.

Kramer, B., 1970, Phys. Status Solidi **41**, 649.

Kramer, B., 1971, Phys. Status Solidi **47**, 501.

Kramer, B., K. Maschke, and P. Thomas, 1971, Phys. Status Solidi **48**, 635.

Kröner, E., 1967, J. Mech. Phys. Solids **15**, 319.

Krumhansl, J. A., 1973, in *Amorphous Magnetism*, edited by H. O. Hooper and A. M. De Graaf (Plenum, New York), p. 15.

Kubo, R., 1957, J. Phys. Soc. Jap. **12**, 570.

Kunz, C., and W. Gudat, 1973, Phys. Status Solidi (to be published).

Lakatos, K., and J. A. Krumhansl, 1969, Phys. Rev. **180**, 729.

Landau, L. D., and E. M. Lifshitz, 1960, *Electrodynamics of Continuous Media* (Addison-Wesley, Reading), p. 45.

Landauer, R., 1952, J. Appl. Phys. **23**, 779.

Landauer, R., 1970, Phil. Mag. **21**, 863.

Landauer, R., and J. C. Helland, 1954, J. Chem. Phys. **22**, 1655.

Langer, J. S., 1960, Phys. Rev. **120**, 714.

Langer, J. S., 1961a, Phys. Rev. **124**, 1003.

Langer, J. S., 1961b, J. Math. Phys. **2**, 584.

Langer, J. S., and T. Neal, 1966, Phys. Rev. Lett. **16**, 984.

Last, B. J., and D. J. Thouless, 1971, Phys. Rev. Lett. **27**, 1719.

Last, B. J., and D. J. Thouless, 1974, J. Phys. C **7**, 699.

Lax, M., 1951, Rev. Mod. Phys. **23**, 287.

Lax, M., 1952, Phys. Rev. **85**, 621.

Lax, M., and J. C. Phillips, 1958, Phys. Rev. **110**, 41.

Lax, M., 1973, American Math. Soc. Colloquium Publication Series, to be published.

Leath, P. L., 1968, Phys. Rev. **171**, 725.

Leath, P. L., 1970, Phys. Rev. B **2**, 3078.

Leath, P. L., 1972, Phys. Rev. B **5**, 1643.

Leath, P. L., 1973, J. Phys. C **6**, 1559.

Leath, P. L., and B. Goodman, 1966, Phys. Rev. **148**, 968.

Leath, P. L., and B. Goodman, 1968, Phys. Rev. **175**, 963.

Leath, P. L., and B. Goodman, 1969, Phys. Rev. **181**, 1062.

Lee, P. M., and P. E. Lewis, 1969, J. Phys. C **2**, 2089.

Lehmann, G. W., and R. E. DeWames, 1963, Phys. Rev. **131**, 1008.

Levin, K., R. Bass, and K. H. Bennemann, 1972, Phys. Rev. B **5**, 1865.

Levin, K., and H. Ehrenreich, 1971, Phys. Rev. B **3**, 4172.

Licciardello, D. C., and E. N. Economou, 1973, Solid State Commun. **12**, 1275.

Lieb, E. H., and D. C. Mattis, 1966, *Mathematical Physics in One-Dimension* (Academic, New York).

Lifshitz, I. M., 1956, Nuovo Cimento Suppl. **3**, 716.

Lifshitz, I. M., 1964a, Usp. Fiz. Nauk **83**, 617 [Sov. Phys.—Usp. **7**, 549 (1965)].

Lifshitz, I. M., 1964b, Adv. Phys. **13**, 483.

Lifshitz, I. M., and G. I. Stepanova, 1956, J. Exp. Theor. Phys. **30**, 938, [Sov. Phys.—JETP **3**, 653].

Lloyd, P., 1969, J. Phys. C **2**, 1717.

Long, D., 1966, Semicond. Semimetals **1**, 143.

Lovesey, S. W., 1968, J. Phys. C **1**, 102.

Lovesey, S. W., and W. Marshall, 1966, Proc. Phys. Soc. Lond. **89**, 613.

Lovesey, S. W., and W. Marshall, 1971, *Theory of Thermal Neutron Scattering* (Oxford U. P., London).

Lukes, T., 1972, J. Noncryst. Solids **8–10**, 470.

Luttinger, J. M., 1951, Philips Res. Rep. **6**, 303.

Lyo, S., 1972, Phys. Rev. Lett. **28**, 1192.

Mabuchi, T., A. Yoshikawa, and R. Onaka, 1971, J. Phys. Soc. Jap. **31**, 1754.

Mahr, H., 1961, Phys. Rev. **122**, 1464.

Maradudin, A. A., 1963, in *Astrophysics and the Many Body Problem*, edited by K. W. Ford (Benjamin, New York).

Maradudin, A. A., 1966, in *Solid State Physics*, edited by F. Seitz and D. Turnbull (Academic, New York), Vols. 18–19.

Martin, T. P., 1967, Phys. Rev. **160**, 686.

Matsubara, T., 1970, Prog. Theor. Phys. Suppl. **46**, 326.

Matasubara, T., and T. Kaneyoshi, 1966, Prog. Theor. Phys. **36**, 695.

Matsubara, T., and Y. Toyozawa, 1961, Prog. Theor. Phys. **26**, 739.

Matsubara, T., and F. Yonezawa, 1967, Prog. Theor. Phys. **37**, 1346.

Matsuda, H., 1964, Prog. Theor. Phys. **31**, 161.

Matsuda, H., 1966, Prog. Theor. Phys. Suppl. **36**, 97.

Matsuda, H., and K. Ishii, 1970, Prog. Theor. Phys. Suppl. **45**, 56.

Messiah, A., 1962, *Quantum Mechanics* (Wiley, New York).

Miller, A., and E. Abrahams, 1960, Phys. Rev. **120**, 245.

Mills, R., 1974, *Analyticity in Binary Alloys*, preprint.

Mitlehner, H., R. Geick, W. Lehman, R. Weber, G. Dietrich, and H. Schoenherr, 1971, Solid State Commun. **9**, 2059.

Møller, H. B., and A. R. Mackintosh, 1965, Phys. Rev. Lett. **15**, 623.

Moore, E. J., 1967, Phys. Rev. **160**, 607.

Mori, H., I. Oppenheim, and J. Ross, 1962, in *Studies in Statistical Mechanics*, edited by J. De Boer (Interscience, New York).

Mott, N. F., 1967, Adv. Phys. **16**, 49.

Mott, N. F., 1968, Phil. Mag. **17**, 1259.

Mott, N. F., 1970, Comments Solid State Phys. **2**, 183.

Mott, N. F., 1972, Phil. Mag. **26**, 1015.

Mott, N. F., 1973, Phys. Rev. Lett. **31**, 466.

Mott, N. F., and E. A. Davis, 1971, *Electronic Processes in Non-Crystalline Materials* (Clarendon, Oxford).

Mott, N. F., and H. Jones, 1958, *Theory of Metals* (Oxford U. P., London).

Mozer, B., 1968, in *Neutron Inelastic Scattering: Proceedings of a Symposium on Neutron Inelastic Scattering held by the International Atomic Energy Agency in Copenhagen, May 20–25, 1968* (IAEA, Vienna), p. 55.

Müller-Hartmann, E., 1973, Solid State Commun. **12**, 1269.

Murata, T., and Y. Nakai, 1967, J. Phys. Soc. Jap. **23**, 904.

Muto, T., 1938, Sci. Pap. Inst. Phys. Chem. Res. Tokyo **34**, 377.

Nagasawa, N., N. Nakagawa, and Y. Nakai, 1968, J. Phys. Soc. Jap. **24**, 1403.

Nagasawa, N., T. Kawasawa, N. Miura, and T. Nauba, 1972, J. Phys. Soc. Jap. **32**, 1155.

Nair, T., and C. T. Walker, 1971, Phys. Rev. B **3**, 3446.

Nakai, Y., T. Murata, and K. Nakamura, 1965, J. Phys. Soc. Jap. **18**, 1481.

Nakamura, K., 1967, J. Phys. Soc. Jap. **22**, 511.

Nakamura, K., and Y. Nakai, 1967, J. Phys. Soc. Jap. **23**, 455.

Ng, S. C., and B. N. Brockhouse, 1967, Solid State Commun. **5**, 79.

Nickel, B., 1974, J. Phys. C (to be published).

Nickel, B. G., and J. A. Krumhansl, 1971, Phys. Rev. B **4**, 4354.

Nicklow, R. M., P. R. Vijayaraghavan, H. G. Smith, G. Dolling, and M. K. Wilkinson, 1968, in *Neutron Inelastic Scattering: Proceedings of a Symposium on Neutron Inelastic Scattering held by the International Atomic Energy Agency in Copenhagen, May 20–25, 1968* (IAEA, Vienna), Vol. 1, p. 47.

Nordheim, L., 1931, Ann. Phys. (Leipz) **9**, 607.

Onodera, Y., and Y. Toyozawa, 1968, J. Phys. Soc. Jap. **24**, 341.

Papatriantafillou, C. 1973, Phys. Rev. **7**, 5386.

Parisot, R., E. Dietz, H. J. Guggenheim, P. Moch, and C. Dugantier, 1971, J. Phys. (Paris) **32**, C1-803.

Parkinson, J. D., 1973, J. Phys. C **6**, 2337.

Parmenter, R. H., 1955, Phys. Rev. **97**, 587.

Payton III, D. N., and W. M. Visscher, 1967, Phys. Rev. **154**, 802.

Payton III, D. N., and W. M. Visscher, 1968, Phys. Rev. **175**, 1201.

Payton III, D. N., M. Rich, and W. M. Visscher, 1967, Phys. Rev. **160**, 706.

Pepper, D. E., 1972, D. Phil. thesis, Oxford University, England (unpublished).

Pepper, D. E., W. J. L. Buyers, and R. J. Elliott, 1972, J. Phys. C **5**, 2611.

Pershan, P. S., and W. B. Lacina, 1970, Phys. Rev. B **1**, 1765.

Plischke, M., 1972, Phys. Rev. Lett. **28**, 361; in *Amorphous Magnetism*, edited by H. O. Hooper and A. M. de Graaf (Plenum, New York,

Plischke, M., and D. Mattis 1971, Phys. Rev. Lett. **27**, 42.

Pohl, R., 1968, in *Localized Excitations in Solids*, edited by R. F. Wallis (Plenum, New York), p. 434.

Polk, D. E., 1971, J. Non-Cryst. Solids **5**, 365.

Lord Rayleigh, 1892, Phil. Mag. Str. 5, **34**, 481.

Robinson, G. W., and H.-K. Hong, 1970, J. Chem. Phys. **52**, 825.

Robinson, G. W., and H.-K. Hong, 1971, J. Chem. Phys. **54**, 1369.

Rosenstock, H. B., and R. E. McGill, 1962, J. Math. Phys. **3**, 200.

Roth, L. M., 1973, Phys. Rev. B **7**, 4321.

Rowell, J. M., W. L. McMillan and P. W. Anderson, 1965, Phys. Rev. Lett. **14**, 633.

Rudnick, J. and E. A. Stern, 1973, Phys. Rev. B **7**, 5062.

Saitoh, M., 1971, Prog. Theor. Phys. **45**, 746.

Saxon, D. S., and R. A. Hutner, 1949, Philips Res. Rep. **4**, 81.

Schmidt, H., 1957, Phys. Rev. **105**, 425.

Schwartz, L. M., 1973, Phys. Rev. B **7**, 4424.

Schwartz, L. and H. Ehrenreich, 1971, Ann. Phys. (N.Y.) **64**, 100.

Schwartz, L., and H. Ehrenreich, 1972a, Phys. Rev. B **6**, 2923.

Schwartz, L., and H. Ehrenreich, 1972b, Phys. Rev. B **6**, 4088.

Schwartz, L., and E. Siggia, 1972, Phys. Rev. B **5**, 383.

Schwartz, L., H. Krakauer, and H. Fukuyama, 1973, Phys. Rev. Lett. **30**, 746.

Schwartz, L., F. Brouers, A. V. Vedyayev, and H. Ehrenreich, 1971, Phys. Rev. B **4**, 3338.

Seib, D. H., and W. E. Spicer, 1970, Phys. Rev. B **2**, 1694.

Sen, P. N., 1973, Phys. Rev. Lett. **30**, 553.

Sen, P. N. and M. H. Cohen, 1972, J. Noncryst. Solids **8–10**, 147.

Shante, V. K. S., and S. Kirkpatrick, 1971, Adv. Phys. **20**, 325.

Sheka, E. F., 1961, Opt. Spektrosk. **10**, 684.

Shiba, H., 1971, Prog. Theor. Phys. **46**, 77.

Shiles, E., and D. Hone, 1970, J. Phys. Soc. Jap. **28**, 51.

Simpson, A. W., 1970, Phys. Status Solidi B **40**, 207.

Sjölander, A., 1964, in *Phonons and Phonon Interactions*, edited by T. A. Bak (Benjamin, New York).

Soven, P., 1967, Phys. Rev. **156**, 809.

Soven, P., 1969, Phys. Rev. **178**, 1136.

Soven, P. 1970, Phys. Rev. B **2**, 4715.

Spicer, W. E., 1972, in *Optical Properties of Solids*, edited by F. Abeles (North-Holland, Amsterdam).

Stern, E. A., 1971, Phys. Rev. Lett. **26**, 1630.

Stocks, G. M., R. W. Williams, and J. S. Faulkner, 1971, Phys. Rev. B **4**, 4390.

Stroud, D., and H. Ehrenreich, 1970, Phys. Rev. B **2**, 3197.

Svensson, E. C., B. N. Brockhouse, and J. M. Rowe, 1965, Solid State Commun. **3**, 245.

Svensson, E. C., B. N. Brockhouse, and J. M. Rowe, 1967, Phys. Rev. **155**, 619.

Svensson, E. C., T. M. Holden, W. J. L. Buyers, and R. A. Cowley, 1969, Solid State Commun. **7**, 1693.

Svensson, E. C., and W. A. Kamitakahara, 1971, Can. J. Phys. **49**, 2291.

Tahir-Kheli, R. A., 1972, Phys. Rev. B **6**, 2808, 2826.

Takeno, S., 1962a, Prog. Theor. Phys. **28**, 33.

Takeno, S., 1962b, Prog. Theor. Phys. Suppl. **23**, 94.

Takeno, S., 1962c, Prog. Theor. Phys. **29**, 191.

Takeno, S., 1968, Prog. Theor. Phys. **40**, 942.

Takeno, S., 1971, J. Phys. C **4**, L118, 121, 123.

Takeno, S., and S. Goda, 1971, Prog. Theor. Phys. **45**, 331.

Tauc, J., 1972, in *Optical Properties of Solids* (North-Holland, Amsterdam), p. 277.

Taylor, D. W., 1967, Phys. Rev. **156**, 1017.

Taylor, P. L., 1967a, Proc. Phys. Soc. Lond. **88**, 753.

Taylor, P. L., 1967b, Proc. Phys. Soc. Lond. **90**, 233.

Thomsen, L., 1972, J. Geophys. Res. **77**, 315.

Thorpe, M. F., D. Weaire, and R. Alben, 1971, Phys. Rev. B **4**, 2508, 3518.

Thorpe, M. F., D. Weaire, and R. Alben, 1973, Phys. Rev. B **7**, 3777.

Thouless, D. J., 1970, J. Phys. C **3**, 1559.

Thouless, D. J., 1972, J. Phys. C **5**, 77.

Thouless, D. J., 1972, J. Noncryst Solids **8–10**, 461

Tonegawa, T., 1968, Prog. Theoret. Phys. **40**, 1195; **41**, 1.

Tong, B. Y., 1970, Phys. Rev. A **1**, 52.

Towers, G. R., 1971, *Phonons*, edited by M. A. Nusimovia (Flammarion, Paris).

Towers, G. R., 1973 (unpublished).

Tsukada, M., 1969, J. Phys. Soc. Jap. **26**, 684.

Tsukada, M., 1972, J. Phys. Soc. Jap. **32**, 1475.

Tyablikov, S. V., 1967, *Methods in the Quantum Theory of Magnetism* (Plenum, New York).

Van Hove, L., 1954, Phys. Rev. **95**, 249.

Velický, B., 1969, Phys. Rev. **184**, 614.

Velický, B., and K. Levin, 1970, Phys. Rev. B **2**, 938.

Velický, B., S. Kirkpatrick, and H. Ehrenreich, 1968, Phys. Rev. **175**, 747.

Velický, B., S. Kirkpatrick, and H. Ehrenreich. 1970, Phys. Rev. B **1**, 3250.

Verboven, E., 1960, Physica **26**, 1091.

Verleur, H. W., and A. S. Barker, 1966, Phys. Rev. **149**, 715.

Visscher, W. M., 1971, Prog. Theor. Phys. **46**, 729.

Wakabayashi, N., R. M. Nicklow, and H. G. Smith, 1971, Phys. Rev. B **4**, 2558.

Walker, L. R., B. C. Chambers, D. Hone, and H. Callen, 1972, Phys. Rev. B **5**, 1144.

Wang, J. C., K. S. Dy, and Shi-Yu Wu, 1973, Phys. Rev. B **7**, 750.

Watson, B. P., and P. L. Leath, 1974, Phys. Rev. B **9**, (to be published).

Watson, K. M., 1956, Phys. Rev. **103**, 489.

Watson, K. M., 1957, Phys. Rev. **105**, 1388.

Weaire, D., 1971, Phys. Rev. Lett. **26**, 1541.

Wolfram, T., and J. Callaway, 1963, Phys. Rev. **130**, 2207

Woll, G. J., 1965, Phys. Rev. **137**, A95.

Woods, A. D. B., and B. M. Powell, 1965, Phys. Rev. Lett. **15**, 778.

Yonezawa, F., 1968a, Prog. Theor. Phys. **39**, 1076.

Yonezawa, F., 1968b, Prog. Theor. Phys. **40**, 734.

Yonezawa, F., and K. Morigaki, 1973, Prog. Theor. Phys. Suppl. **53**, 1.

Yonezawa, F., and T. Matsubara, 1966a,b Prog. Theor. Phys. **35**, 357 759.

Yonezawa, F., and M. Watabe, 1973, Phys. Rev. B **8**, 4540.

Yussouff, M., and J. Mahanty, 1965, Proc. Phys. Soc. Lond. **85**, 1223.

Yussouff, M., and J. Mahanty, 1966, Proc. Phys. Soc. Lond. **87**, 689.

Yussouff, M., and J. Mahanty, 1967, Proc. Phys. Soc. Lond. (6b) **90**, 519.

Zeller, H. R., 1973, *Advances in Solid State Physics* (Pergamon, New York), Vol. XIII.

Ziman, J. M., 1966, Proc. Phys. Soc. Lond. **88**, 387.

Ziman, J. M., 1969, J. Phys. C **2**, 1230.

Zubarev, D. N., 1960, Usp. Fiz. Nauk **71**, 71 [Sov. Phys.—Usp. **3**, 320 (1960)].